



# itw

Institute for Transuranium Elements

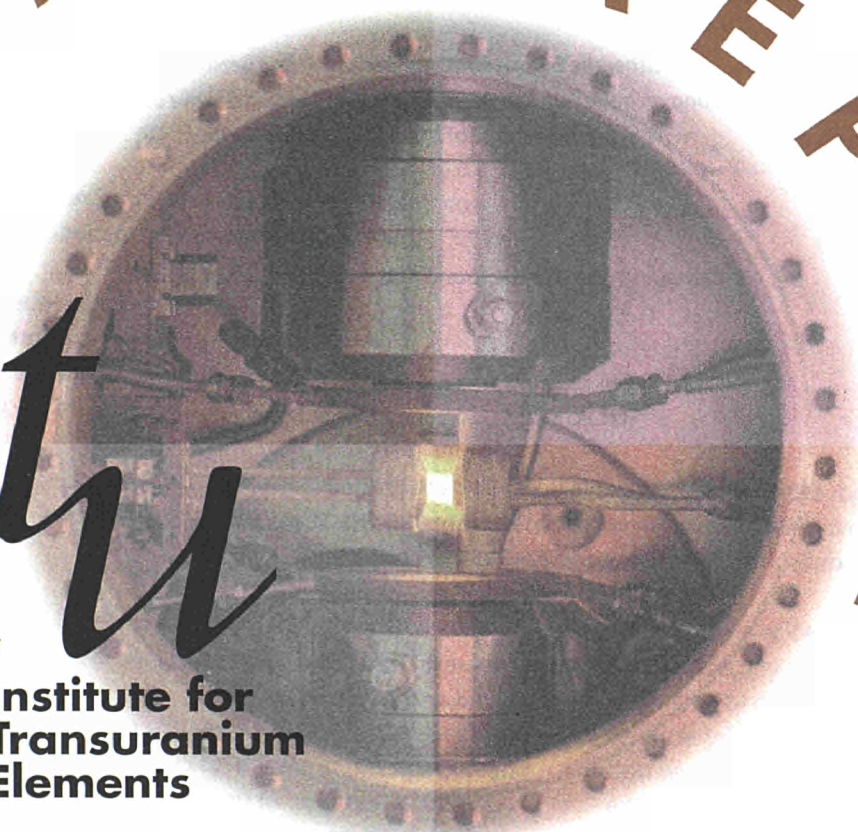
Annual Report

# 98

JOINT RESEARCH CENTRE  
EUROPEAN COMMISSION  
Report EUR 18715 EN



# ANNUAL REPORT 1998



*itu*

**Institute for  
Transuranium  
Elements**

Published by the  
**EUROPEAN COMMISSION**  
Directorate-General JRC

**Institute for Transuranium Elements**

## LEGAL NOTICE

*Neither the European Commission nor any person acting on behalf of the Commission is responsible for the use which might be made of the following information.*

Cataloguing data can be found at the end of this publication

This report was compiled and edited by  
R. Schenkel, J. Richter, J. Magill, D. Pel

Inquiries for more details should be addressed to the Programme Office,  
Institute for Transuranium Elements, P.O. Box 2340, D-76125 Karlsruhe,  
phone +49 7247 951386, fax +49 7247 951591  
e-mail: roland.schenkel@jrc.org

This publication and more information on the Institute  
may be found on the Web page:

<http://www.jrc.org/>

Graphic design:  
Public Relations, Documentation and Publications Unit • JRC Ispra

EUR 18715 EN

Luxembourg: Office for Official Publications of the European Communities

ISBN 92-828-6580-0

© European Communities, 1999

*Printed in Germany*

An Annual Report is the occasion to demonstrate the progress and achievements reached during a year and to acknowledge scientists, technicians and support staff for their engagement and contributions.

**In many respects, 1998 has been a remarkable year for ITU:**

- The highlights described in part A of the Annual Report provide a selection of particularly interesting achievements in 1998.
- From our own research programme, and our many collaborations, 140 publications have resulted:
  - 54 to refereed journals
  - 46 to conference proceedings or reports
  - 40 contributions were submitted in the form of abstracts.
- Reflecting the increased orientation towards innovation and technology transfer, 4 patent applications were submitted.
- In the area of work for third parties, contracts with a volume of 6.6 MEURO were signed in 1998.
- In March 1998, the effort to streamline major "processes" within ITU led to the official DQS certificate in accordance with ISO 9001. This is a vital first step in quality management, but the process of continuous improvement needs to be pursued.

**1998 has also been a year of change :**

During the last year of the 4th Framework Programme, activities for the 5th Framework Programme were proposed based on a thorough evaluation of the needs of our customers in research, industry, authorities, inspectorates and Commission services. In addition, the mission of the JRC has been changed with a major shift in emphasis towards supporting the policies of the European Union. ITU is therefore increasing its support to DG IA (in the area of nuclear safety and safeguards for Eastern countries), to DG XI (radioactivity in the environment) while maintaining its established support to DG XVII.



**J. van Geel**  
*Director*

- New installations are being established at ITU which open or widen new avenues of research and provide opportunities for collaboration:
  - set up of a hot cell to study electrorefining of spent fuel and highly active wastes
  - extension of the laboratory for alpha-immunotherapy to cope with the increasing demands for collaboration with hospitals.
  - extension of Minor Actinide Laboratory for targets fabrication for transmutation experiments.
- A large number of young researchers is expected to arrive at ITU as a result of the retirements of experienced and specialised staff. This places a challenge on all personnel to maintain quality, experience, safety and our ITU corporate culture in the years to come.

In the year ahead, some outstanding issues, like the renovation and the upgrading of the Institute's infrastructure and the further discharge of old gloveboxes and radioactive wastes will have to be tackled.

I trust that the Institute's staff will continue to provide a major contribution to the goals and objectives of the Institute in the year ahead.



## Table of contents

### A - General Part

3	Foreword
6	Mission of the Institute for Transuranium Elements
7	Research and Technological Development on Actinides and Fuel Cycle Safety
14	Highlights 1998
26	Nuclear Forensics – the Investigation of Smuggled Nuclear Materials (review article)
36	Information-dissemination
37	Organisation Chart of the Institute
38	Publications, PhD'S and Patents
40	Institute Staff Resources
41	Budget Resources

### B - Scientific/Technical Part

45	Table of Contents (Part B)
47	Research in Fuel Cycle Safety
47	1. Basic Actinide Research
71	2. Safety of Nuclear Fuel
83	3. Mitigation of Long Lived Actinides and Fission Products
97	4. Spent Fuel Characterization in View of Long Term Storage
103	5. Safeguards Research and Development
107	6. Scientific and Technical Support to DG XVII
113	7. Scientific and Technical Support to DG I (Safeguards)
115	Annexes

# Mission of the Institute for Transuranium Elements

The Institute for Transuranium Elements provides impartial and independent expertise for the protection of the population against risks associated with the handling and storage of highly radioactive transuranium elements.

## ITU's particular aims are

- to do customer-driven R&D of the highest quality and integrity in support of EU policies
- to further enhance the Institute's role as a recognised centre of European basic actinide research
- to contribute to an effective nuclear safeguards system in Europe and elsewhere
- to strengthen the position of the European industry by

evaluating and testing the potential for technological and medical applications of transuranium elements.

## In line with the European Commission's R&D programme, ITU

- PERFORMS and PROVIDES Institutional Research and Support on a multiannual basis
- PARTICIPATES in European Networks to enhance co-operation and to avoid duplication
- SOLICITS Work under Contract from Third Parties
- CO-OPERATES with Eastern countries in the areas of nuclear safety

PURSUES Exploratory Research to open up new avenues.



# Research and Technological Development on Actinides and Fuel Cycle Safety

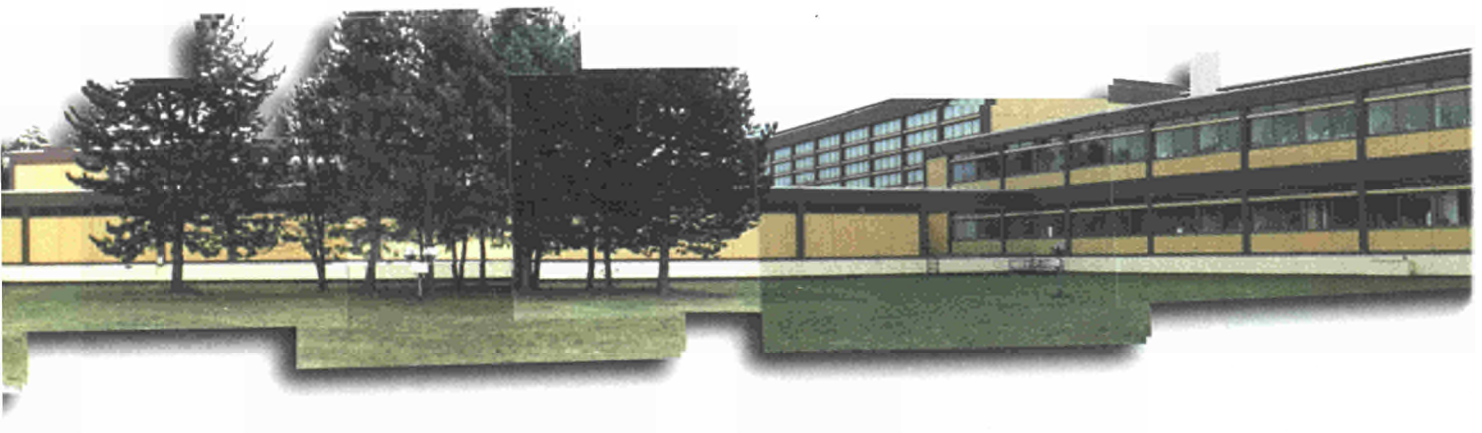
## This is the rationale of ITU's activities

ITU's work is anchored in the EURATOM Framework Programme on "Nuclear Fission Safety". It comprises so-called institutional research and scientific and technical support activities, which can be grouped under six main headings

- Basic Actinide Research
- Safety of Nuclear Fuels
- Mitigation of Long-lived Actinides
- Spent Fuel Characterization, in View of Long Term Storage
- Nuclear Safeguards
- Support to Policies of the European Union in Fields of Nuclear Safety and Safeguards

In addition to these activities, the Institute performs work for third parties, mainly for industry, with a volume of between 10 and 15 % of the institutional budget.

Brief descriptions of these sub-themes are given in the subsequent pages.



## Basic Actinide Research

The actinide elements consist of four natural (actinium to uranium) and eleven man-made radionuclides (neptunium to lawrencium) which were synthesized for the first time between 1940 and 1961 by transmutation.

Actinides are available in very small ( $\mu\text{g}$  to g) and very large quantities (kilotonnes and more) depending on the use. For the production of energy, uranium and plutonium are available in large quantities.

The continuing and rapidly growing interest in the actinides results from three reasons:

(a) the application of the two "major" actinides (uranium and plutonium) in the fuel cycle and the interest in the separation and transmutation of some "minor" actinides (neptunium, americium and curium) in the framework of waste management,

(b) the interest of the scientific community in the multiplicity of very unusual and highly interesting chemical and physical phenomena, such as the multitude of oxidation states, changes of crystal structures, variety of transport, thermody-

amic, spectroscopic and magnetic properties and the co-existence of magnetism and superconductivity. This results from the successive filling of the inner 5f-electron shell and the complex interaction of these 5f-electrons with the outer conduction band electrons,

(c) the potential application of actinides in nuclear medicine. A recent example is the ongoing work to use the high energy low range alpha particles, coupled to suitable antibodies, to combat cancer.

The transmutation of separated plutonium (from military as well as civil applications) and of long-lived actinides from spent fuel in special burner reactors requires the development and characterization of new types of fuel. For these new fuels a variety of basic physical, chemical, material and thermodynamic data are required to assess their suitability.

The growing interest in the scientific community is reflected in the extension of ITU's capabilities as a user laboratory for university and research centre staff and as a supplier of encapsulated actinide containing samples.



*Dieter Kolberg (doctoral grant holder)  
loading a sample in the SQUID magnetometer.*

## Safety of Nuclear Fuel

In order to increase cost-effectiveness of nuclear power production, research and development is underway to increase the fuel residence time in the reactor, i. e. the burn-up of the fuel, without putting safety at stake. In this way, the fuel inventory, reprocessing, transport and storage costs can be reduced. Furthermore, longer use of the fuel assemblies require fewer shutdowns for refuelling and thus reduced reactor operation costs.

The Institute is analysing some of those basic phenomena, which occur at extended burn-up of fuel and which may impose an upper limit to burn-up extension. Such factors are the fuel-cladding chemical and mechanical interaction, the increase of the fission gas pressure inside the fuel rod, the outer corrosion of the zircaloy cladding and the resulting hydrogen pick-up after prolonged irradiation time. The experimental investigation of the behaviour of uranium oxide and MOX (mixed uranium-plutonium oxide) LWR (light water reactor) fuel at high burn-up is therefore a major focus of ITU's activities.

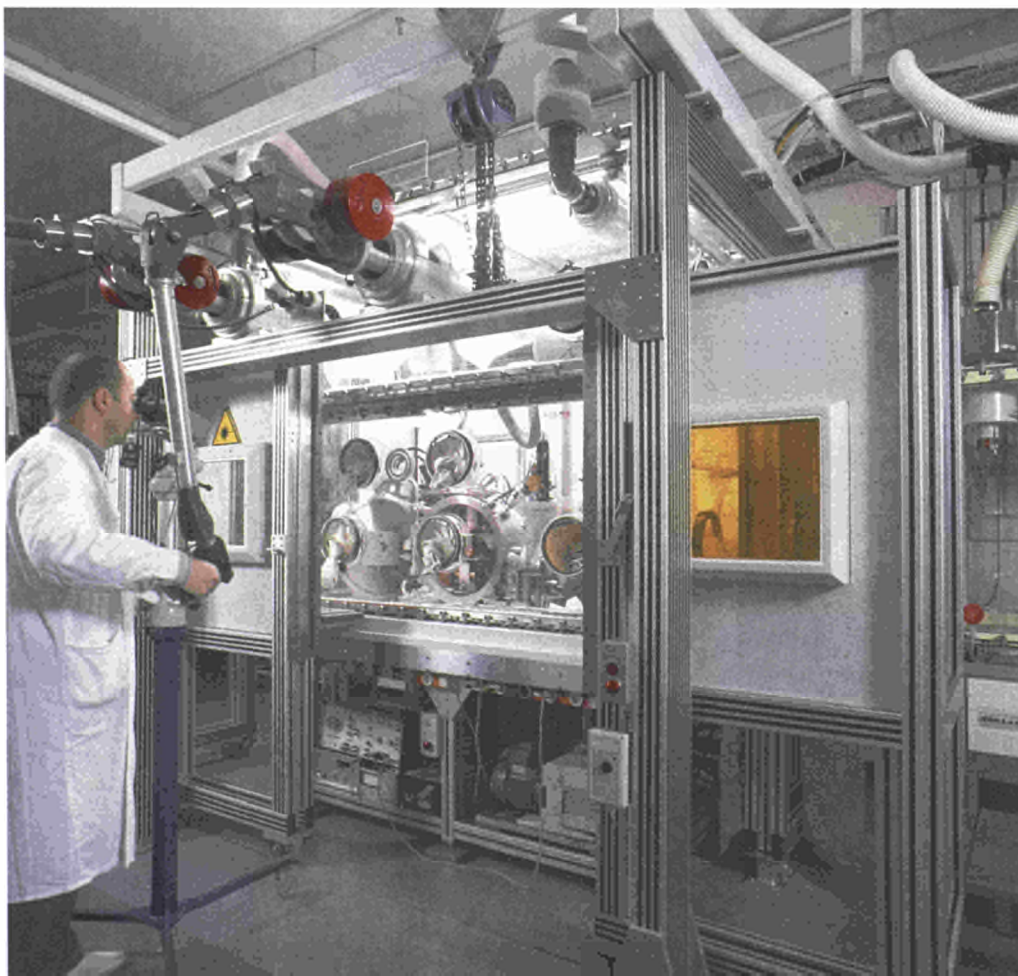
These investigations are complemented by the determination of mechanical, thermal and thermodynamic properties

of the material in a large temperature range and take into account radiation damage effects. The experimental data form the basis for the extension of the TRANSURANUS code, used by industry and licensing authorities to calculate in detail the thermal and mechanical in-pile behaviour of fuel rods under normal and transient conditions.

Of particular interest are investigations on the release of fission products from irradiated fuel, the radiotoxic inventory (source term) of fuel rods and the possible release mechanisms under accident conditions.

In the framework of the Phebus FP project, the Institute is investigating melted fuel rod bundles. The experience will improve the knowledge of the behaviour of nuclear fuel rods under accident conditions.

Advanced fuel fabrication techniques for the next generation of MOX fuel fabrication will be developed and tested with a view to achieving lower occupational risks by fully automated and almost dust-free processes.



*Dr. Mikhail Sheindlin testing the gamma shielded facility with an apparatus for high precision measurements of thermophysical properties of highly radioactive materials.*

# Mitigation of Long-Lived Actinides and Fission Products

The safe disposal of highly active wastes dominates the nuclear debate in several countries. The major issue is the potential risk due to the long-term radiotoxicity of trans-uranium elements and some long-lived fission products, such as technetium-99 ( $T_{1/2} \approx 210\,008\text{ a}$ ) and, for example, iodine-129 ( $T_{1/2} \approx 16\text{ Mio a}$ ).

To further reduce the potential long-term hazard of such wastes, partitioning and transmutation (P+T) research is being performed in several countries. The objective is to separate the long-lived nuclides from the waste, to recycle them in reactors and to "transmute" or "burn" them by neutron capture or fission into nuclides with much shorter half-lives.

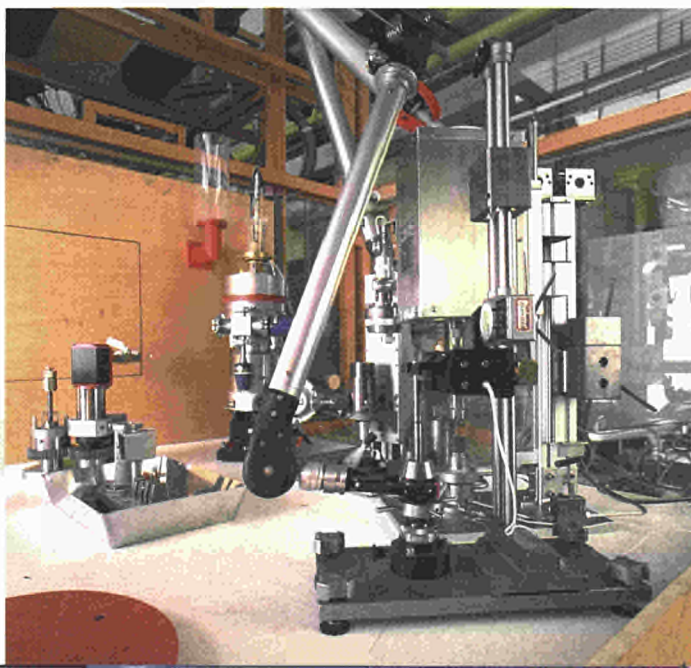
Current recycling of plutonium and reuse as MOX fuel in thermal reactors can be seen as an example of P+T for plutonium. The objective of P+T research is to provide basic data on the chemical separation, fuel fabrication, in-pile behaviour, reprocessing and recycling in order to assess whether

the technology is feasible and whether a reduction of the radiotoxicity hazard by a factor of about 100 can be achieved at reasonable cost.

In order to reduce the further build-up of plutonium and/or minor actinides, so-called inert matrices, i. e. uranium and/or plutonium free matrices, such as spinel ( $\text{MgAl}_2\text{O}_4$ ), are under investigation.

The Institute's activities involve testing new extractants for partitioning of actinides and fission products, the feasibility of fabrication of minor actinide and fission product containing fuels, and post-irradiation examination of such fuels following irradiation in a reactor.

The work performed by the Institute is in close collaboration with its European partners including the Commissariat à l'Energie Atomique (CEA) in France, the Forschungszentrum Karlsruhe (FZK) in Germany and the Nuclear Research Consultancy Group (NRG) in Petten, Netherlands.



*Mock-up cell to test equipment before introduction in the hot cells.*

## Spent Fuel Characterization in View of Long Term Storage

For the management of spent fuel discharged from power reactors, Member States of the European Union have adopted one (or a combination) of the following approaches:

- intermediate dry or wet storage with subsequent conditioning for final disposal in geological formations,
- intermediate storage followed by reprocessing, i. e. recycling of uranium and plutonium and subsequent conditioning of highly active wastes for final disposal in geological formations.

For the direct long-term storage of spent fuel, i. e. without reprocessing, the behaviour and interaction of the fuel with its surroundings need to be well known and understood.

The Institute is therefore performing work to characterize spent fuel with regard to the source term (i. e. the actinide and fission product inventory), the corrosion and leaching behaviour under different storage conditions, the evolution of the radiotoxicity as a function of storage time and the interaction of the fuel with structural materials. The work is complemented by equipment development for non-destructive assay of the actinide and fission product content of fuels.

The basic phenomena of corrosion kinetics and the near field behaviour of the different radionuclides in the repository are examined in close collaboration with European partners on real spent fuel or other highly active waste forms under hot cell conditions.

*Messrs. Paulo Nascimento and Didier Pellottiero working at a hot cell facility for post-irradiation examination of spent nuclear fuel.*



## Nuclear Safeguards

Stopping the further spreading of nuclear weapons is a complex task requiring international co-operation and confidence-building at all levels: bilateral, regional and global.

Nuclear safeguards are a set of activities by which the International Atomic Energy Agency (IAEA) in Vienna seeks to verify that a State is not using nuclear material or equipment to develop or produce nuclear weapons. Safeguards are not directly linked with either the safety of nuclear installations or with the physical security of nuclear material.

The Euratom Safeguards Directorate of the European Commission in Luxembourg is a regional inspection system which contributes to the IAEA's worldwide non-proliferation regime.

The Institute is a long-standing partner of both inspectorates in performing research and development as well as providing analytical services and support to both inspectorates.

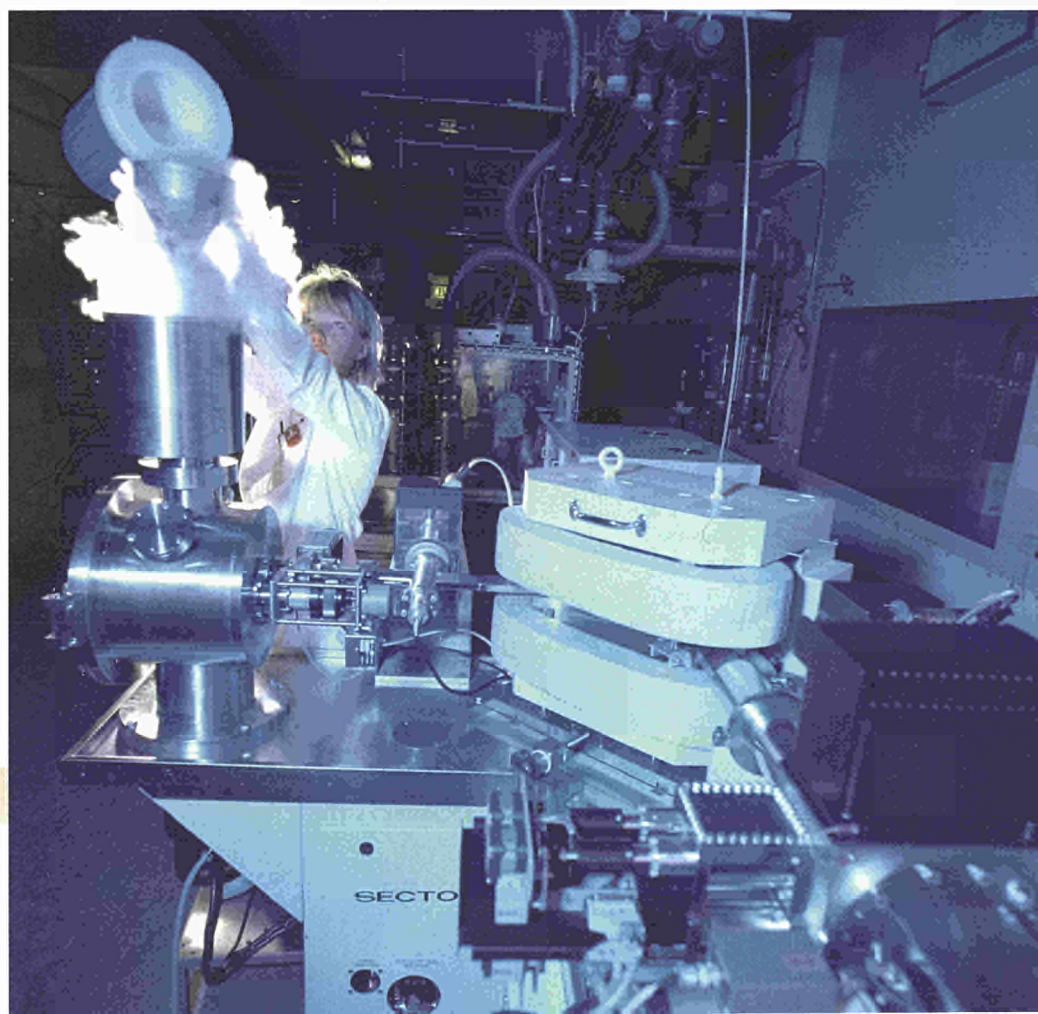
Analytical measurements on safeguards samples have been performed at ITU for about 20 years (ECSAM). Safeguarding

major reprocessing facilities involves a large number of samples being analysed. These samples will be measured in on-site laboratories at Sellafield and La Hague, which are being installed and operated by ITU.

The discovery of a clandestine nuclear weapon programme in Iraq after the Gulf War demonstrated serious shortcomings in the ability of the IAEA safeguards system to detect possible undeclared nuclear activities.

In close collaboration with the Euratom Safeguards Directorate and Member States of the European Union, the Institute has helped to accelerate the process of strengthening the IAEA safeguards system by developing and implementing facilities and equipment for the analysis of tell tale traces of radionuclides inside and outside nuclear plants. The new technique is called environmental monitoring or high precision trace analysis.

The Institute will pursue its efforts to develop inter alia these new techniques to their full potential in line with the needs of our customers.



*Maria Wallenius (doctoral grant holder) filling liquid nitrogen into the Thermal Ionisation Mass Spectrometer (TIMS).*

# Support to Policies of the European Union in the Fields of Nuclear Safety and Safeguards

## Support to Policies of the European Union in the Fields of Nuclear Safety and Safeguards

The European Union is cooperating with the countries of Eastern and Middle Europe as well as the Commonwealth of Independent States in a variety of ways and via different organizations. As a European Commission nuclear research body with core competences in the area of nuclear safety and safeguards, the Institute is contributing to various projects, such as:

- transfer of a fuel rod performance code for reactor safety evaluations to licensing authorities and nuclear research institutes in the framework of the Commission's PHARE programme,
- co-operation with state authorities and nuclear research institutes of Eastern countries to combat illicit trafficking of nuclear materials under the PHARE and TACIS programmes,
- co-operation with the Russian Federation in the set-up of a database for the identification of nuclear material with unknown origin,

- co-operation with the Russian Federation in the area of nuclear safeguards, for example in the design and set-up of analytical laboratories for metrological, nuclear material accountancy and forensic applications,
- co-operation with Russian research institutions via the International Science and Technology Center (ISTC) in Moscow,
- review of the equation of state of uranium oxide up to the critical point in a scientific cooperation under the INTAS programme (International Association for the Promotion of Cooperation with Scientists from the Independent States of the Former Soviet Union).

The Institute also participates in the International Technical Working Group (a subgroup of the P-8 Non Proliferation Committee) on illicit trafficking and in activities concerning the co-operation of the European Union with institutions in other third countries, like the United States and Japan, where research agreements on nuclear issues are included.



*Consolidating ties with Russian scientists from the Bochvar Institute, Moscow.  
(from left to right): Klaus Mayer, ITU, Ronald Schenkel, ITU,  
Jacques van Geel, ITU, Nikolai Babel (translator),  
Prof. Yury Bibilashvili, Deputy Director of Bochvar Inst.,  
Prof. Mikhail Solonin, Director of Bochvar Inst.*

# Highlights 1998 Strong Pressure Dependence of the Transport Properties of PuTe

Among actinide compounds with the simple NaCl-structure, the Pu monochalcogenides have a special place. They do not order magnetically and at low temperature show resistivity that increases with decreasing temperature, whereas most metallic compounds show the reverse. Because of the simplicity of their atomic structure and their exceptional properties, many different proposals have been made concerning their electronic ground state.

A recent theoretical investigation of the electronic structure suggests that these compounds are semimetals with a quasigap [1]. Therefore, it is believed that their electronic properties strongly depend on the value of the lattice parameter. An excellent way of tuning this parameter is the application of external pressure.

The four high-pressure experiments available in ITU (previous reports) are all based upon the opposing diamond-anvil technique. In the resistivity and X-ray diffraction experiments mentioned here (see Fig. 1), high-pressures up to 300 kbar (30 GPa) and 500 kbar (50 GPa) can be achieved, respectively.

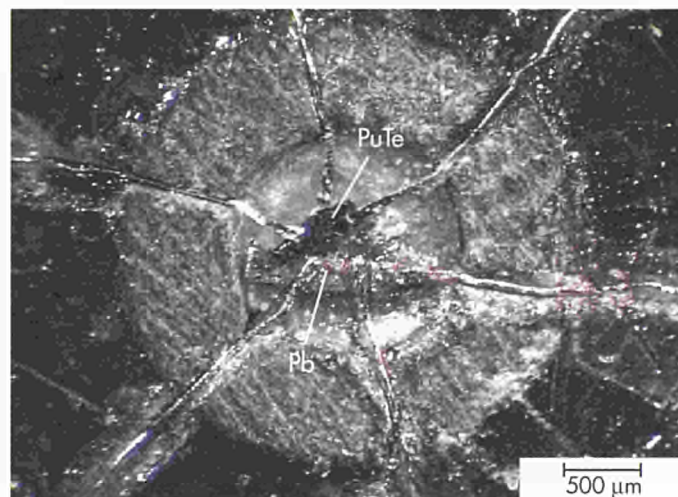
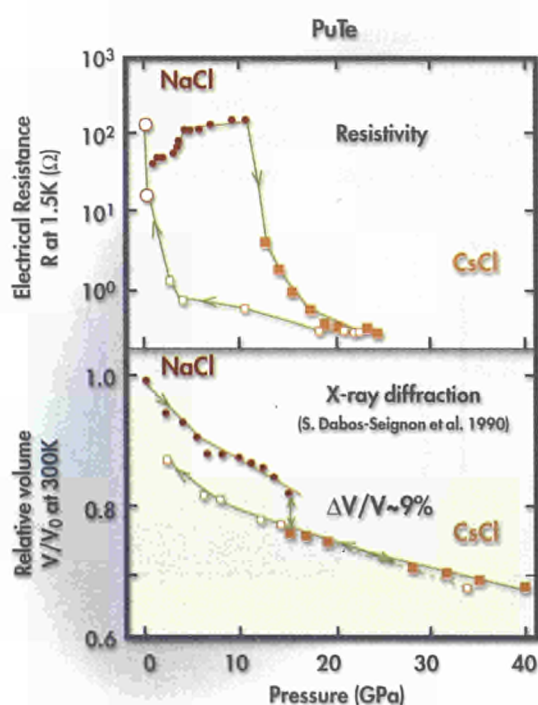


Fig. 1 Diamond anvil technique - View of the pressure cell used for high-pressure resistivity experiments. The diameter of the gasket (grey pyrophyllite ring) is only 2 mm. With this type of cell, pressures of between 250-300 kbar (25-30 GPa) can be achieved. The single crystal of PuTe is rather small ( $\sim 480 \times 100 \times 30 \mu\text{m}^3$ ). The piece of lead (Pb) is the manometer and the six platinum wires are used to measure the electrical resistance. The preparation of the pressure cell is carried out in a glove box as the diamond anvils are contaminated.

In our first series of experiments on these materials at ITU with the high-pressure resistivity technique we have chosen PuTe; excellent crystals of which were grown at ITU some years ago.

Fig. 2 shows the electrical resistance  $R$  at 1.5 K and the relative volume of PuTe as a function of pressure. The pressure dependence of  $R$  is unusual and clearly displays two regimes ( $\bullet$ ,  $\blacksquare$ ): an initial increase and then, above  $\sim 11$  GPa, a strong decrease by around 2 orders of magnitude. From X-ray data [2] we can

identify both regimes and attribute them to the NaCl and CsCl crystallographic structures, respectively. The initial increase of the resistance is rather surprising and could be due to an increase of the quasigap with reduced lattice parameter; a possibility suggested by recent theoretical investigations [1]. The decrease of  $R$  observed in the CsCl structure is in qualitative agreement with previous theory, which predicted an increase of the density of states at the Fermi surface in the CsCl phase [3].



#### References

- [1] P.M. Oppeneer, T. Kraft, M.S.S. Brooks, Electronic structure of Plutonium Monochalcogenides, to be published in Physical Review B
- [2] S. Dabos-Seignou, U. Benedict, S. Heathman, J.C. Spirlet, Journal of the Less-Common Metals 160 (1990) 35-52
- [3] B. Johansson, O. Eriksson, M.S.S. Brooks, H.L. Skriver, Inorganica Chimica Acta 140 (1987) 59-66

Fig. 2. Electrical resistance at 1.5 K shown in logarithmic scale and relative volume at 300 K of PuTe as a function of pressure. The two regimes observed in the resistivity ( $\bullet$ ,  $\blacksquare$ ) are attributed to the NaCl-CsCl structural transition which is observed in the X-ray data. The open symbols ( $\circ$ ,  $\square$ ) show the data obtained as the pressure was decreased. Large hysteresis is common in these kinds of measurements.

# Thin Films of Actinides and their Study by Photoemission

Thin films are used to study the localization phenomena of 5f electrons in actinides. This specific issue of the electronic structure controls many physical and chemical properties of actinides such as surface valence and reactivity, magnetism or heavy fermion properties. The surface is a particularly important part of actinides and nuclear systems because it constitutes the contact interface to the environment. Leaching or corrosion properties of waste systems directly depend on the surface properties such as the valence.

The central question is under what conditions 5f electrons participate in surface chemical bonding, i.e. if they are initially delocalized, and what happens to the surface reactivity as

they become localized? To investigate this we modulate the chemical environment (atomic coordination) of surface actinide atoms and study the evolution of the electronic structure by photoemission spectroscopy. Decreasing coordination suppresses the chemical bonding and hence 5f localization can be varied. The exact surface electronic structure depends also on the strength of overlayer-substrate interactions. *Fig. 1* compares different surface systems with a decreasing coordination. The embedded atoms are almost bulk-like. The thin film (one to several monolayers) results in suppression of solid state bonding which becomes more suppressed as the film thickness decreases. Surface clusters may behave almost like isolated atoms.

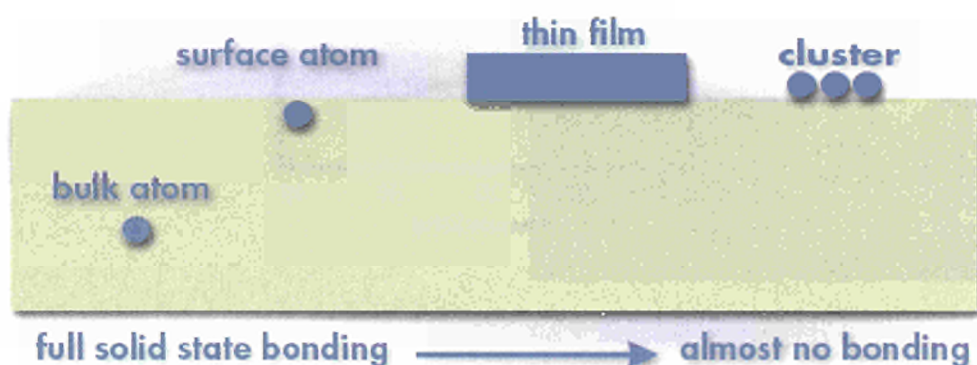


Fig. 1 The chemical bonding of atoms decreases from the bulk to the surface, thin film and eventually cluster.

An example for the changing electronic structure is shown in Fig. 2, where we studied Pu overlayers on various substrates. The substrates, in order of increasing affinity to Pu are: Mg, Al and Si. The thin films are compared to two bulk phases of Pu, which differ in the extent of 5f localization: in  $\alpha$ -Pu the Pu 5f electrons are more delocalized, while in  $\delta$ -Pu they become more localized. With approaching localization, the maximum at the Fermi-level ( $E_F$ ) splits into a narrow resonance right at  $E_F$  and a small peak at roughly 1 eV. Between them an intensity minimum (gap) appears. All thin film spectra are very similar to  $\delta$ -Pu, despite the different substrates and the varying interaction with the Pu overlayer. Details in overlayer-substrate bonding seem to affect the electronic structure only weakly. The overlayer on the non interacting Mg is virtually identical to  $\delta$ -Pu. On Al and Si, the gap at 0.5 eV becomes more pronounced pointing to more localized 5f states.

A description of these systems in terms of band structure is problematic. Because of the strong correlation the electrons cannot be treated as belonging to a nearly free electron gas. Simple interpretation of photoemission spectra in terms of electron binding energies, which may be compared to band structure calculations, is no longer possible. Instead many-

body final-state effects influence the spectra. One result may be the temperature dependence observed for spectra of Pu/Si (Fig. 3), which is totally unexpected from band structure models. The strong intensity variation of the peaks at low binding energy cannot be attributed to temperature broadening of the Fermi-level. A similar effect was observed previously this year for PuSe, and is discussed in more detail elsewhere. This appears to be the first time that such strong effects are observed in photoemission in the absence of structural changes.

The above examples show the applications of thin films for studying the electronic structure of actinides. Film deposition is a well established method for producing high quality samples. Complex systems of varying composition and defect concentrations may be produced allowing a simulation of actinide waste systems. For working with higher actinides we developed a film source using minor amounts. The films themselves contain nano- to micrograms of actinides. Ongoing and future thin film research involves study of the electronic structure, and surface reactivity of nuclear waste systems e.g. by electrochemistry, surface corrosion and overlayer-bulk interdiffusion.

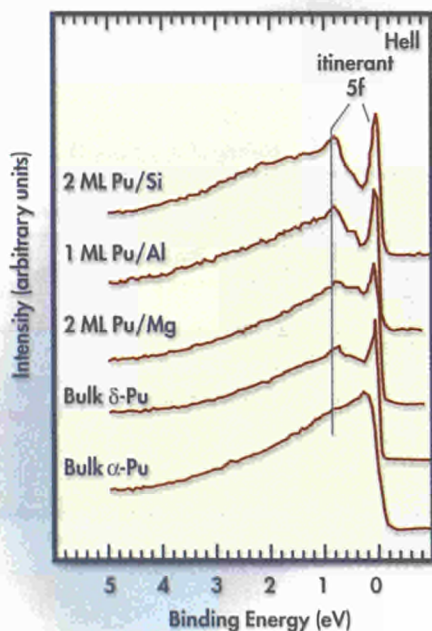


Fig. 2 UPS-Hell spectra of Pu overlayers on Mg, Al and Si. For comparison spectra of  $\alpha$ - and  $\delta$ -Pu are shown. ML = monolayer.

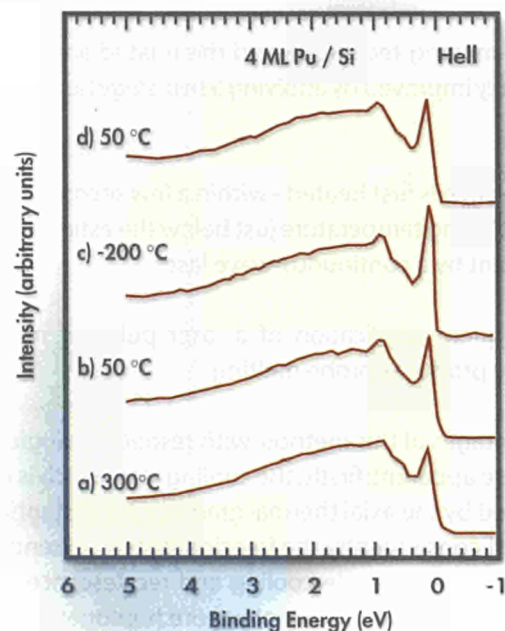


Fig. 3 UPS-Hell spectra of Pu/Si recorded at different temperatures. The spectra have been taken in the following order: a, b, c, d. The identical shape of b) and d) shows that there is no time dependence. Any possible explanation by surface evolution (e.g. amorphous – crystalline transition) is ruled out. Also no other Pu phases below the  $\alpha$ -phase at 115°C are known.

# High-Precision Melting Point Measurement of MOX Nuclear Fuel

The high temperature thermophysical properties of nuclear reactor fuels, investigated in our Institute, are of primary importance in different contexts: first in optimising the fuel rod design; secondly in defining the safe operation limits of the fuel elements, and, finally, in predicting the consequences of hypothetical reactor accident scenarios. In this respect, fuel melting represents, from the one side, a not-transgressible limit during normal and off-normal reactor operation, and, from the other side, a crucial reference event for accident analysis. The accurate determination of the melting point of different types of fuels is therefore an essential part of our research programme.

The melting behaviour of refractory actinide oxides is customarily investigated in our Laboratory by heating the surface of the sample with a pulsed laser-beam. The effect of the melting phase transition is observed as a more or less pronounced temperature arrest during heating (*solidus*) and/or cooling (*liquidus*). In practice, the experimental thermograms may present a rather complex trend, which may be affected both by the nature of the investigated phase transition (e.g. non-congruent melting) and by the heating method itself that, unavoidably, produces large axial gradients beneath the heated surface.

The laser-melting technique and the related analysis, were considerably improved by applying a two-stage heating method, i.e.:

1. The sample is first heated - within a few seconds - up to a conditioning temperature just below the estimated melting point by a continuous-wave laser.
2. Subsequent application of a laser pulse of moderate energy produces probe melting.

The advantages of this method, with respect to single-pulse heating, are apparent: firstly, the cooling rate, which is mainly determined by the axial thermal gradient, is substantially lowered, and, consequently, the freezing plateau extended, with less pronounced undercooling and recalescence effects. Secondly, a thicker and thermally more homogeneous molten pool can be produced with relatively low heat pulses, ensuring a more precise determination of the transition temperature.

A special set-up was designed and mounted to this purpose in an alpha-glove box. During 1999 a biological lead shielding will be implemented, enabling two-stage melting experiments to be carried out also on irradiated nuclear fuel.

Two-stage laser melting was successfully applied to a number of materials. Fig. 1 presents the results of a measurement in a 25%-Plutonium MOX fuel. It can be seen that the thermal arrest due to freezing at 3086 K is well indentified on the cooling branch of the thermogram, after a recalescence of less than 5 K, by a 10 ms-long plateau, with a precision of the order of 1 K.

The melting point of MOX is found to depend both on the plutonium content and on the O/M ratio of the oxide (note that of the melting point of  $UO_2$  is 3150 K). In this respect, the technique offers the double advantage of rapid measurements and of heating in an arbitrary gas atmosphere (an autoclave is being constructed enabling melting studies to be carried out under pressures up to 2000 bar). Though the experiments are not performed under equilibrium conditions, in most cases changes of the initial chemical composition of the sample can be kept within pre-fixed limits.

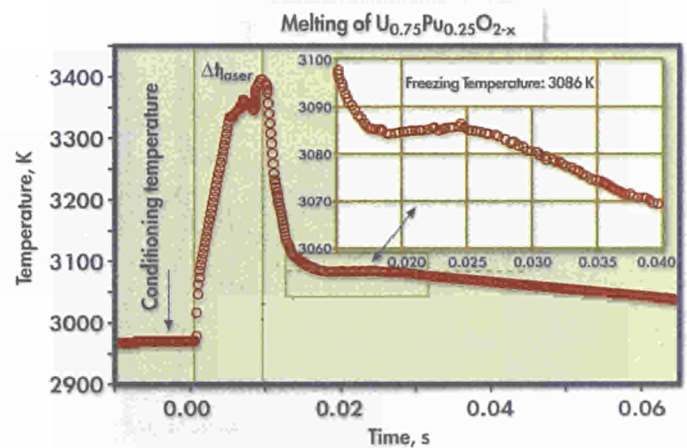


Fig. 1 Thermogram of a MOX melting experiment: the thermal-arrest plateau, due to recovering of the latent heat of fusion, is magnified in the inset. The accuracy of the freezing temperature measurement is in the order of 10 K.

# Effect of $\alpha$ -radiolysis on leaching of $\text{UO}_2$ in water

After a few hundred years storage, the radiation field in and around spent nuclear fuel will be almost entirely due to  $\alpha$ -emission of actinides. The radioactivity of the irradiated fuel available today is, in contrast, characterized by the strong  $\beta$ - and  $\gamma$ -contribution of fission products. In the unlikely event of failure of a container and water access to the repository, the dissolution behaviour of the  $\text{UO}_2$  matrix in contact with ground water could be enhanced by  $\alpha$ -radiolysis.

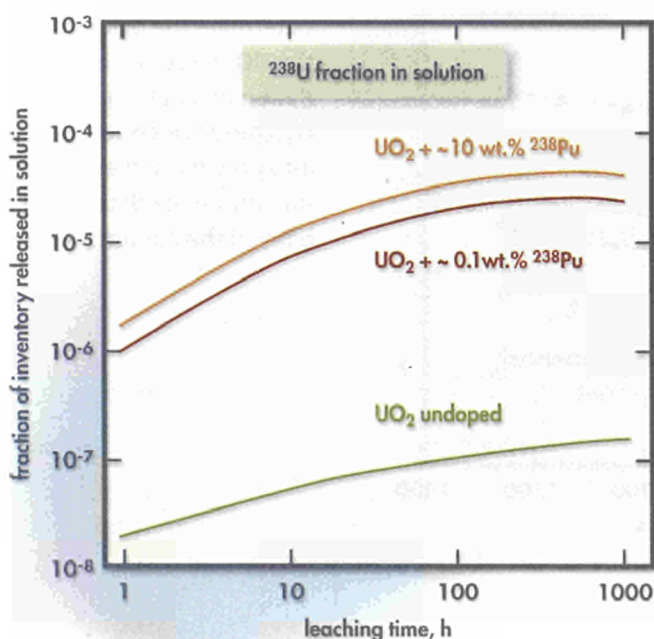
It is well known, that water radiolysis enhances fuel dissolution of spent  $\text{UO}_2$  fuel [1] but these results are not representative for storage times of a few hundred years, i.e. times beyond the guaranteed lifetime of the containers.

To study the effect of high  $\alpha$ -emission rates on fuel dissolution,  $\text{UO}_2$  with 10 or 0.1 w/o  $^{238}\text{PuO}_2$  was produced. Homoge-

neous pellets were achieved by using a sol-gel method to produce the starting material for pressing and sintering of the pellets.

First leach tests in demineralized water at room temperature and under anoxic conditions showed a significant radiolysis effect which must be due to  $\alpha$ -radiolysis because of the absence of any significant  $\beta$ -,  $\gamma$ -radiation field. Compared with  $\text{UO}_2$ , the  $^{238}\text{PuO}_2$  containing pellets showed leach rates of U higher by factors of up to  $10^2$  (see Fig. 1). The ratio of Pu/U in the leachate was higher than 0.1 indicating significant release of Pu in addition to increased bulk leaching rates.

These experiments will be continued to quantify the observed  $\alpha$ -radiolysis effect as a function of ground water composition and temperature as well as  $\alpha$ -decay rate of the specimens.



## Reference

- [1] S.Sunder, D.W. Shoesmith, H. Christensen and N.H. Miller, J. Nucl. Mater. 190 (1992) 79

Fig.1 Leaching of U from undoped  $\text{UO}_2$  is seen to be smaller by about a factor of 100 than leaching from  $\text{UO}_2$  doped with short-lived  $^{238}\text{PuO}_2$  causing  $\alpha$ -radiolysis in the water.

# Interaction of an oxidic corium melt with water: the puzzle of H<sub>2</sub>-production

An oxidic corium melt (80 wt% UO<sub>2</sub>, 20 wt% ZrO<sub>2</sub>) would, on first sight, not be expected to form hydrogen when interacting with water. However, noticeable amounts of hydrogen were found [1] in recent tests performed in the framework of the international FARO-LWR Research Programme, when batches of the above oxidic corium melt were poured by gravity into water. To solve this puzzle, debris from different locations of the test equipment and batches of the starting material were shipped from JRC Ispra to ITU.

These batches were analyzed in ITU with a variety of techniques in order to investigate the differences existing between the genuine UO<sub>2</sub>-ZrO<sub>2</sub> charge mixture, the re-solidified melt remaining in the furnace, the debris deposited in the melt release path before interacting with the water and the debris resulting from the interaction of the melt with the water.

The techniques applied were optical microscopy, scanning electron microscopy with EDX analyses, thermogravimetry, oxygen potential measurements, X-ray diffraction, Auger electron spectroscopy and Rutherford backscattering spectroscopy with 2 MeV He-ions.

The combined results show clearly

- all specimens are mixed (U,Zr)O<sub>2</sub>
- the melt is substoichiometric, the quenched material contains inclusions of U-metal (probably due to evaporation of UO<sub>3</sub> from the melt)
- due to the interaction with the water, the melt oxidizes from (U,Zr)O<sub>2-x</sub> to (U,Zr)O<sub>2+x</sub>
- the total amount of oxygen take-up from the water produces a large amount (~ 60 to 75 mol) of hydrogen, thus giving a well-founded explanation why the oxidic melt produces hydrogen
- as an additional result, the annealing tests performed to determine the oxidation state of the debris showed that the UO<sub>2</sub> structure is stabilized by the dissolved ZrO<sub>2</sub>: oxidation in air at e.g. 650 °C does not lead to formation of U<sub>3</sub>O<sub>8</sub> and does not cause disintegration of the fuel pieces into powder. Rather, the ZrO<sub>2</sub> stabilized the fluorite structure during oxidation and increased the mechanical stability of the corium pieces.

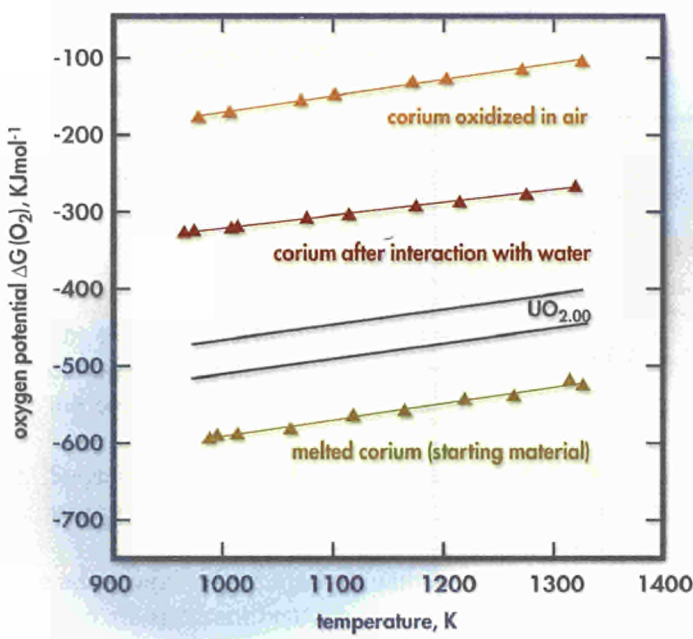


Fig. 1. Oxygen potential measurements of the melted starting material, of the corium after interaction with water and of the corium oxidized in air, compared with typical results for UO<sub>2</sub> (data band). The melted material is clearly substoichiometric, and the corium clearly oxidized due to the interaction with the water. These and the other above-mentioned measurements yielded the proof that ~ 60 to 75 mol H<sub>2</sub> were produced in the test, the debris of which was analyzed.

## Reference:

- [1] D. Magallon, A. Annunziato, FARO LWR Programme L-19 Test, Quick Look Report I.96.27 (1996)

# Partitioning of Minor Actinides from Genuine High Level Waste by Means of the DIAMEX process

Today many countries in the world investigate partitioning and transmutation as a promising nuclear waste management option. Transmutation of long-lived fission products and minor actinides in fast reactors or accelerator driven systems would considerably reduce the radiotoxicity of nuclear waste. The feasibility of transmutation depends, however, strongly on an effective partitioning process. The main goal is to recover the relevant radiotoxic elements from irradiated fuel materials with the highest possible efficiency. Several advanced liquid-liquid extraction processes were developed world-wide to achieve this goal in combination with the well-established PUREX process.

For the separation of minor actinides, one of the most promising is the French DIAMEX process, which uses diamides in an organic diluent as organic solvent. Besides the excellent extraction capabilities, the adaptation to the PUREX process is very easy. Furthermore the solvent is completely combustible and leaves no solid residue.

In 1998 a combined PUREX - DIAMEX process scheme was tested for the first time at ITU on genuine spent commercial

LWR fuel (see figure). The tests were carried out in a centrifugal extractor battery operated in a continuous counter-current mode. An efficient U and Pu separation with decontamination factors of  $10^5$  and  $10^3$  respectively was achieved in the PUREX part of the process. For the following minor actinides separation from the high level liquid waste effluent by the DIAMEX scheme, an optimised flow-sheet was used. An oxalic scrubbing step was included to prevent co-extraction of trouble-making fission products Mo and Zr.

The process showed an excellent compromise between very good extraction and even better back-extraction properties for Am and Cm. Thus, a recovery better than 99.8% for Am and Cm was achieved, i.e. the losses of these elements in the process are very low.

This is only the second hot verification of the process (the first outside France and also the first carried out with centrifugal extractors). The results were in all cases higher than those set as target values on the basis of French process code calculations [1].

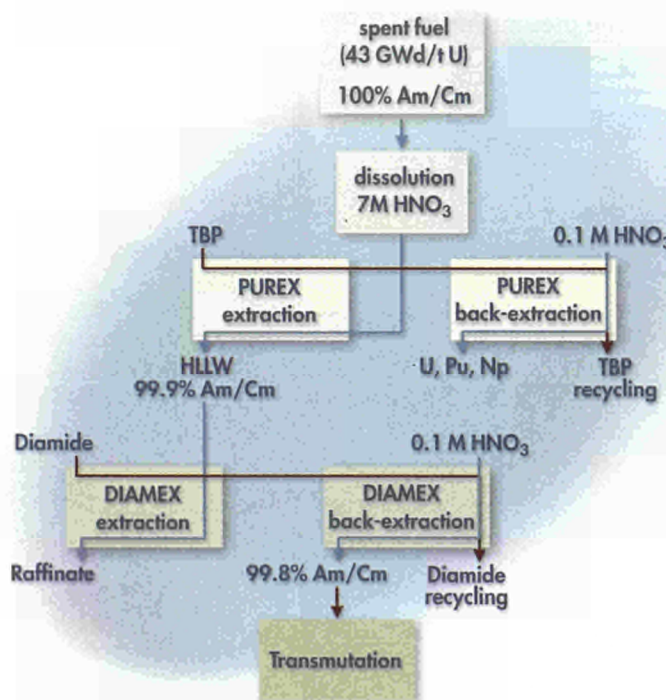


Fig. 1 Minor actinide partitioning scheme.

**Reference:**

[1] B. Dinh, B. Mauborgne, P. Baron, "Dynamic simulation of extraction operations: application in nuclear fuel reprocessing" ESCAPE 2, (1992), Toulouse, France.

# NUCLIDES 2000: An Electronic Chart of the Nuclides on Compact Disc

Radionuclides have many applications in agriculture, medicine, industry and research. For basic information on such radioactive materials, the *Chart of the Nuclides* has proved to be an indispensable tool for obtaining data on radionuclides and working out qualitatively decay schemes and reaction paths. These *Charts* are, however, of limited use when one requires quantitative information on the decaying nuclide and its daughters. In such cases one must further process the data to obtain, for example, the activities, gamma emission rate, dose rates, neutron emission rates, radiotoxicities, and isotopic powers.

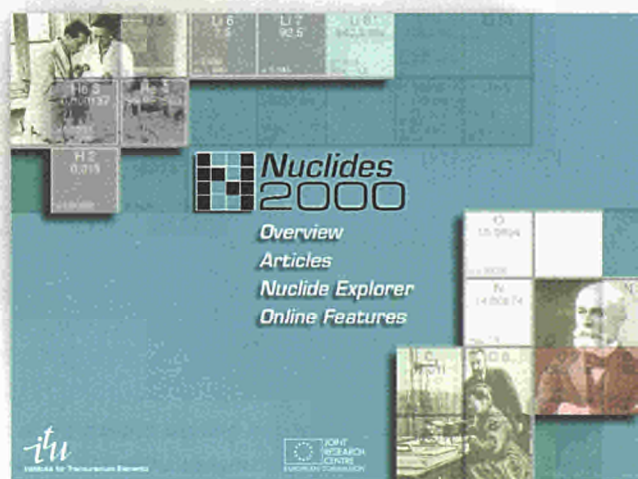
This was the motivation for the development of the NUCLIDES 2000 software package. Although information-processing tools have been available for many years within the Institute for such calculations, it was felt that there was a demand for an integrated and more user friendly software package for such calculations. Over the past year, a technology transfer support was provided by the EC DGXIII to develop such a package.

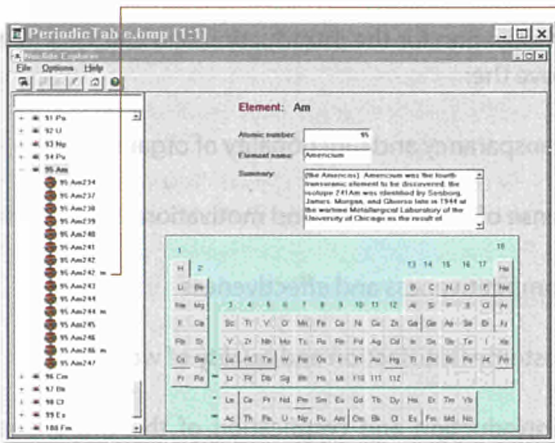
The radioactive decay data used in NUCLIDES 2000 is based on the Joint Evaluated File (JEF) version 2.2, with a few corrections for known inaccuracies in the file. The present version

of the program contains information on approximately 2700 radionuclides. A powerful navigational interface allows fast access to the nuclides through a periodic table, an isotope list box, and a Segre chart. A search facility is also available for searching the database for particular nuclides. The basic data provided consists of the type of decay (alpha,  $\beta^-$ ,  $\beta^+$ /EC, IT, n, p, etc.), half-life, decay energies (average and spectral), branching ratios, annual limits of intake for ingestion and inhalation etc. This basic data can be edited and appended and the changes are stored in a personal database. Derived data consists of activities, gamma dose rate, neutron emission rate, isotopic power etc. Through the decay engine, one can investigate the full decay scheme of any radionuclide to obtain the total activity, dose rate, etc. accounting for all the daughters starting from an initial mass or activity of the parent nuclide. An option to plot the results is also available. In addition an encyclopaedia of articles covering all aspects of radionuclides is included.

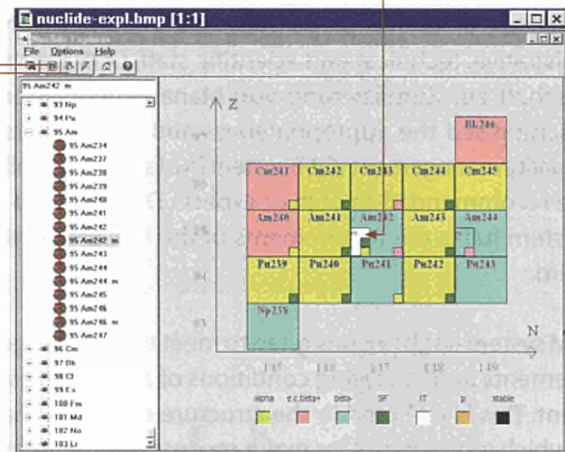
NUCLIDES 2000 will be available by Spring 1999 on CD for Windows 95, 98, NT operating systems. Further information can be obtained from the NUCLIDES 2000 website at:

[http://itumagill.fzk.de/NUCLIDES\\_2000/](http://itumagill.fzk.de/NUCLIDES_2000/)

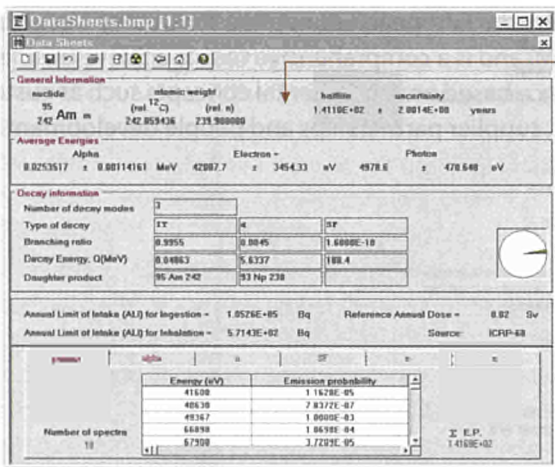




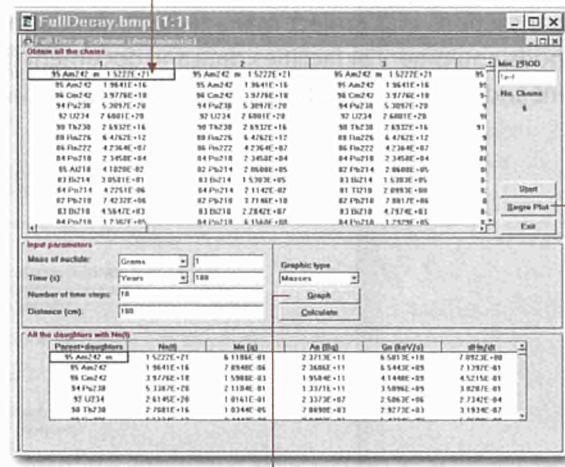
a) Powerful Navigational Interface: Select the element from the periodic table and the isotope list box shows all isotopes or use the direct input box (top left).



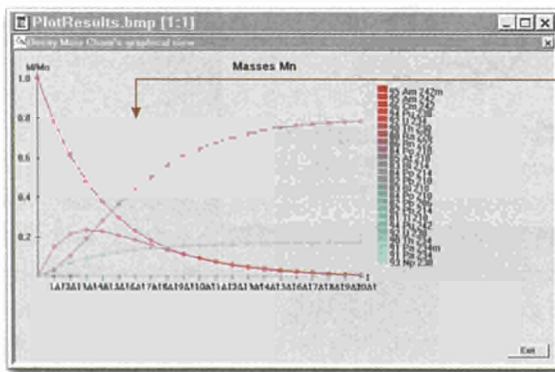
b) Select an isotope from the list box to obtain its position in the "Segre Chart". Colour schemes used to indicate the mode of decay (e.g. Karlsruhe, Strasbourg, user defined) can be changed in the options menu.



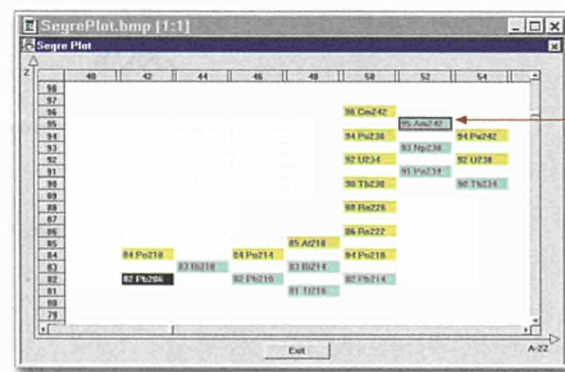
c) Data Sheets: Radioactive decay data on over 2700 nuclides based on the JEF 2.2 datafile. Sheets also contain derived data such as specific activity, isotopic power, neutron emission rate (from SF), specific gamma dose rate.



d) Full Decay Scheme: In the top window, all the possible decay chains are identified. In the centre window the input parameters are set. In the bottom window, the results of evaluating the Bateman solutions are given.



e) Plotting the Results: Following the calculations the results (masses, activities, gamma emission rate, gamma dose rate etc.) can be plotted.



f) Compacted Segre plot showing the decay of Am-242. For compactness, the number of protons Z, versus A-ZZ is plotted.

## ISO 9001 Certificate for ITU

After a phase of intense preparation and training, involving administrative, technical and scientific staff, DQS Deutsche Gesellschaft zur Zertifizierung von Managementsystemen mbH scrutinised the appropriateness and effectiveness of ITU's quality management (QM) system in March 1998. Following the recommendation of their experts, DQS certified that this system fulfils the requirements of the DIN EN ISO 9001 standard.

The QM system has been designed to meet the specific goals, requirements and operating conditions of a research establishment. This is reflected in the structure of the QM handbook, which is based on nine major processes rather than on the 20 elements of the norm.

These major processes are: management, staff development and training, purchasing, safety and radiation protection, order transactions and project management, development of methods, equipment or facilities, data and document management and general improvement procedures.

The motivation for the introduction of a QM system was to improve the:

- transparency and functionality of organisation
- sense of responsibility and motivation
- competitiveness and effectiveness
- customer satisfaction and quality of work.

The introduction and certification of the QM system has initiated a positive and dynamic development to strive for continuous improvement.

Steps have been initiated to enhance the QM system towards Total Quality Management. The model chosen has been created by the European Foundation for Quality Management (EFQM) and is a comprehensive tool to achieve business excellence based on fundamental concepts such as customer focus, supplier partnerships and people development.



# C E R T I F I C A T E

**DQS Deutsche Gesellschaft zur Zertifizierung  
von Managementsystemen mbH**  
Qualitäts- und Umweltgutachter

hereby certifies that the



**European Commission  
Directorate-General JRC  
Institute for Transuranium Elements  
(ITU)**



Gebäude Nr. 805  
Forschungszentrum Karlsruhe  
Hermann-von-Helmholtz-Platz Nr. 1  
D-76344 Eggenstein-Leopoldshafen

Contractual work regarding examination and production of nuclear fuels,  
radioactive material, samples as well as development and operation  
of laboratory and measurement equipment

has implemented and maintains a

**quality system.**

A quality audit, documented in an audit report, has verified  
that this quality system fulfills the requirements  
of the following standard:

**DIN EN ISO 9001**

issue August 1994

This certificate is valid until 2001-04-02

Certificate Registration No. 59429-01

Frankfurt am Main, Berlin 1998-04-03

Dr.-Ing. K. Petrick

MANAGING DIRECTORS

Dipl.-Ing. J. Pörsch



Offices: D-60433 Frankfurt am Main, August-Schanz-Straße 21  
D-10787 Berlin, Burggrafenstraße 6



The Certificate provided by DQS Deutsche Gesellschaft zur Zertifizierung von Managementsystemen mbH

L. Koch, I.L.F. Ray, M. Betti and A. Schubert

## 1. Introduction

Since the beginning of the 1990s, following the breakup of the Soviet Union, an increasing number of cases involving attempts to sell smuggled nuclear material has been detected. Some of the materials were sent to the Institute for investigation following requests from the government of the Federal Republic of Germany through the EURATOM Safeguards Directorate, ESD, Luxembourg. The primary objective of the analyses was to identify the material to determine its category with reference to the German "Atomgesetz" or "Kriegswaffenkontrollgesetz". The second priority was a request to characterize the material in view of establishing its intended use and possible origin.

As a result of these incidents, an International Technical Working Group (ITWG) on smuggled nuclear material was set up which had its first meeting at Karlsruhe in January/ February 1996. One of its first tasks was to make an inventory of the technical tools available at the time and the group submitted a report on the "status of international co-operation on nuclear smuggling forensic analysis" [1] to the P-8 meeting in Moscow on April 19-20, 1996. In this report nuclear materials were divided into the three categories defined in *Tab. 1*.

<b>Pu-239</b>	<b>higher than 90%</b>	<b>weapons grade</b>
<b>Pu-239, Pu-241</b>	<b>any concentration</b>	<b>weapons-utilisable</b>
<b>U-235</b>	<b>enrichment above 20%</b>	
<b>U-235</b>	<b>enrichment below 20%</b>	<b>non-weapons utilisable</b>

*Tab. 1 Nuclear materials divided into three categories following the status report in reference 1.*

The nuclear fuels used in electric power generating reactors, except for MOX fuel containing Pu, fall under the category of non weapons-utilisable material. When the seized material which has been investigated at ITU is categorized according to the criteria in *Tab. 1*, we see that most of it belongs to the category of nuclear fuels.

## 2. Methodology

In order to characterize material to the required extent a new methodology - nuclear forensics - had to be developed. The methodology followed the principle of diagnosis, i.e. the progressive steps of the investigation were guided by the results of the preceding steps, according to which the tools and techniques for the further investigation were selected.

The "toolbox" for this investigation consisted of existing techniques for determining the nuclide abundance and the isotopic composition of the elements (which are changed by exposure in nuclear reactors) and the material properties which are typical for such materials.

In order to extend the investigation to answer questions about the age of the material and the period that it was exposed under certain specific conditions, and to determine the local characteristic properties of the material which might lead to identification of its place of origin, it was soon recognized that new methods had to be developed and that a databank would be required to relate the results of the investigation to a particular time and place.

The standard analytical equipment already available in the Institute had to be modified to adapt it to the specific requirements of the material, especially for samples containing plutonium. Nuclide abundance can be obtained non-destructively by using pure Ge or Ge/Li gamma spectroscopy, a technique which can already be applied at the site of seizure or before the material is unpacked in the laboratory.

Because of its higher sensitivity and accuracy, mass spectrometry is applied: in the case of bulk materials Thermal Ionisation Mass Spectrometry (TIMS), and for identifying trace elements Inductively Coupled Plasma Mass Spectrometry (ICP-MS) and Glow Discharge Mass Spectrometry (GDMS).

In those cases where the sample itself is a powder, or particles are found on the surface of the material or on the packing, then Scanning Electron Microscopy (SEM) coupled with Energy Dispersive X-ray Analysis (EDX) and Secondary Ion Mass Spectrometry (SIMS) are the techniques chosen. SEM is used to determine the particle morphology and the types of component present, which can then be isotopically characterised by SIMS. If necessary, particles can be selected for further analysis by Transmission Electron Microscopy (TEM), giving a unique identification of the crystal structure by electron diffraction.

In those cases where the samples are in the form of pellets, the geometrical dimensions are of primary importance, followed by the microstructure determined by SEM and TEM, the composition by EDX and the crystal structure from x-ray or electron diffraction.

Examples will be given here of the applications of SEM/TEM and SIMS/GDMS in the investigation of vagabonding samples which have been sent to the Institute. Finally, the structure, content and use of the database will be discussed.

### 3. Electron Microscopy

Electron microscopy has established itself as a major technique in criminology and conventional forensic science over the last thirty years. However, in the specialised field of nuclear forensics the instruments have to be modified to meet the requirements for examining radioactive materials.

The Electron Microscopy Laboratory of the Institute possesses a Hitachi H 700 TEM, a Philips 515 SEM and a newly installed Philips XL 40 SEM; all the microscopes are equipped with Energy Dispersive X-ray Analysis facilities for the chemical analysis of the samples.

The Philips XL 40 SEM has the microscope column separated from the control console and mounted inside a glovebox so that it can be used for the examination of radioactive samples, and is being equipped with a "Gunshot Residues" software package for the automatic identification, analysis and location of particles of interest. A remotely controlled micromanipulator will enable the separation and retrieval of individual small particles down to a size of 1.0  $\mu\text{m}$  to be made, which can then be transferred to the TEM for electron diffraction analysis, or to a mass spectrometer for isotopic determination. This microscope is shown in *Fig. 1*.

The Hitachi H 700 TEM is also attached to a glovebox system for the handling and loading of radioactive samples [2,3], and is fitted with a scanning attachment (STEM). This microscope plays a special role in nuclear forensics, since there is a requirement in some cases for microstructural analysis (for example, to give information on the fabrication process) and for the crystallography of the sample to be determined by electron diffraction (for example, the phase determination for Pu metal).



*Fig. 1 The newly installed Philips XL 40 SEM with the microscope column separated from the control console and mounted inside a glovebox.*

#### 3.1 Information which can be obtained by Electron Microscopy

The information which can be obtained by electron microscopy (using a combination of SEM and TEM) on a powder sample can be summarised as follows:

1. Whether the sample consists of a single material, or is multicomponent, and whether the particles themselves are homogeneous on a microscopic scale. This is an essential prerequisite to an analysis by TIMS, GDMS and ICP-MS, since multicomponent samples must be separated out for individual analysis.
2. The morphology and size distributions of the different types of particle which are present in the sample, down to a particle size of 10 nm (SEM). Identification and location of particles of interest proceeds automatically using a back-scattered electron detector (BSE) tuned to the appropriate window of signal strengths.
3. High resolution information concerning the surface structure, porosity and grain size of the component particles (SEM; resolution < 3 nm), and high resolution information about the internal structure, lattice defects and porosity (TEM; resolution < 0.5 nm).
4. The overall chemical composition of the particles and the elemental distribution within individual particles (EDX; spatial resolution < 0.01  $\mu\text{m}$  in TEM, < 0.1  $\mu\text{m}$  in SEM).

5. The crystallographic structure of the components using electron diffraction in the TEM.

A combination of these techniques is usually sufficient to give a unique identification and characterization of the material under analysis, apart from the isotopic ratios of the different elements present, which can then be further analysed by SIMS or TIMS.

On bulk samples the same information on surface structure, composition, grain size and porosity can be obtained directly by SEM, but TEM analysis requires the preparation of a suitably thin sample from the bulk material.

#### 4. Secondary Ion Mass Spectrometry

Secondary ion mass spectrometry utilises a beam of primary ions directed at a sample to sputter off secondary ions from the sample surface. The secondary ions, having various initial velocities according to their mass/atomic number ( $m/z$ ) ratios, pass through a stigmatic-focusing mass spectrometer which focuses them to a single point according to the  $m/z$  ratios.

The SIMS apparatus in the Institute is a CAMECA IMS 6f, shown in Fig. 2. This instrument consists of a double-focusing mass spectrometer that allows fast switching between the masses. In addition, it has microfocus ion sources (caesium and duoplasmatron with oxygen or argon gas) that can be used either in the microscope or microprobe mode. Small particles of actinides and other elements can be identified and the isotopic composition determined. Using ion mapping, the elements associated with individual particles can also be determined.

##### 4.1 Information which can be obtained by SIMS

SIMS is at present the only technique [4] that makes it possible to perform ultrasensitive elemental and isotopic analysis in combination with sub-micrometer spatial resolution. Moreover, since the detection limits for all elements (with the exception of the noble gases which are hard to ionise), are around a few parts per billion, SIMS provides an extremely sensitive method for indicating the chemical composition of the sample. Statistically meaningful results can be obtained from a specimen containing as few as  $10^4$  atoms of the

element analysed. Its high sensitivity, along with the potential for investigating all solid samples and measuring secondary ions over a dynamic range greater than  $10^{10}$ , gives SIMS an unsurpassed capability for determining the compositions of samples as small as a few picograms.



Fig. 2 The Cameca IMS 6f SIMS used in the nuclear forensic analyses.

In view of these features SIMS was chosen for the isotopic analysis of single particles [5-7]. SIMS can be used both in microscope and microprobe modes. In both cases a high mass resolution, magnetic sector mass spectrometer, with ion-counting detection is employed. A resolution up to 10,000 can be achieved. With each mode mass resolved images can be acquired as the primary beam erodes the specimen surface. The resulting three-dimensional analysis provides a complete record of the chemical composition of the sample and isotopic variations, with simultaneous lateral resolution. This unique capability is particularly effective in analysing the chemically heterogeneous materials often encountered as forensic specimens.

The ion microscope mode employs a defocused primary ion beam (diameter greater than  $100\ \mu\text{m}$ ). A real image of the sample surface in mass-separated secondary ions is obtained. The result is a mapping of trace-element and isotopic distribution over the entire field of view with a spatial resolution of about  $1\ \mu\text{m}$ .

The ion microprobe mode uses a finely focused primary ion beam, typically with a diameter of 1 to  $10\ \mu\text{m}$ , to sputter a small region of the sample. Secondary ion images can be produced by rastering the primary beam over the specimen. The lateral resolution is determined by the primary beam diameter, and can approach  $0.2\ \mu\text{m}$ .

The instrument is equipped with a resistive anode encoder (RAE) used for the mapping of the entire sample surface

## 5. Glow Discharge Mass Spectrometry

Glow discharge (GD) sources have a long history in analytical chemistry, principally as sources for optical emission spectrometry. More recently GD sources have been coupled with mass spectrometry (GDMS) and the combination of these two established methods has led to a new technique for the analysis of solid samples being available to the analytical chemist.

In 1992 a GDMS was installed in a glove-box at the Institute for the handling of nuclear material and this is still the only installation of its kind in the world [8]. The mass spectrometer used is a VG 9000 GDMS instrument. It consists of a dc GD ion source coupled to a double-focusing mass spectrometer of reverse (Nier-Johnson) geometry. This configuration provides a high transmission (> 75%) and sensitivity whilst operating at a mass resolution of 5000 with 10% valley definition.

### 5.1 Information which can be obtained by GDMS

The advantage of MS over conventional optical emission spectrometry techniques lies in the increased sensitivity obtained by direct sampling of the ions, and a much simpler spectrum which makes the determination of a wider range of elements possible. This is accompanied by much simpler elemental quantification. Plasma sources coupled with mass spectrometers have thus considerably extended both elemental coverage and detection limits in quantitative trace element analysis. This is both true of GDMS and the inductively coupled plasma ICP-MS techniques.

The GDMS is an analytical tool which is ideally suited for the analysis of solid samples of nuclear origin, requiring minimum chemical treatment of the samples [9]. The elemental and isotopic identification capabilities can be fully applied to materials having non-natural isotopes and/or non-natural isotopic abundances [10]. Other advantages of GDMS are:

1. all elements can be determined, except hydrogen,

2. the dynamic range over 11 orders of magnitude of the detector allows the determination of both major components and trace constituents within the same analytical cycle,
3. decoupling of the atomisation and ionisation process gives place to matrix effects to a very low extent.

The GDMS technique is capable of detecting and measuring trace constituents in a sample at the ng/kg level.

## 6. Some Recent Investigations of Smuggled Nuclear Materials

### 6.1 Case 1: A Mixed Powder Sample Containing Plutonium and Uranium

A specimen of powder from an illicit sample seized by the German authorities was analysed by a combination of SEM and TEM

The SEM analysis showed that this was not a homogeneous powder sample, but was a mixture of three distinct components characterised by their morphology and chemical composition, and an example of a secondary electron image recorded on this sample is shown in Fig. 3.

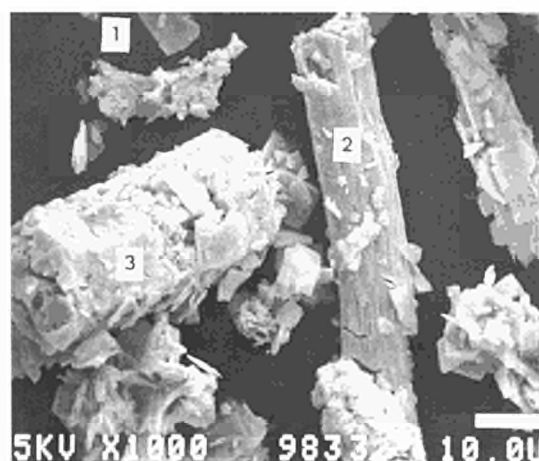


Fig. 3 An SEM micrograph of the powder showing the three separate components which could be identified in the sample.

In this image the different components can be identified as follows:

- Component 1:  $\text{PuO}_2$  platelets with an average size of  $3.4 \mu\text{m}$ , containing U as a minor component with about 9 w/o content, forming the largest fraction of the mixture analysed. These were identified by EDX and the structure confirmed uniquely by electron diffraction in the TEM. An example of this component is shown in Fig. 4.
- Component 2:  $\text{PuO}_2$  particles with a rod-shaped form with an average diameter of  $9 \mu\text{m}$  and length of  $25 - 75 \mu\text{m}$ , forming about 5% of the total, identified by EDX and confirmed by electron diffraction in the TEM.
- Component 3: Uranium oxide particles with a strongly characteristic and constant morphology, being hexagonal in cross section with a  $12 \mu\text{m}$  side and an average length of  $50 \mu\text{m}$ . This component was identified by electron diffraction to consist of  $\text{U}_3\text{O}_8$ . A secondary electron micrograph showing this highly characteristic form is reproduced in Fig. 5.

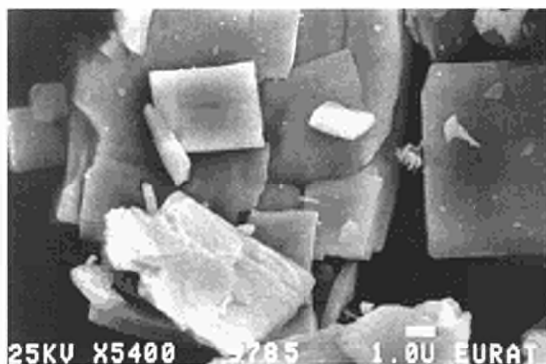


Fig. 4 SEM micrograph of component 1 of the sample consisting of small, thin platelets of  $\text{PuO}_2$ .

Each of these components was also examined by TEM, and the  $\text{PuO}_2$  components showed microstructural differences which reflect the manner in which they were prepared. Fig. 6 shows a high resolution transmission electron micrograph of one of the platelets forming component 1, showing that the  $\text{PuO}_2$  grain size is very small, with an average value of  $12.7 \text{ nm}$ . The diffraction pattern from this area is shown inset, and indexes to  $\text{PuO}_2$ . This extremely fine grain structure of the  $\text{PuO}_2$  platelets observed by TEM is a very significant re-

sult in assessing the possible origin of the material, since it provides information on the process used to produce the platelets. This platelet morphology is typical of  $\text{PuO}_2$  which has been prepared by precipitation as oxalate, followed by calcination to the oxide.

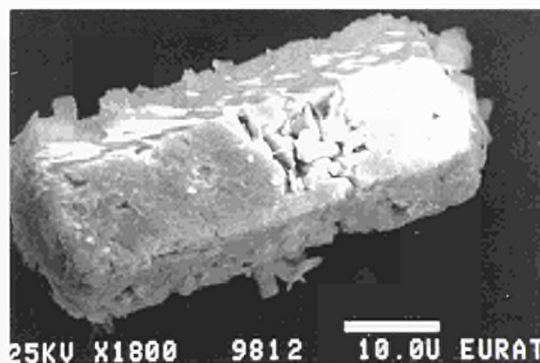


Fig. 5 SEM micrograph of component 3 of the sample consisting of particles of  $\text{U}_3\text{O}_8$  with a characteristic form.

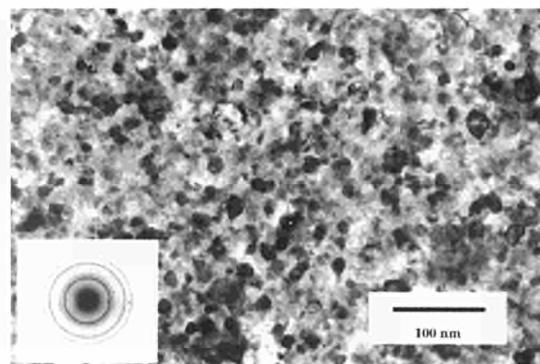


Fig. 6 TEM micrograph of one of the  $\text{PuO}_2$  platelets forming component 1, indicating the very fine grain structure.

The microstructure of the other form of  $\text{PuO}_2$  designated component 2 is, however, quite different, as shown in the transmission electron micrograph reproduced in Fig. 7. In this case the average grain size of  $0.29 \mu\text{m}$  is much larger, and the grains are relatively defect free, indicating that the conversion to oxide has probably been performed at a higher temperature than for component 1. The electron diffraction pattern is shown inset, and indexes to  $\text{PuO}_2$ .

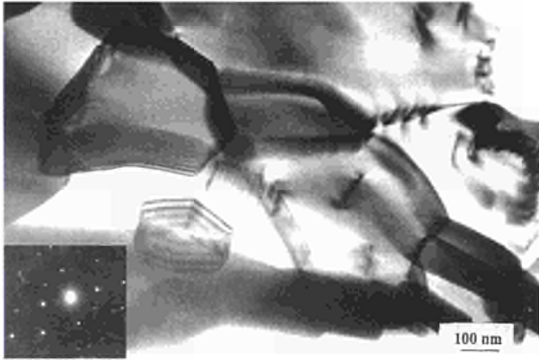


Fig. 7 TEM micrograph of the  $\text{PuO}_2$  rods forming component 2, which has a very much larger grain structure.

A rather crude but nevertheless effective method was used to separate out the individual components for analysis by TIMS, using a micromanipulator in a glovebox under a stereo microscope. This is now being superseded by the installation of a micromanipulator in the specimen chamber of the Philips XL 40 SEM which will enable the direct extraction of micron-sized particles to be made under SEM observation.

## 6.2 The Analysis of a Powder Sample containing Weapons-grade Plutonium Metal

A specimen of Pu metal, mixed with various other substances containing Hg, Sb and I, was investigated using TEM, SEM and GDMS. The metal had been shown by TIMS to consist of 99.8% isotopically pure  $^{239}\text{Pu}$ , containing a small amount of Ga.

Fig. 8 is a low magnification optical stereo micrograph of the sample in which it can be seen to consist of several components, including globules of metallic Hg. The large grey particles are Pu metal, showing light surface oxidation.

Fig. 9 reproduces a TEM micrograph of the Pu metal, revealing a very small grain size ranging from 25 nm to 0.25  $\mu\text{m}$ . The microstructure was homogeneous and free from lattice defects.

Electron diffraction of the sample supported on a gold calibration film indicated that the material was  $\delta$  - phase Pu metal. Faint rings superimposed on the patterns arose from surface oxidation of the particle, and indexed to  $\text{PuO}_2$ .

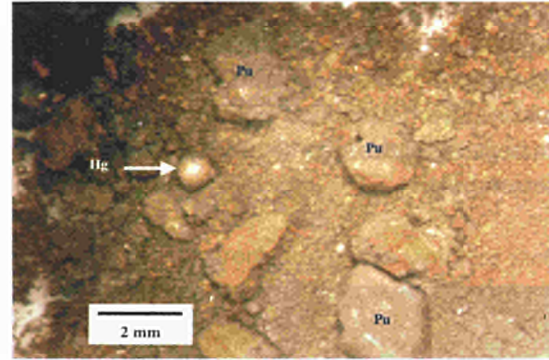


Fig. 8 An optical stereo-micrograph of the powder sample showing globules of metallic Hg, particles of metallic  $^{239}\text{Pu}$ , mixed with other components.

The rest of the powder consisted of a mixture of three other compounds, and apart from Pu and Hg in metallic form, these could be characterised and identified by a combination of EDX and electron diffraction in the TEM.

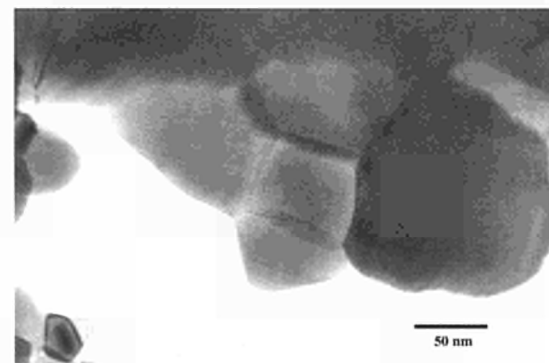


Fig. 9 TEM micrograph showing the fine-grained structure of the weapons-grade  $^{239}\text{Pu}$  metal.

The following components were found:

1. A fibrous compound containing Pu and Sb in the constant ratio  $\text{Pu}:\text{Sb} = 4:1$  (a/o). An example of this fibrous material, which formed a large proportion of the sample, is shown in Fig. 10.
2. A component in the form of small particles which were very sensitive to the electron beam, and which contained Hg and I in the constant ratio  $\text{Hg}:\text{I} = 1:1$  (a/o). This could be identified directly as the compound  $\text{Hg}_2\text{I}_2$ .

- A third component containing all three of the elements Hg, Sb and I, but no Pu, in the ratio Sb:Hg:I = 2:4:1 (a/o). This component may be a mixture of oxides, but this could not be determined uniquely by electron diffraction because of the high instability of the material in the electron beam.

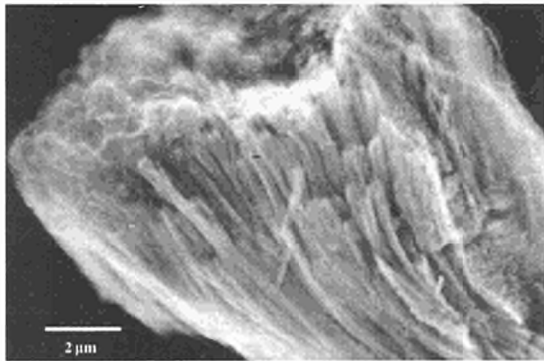


Fig. 10 SEM micrograph of the fibrous component containing Pu and Sb which was found in the sample.

The examination by GDMS was performed on a sample of the powder compacted into a disc with a diameter of 6 mm. During the compaction of the disc it was observed that metallic mercury squeezed out, consequently, no reliable results for mercury could be obtained by GDMS. No chemical treatment of the sample was performed, only a pre-sputtering before the analytical measurement.

The major components of the sample were determined to be O, Ga, Sb, Hg, and Pu and these were measured using the Faraday cup detector. The ratio of Ga to Pu was 0.0144. In Fig. 11 an example of the acquisition of the elements determined quantitatively by GDMS is given.

Six independent runs for the quantitative determination of the elements found were performed. From the results obtained by GDMS and Inductively Coupled Plasma Mass Spectrometry (ICPMS) the following stoichiometric relationship between antimony, mercury and oxygen, Sb: Hg: O = 2: 6: 8 was calculated. From this analysis it could be concluded that the powder sample consisted mostly of a component with an overall formula of  $Hg_2Sb_2O_7$  to which  $Hg_2O_2$  had been added. The latter had partially reacted with metallic Pu-powder. The presence of Ga in this concentration and a  $^{239}Pu$  of 99.8% pointed to  $\delta$ -stabilized Pu-alloy which is high-grade weapons plutonium.

### 6.3 An Investigation by SIMS and SEM of a Sample Containing Highly Enriched Uranium Particles

Swipe tests following the standard IAEA and Euratom techniques used for particle collection [11] were taken from the inner surfaces of two empty stainless steel containers which were suspected of having been used to store radioactive material. The swipe tests revealed radioactivity and were then treated in the Institute laboratories for the recovery of particles and their subsequent analysis by SIMS and SEM.

After the introduction of the samples into the SIMS source a positively charged oxygen beam was used to sputter secondary ions from the sample surface. The microscope mode was used to obtain the images of the uranium isotopes. Once the image was obtained a computer programme, developed in the Institute, was used for the initial evaluation to estimate the isotopic ratios from the intensity of the images obtained for the different isotopes. For a more specific analysis, the ion beam was focused on individual particles and the

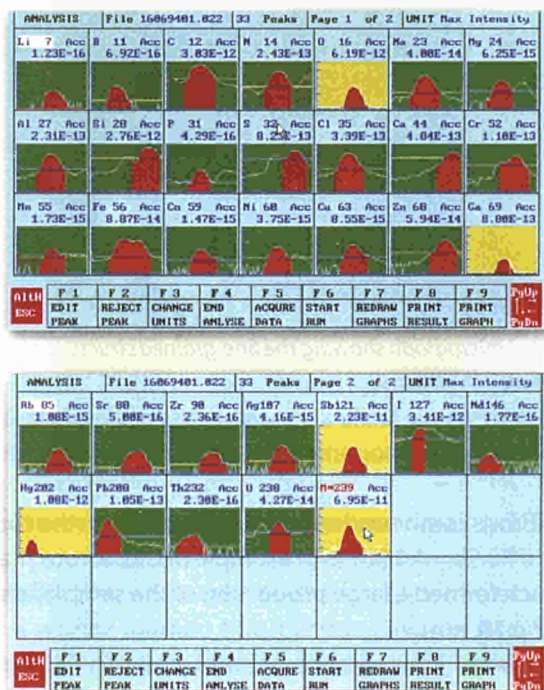


Fig. 11 GDMS acquisition for the quantitative determination of the chemical composition of the sample.

acquisition for the determination of the isotopic ratios was performed. The enrichment of the particles was determined by focusing the primary ion beam onto the particles and acquiring the uranium isotopes (234, 235, 236 and 238) using a method described elsewhere [5]. Using this method an accuracy and precision of 0.5% for the ratio 235/238 and 2.0% for the ratio 234/238 can be obtained. The size of each particle detected was estimated from its image and values between 2  $\mu\text{m}$  and 10  $\mu\text{m}$  were found.

The particles characterised by SIMS consisted of  $\text{UO}_2$  enriched up to 90% in U-235, and fluorine was not detected. The analysis of trace elements in the particles was also performed by SIMS. The results revealed light elements (such as C, Na, Mg, Al, Si, K, Ca, Cr and Fe) characteristic of the pyrochemical process for the production of  $\text{UO}_2$ .

The swipe tests were examined by SEM and EDX to identify the individual particles for characterization. The direct analysis of the swipe test was complicated by the open fibrous structure of the material, which required a fairly thick coating of Au to prevent surface charging. An alternative method was developed in which a small piece of conducting adhesive tape was used to collect and concentrate the particles from the swipe material, and this could be directly analysed by SEM without coating.

Small particles containing uranium were identified by EDX in the size range 2.5  $\mu\text{m}$  to 9  $\mu\text{m}$ , and from the morphology of the particles it was possible to identify them as  $\text{UO}_2$ . An example of such a particle is shown in the SEM image in Fig. 12.

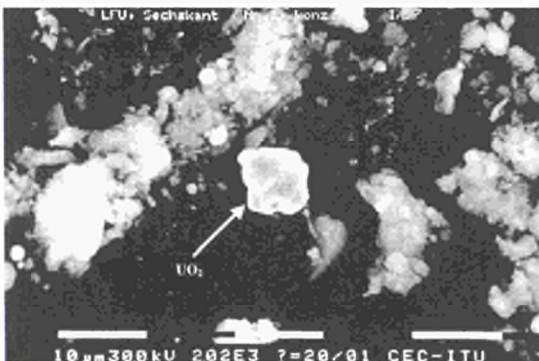


Fig. 12 SEM micrograph of a small particle of highly enriched  $\text{UO}_2$  recovered from a swipe test taken on a suspect steel container.

When this examination was performed it was necessary to analyse each suspect particle by hand in the SEM which involved large expenditure of time. The BSE imaging facilities combined with the computer control of the digital stage on the Philips XL40 SEM will enable automatic analysis of such samples to be made very rapidly.

A small metal strip cut from one of the stainless steel containers was also examined by EDX in the SEM, and revealed that the containers were made of a titanium-stabilised stainless steel, with the approximate composition Fe:Cr:Ni:Ti = 71:20:8:0.5 (w/o).

## 7. The Nuclear Materials Databank

For supporting the analysis of nuclear materials of unknown origin, ITU Karlsruhe has developed a relational database system containing characteristic parameters of nuclear fuels used for power as well as research reactors. In order to cover material of both West and East European origin this development has been made in close co-operation with the Bochvar All-Russia Research Institute for Inorganic Materials (VNIINM) in Moscow.

The main structure of the system (implemented in an ORACLE™ environment) has been described in previous ITU annual reports (TUAR-96, p. 22 and 135-136, TUAR-97, p. 113). It provides the backbone for conceiving a retrieval algorithm based on the principle of diagnosis. Starting from basic parameters, such as macroscopic geometry and main element composition of the sample, the potential origin of the material can be progressively narrowed by measuring case-specific impurity and microstructural parameters. This approach represents an iterative exclusion procedure which is complemented by the subsequent attribution of relative probabilities as illustrated in Fig. 13.

The iterative exclusion algorithm was used as concept for the retrieval software NucSearch developed at ITU in 1998 which is interfaced with the relational database system. NucSearch allows the user to perform a step-by-step narrowing of the potential origin of a nuclear material and guides him to the most relevant analytical parameters to be measured [12].

The operation of the retrieval system can be demonstrated using the example of the identification of the production

plant for a batch of nuclear fuel pellets seized as vagabonding material in 1996. In a 24-hour express analysis the following analytical results were obtained in the Institute:

Content of  $^{235}\text{U}$ :  $4.398 \pm 0.002$  w/o  
 Diameter:  $7.55 \pm 0.05$  mm  
 Annular Diameter:  $2.43 \pm 0.05$  mm

From the first query to the macroscopic section of the database, a list of 34 different combinations for the vector of origin and intended use could be compiled, [13]. As an additional result the retrieval system informs the user that in this case impurity specifications cannot support further distinction between the two potential fuel suppliers in Elektrostal, Russia (MZ) and Ust-Kamenogorsk, Kazakhstan (UMP), respectively. Real ranges of impurity levels, however, do allow for a more detailed probability attribution.

Because of their commercial sensitivity, such plant-specific reference data are stored in separate sectors of the database system being developed at both VNIINM and ITU. These parts contain sensitive data not accessible to the partner institute. However, a qualitative description can be given because, in the context of a bilateral agreement on confidentiality, both institutes can issue query requests to each other's separate sector.

The elements F, Cl, N, Fe, Cr and Al are the most characteristic for distinguishing powder and pellet material stemming either from the UMP or the MZ production plant. In addition, impurity levels encountered in material from these facilities differ significantly from those of analogous production plants located in Western Europe.

The information so far stored in this databank is obtained under confidentiality agreements. Nevertheless, ITU and VNIINM are prepared to conduct searches for specific cases from the outside and would provide - if it is within the scope of the present data file - information on material in question.

A set of data obtained from the first series of impurity measurements by ICP-MS is shown in Tab.2. As expected, all measured impurities are in accordance with the specification limits of both facilities. However, by comparison with real impurity ranges of Al and Cr, the corresponding analytical results indicate a high exclusion probability for the MZ origin and a significantly higher relative probability for UMP compared with MZ.

Element	Concentration (ppm)
Mg	5.0
Al	18
Cr	19
Mn	8.1
Fe	73
Ni	26
Sr	0.5
Ba	167

Tab.2 Impurities measured by ICP-MS in the case used as an example.

The remaining elements measured do not assist in the identification. On the other hand, the database query at VNIINM stated that in this specific case more detailed data on the impurity concentrations of N, C, F, and Cl will allow further conclusions to be drawn. Corresponding measurements are underway, making use of ITU's GDMS. On the basis of such results further conclusions concerning the production period of the seized nuclear materials are also expected.

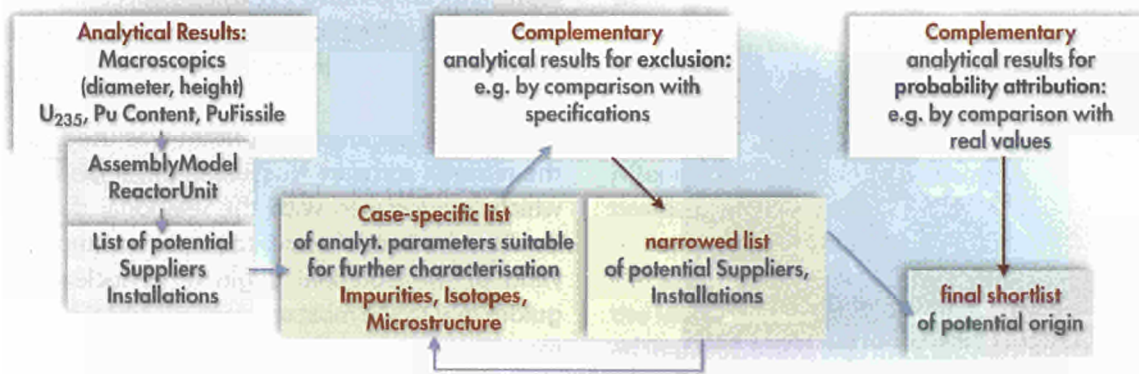


Fig. 13 Basic algorithm for material identification used as the concept for the retrieval system NucSearch.

## 8. The Outlook for the Future

Nuclear forensics is a new field which has only developed, out of urgent necessity, over the last five years. The Institute was in the fortunate position of having many of the necessary analytical techniques already available for handling the seized radioactive materials and was thus able to take an early lead in the investigations and establish a reputation in the field.

These techniques have now been optimised for the investigation of any more cases which may come to light in the future.

Future developments will concentrate on the following areas:

1. Sample geolocation. This involves tracing the source of a sample and the route which it has taken, and a combination of nuclear forensic techniques and conventional forensic science is being developed. The nuclear techniques involve the identification of traces specific to particular locations such as the measurement of oxygen isotopes by SIMS, and gas chromatography for gaseous fission products and characteristic process-related organics substances.

Conventional forensic science techniques involving the examination of samples and packaging materials for dust, fibres and other environmental traces will also be used. Of particular interest is the potential application of the analysis of pollen and other biological materials by SEM and mass spectrometry.

2. Sample age. SIMS techniques are being developed to date samples of material by measuring the U and Pu isotopic ratios, and the presence of daughter products. On bulk samples this analysis will be performed by TIMS.
3. Classic forensics. The potential benefits to classical forensic science from applying the new analytical techniques available from nuclear forensics is being investigated. This will lead to possible spin-off applications in environmental studies such as the detection of trace elements in pollen using highly sensitive mass spectrometry techniques.
4. Based upon historical data resulting from the database, current techniques are being appropriately modified where necessary for the investigation of old samples.

The development of these techniques coupled with the enlargement of the scope and application of the database will assure that the Institute will play a key role in the future of nuclear forensics.

### References

- [1] Status of International Co-operation on Nuclear Smuggling Forensic Analysis - A report on recent international progress for enhancing nuclear forensic capabilities for cases of illicit nuclear materials, L. Koch, S. Niemeyer, March 20, 1996.
- [2] I. Ray, H. Thiele, "Hot Laboratories and Remote Handling" Working Group, Karlsruhe (1981).
- [3] I.L.F. Ray, H. Thiele, H. Blank, J., 10th Int. congress on X-Ray Optics and Microanalysis, ICXOM-10, 5-9 Sept. 1983, Toulouse, France. Proceedings, *J. de Physique* 45 (1984), C2, 849-851.
- [4] A. Benninghoven, F.G. Rüdener, H.W. Werner, Secondary Ion Mass Spectrometry, Wiley, New York, 1997. ISBN 0-471-95897.
- [5] G. Tamborini, M. Betti, V. Forcina, T. Hiernaut, B. Giovannone, L. Koch, *Spectrochimica Acta B* 53 (1998), 1289-1302.
- [6] M. Betti, Mass spectrometric techniques applied for the determination of radionuclides traces, Proc. Int. Workshop on the status of measurements techniques for the identification of Nuclear Signatures, 25-27 February, Geel (Belgium). EUR 17312 EN.
- [7] M. Betti, G. Tamborini, V. Forcina, T. Hiernaut, L. Koch, Identification of nuclear activities by the characterization of single microparticles, in: Proc. Inter. Symp. on International Safeguards, IAEA, Vienna, 13-17 October 1997.
- [8] M. Betti, G. Rasmussen, T. Hiernaut, L. Koch, D.M.P. Milton, R.C. Hutton, *J. Analytical Atomic Spectrometry*, 9 (1994), 385-391.
- [9] M. Betti, *Analytical Atomic Spectrometry*, 11 (1996), 855-860.
- [10] M. Betti, G. Rasmussen, L. Koch, *Fresenius' J. Analytical Chemistry*, 355 (1996), 808-812.
- [11] J. N. Cooley, E. Kuhn and D.L. Donohue, "Current status of the environmental sampling for IAEA Safeguards", Proc. 19th Annual ESARDA Symposium of Safeguards and Nuclear Material Management, Montpellier, 1997. EUR 17665.
- [12] A. Schubert, G. Janssen, L. Koch, P. Peerani, Yu.K. Bibilashvili, N.A. Chorokhov, Yu.N. Dolgov, A Software Package for Nuclear Analysis Guidance by a Relational Database, Proceedings of the ANS International Conference on the Physics of Nuclear Science and Technology, Long Island, New York, October 5-8 (1998), 1385-139.
- [13] Yu. Dolgov, Yu. Bibilashvili, N. Chorokhov, L. Koch, R. Schenkel, A. Schubert, Case Studies with a Relational Database for Identification of Nuclear Material of Unknown Origin. Russian International Conference on Nuclear Material Protection, Control and Accounting, Obninsk (Russia), March 9-14, 1997, proceedings, pp.116-120.

## Meeting Point ITU

Interest in ITU and its activities remained at a high level. The number of visitors to the Institute reached last year's score with ITU's geographical sphere of influence widened. 80% of the 30 major meetings convened long-standing co-operation partners in industry, research laboratories, universities, regulatory authorities, other Commission DGs. Research issues were discussed, existing co-operation agreements assessed, and new fields for collaboration fathomed. A 20% share went into consolidating ties with Russian partners and creating new contacts with Swedish, Finnish, Argentinean, Brazilian, and South Korean institutions. Topical subjects dealt with in workshops were analytical methods in nuclear forensics, high performance trace analysis, partitioning and transmutation, and waste minimisation.

## Training Centre ITU

In-house experience and know-how were passed on to 60 specialists in ITU training courses. These centred around nuclear safety subjects such as fuel behaviour (TRANSURANUS code for seven East European countries, in co-operation with IAEA); running the newly installed safeguards laboratories in Moscow (1-month hands-on training for eleven Russian scientists at ITU); new analytical techniques (High Performance Trace Analysis and Environmental Sampling for Euratom, IAEA and ABACC inspectors).

## Window on ITU

"Au service du citoyen européen: le CCR", the one-week exhibition at the European Parliament in Strasbourg, was the plat-

form for illustrating ITU contributions to non-proliferation (detecting clandestine nuclear activities) and to fighting cancer (alpha-immuno therapy).

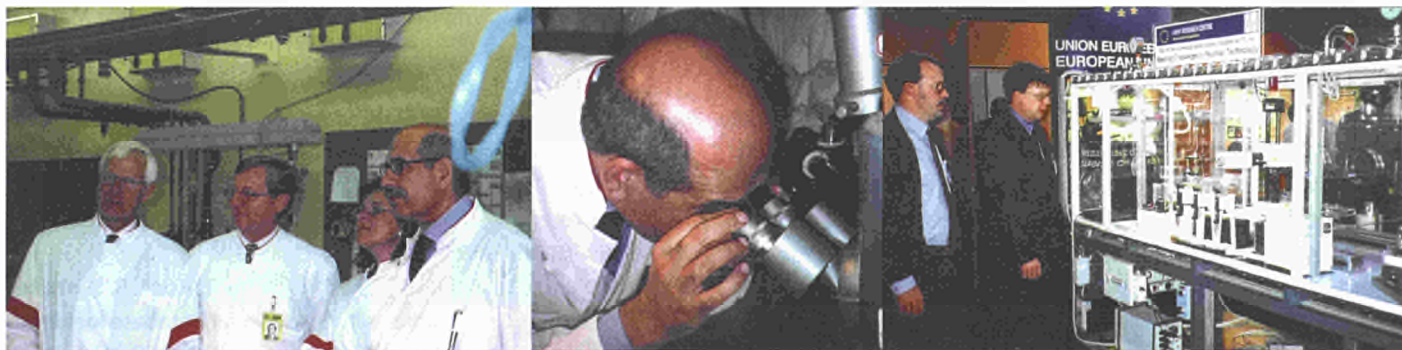
Examples of ITU's technological capabilities (robotised analyses, fabrication of fuel rods and pellets, filling of capsules inside glove boxes; hot cell facilities and Minor Actinide laboratory) attracted numerous visitors during the 4-day "International Nuclear Energy Congress and World Exhibition" in Nice (France).

ITU and its work were quoted in newspapers, magazines, and speeches. The Alpha-Immunotherapy project continued to be in the fore of public attention. Articles appeared in "Einblick", the journal of Deutsches Krebsforschungszentrum, "Deutsches Ärzteblatt", and "Le Quotidien du Médecin". In her address to the participants in the "Congrès international des traitements anticancéreux" in Paris, Commissioner Edith Cresson gave credit to the ITU research.

ITU safeguards work featured in an article of "Nuclear Europe". Methods for detecting illicit trafficking of nuclear materials created an interest with RAIUNO's "Giorni d'Europa" and "SuperQuark" TV magazines.

Details on ITU's certification according to ISO 9001 were posted on the JRC, ITU, and Cordis web sites. Also ITU's role in KEIM (Karlsruher Existenzgründer Impuls), the German innovation project, was announced, leading to requests for information and collaborations.

A new ITU brochure was published in 1998 and is available on request.



Explaining ITU installations to visitors: (from left to right) Professor M. Popp, Chairman of the Board, Forschungszentrum Karlsruhe, Professor J. van Geel, ITU, Mrs. and Dr. M. ElBaradei, IAEA. – Dr. M. ElBaradei, IAEA Director-General, taking a close look through an ITU electron microscope at seized plutonium. – ITU presenting its technological capabilities at the NEC '98 International Congress and World Exhibition in Nice (F).

# Organisation Chart of the Institute



# Publications, PhD's, and Patents

## Informing scientific circles and customers

Annex I of part B of this report lists the publications, which were printed in refereed journals or books. Also details on contributions made at various conferences can be found there.

In addition to the general descriptions presented to the public at exhibitions such as the ones mentioned above, numerous more specialised posters illustrated new scientific findings at conferences.

Previous publications of the Institute can be retrieved from the database "Publications" of the Community Research and Development Information Service (CORDIS) located in Luxembourg: <http://www.cordis.lu/>

Direct access to the CORDIS Publications Form: Query Advanced Search: [http://apollo.cordis.lu/cordis/en\\_public\\_search.html](http://apollo.cordis.lu/cordis/en_public_search.html)

A printed version is provided by the Publications Bulletin, published annually by the Public Relations and Publications Unit of the JRC Ispra (Italy).

More information on the Institute can be found in the sections *Guided Tour/ITU* and *Contacts/ITU* on the Web page of the JRC: <http://www.jrc.org/>

Link to the local URL of the Institute: <http://itumagill.fzk.de>

## Three doctoral grantees from the Institute have obtained their PhD

*L. C. de J. Pereira Waerenborgh*

"Compostos Intermetálicos da Família An<sub>2</sub>T<sub>2</sub>X, An = U, Np, Pu e Am, T = Metal de Transição dos Grupos 8 a 12, X = In e Sn Universidade de Lisboa, Dezembro de 1997.

*J. Cobos Sabate*

"Simulación de combustible nuclear de grado de quemado muy alto. Fabricación, caracterización y comportamiento a la oxidación".

Universidad Complutense de Madrid, Noviembre 1998.

*G. Tamborini*

"Développement de la technique SIMS pour l'analyse de particules et ses applications à différent échantillons".

Université Paris Sud – Orsay, Décembre 1998.

## Application for patents in 1998

(inventor names in alphabetical order)

*J.-P. Glatz, W. Janssens, L. Koch, K. Niemax, B. Ocker*

Verfahren und Vorrichtung zur isotopenselektiven Messung chemischer Elemente in Materialien.

LU 2553 (90296 • 7.10.1998).

*G. Dockendorf, H. Ottmar*

Sample changer for transferring radioactive samples between a hot cell and a measuring apparatus.

LU 2585 (90270 • 5.8.1998).

*C. Apostolidis, W. Janssens, L. Koch, J. McGinley, J. Möllenbeck, R. Molinet, M. Ougier, H. Schweickert, J. van Geel*

Method for producing Ac-225 by irradiation of Ra-226 with protons.

EP 2588 (98109983.1 • 2.6.1998).

*C. Apostolidis, B. Brandalise, W. Janssens, L. Koch, R. Molinet, J. van Geel*

Method and apparatus for preparing Bi-213 for human therapeutic use.

EP 2596 (98111442.4 • 22.6.1998).

## Patents granted in 1998

(inventor names in alphabetical order)

*R. Beukers, W. Heinz, J.-P. Hiernaut, C. Ronchi, R. Selfslag*

Pirometro multi-comprimentos de onda.

95405 • 27.03.1998 • Country PT.

*D. Baron, M. Coquerelle, J. Spino, P. Werner*

Vorrichtung zur Materialprüfung mit einem Mikrostempel.

88821 • 01.04.1998 • Country LU.

*J. Fuger, L. Koch, J. van Geel*

Processo para a recuperação de actínio-225 e bismuto-213.

96843 • 13.04.1998 • Country PT.

*J. Magill, P. Werner*

Machine for separating aerosol particles.

5827350 • 27.10.1998 • Country WO US.

## Les promesses de la recherche européenne en cancérologie

### einblick

Zeitschrift des Deutschen Krebsforschungszentrums  
1/98

#### Gezielt in kleinen Dosen

Radioaktive Antikörper starten das Selbstmordprogramm der Zelle

#### RESEARCH CENTER NEWS

ITU Karlsruhe goes East: toward a common safety & safeguards culture

The European Institute for Transuranium Elements (ITU) does R&D on basic properties of actinide elements and on nuclear fuel cycle safety. The latter area covers safety of nuclear fuel, partitioning and transmutation and characterization of spent fuel.

sions in the framework of the non-proliferation expert group (NPEG) of the G-8/P-8, the institute participated actively in the international technical working group on smuggled materials. Since 1996, the Institute is setting up, in close cooperation with the A. A. Bochvar All-Russia Research Institute

Nuclear Europe Worldscan 1-2/1998

Forschungszentrum Karlsruhe  
Technik und Umwelt

#### Hausmitteilungen

3

1998

- ITU schafft QM-Norm ISO 9001
- Partitioning & Transmutation

Wissenschaftler aus den EU-Ländern im Forschungszentrum über die Abtrennung und Umwandlung nuklearer Abfälle

MEDIZINREPORT Deutsches Ärzteblatt 95, Heft 15, 10. April 1998 (17)

#### Zielgerichtete Krebsbekämpfung

### Alpha-Immuntherapie bei myeloischer Leukämie

Neue Form der Strahlenbehandlung mit wismutbeladenen Antikörpern; stark zytotoxisch bei kurzer Reichweite

Radiochim. Acta 82, 3-9 (1998)

© R. Oldenbourg Verlag, München 1998

### The Enthalpies of Solution of Lanthanide Metals in Hydrochloric Acid at Various Concentrations. Relevance to Nuclear Waste Long Term Storage

Mikrochim. Acta (Suppl.) 15, 191-200 (1998)  
© Springer-Verlag 1998

EPMA of Melted UO<sub>2</sub> Fuel Rods from the Phebus-FP Reactor Accident Experiment

Paul D. W. Bottomley, François Montigny, Achilles D. Stalios, and Clive T. Walker\*

Institut für Transuranelemente, European Commission, Joint Research Centre, Postfach 2340, D-76125 Karlsruhe, Federal Republic of Germany

Radiochim. Acta 83, 21-25 (1998)  
© R. Oldenbourg Verlag, München 1998

Development and Validation of a Simple, Rapid and Robust Method for the Chemical Separation of Uranium and Plutonium

VOLUME 81, NUMBER 19

PHYSICAL REVIEW LETTERS

9 NOVEMBER 1998

#### Enhancement of Magnetic Fluctuations on Passing below $T_c$ in the Heavy Fermion Superconductor UPd<sub>2</sub>Al<sub>3</sub>

N. Bernhoeft,<sup>1</sup> N. Sato,<sup>2</sup> B. Roessli,<sup>3</sup> N. Aso,<sup>2</sup> A. Hiess,<sup>1</sup> G. H. Lander,<sup>4</sup> Y. Endoh,<sup>2</sup> and T. Komatsubara<sup>3</sup>

<sup>1</sup>Institut Laue Langevin, BP 156X, F-38042 Grenoble, France

<sup>2</sup>Physics Department, Tohoku University, Sendai 980-77, Japan

<sup>3</sup>Laboratory for Neutron Scattering, ETH Zurich and Paul Scherrer Institut, CH-5232 Villigen, Switzerland

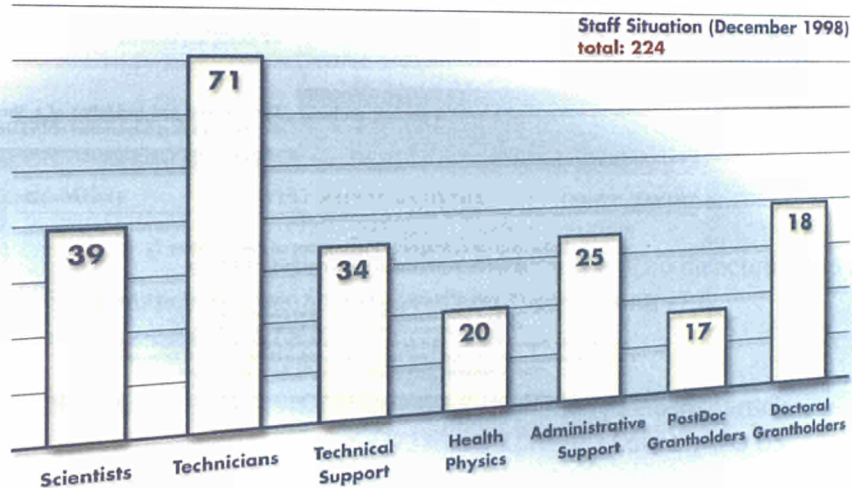
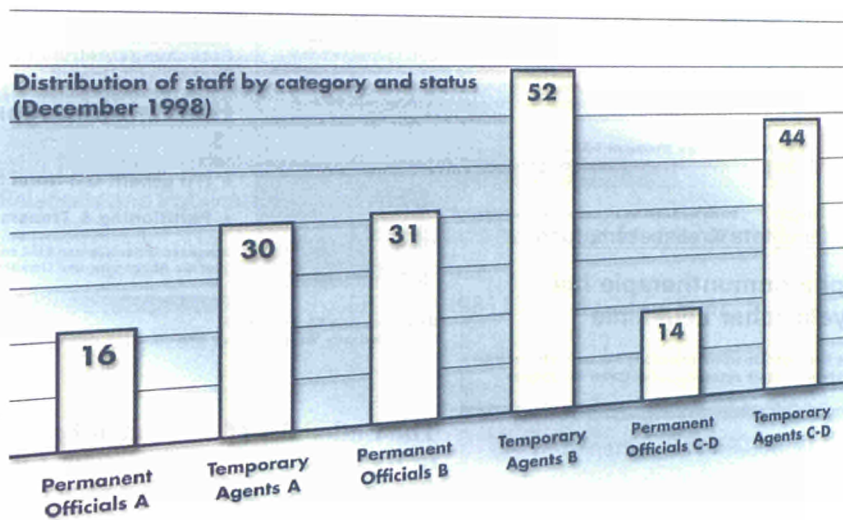
<sup>4</sup>European Commission, JRC, Postfach 2340, Institute Transuranium Elements, D-76125 Karlsruhe, Germany

<sup>5</sup>Low Temperature Science, Tohoku University, Sendai 980-77, Japan

# Institute Staff Resources

The staff situation as of december 1998 is presented in the chart below. The total of statutory staff, i.e. employees of the European Commission, was 189 (188). In addition, 17 (7) post docs, 18 (11) doctoral grantholders worked during 1998 in the Institute. The figures from the previous year are given in brackets.

The distribution of staff by category and status is given in the chart below. Category A grade means scientists and engineers with an university degree, category B corresponds to technicians and category C/D means laboratory attendants or craftsmen.

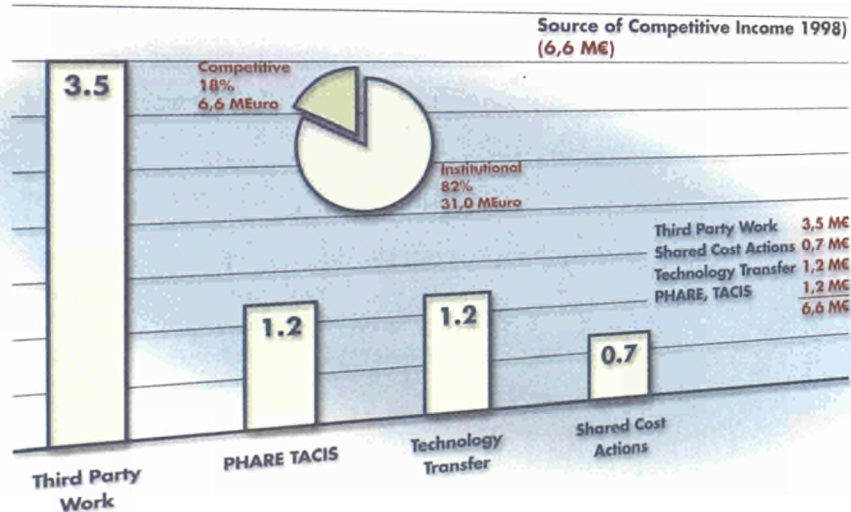
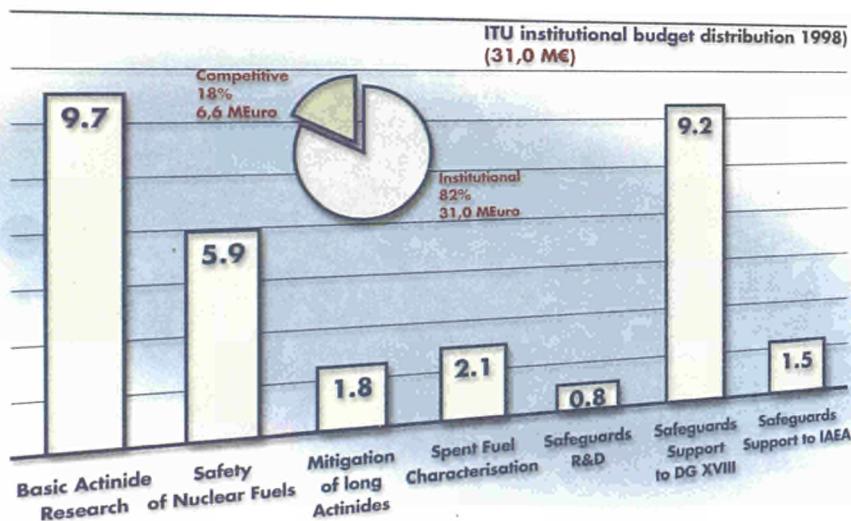


## Budget Resources

Two major categories of activities are performed by the Institute. So-called "institutional" activities, i.e. activities carried out on behalf of the European Union and paid for by the European Commission. These activities include basic research in the area of fuel cycle safety and nuclear safeguards and scientific technical support to the different Directorate Generals of the Commission, i.e. support to policies of the European Union (safeguards, nuclear safety in Eastern countries etc.).

The second category of activities comprises so-called "competitive" work, i.e. activities performed against payment. This category includes work for third parties, shared cost actions (DG XII) and work for other Directorate Generals of the Commission following a call for tender.

The distribution of the institutional budget to the different research and support activities and the source of competitive income for 1998 is shown below.





SCIENTIFIC  
TECHNICAL  
PART B

*itu*

Institute for  
Transuranium  
Elements





# Table of contents (Part B)

## Research in Fuel Cycle Safety

<b>1. Basic Actinide Research</b>	<b>47</b>
1.1 Preparation and Characterisation	47
1.2 Solid-State Physics Studies	50
1.3 Photoemission Studies	53
1.4 High-Pressure Studies	54
1.5 Scattering Studies	58
1.6 Theory	62
1.7 Thermodynamic Properties	63
1.8 Alpha-Immunotherapy	69
<b>2. Safety of Nuclear Fuel</b>	<b>71</b>
2.1 Structural Investigations and Basic Studies on High Burn-up Fuel	71
2.2 Studies of High Temperature Properties of Nuclear Fuels	76
2.3 The Fuel Performance Code TRANSURANUS	79
2.4 Development of Advanced Fuel Fabrication Techniques	80
<b>3. Mitigation of Long Lived Actinides and Fission Products</b>	<b>83</b>
3.1 Fabrication of Fuels and Targets for Transmutation Experiments	83
3.2 Basic Work on Inert Matrices	85
3.3 Partitioning and Transmutation Experiments	88
<b>4. Spent Fuel Characterization in View of Long Term Storage</b>	<b>97</b>
4.1 Characterization and Leaching Experiments	97
4.2 Corrosion Measurements with Electrochemical Techniques	100
4.3 Source Term of Spent Fuel	101
<b>5. Safeguards Research and Development</b>	<b>103</b>
5.1 High Sensitivity Isotope Mass Spectrometry	103
5.2 Environmental Monitoring/High Performance Trace Analysis	103
5.3 Non-Destructive Assay of Spent Nuclear Fuel	104
5.4 Relational Database for Identification of Nuclear Material of Unknown Origin	104
<b>6. Scientific and Technical Support to DG XVII</b>	<b>107</b>
6.1 On-Site Laboratory (OSL), Sellafield	107
6.2 Laboratoire Sur Site (LSS), La Hague	108
6.3 Development for the LSS and OSL	109
6.4 In-Field Verification Activities	111
6.5 European Commission's Safeguards Analytical Measurements	112
6.6 High Performance Trace Analysis	112
<b>7. Scientific and Technical Support to DG I (Safeguards)</b>	<b>113</b>
7.1 Support to IAEA	113
7.2 Assistance to Central and East European Countries	113
7.3 Design and Set-up of Analytical Laboratories at the Bochvar Institute, Moscow	113
<b>Annexes</b>	<b>115</b>
I. Publications 1998	115
II. List of Collaborations with External Organisations	125
III. List of Contributors to the Various Chapters	129
IV. Glossary of Acronyms and Abbreviations	131
V. List of Previous Progress Reports	135



# Research in Fuel Cycle Safety

## 1. Basic Actinide Research

### Introduction

Actinide research has as its main goal the understanding of the physics and chemistry of such systems. Our level of knowledge of actinide metals and compounds is far inferior to that of the rest of the periodic table, mainly because of the difficulty of handling transuranium materials, but also because of the inherent difficulty of understanding the behaviour of the 5f electrons. Their spatial extent and tendency to interact with electrons on ligand sites give actinide materials a complexity unique in the periodic table. Experiments and theory are performed with a view to improved understanding rather than applications. The long-term impact may be viewed in terms of a database for fuels development, for the treatment of waste, and as a contribution to our knowledge of materials in general.

First and foremost in our tasks is the preparation of materials, both in polycrystalline and single crystal form. A second major task is to develop measurement capabilities that can be used both to characterize the material and reveal interesting properties. Since many laboratories are now unable to work with transuranium elements (and sometimes not even with uranium), we have undertaken to construct a "User's laboratory" in Karlsruhe. It is possible for interested staff from universities and other institutes to come to ITU and use these facilities. We are conscious of the need to develop state-of-the-art techniques at ITU, and a good example is our emphasis on developing thin film capabilities and analysis techniques in conjunction with our photoemission effort. Some of the materials prepared (and characterized) in this effort are now finding use in applications in the Institute.

Following the characterization and initial measurements, usually at ITU, the further understanding of the basic properties often requires the use of other measuring techniques that are available only at large facilities (e.g. neutrons, synchrotron X-rays, and muons) or to perform specialized measurements at other laboratories. In most cases the samples must then leave ITU, and for this aspect we have developed a large number of different capsules. Encapsulation and transportation are then arranged by staff at ITU.

Another important aspect of the work is the training of students and postdoctoral candidates, and we have ~10 attached to the group at any one time. The students, in particular, are cement bonds between our work and that in universities, and help to sustain and spread the knowledge of acti-

nide science. The progress of our work is documented in papers in the open literature, conference reports, seminars, and review chapters.

### 1.1 Preparation and Characterisation

Progress in actinide solid state physics depends on the availability of adequate samples with a well-defined structure, well-known purity and appropriate dimensions. Our synthesis facilities permit the preparation of transuranium systems in various states from amorphous to single crystalline samples. The type of samples prepared and investigated are based on the evolution of our understanding and/or questions arising from the progress of physical property measurements performed by external or internal users.

In 1998, we continued our efforts presented in previous reports on the preparation of pure metals, alloys and intermetallic compounds with some new aspects. A major objective of our preparation work is the encapsulation of characterised samples for collaborative studies.

#### 1.1.1 Preparation of pure metals

Obtaining actinide samples for solid state physics investigation needs high purity metals. Electropositive actinide metals are prepared by metallothermic reduction of the halide, oxide and carbide and by electrolysis in a molten salt [1,2]. In the last reporting period (TUAR-97, p. 48) we presented the achievement of a high-vacuum radio-frequency oven for the preparation of  $^{242}\text{Pu}$ -metal by metallothermic reduction of the oxide. In 1998, we conducted the first run in active conditions with this arrangement. Some hundreds of milligrams of metal were obtained, however the yield of the process remained quite low (50-60%). Improvements of the experimental conditions are necessary and will continue.

As presented recently by a Japanese group, an alternative method to produce actinide metals is to proceed by electrochemical reduction in aqueous solution via an amalgamation process. Uranium and neptunium metals were successfully prepared by the thermal decomposition of electrochemically prepared amalgams from the aqueous solutions [3,4]. We intend to study further this technique by starting a collaboration with our Japanese colleagues and welcomed Prof. Y. Shiokawa (Tohoku University, Sendai) in our laboratory to

set up such facility. An electrochemical cell and a decomposition furnace were developed and installed. Preliminary tests were performed on the reduction of Np-oxide. Neptunium amalgams were synthesised from acetate buffer solutions and metallic buttons of neptunium metal were obtained. Fig. 1.1 shows the electrochemical cell used for this synthesis. Several charges of Np were prepared with a process yield over 90%. Chemical characterisations (impurities and N, C, O, H contents) of the metal obtained are still in progress.

This method is relatively simple, with high yields and therefore suitable for metal production on the laboratory scale. The preparation of plutonium metal should also be feasible by this technique and attempts are planned for next year.



Fig. 1.1 Electrochemical cell for reduction-amalgamation process.

### 1.1.2 Preparation of compounds and single crystal growth

The discovery of uranium intermetallics which exhibit heavy-fermion behaviour, i.e. an enhanced value of the coefficient  $\gamma$  of the electronic specific heat, has led to an increasing amount of work on uranium systems in the last decade [see for review 5]. This interest was greatly enhanced with the dis-

covery of heavy-fermion superconductors. By having several related compounds, with only the nature of the local moment varying, there is a chance of achieving a better understanding of how superconductivity and the local moments interact to produce the low-temperature ground state of these compounds. In this field, the investigation of related transuranium elements based systems contributes to complete this quest.

In 1998, several new compounds were successfully prepared and attempts of single crystal growth performed. Compounds obtained and their lattice parameters are summarised in Tab. 1.1.

Compounds	Structure Type	Lattice Parameters	
$(U_xNp_{1-x})_4Ru_7Ge_6$ x = 0 x = 0.005 x = 0.01 x = 0.05 x = 0.1 x = 1	Cubic $U_4Re_7Ge_6$	a (pm)	
		831.2(1)	
		830.9(2)	
		830.6(1)	
		830.7(1)	
		830.6(1)	
		829.8(1)	
$U_{1-x}Np_xNi_2Al_3$ x = 0 x = 0.1 x = 0.3 x = 0.5 x = 0.7 x = 0.9 x = 1	Hexagonal $PrNi_2Al_3$	a (pm)	c (pm)
		521.1(1)	402.1(1)
		520.9(1)	402.0(1)
		519.8(5)	402.0(4)
		521.3(1)	401.7(1)
		521.8(1)	401.7(1)
		521.6(2)	401.1(2)
522.2(2)	399.5(1)		
$PuSn_3$ $PuIn_3$	Cubic $AuCu_3$	a (pm)	
		463.1(1) 461.4(1)	

Tab. 1.1 Structure types and lattice parameters of new compounds prepared and characterised in 1998.

We started also some preliminary research on the preparation of new magnetic superconductors, the  $RNi_2B_2C$  series for which the salient energy scales for antiferromagnetic order and superconductivity can be varied over a wide range and examined in two different limits –  $T_C > T_N$  and  $T_C < T_N$  [6], with uranium and neptunium. However we were, for the moment, unable to produce pure enough samples and our efforts will continue.

### 1.1.3 Encapsulation for collaborative studies

New capsules were designed and in house fabricated for:

- EXAFS (Extended X-ray Absorption Structure) on PuX small samples (few mg),
- SQUID measurements on oriented single crystal
- X-ray magnetic scattering on single crystals

Compounds encapsulated for various physical properties measurements performed in house or in external institutions in collaborative studies are listed in *Tab. 1.2*.

An oriented single crystal of UO<sub>2</sub> was provided to Cardiff University (GB) on a cost-reimbursement basis.

### References

- [1] J.C. Spirlet, O.Vogt; in "Handbook on the Physics and Chemistry of the Actinides", eds. A.J. Freeman and G.H. Lander, North Holland Publishing (Elsevier Science Publishing Co.), Amsterdam, Vol.1 (1984) 79; ISBN: 0-444-86903-4
- [2] R.G. Haire, *J. Less-Common Met.* 121 (1986) 379
- [3] Y. Shiokawa, K. Hasegawa, K. Konashi, M. Takahashi, K. Suzuki, *J. Alloys Comp.* 225 (1996) 98-101
- [4] K. Hasegawa, Y. Shiokawa, M. Akabori, Y. Suzuki, K. Suzuki, *J. Alloys Comp.* 271-273 (1998) 680-684
- [5] V. Sechovsky, L. Havela, in "Handbook of Magnetic Materials", ed. K.H.J. Bushow, North Holland Physics Publishing (Elsevier Science B.V.), Amsterdam, Vol. 11 (1998) 1-289
- [6] P.C. Canfield, P.L. Gammel, D.J. Bishop, *Physics Today* Oct. 1998 (1998) 40-46

MEASUREMENTS	LABORATORIES	COMPOUNDS	FORM
EXAFS	CEA-Marcoule SSRL-Stanford LURE-Orsay	PuN, PuS, PuSe, PuTe	P, G-SC
Resistivity Magneto-Resistance	ITU-Karlsruhe	NpPd <sub>2</sub> Ge <sub>2</sub> U <sub>4</sub> Tc <sub>7</sub> Si <sub>6</sub> , Np <sub>2</sub> Mo <sub>3</sub> Si <sub>4</sub> , U <sub>0.95</sub> Np <sub>0.05</sub> Pd <sub>2</sub> Al <sub>3</sub> PuTe	AcM AcM SC
Mössbauer Spectroscopy	ITU-Karlsruhe	(U <sub>x</sub> Np <sub>1-x</sub> ) <sub>4</sub> Ru <sub>7</sub> Ge <sub>6</sub> U <sub>1-x</sub> Np <sub>x</sub> Ni <sub>2</sub> Al <sub>3</sub> U <sub>0.95</sub> Np <sub>0.05</sub> Ru <sub>2</sub> Si <sub>2</sub>	AcM AcM AcM
Neutron Scattering	ILL-Grenoble	UPtGe, Np(As <sub>1-x</sub> Se <sub>x</sub> ) (x = 0.15, 0.2)	SC
Magnetism	ITU-Karlsruhe	U <sub>1-x</sub> Pu <sub>x</sub> Sb (x = 0.25, 0.5, 0.75) oriented along <111>, <100> and <110> U <sub>1-x</sub> Lu <sub>x</sub> RhAl	SC AcM
	FZ-Jülich	UO <sub>2</sub>	SC
Magnetic X-ray Scattering	ESRF-Grenoble	U <sub>0.95</sub> Np <sub>0.05</sub> Ru <sub>2</sub> Si <sub>2</sub> , U <sub>0.99</sub> Np <sub>0.01</sub> Ru <sub>2</sub> Si <sub>2</sub> , UO <sub>2</sub> , NpP, CeFe <sub>2</sub> , NpCo <sub>2</sub> , Np(As <sub>1-x</sub> Se <sub>x</sub> ) x = 0.05, 0.1, 0.15, 0.2	SC SC SC
	BNL-Brookhaven	UO <sub>2</sub>	SC
High-Pressure X-ray Diffraction	ITU-Karlsruhe	PuX <sub>3</sub> (X= Sn, In) PuBi	AcM G-SC
High-Pressure Resistivity	ITU-Karlsruhe	PuTe, NpTe	SC

AcM = arc melting SC = single crystal P = powders, polycrystalline sample  
G-SC= grinding single crystals

Tab. 1.2 *Samples prepared, characterised and encapsulated in 1998 for the indicated measurements.*

Contact (1.1): Franck Wastin • tel.: +49 7247 951 387 • fax: +49 7247 951 599 • wastin@itu.fzk.de

## 1.2 Solid-State Physics Studies

A major task is to develop measurements capabilities that can be used both to characterise the material and reveal interesting properties. A number of solid-state physics studies have been performed this year at the ITU. Most of them have been conducted in collaboration with outside users of our facilities.

### 1.2.1 Development of multi-users physical properties measurements facility

Since many laboratories are now unable to work with transuranium elements (and sometimes not even with uranium), we have undertaken to construct a "User's laboratory" in Karlsruhe. It is possible for interested staff from universities and other institutes to come to ITU and use these facilities. Various pieces of equipment for basic physical property measurements are available for:

- Mössbauer spectroscopy experiments down to 1.5 K at ambient or high pressure (up to 4 GPa),
- resistivity measurements down to 1.5 K and up to 1000 K,
- magneto-resistance in a cryostat equipped with a 9 Tesla magnet field,
- magnetic susceptibility and magnetisation with a Quantum Design SQUID (MPMS-7) apparatus equipped with a 7 Tesla magnet and able to perform magnetic measurements from 2 K to 700 K.

MEASUREMENTS	USERS	COMPOUNDS
Resistivity	Prague Univ. (CZ) Ancona Univ. (I)	NpIrSn CeFe <sub>2</sub>
Magneto-Resistance	Prague Univ. (CZ) Ancona Univ. (I) Augsburg Univ. (D)	NpIrSn CeFe <sub>2</sub> NpPd <sub>2</sub> Ge <sub>2</sub>
Magnetism	Braunschweig Univ. (D) Prague Univ. (CZ) Ancona Univ. (I)	U <sub>1-x</sub> Pu <sub>x</sub> Sb U <sub>1-x</sub> Lu <sub>x</sub> RhAl CeFe <sub>2</sub>

CZ: Czech Republic, I: Italy, D: Germany

Tab. 1.3 Measurements on samples performed by outside users.

In Tab. 1.3, we present a summary of the measurements performed by outside users and the compounds studied.

For the coming year we expect to continue to develop our capabilities and increase our possibilities to welcome new users.

### 1.2.2 Measurements of bulk physical properties

#### Mössbauer studies

Mössbauer spectroscopy is a unique tool giving access to local magnetic and electronic properties of solids. Four large isostructural families of intermetallic actinide compounds were investigated by <sup>237</sup>Np Mössbauer spectroscopy and yielded interesting results, completing the study of some series (e.g. Np<sub>2</sub>Ir<sub>2</sub>In) or constituting the first magnetic investigations in other ones (e.g. Np<sub>2</sub>T<sub>3</sub>X<sub>4</sub>). A summary of relevant hyperfine parameters is given in Tab. 1.4 and details of investigated systems are discussed below:

- Np<sub>2</sub>T<sub>2</sub>X (X=In, Sn): The electronic and magnetic properties of this large family were investigated in the recent years, in particular by Mössbauer spectroscopy, except its last known member, Np<sub>2</sub>Ir<sub>2</sub>In [1,2]. Our Mössbauer experiments on this compound complete the Mössbauer study of the whole Np<sub>2</sub>T<sub>2</sub>X series. As expected from general trends in actinide intermetallics, Np<sub>2</sub>Ir<sub>2</sub>In orders magnetically at low temperature and exhibits a weaker moment and a lower ordering temperature than Np<sub>2</sub>Pt<sub>2</sub>In.
- Np<sub>2</sub>T<sub>3</sub>X<sub>4</sub> [3]: Our Mössbauer investigations in this series reveal that Np<sub>2</sub>Mo<sub>3</sub>Si<sub>4</sub> and Np<sub>2</sub>Tc<sub>3</sub>Si<sub>4</sub> order magnetically (at 47 K and 19 K respectively). Np<sub>2</sub>Tc<sub>3</sub>Ge<sub>4</sub> exhibits at 4.2 K a very weak magnetic ordering coexisting with a dominant paramagnetic phase. Further measurements below 4.2 K are planned to explore the evolution of these phases.
- Np<sub>2</sub>T<sub>3</sub>X<sub>5</sub> [3]: Np<sub>2</sub>Re<sub>3</sub>Si<sub>5</sub> does not order magnetically down to 4.2 K.
- NpT<sub>2</sub>X<sub>2</sub>: Np<sub>0.05</sub>U<sub>0.95</sub>Ru<sub>2</sub>Si<sub>2</sub> was measured to complete the previous investigations in the Np<sub>x</sub>U<sub>1-x</sub>Ru<sub>2</sub>Si<sub>2</sub> series (0.1 < x < 1) [4]. URu<sub>2</sub>Si<sub>2</sub> orders antiferromagnetically at T<sub>N</sub> ≈ 17.5 K with a very small moment (μ<sub>U</sub> (4.2 K) ≈ 0.03 μ<sub>B</sub>) whereas NpRu<sub>2</sub>Si<sub>2</sub> orders at T<sub>N</sub> ≈ 27.5 K (μ<sub>Np</sub> (4.2 K) ≈ 1.5 μ<sub>B</sub>). Though the Np concentration in Np<sub>0.05</sub>U<sub>0.95</sub>Ru<sub>2</sub>Si<sub>2</sub> is very low, an exploitable spectrum could be obtained by counting over a long period. It reveals that no major change of the electronic and magnetic properties has occurred from Np<sub>0.1</sub>U<sub>0.9</sub>Ru<sub>2</sub>Si<sub>2</sub> to Np<sub>0.05</sub>U<sub>0.95</sub>Ru<sub>2</sub>Si<sub>2</sub>.

COMPOUND	T = 4.2 K					T <sub>ord</sub> (K)	T > T <sub>ord</sub>				
	$\mu_{Np}$ ( $\mu_B$ )	$\delta_{IS}$ (mm/s)	$e^2qQ$ (mm/s)	W (mm/s)	I <sub>site</sub>		$\delta_{IS}$ (mm/s)	$e^2qQ$ (mm/s)	W (mm/s)	I <sub>site</sub>	$\eta$
Np <sub>2</sub> Ir <sub>2</sub> In extra phase	0.74(1)	-14.1*	3(1)	9.8	45%	30	-14.1(1)	31(1)	2.9(1)	72%	0.4(1)
	0	-19.7*	10.2*	3.8(1)	55%	-	-19.7(1)	10(1)	4.7(1)	28%	0
Np <sub>2</sub> Mo <sub>3</sub> Si <sub>4</sub>	1.12(1)				31%	47					0.4(1)
	1.06(1)	-3.2(1)	-30(1)	4.3(1)	57%		-3.9(1)	41(1)	3.7(1)	100%	
	0.98(1)				12%						
Np <sub>2</sub> Tc <sub>3</sub> Si <sub>4</sub>	0.79(1)				46%	19					1.0(1)
	0.54(1)	-4.0(1)	-44(2)	6.0(2)	22%		-2.6(1)	31(1)	2.6(1)	100%	
	0.19(1)				32%						
Np <sub>2</sub> Tc <sub>3</sub> Ge <sub>4</sub>	0	2.6*	28*	3*	66%	6?					0.9(1)
	0.55(1)	0.2(1)	-7(1)	9.8(5)	14%		1.7(1)	28(1)	2.6(1)	100%	
	0.17(1)	0.2(1)	-7(1)	9.8(5)	20%						
Np <sub>2</sub> Re <sub>3</sub> Si <sub>5</sub>	0	5.7(1)	55.8(1)	2.7(1)	100%	-					0.2(1)
Np <sub>0.05</sub> U <sub>0.95</sub> Ru <sub>2</sub> Si <sub>2</sub>	1.57(1)	-0.6(1)	-65(1)	3.5(1)	100%						0
NpPd <sub>2</sub> Ge <sub>2</sub>	2.03(1)	18.9(1)	-13.9(1)	3.6(1)	100%	60	19.5(1)	5.4(4)	3.2(1)	100%	0

Tab. 1.4 Local magnetic moment  $\mu_{Np}$ , isomer shift  $\delta_{IS}$ , quadrupolar interaction parameter  $e^2qQ$ , line width  $W$ , site intensity  $I_{site}$ , magnetic ordering temperature  $T_{ord}$  and asymmetry parameter  $\eta$  at 4.2 K and above  $T_{ord}$ , for Np<sub>2</sub>T<sub>2</sub>X, Np<sub>2</sub>T<sub>3</sub>X<sub>4</sub>, Np<sub>2</sub>T<sub>3</sub>X<sub>5</sub> and NpT<sub>2</sub>X<sub>2</sub> compounds investigated by Mössbauer spectroscopy. The local magnetic moment of Np is derived from the magnetic hyperfine field relation ( $H_{hf}/\mu_{Np} = 2150$  kG/ $\mu_B$ ). Isomer shifts are given relative to the standard absorber NpAl<sub>2</sub>. Parameters marked with a star (\*) were fixed in the fit. The hyperfine field and the corresponding moment values of NpPd<sub>2</sub>Ge<sub>2</sub> are mean values inferred from the  $H_{hf}$  distribution.

NpPd<sub>2</sub>Ge<sub>2</sub> was also investigated. Typical NpPd<sub>2</sub>Ge<sub>2</sub> Mössbauer spectra at 4.2 K and 64 K are shown on Fig. 1.2. At 64 K, the spectrum consists of a pure quadrupolar splitting, as expected in the paramagnetic state. The value of the isomer shift ( $\delta_{IS} \approx 19.5$  mm/s vs NpAl<sub>2</sub>) indicates a Np<sup>3+</sup> charge state. At 60 K the spectrum begins to broaden, indicating the occurrence of magnetic ordering. At 4.2 K the hyperfine splitting reveals the presence of magnetic order. The spectrum can be well reproduced assuming an hyperfine field distribution around the mean value  $H_{hf} \approx 436$  kG which corresponds to an average moment  $\mu_{Np} \approx 2.03 \mu_B$ . Two other compounds of this series, NpPd<sub>2</sub>Si<sub>2</sub> and NpPt<sub>2</sub>Si<sub>2</sub>, order also around 60 K, but exhibit weaker magnetic moments [3].

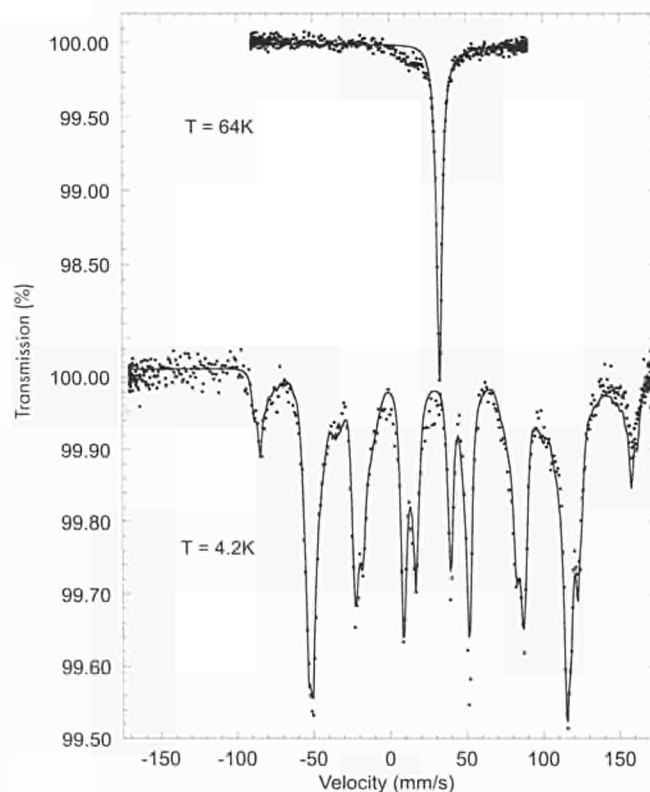


Fig. 1.2 Mössbauer spectra of NpPd<sub>2</sub>Ge<sub>2</sub> at 4.2 K and 64 K.

## Magnetic response of CeFe<sub>2</sub>

The magnetic response of CeFe<sub>2</sub> single crystals was studied by linear and non-linear ac susceptibility, dc magnetisation and magnetoresistance measurements. Several anomalies have been observed below the Curie temperature ( $T_C = 228$  K). A kink near 30 K in the real component of the linear susceptibility,  $\chi'_1(T)$ , is accompanied by a frequency dependent peak in both the linear imaginary part,  $\chi''_1(T)$ , and the third-harmonic non-linear susceptibility,  $|(3/4)\chi_3H_0^2|$ . It is suggested that these features are related to the development of antiferromagnetic spin fluctuations of growing spatial extension. An electronic instability below 80 K is further indicated by a transition from negative, and small, to positive and fairly large magnetoresistance.

## Magnetic properties of Pu<sub>x</sub>U<sub>1-x</sub>Sb single crystals

The actinide compounds PuSb and USb, crystallising in the sodium chloride structure, are amongst the most interesting and most studied magnetic materials. USb shows a complicated triple-k structure (see e.g. [5]). The situation in PuSb is even more complicated: Below a high-temperature paramagnetic region the system first undergoes a transition to antiferromagnetism at 85 K, whereas below 69 K one observes a second transition to ferromagnetism. A strong anisotropy, with  $\langle 100 \rangle$  as the easy magnetic axis, develops at these low temperatures. The field and temperature dependent phase diagram is shown in [6].

Large single crystals of Pu<sub>x</sub>U<sub>1-x</sub>Sb with concentrations  $x = 0.25, 0.50$  and  $0.75$  were grown in ITU and encapsulated with regard of the three main crystallographic directions  $\langle 100 \rangle$ ,  $\langle 110 \rangle$  and  $\langle 111 \rangle$ . Our goal is to study the transition from the antiferromagnetism in USb to the complex behaviour found in PuSb. Magnetisation curves were obtained by the use of our SQUID magnetometer in a temperature range of 2 K - 310 K and in magnetic fields up to 7 Tesla.

Fig. 1.3 shows the susceptibility as a function of temperature of a single crystal Pu<sub>0.75</sub>U<sub>0.25</sub>Sb. Similar to the pure PuSb one can distinguish three magnetic regimes: The sample is paramagnetic at high temperatures following a Curie-Weiss law (localised magnetic moments). The onset of antiferromagnetism is observed at 93 K. If the temperature decreases below 55 K we see a transition to ferromagnetism as expected from the behaviour of the pure PuSb. These transition temperatures are in good agreement with former resistivity studies on Pu<sub>x</sub>U<sub>1-x</sub>Sb done at ITU [7].

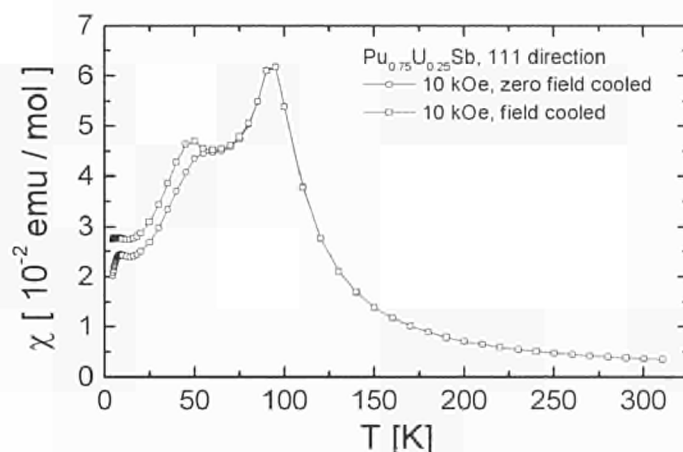


Fig.1.3 Magnetic susceptibility versus temperature of Pu<sub>0.75</sub>U<sub>0.25</sub>Sb.

Contrary to the case of PuSb only small anisotropy is seen at low temperatures.

For the low concentrations of Pu no clear ferromagnetic signal is observable. These samples mainly show the features of USb with paramagnetic-antiferromagnetic transition temperatures  $T_N$  being changed according to Vegard's law, namely 155 K for Pu<sub>0.50</sub>U<sub>0.50</sub>Sb and  $T_N = 200$  K for Pu<sub>0.25</sub>U<sub>0.75</sub>Sb. At high temperatures the data follow a Curie-Weiss formula. The average effective magnetic moment changes almost linearly with concentration  $x$  between the values for USb and PuSb.

Magnetisation measurements at temperatures up to 800 K are planned as well as neutron studies with and without magnetic fields.

## References

- [1] M.N. Perón, Y. Kergadallan, J. Rebizant, D. Meyer, J.M. Winand, S. Zwirner, L. Havela, H. Nakotte, J.C. Spirlet, G.M. Kalvius, E. Colineau, J.L. Oddou, C. Jeandey, J.P. Sanchez, J. Alloys Comp. 201 (1993) 203.
- [2] J.P. Sanchez, E. Colineau, C. Jeandey, J.L. Oddou, J. Rebizant, A. Seret, J.C. Spirlet, Physica B206 & 207 (1995) 531.
- [3] F. Wastin, PhD Thesis, Université de Liège (Belgique), 1991.
- [4] S. Zwirner, J.C. Waerenborgh, F. Wastin, J. Rebizant, J.C. Spirlet, W. Potzel, G.M. Kalvius, Physica B 230 (1997) 80.
- [5] J. Jensen, P. Bak, Phys. Rev. B 23 (1981) 6180-6183.
- [6] O. Vogt, K. Mattenberger; in Handbook on the Physics and Chemistry of Rare Earths, eds. K. A. Gschneidner Jr, L. Eyring, G.H. Lander, G.R. Choppin, North-Holland Physics Publishing Co., Amsterdam, Vol. 17 (1993), Chap. 114; 301-407.
- [7] J. Rebizant, F. Wastin, C. Rijkeboer, E. Bednarczyk and P. Lefèbvre, J. Alloys Comp. 271-273 (1998) 490-4.

## 1.3 Photoemission Studies

### 1.3.1. PuSe: Band Structure or Kondo effect?

Photoemission studies of thin films of PuSe have been done to complement previous solid state physical (resistivity, neutron diffraction, magnetic susceptibility) [1] and theoretical investigations [2] of Pu monochalcogenides, one of the most puzzling group of actinide compounds. One of the main issues is the degree of delocalization of the  $5f$  states, and it seems that experimental evidence available so far is rather ambiguous. In particular, the band approach predicts PuSe to be a relativistic semiconductor [2], which is supported by high temperature resistivity data [3]. On the other hand, measurements of the electronic specific heat point to an appreciable density of quasiparticle states at the Fermi level. Previous photoemission investigations performed on bulk PuSe showed an intense peak at the Fermi energy  $E_F$  pointing to a high density of states  $N(E_F)$  [4]. However these measurements suffered from the problem of clean surface preparation. Conventional sputter cleaning led to off-stoichiometric surfaces. Scraping, which produces stoichiometric surfaces, resulted in a rapid deterioration of the sample so that it could be used in only a few measurement cycles.

Present studies were carried out on thin films of PuSe. The films were prepared from a microtarget of 100 mg PuSe by sputter deposition. This technique allows production of a large number of clean films of a bulk-like stoichiometry in contrast to scraping (about 70 films compared to three surfaces by scraping). Deposition on a clean single crystalline Si substrate of high purity resulted in no surface segregation of impurities even at high temperatures. Thus excellent quality photoemission spectra could be taken at a temperature of 673 K, while bulk PuSe samples showed strong surface segregation of O already at 373 K. In the first stage, we did not concentrate on the interaction of the PuSe layers with the substrate, but relatively thick films ( $d > 15$  monolayers) were studied to make comparisons with bulk PuSe samples.

Fig. 1.4 shows UPS Hel and Hell room temperature spectra of thin films deposited at high temperature (623 K). All features observed in valence band spectra of PuSe layers prepared under different conditions can be identified with features which were observed for the bulk PuSe sample. Besides the peak between 3 eV and 5 eV binding energy, which dominates for the Hel - 21.2 eV excitation, and can be thus associated with emission from the Se  $4p$  states, we observe 4

distinct peaks related clearly to a  $5f$  emission. Most of the  $5f$  spectral intensity, dominating the spectra with Hell - 40.8 eV excitation energy, concentrates into a broad triangular peak centered roughly at 2 eV. Besides this robust feature, which we tentatively attribute to a  $5f$  localized ( $5f^{\text{loc}}$ ) state with unresolved multiplet structure, we observe two additional very sharp (FWHM  $\approx 0.15$  eV) peaks, located at 0.85 eV and 0.5 eV, respectively, and similarly sharp but more intense peak at the Fermi level.

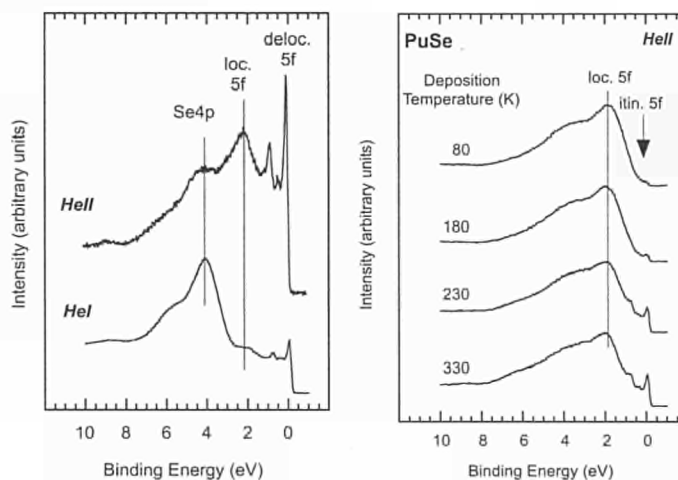


Fig. 1.4 Hel and Hell spectra of a PuSe film deposited at high temperature.

Fig. 1.5 UPS-Hell spectra of PuSe films deposited at different temperatures. At high temperature crystalline films are favored and this has an unexpected strong influence on the low binding energy features.

The intensity of the last three features depends strongly on the surface composition and deposition temperature. It is considerably reduced for the surface of the bulk sample cleaned by sputtering using Ar ions, which leads to a Se-depleted surface. A similar effect is seen for layers prepared under sputter conditions yielding Se-deficient composition (no Se-rich layers could be prepared). Most dramatic is the effect of deposition temperature (Fig. 1.5). For layers prepared at  $T = 80$  K the features close to  $E_F$  are absent, and this fact can be attributed to the amorphous state, which should be formed preferentially at low deposition temperatures. For layers prepared at such low temperature the spectra are not changed by any short time exposure to higher temperatures (tested up to 623 K). The same dependence of the three sharp features on stoichiometry and defects points to their common origin, and they apparently reflect band electron or quasiparticle states. On the other hand, the dispersion must be small due to their observed narrow width.

The above mentioned picture of the  $5f$  emission consisting of a "localized" peak and features reflecting itinerant states, the latter being very sensitive to any defects, is corroborated by Pu- $4f$  core level spectroscopy, where the twofold nature of valence band states is reflected by two different screening channels of the  $4f$  hole. According to the standard approach [5], itinerant  $5f$  states participating in the screening of the  $4f$  hole yield  $4f$  peaks at lower binding energy (good screening) than if the  $4f$  hole has to be screened by non- $f$  valence-band electrons because of  $5f$  localization (poor screening). Fig. 1.6 shows Pu $5f_{7/2}$  spectra of PuSe films. The comparison with elemental plutonium spectra [5] shows that the main  $4f$  peaks are located at energies corresponding to poor screening in PuSe, whereas more or less intense satellites appear on their low binding energy side, where well screened  $4f$  peaks are expected. By comparison with Hell spectra of films prepared under the same conditions we can see that the intensity of such satellites scales qualitatively with the intensity of the band  $5f$  features in the valence band of PuSe.

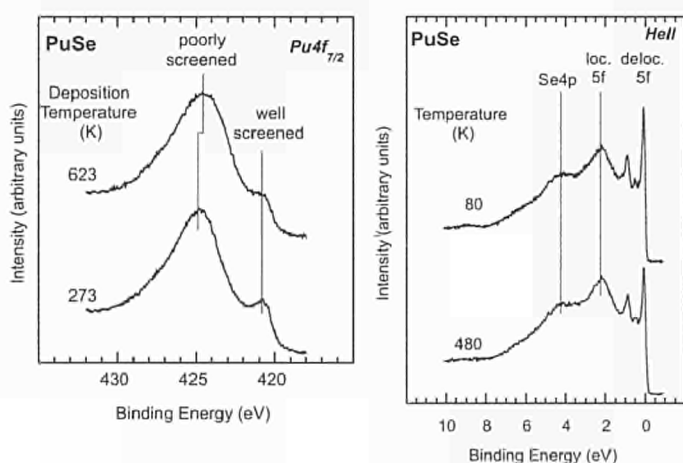


Fig. 1.6 XPS-Pu  $4f_{7/2}$  core level spectra of PuSe films deposited at different temperatures. For high temperature crystalline films are favored and this results in the increase of the well screened peak.

Fig. 1.7 UPS-Hell spectra taken at different temperatures. The films have been deposited at 673 K. With decreasing temperature all three low energy band like peaks increase in intensity.

A striking feature in the photoelectron spectra of PuSe is the strong temperature dependence of both the well screened peaks in the  $4f$  spectra, and of the three  $5f$  band features in the valence band spectra (Fig. 1.7). Such intensity variations

cannot be explained by standard phonon assisted processes. They may reflect temperature variations of the quasiparticle density of states, i.e. an analogy of the Kondo effect [6], which is well known in the context of a single impurity problem, but its observation in periodic systems is a matter of controversy. To be more conclusive about the nature of the sharp spectral features with their temperature dependence, we propose to perform analogous experiments on PuSb, in which magnetic order and sizeable Pu moments should suppress any Kondo-like effect.

## References

- [1] E. Gómez Marín, PhD Thesis, University Joseph Fourier, Grenoble 1997
- [2] M.S.S. Brooks, J. Magn. and Magn. Mat. 63 & 64 (1987) 649
- [3] E. Gomez Marin, J.M. Fournier, J.C. Spirlet and F. Wastin, J. de Physique (submitted)
- [4] J.R. Naegele, 20<sup>èmes</sup> Journées des Actinides, Charles University Prague, 1990
- [5] J.R. Naegele, J. Ghijsen and L. Manes, in Actinides - Chemistry and Physical Properties (Structure and Bonding 59/60), Springer-Verlag, Berlin Heidelberg Tokyo New York (1985) 199
- [6] D. Malterre, M. Grioni and Y. Baer, Adv. Phys. 45 (1996) 299

## 1.4 High-Pressure Studies

### 1.4.1 High-pressure resistivity

Development of equipment for temperatures below 1.5 K

In the previous report (TUAR-97, p. 55-56), we explained the goal of our project and showed our prototype of a  $^3\text{He}$  refrigerator which gave satisfactory results down to a temperature of  $\sim 320\text{mK}$ . For high-pressure experiments the refrigerator should be able to cool the pressure cell. Our previous tests showed that the refrigerator cools  $\sim 500\text{g}$  of copper to  $320\text{mK}$ . It turned out that the minimum temperature increases for higher masses. Therefore we designed and constructed 2 small pressure cells ( $< 500\text{g}$ ) on the basis of a technique used in CEA, Grenoble. We also designed modified capsules to handle the pressure cells. This technique requires an external press to apply the force, which we need to adapt for the contaminated cells. To continue the tests at low temperature we received a new cryostat, associated equipment and electronics. The installation of this equipment is in progress.

## Transuranium experiments

In addition to the high-pressure study on PuTe (see highlight) we have started a preliminary study on NpTe up to 6 GPa. At ambient pressure, NpTe is antiferromagnetic and a very small anomaly was observed at the magnetic transition (~ 43 K) in the temperature variation of the resistivity [1].

Under pressure, the low-temperature resistance increases up to 0.6 GPa and then decreases. This is accompanied by the progressive suppression of the maximum at 50 K and the disappearance of the high-temperature Kondo anomaly. We observed the latter effect in NpAs, NpBi, and NpGa<sub>3</sub> previously. The room temperature resistance, however, is nearly constant up to 6 GPa. The anomaly at the magnetic order is not visible in our measurement and we have no information on the pressure variation of the ordering temperature.

### Reference

[1] M. Amanowicz, PhD Thesis, University of Grenoble (1995).

### 1.4.2 High pressure X-ray diffraction studies

Samples of <sup>243</sup>Am and <sup>248</sup>Cm were loaded into three types of high pressure cell at the Oak Ridge National Laboratory in the USA and shipped to the ESRF Grenoble where they were mounted in specially made containers for study at the high pressure beamline ID30. Extra precautions were taken to ensure that these samples remained confined during the experiments by the use of double or triple sealing of the cells with Mylar, Kapton and Be windows. The cells used were of the Holzapfel, Mao-Bell and Cornell types to allow as much flexibility as possible with accurate determination of low and high pressure sample phases as well as a certain flexibility to choose optimal wavelengths and diffraction angles for the detector system.

We used the ID30 high pressure beam line in angle dispersive mode and collected data containing the full diffraction cones on the fast scan image plate detector. A micro-focused beam of 25x25 μm<sup>2</sup> obtained with two bent mirrors and passed through a pinhole was used for the Cornell cells.

<sup>243</sup>Am was loaded into Holzapfel and Cornell cells whilst the <sup>248</sup>Cm was loaded into the Mao-Bell cell allowing a certain redundancy in case of problems with one of the cells. Exposure times ranged from only 15 seconds for the larger samples in

the low pressure range to 60 seconds for the highest pressures. The aims of the experiment were to probe the fundamental chemistry and physics of these elements by decreasing interatomic distances with applied pressure and in particular to solve the structures of Am III and Am IV as well as hopefully finding a new fourth phase of Cm above 60 GPa.

The selection of Cm and Am for investigation of high-pressure behaviour of transplutonium elements was especially attractive as <sup>248</sup>Cm and <sup>243</sup>Am isotopes, which have a relatively low specific-activity, were available at ORNL for the study.

We achieved most of our goals except that of reaching the Cm high pressure phase which was compensated for by the unexpected appearance of a fifth phase of Am. Structure refinement of the Am III and IV phases is in progress.

### Results for <sup>243</sup>Am

Both pressure cells behaved correctly and we were able to observe a total of five high pressure phases with a far higher resolution than any previous work.

The initial dhcp structure transformed to fcc at 6 GPa, to a monoclinic structure at 11 GPa, to a possible orthorhombic structure above 18 GPa and then to an as yet unidentified fifth phase at around 100 GPa. The sequence of structural changes is shown in Fig. 1.8.

### Results for <sup>248</sup>Cm

Cm (element 96) is one of the most interesting transplutonium elements as it has a stabilising ground state electronic configuration of : [Rn core] 5f<sup>7</sup> 6d 7s<sup>2</sup>. This half-filled 5f-shell greatly influences the pressure behaviour of Cm; which displays higher structural transition pressures and resists f-electron delocalisation. The low pressure region was studied using the Mao-Bell pressure cell up to 20 GPa.

We were not able to further increase the pressure with this series because of deformation of the gasket hole which could have eventually led to diamond breakage. The <sup>248</sup>Cm sample studied remained in the dhcp phase shown in Fig. 1.9 throughout the measurement.

Further experiments on Cm as well as alloys of Am/Cm are required and these studies will be carried out in 1999 again at the ESRF beam line ID30.

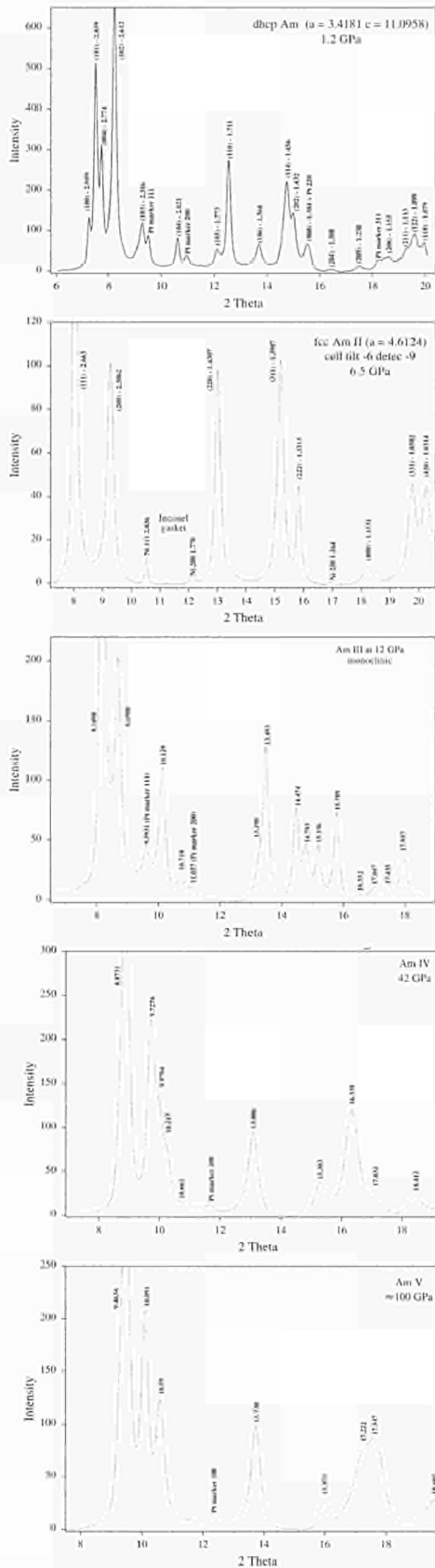


Fig. 1.8 The five structural phase transitions observed for Am (pressure transmitting fluid: Silicone Oil).

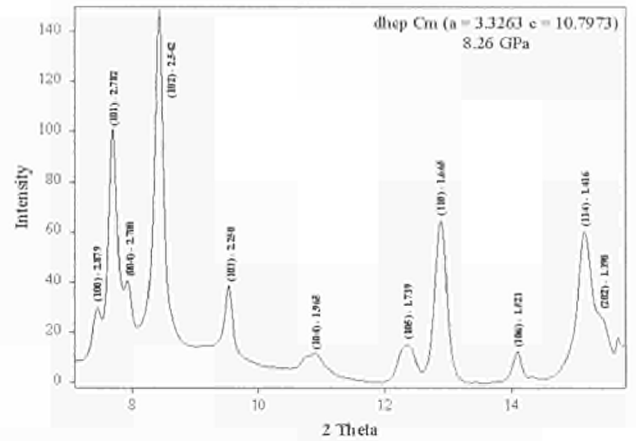


Fig. 1.9 dhcp phase of Cm observed at 8.26 GPa.

### GdNi<sub>2</sub>, YNi<sub>2</sub>, SmNi<sub>2</sub>

These compounds were studied under pressure at the Hasy-lab DESY synchrotron source and can be indexed with the cubic space group  $Fd\bar{3}m$  ( $N^{\circ} 227$ ). The X-ray patterns taken at ambient pressure with our measurements show *additional lines* which cannot be indexed in the same space group. In general, these extra lines are characterised by low intensity and with a tungsten tube as X-ray source they are usually lost in the background. The compounds in fact show a defect superstructure of cubic Laves phase C15.

As can be observed in Fig. 1.10, pressure causes the progressive extinction of these peaks. Vertical arrows indicate the peaks of the superlattice. The same behaviour was observed for GdNi<sub>2</sub> and SmNi<sub>2</sub>.

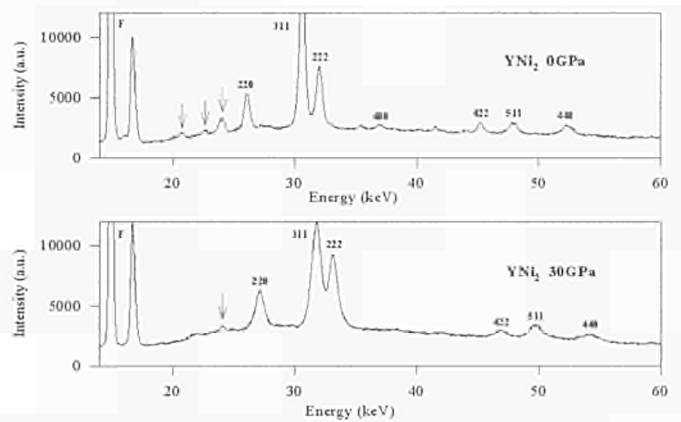


Fig. 1.10 Spectra of YNi<sub>2</sub> showing extinction of superlattice peaks (indicated by arrows) under pressure.

The pressure / volume curve shown in Fig. 1.11 does not show any phase transformation in the investigated pressure range except for the disappearance of the superstructure lines. The incompressibility anomaly at 8-10 GPa is due to the solidification of the silicone oil used as the pressure transmitting medium.

The Bulk modulus parameters determined for  $\text{YNi}_2$  and  $\text{SmNi}_2$  were 208 GPa and 200 GPa respectively.

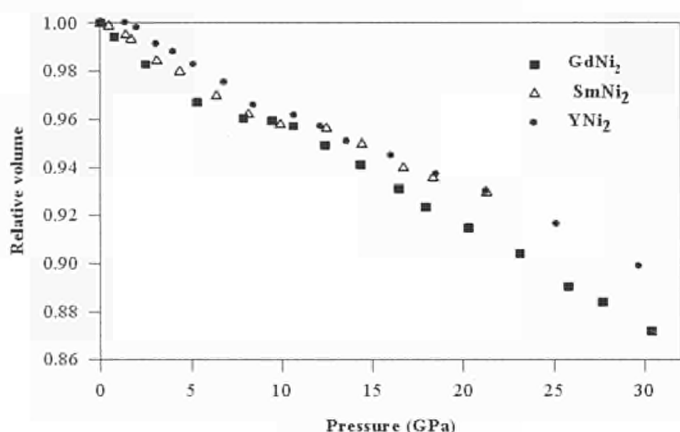


Fig. 1.11 Relative volume vs pressure of  $\text{GdNi}_2$ ,  $\text{SmNi}_2$  and  $\text{YNi}_2$ .

increase under pressure there must be a second structure for the high pressure range which must be found. From the compressibility of the first phase at low pressure we obtain a  $B_0$  of 82 GPa and for the higher pressure phase around 263 GPa. It would appear that the literature  $B_0$  value is taken from the higher pressure phase and that the real low pressure compressibility should be 82 GPa which is consistent with values for other Laves phase compounds.

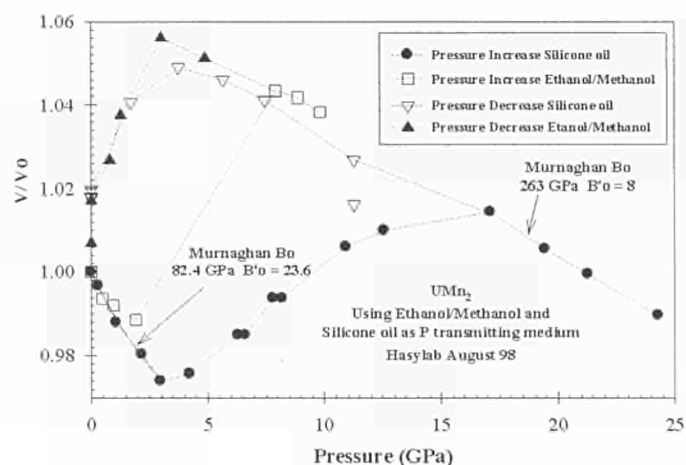


Fig. 1.12 Pressure behaviour of  $\text{UMn}_2$  up to 25 GPa.

### $\text{UMn}_2$

This sample was studied to determine why the literature value of its bulk modulus is so high at 320 GPa compared to lanthanide  $\text{X}_2$  compounds such as  $\text{ScMn}_2$  with a  $B_0$  of only 80 GPa.

We obtained a most unexpected result whereby after a normal compressibility behaviour up to about 2.5 GPa the sample volume steadily increased until about 7.5 GPa and then behaved normally again. The cubic  $\text{Fd}3\text{m}$  Laves phase starting sample had a lattice parameter of 715.17 pm which increased to 726.87 pm at 8 GPa as shown in Fig. 1.12.

The first loading was performed using an ethanol/methanol mixture as the pressure medium, so to eliminate any possibility of reaction between the sample and medium we carried out a second experiment using silicone oil which gave the same result and confirmed the unusual behaviour. Both the low and high pressure structures fit perfectly to the same  $\text{Fd}3\text{m}$  structure, but as it is impossible for the volume to

### US and Use

These samples were studied in two series of measurements to try to observe if a rhombohedral or other form of distortion could be detected as a function of pressure. Previous studies have yielded poor or inconclusive results whereas our studies of  $\text{NpS}$  and  $\text{PuS}$  showed no such distortion. Pure single crystals of US were ground to a fine powder in a glove box under argon to prevent any oxidation, and the powder samples diffracted extremely well. The fcc structure did indeed behave completely differently from  $\text{NpS}$  and  $\text{PuS}$  under pressure with clear changes to the lattice occurring progressively with pressure increase.

Use was prepared in an identical manner to the US, and under pressure also showed the same effect confirming the rhombohedral distortion. We show the results for Use (Fig. 1.13) because of its importance for the optical reflectivity.

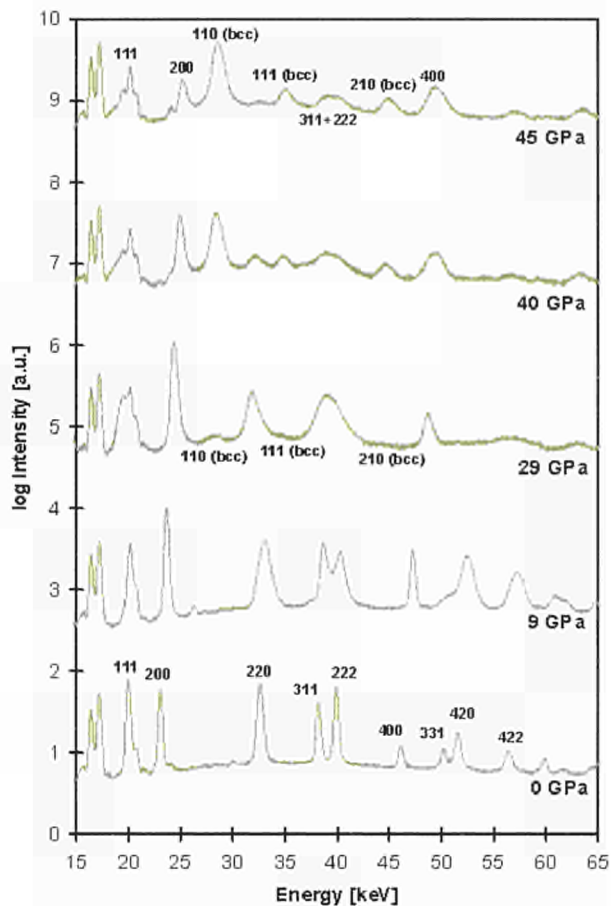


Fig. 1.13 Rhombohedral distortion and phase transition in USe.

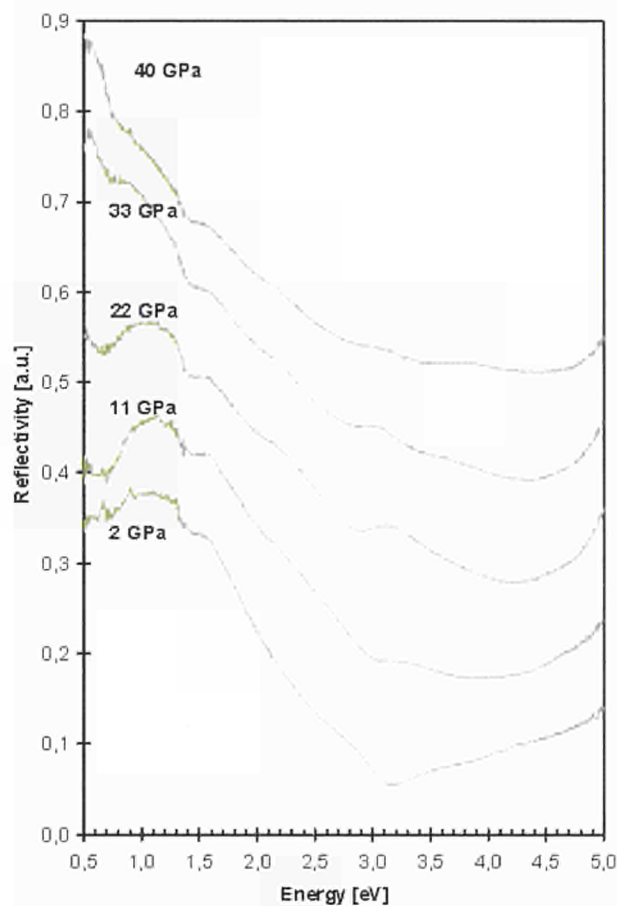


Fig. 1.14 Increasing f-d transitions and metallic behaviour in USe.

#### 1.4.3 Optical properties under pressure

We have started a programme to measure the optical properties of uranium compounds under pressure. In view of the considerable interest in actinide monochalcogenides expressed elsewhere in this report, we have started with these uranium compounds.

Fig. 1.14 shows reflectivity measurements from 0.5 eV to 5.0 eV on USe performed at the ITU as a function of pressure.

The measurements show an f-d transition that is increasing with pressure. The structural phase transition shown in Fig. 1.13 results in a new peak at 3.9 eV in the optical reflectivity (Fig. 1.14) that becomes visible around 33 GPa. In the low energy range a metallic like behaviour is recognized for increasing pressures. Similar experiments have been made on US.

### 1.5 Scattering Studies

A number of neutron experiments have been performed this year at the Institut Laue-Langevin (ILL, Grenoble). Good progress was made in understanding the crystal and magnetic structures of the  $U_2T_2In$  ( $T = Ni, Pd, \text{ and } Pt$ ) compounds. The Pt compound is especially interesting as it has a modified crystal structure with two independent U positions and these positions have a slightly different nearest neighbour configuration and different magnetic susceptibilities. Progress was also made on our study of  $UGa_3$ , and we expect work on this to be completed in 1999.

In this report we describe further neutron inelastic experiments on  $UPd_2Al_3$  showing how the complete inelastic response at low-energy transfers has been measured, and emphasizing the dramatic changes that occur at the superconducting temperature,  $T_c$ . We also present some new work on the examination of the phonons in alpha-uranium, show-

ing how they are connected to the low-temperature transition of this material into a charge-density wave.

X-ray magnetic scattering investigations have continued at both Brookhaven Nat. Lab., USA and at the European Synchrotron Radiation Facility (ESRF) in Grenoble. Experiments on the  $(\text{Np}_x\text{U}_{1-x})\text{Ru}_2\text{Si}_2$  series should be complete in 1999. New experiments on  $\text{NpO}_2$  have just been started and have already observed the magnetism long thought to exist in  $\text{NpO}_2$ , but previously uncharacterised. Here we describe experiments on thin films of  $\text{UPd}_2\text{Al}_3$ .

### 1.5.1 Neutron inelastic scattering

#### A. Heavy-fermion superconductors

We have completed the characterisation of the magnetic response in  $\text{UPd}_2\text{Al}_3$  as a function of momentum transfer ( $Q$ ), energy ( $E$ ) and temperature ( $T$ ). This material orders antiferromagnetically with an ordered wavevector  $Q_0 = [0, 0, 1/2]$  and the most interesting part of the magnetic response is found around  $Q_0$ , as shown in Fig. 1.15. The top four panels show the evolution of the response as a function of temperature. Near  $T_N$  (Fig. 1.15a) the response is quasielastic (i.e. it has its maximum at  $E = 0$ ) and has relatively little  $Q$  dependence. This is a normal situation for an antiferromagnet near  $T_N$ . At  $T_N/2$  (Fig. 1.15b) the main spectral weight is still quasielastic, which is unusual, and a weak spin wave can be seen at higher energy. On further cooling (Fig. 1.15c), the spin-wave response strengthens, but the quasielastic response remains and now becomes very sharply peaked in  $Q$ -space. Finally, below  $T_c$  (1.8 K), as shown in Fig. 1.15d, a gap opens in the spectrum, i.e. the pole of the previously quasielastic response moves away from  $E = 0$ . It is this latter effect, clearly strongly associated with the development of superconductivity, that is so surprising.

Our experiments [1], and complementary ones of Metoki et al. [2], together with further analysis [3], suggests that quasielastic part of the response (for  $T > T_c$ ) may be associated with the quasiparticles, or heavy electrons, present in  $\text{UPd}_2\text{Al}_3$ . It is then tempting to speculate that it is the interaction between these quasiparticles and the "localised" part of the  $5f$  response that drives the superconductivity. Support for such speculation is the temperature dependence of the gap (shown in Fig. 1.16). The fact that this curves follows BCS theory

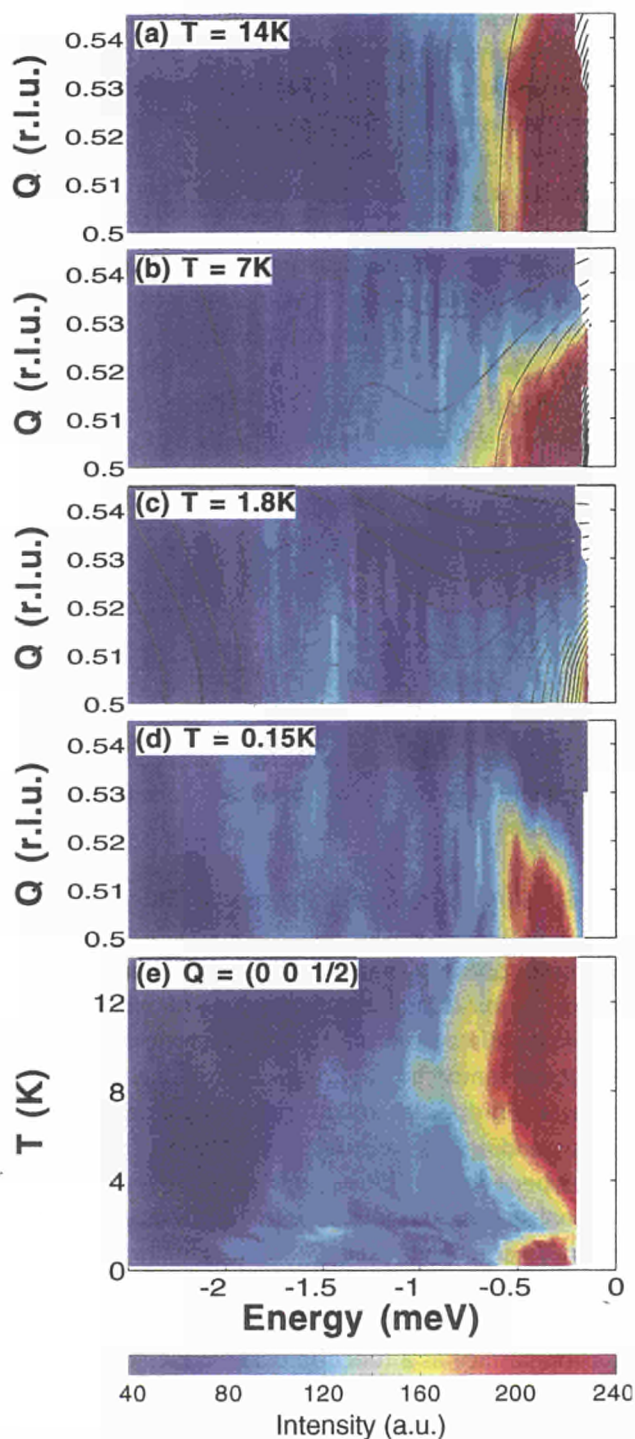


Fig. 1.15 Contour plots at four temperatures (as marked) of intensity as a function of  $Q$ ,  $Q = (0, 0, Q)$ , and neutron energy loss. The section at the smallest energy transfers is inaccessible due to the incoherent elastic scattering, and, at  $Q_0$  due to the antiferromagnet Bragg peak. The solid lines are fits to a theory described in Ref. [1,3]. Bottom panel: intensity at  $Q_0$  as a function of  $T$  and neutron energy loss. A substantial change is seen in the spectrum below  $T_c$ .

does not imply that the superconductivity is *s*-wave in form, which is certainly not the case, but simply that the quasiparticles are strongly involved in the formation of the superconducting state.

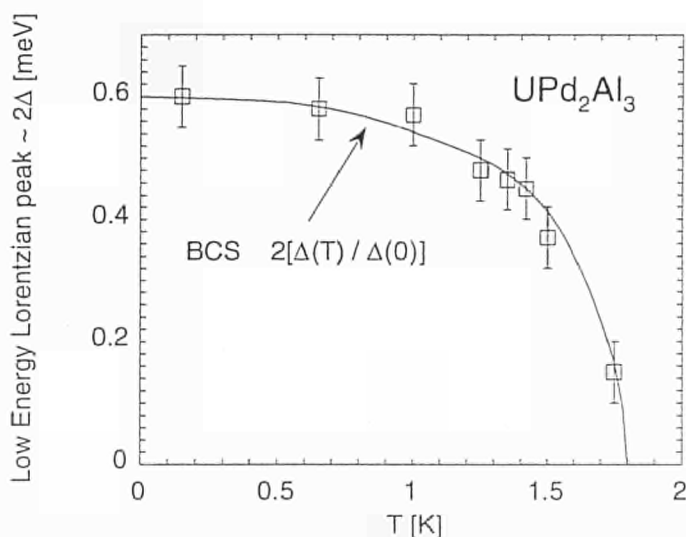


Fig. 1.16 The thermal evolution of the low-energy Lorentzian pole in the superconducting state. The solid line shows the canonical form for the BCS theory.

### B. Alpha-uranium: hints of the charge-density wave?

The ambient phase of uranium metal, the alpha phase with an orthorhombic crystal structure, is the only element, so far, to manifest a distortion to a so-called charge-density wave (CDW) at low temperature ( $T_0 \sim 43$  K) [4]. This changes many of its physical properties, and much research has been aimed at understanding this unusual phenomenon. The transition itself has been known for some time to be coupled to the vibrational spectra (phonons) of the metal, and recently at the Institut Laue Langevin in Grenoble we have performed high resolution measurements of the phonon frequencies at temperatures close to, but above,  $T_0$  [5]. Fig. 1.17 shows the dispersion surface as a function of momentum transfer taken at 55 K, i.e.  $T_0 + 12$  K. An earlier theory [6] presumed that the phonon frequencies in this region of momentum space were dependent *only* on  $q_x$ , the component of momentum in the [100] direction. This would be reflected in a simple parabola dependent only on  $q_x$  in Fig. 1.17, which is clearly not the case. Another interesting feature is that the minimum is not at  $q_x = 0.5$ , but rather at a slightly lower value. Preliminary experiments at higher temperatures suggest that the form of the dispersion surface is relatively independent of tempera-

ture, although the frequencies themselves change. The irregular shape of the dispersion surface in Fig. 1.17 is unusual, and indicates that the origin of the CDW is electronic in origin, and is actually present in  $\alpha$ -U even at much higher temperatures. The elastic constants, for example, start to show anomalies at  $\sim 200$  K. Our experiments provide confirmation of the recent theory that the CDW in  $\alpha$ -U is driven by a so-called Peierls instability arising from the unique nature of the Fermi surface [7]. Together with theory [7], the experiments point to the unusual influence of the 5*f* bonding in this classical actinide element, and open the possibility for precise predictions about the structures of the transuranium metals.

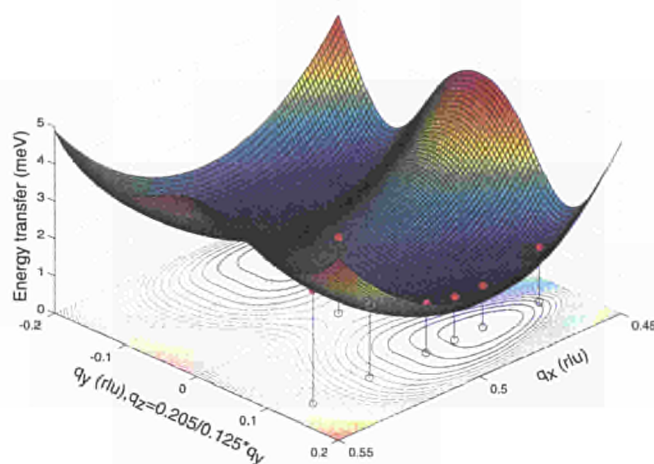


Fig. 1.17 A three dimensional view of the dispersion surface in  $\alpha$ -U, showing the position  $q' = [\sim 0.5, 0, 0]$  of the saddle point, and the minimum in the oblique direction:  $q_{\min}(55 \text{ K}) = 0.483 a^* \pm 0.125 b^* \pm 0.205 c^*$ . The red circles show the experimentally measured phonon frequencies at  $T = 55$  K.

### 1.5.2 Synchrotron magnetic scattering

Aspects of the coherent features of the X-ray beam

Photons beams from the new 3rd generation synchrotrons, such as the ESRF in Grenoble, have the property that the radiation is approaching a certain degree of *coherence*. A measure of this effect is the longitudinal coherence length, defined as  $\xi = \lambda / (\Delta\lambda / \lambda)$ , where  $\lambda$  is the wavelength of the photon beam, and  $\Delta\lambda / \lambda$  is the degree of monochromaticity. For laboratory X-ray sources, the latter is  $\sim 1\%$ , making  $\xi \sim 15$  nm, much less than the absorption length of photons

in materials or the natural coherence length of structures. However, from an undulator source with a perfect Si monochromator  $\Delta\lambda/\lambda \sim 10^{-4}$  so that  $\xi \sim 3 \mu\text{m}$  for the long wavelength photons we use for examining the actinides at the M edges. This distance is *longer* than the absorption length ( $1/\mu \sim 0.25 \mu\text{m}$ ) found at the  $M_4$  resonance energy. Under these conditions, the normal treatment for absorption of photons beams (which assumes an incoherent photon beam) is invalid and the formula must take into account the intrinsic coherence of the probe [8].

We have demonstrated these effects with a series of magnetic X-ray experiments on thin epitaxial films of  $\text{UPd}_2\text{Al}_3$  [9]. Although the coherence of the incident beam can also change the wavevector dependence, it is in the energy dependence of diffraction peaks that the most dramatic effects are seen. This is because the resonant enhancements are sharp in energy, and the absorption changes appreciably as the phonon energy sweeps through the edge. Fig. 1.18 shows the measured half-width at half maximum (HWHM) plotted as a function of optical path through the different films and for different reflections at the  $M_4$  uranium edge. The fit to the theory is excellent – clearly coherence effects must be included to understand these data.

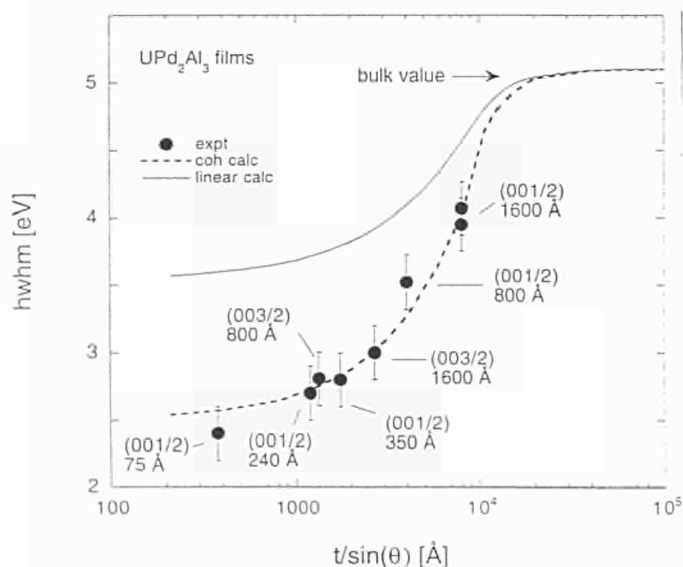


Fig. 1.18 Energy HWHM of the antiferromagnetic peaks (at  $T = 4 \text{ K}$ ) measured at the  $M_4$  absorption edge as a function of optical path ( $t = \text{film thickness}$ , and  $\theta$  is the Bragg angle for a reflection) of the photon beam in the thin films. The heavy dashed curve is the numerical simulation in the coherent approximation. The continuous line is calculated assuming the classical (incoherent) summation of intensities.

One consequence of this approach is that the energy profile of the scattering function may be used to locate the source of the scattering below the surface, which is not possible in the incoherent approximation. We demonstrate this in Fig. 1.19. For the 160 nm film at low temperature the HWHM is  $\sim 4 \text{ eV}$  (see Fig. 1.18), but on warming to near the temperature at which the antiferromagnetism disappears ( $T_N \sim 14 \text{ K}$ ) the energy width actually decreases. The profile may be fit (Fig. 1.19) only by the coherent approximation with the scattering potential located in the top  $60 (\pm 5) \text{ nm}$  of the film. A quite different profile would be obtained if the scattering volume was located at the base of the film. This implies that the film starts to order magnetically from the *top* of the film.

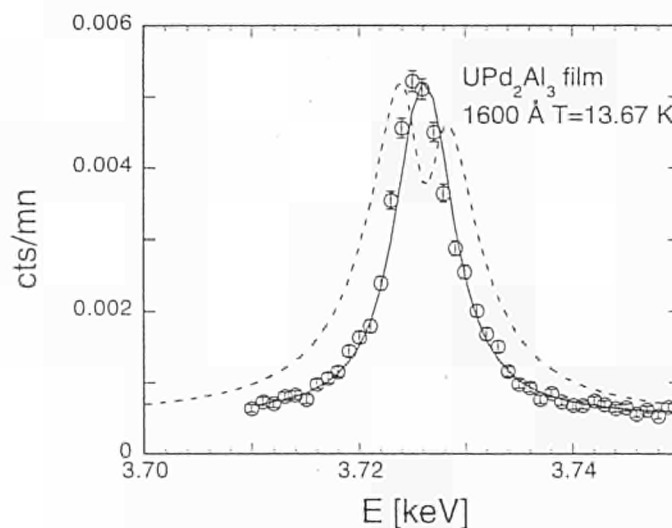


Fig. 1.19 Energy profile of the  $(0, 0, 1/2)$  reflection measured from a 160 nm film at 13.67 K, near  $T_N$ . The solid line is the calculation assuming that the scattering volume comprises just the first 60 nm, whereas the dashed line is the expected profile if this scattering volume is placed at the base of the film.

These experiments have been used to demonstrate the importance of taking account of the coherence of the incident probe, especially in the situation where large absorption is present. The observation of intense magnetic scattering from films of  $< 10 \text{ nm}$  in thickness and the high information content will be especially useful in actinide research, where there is a need to reduce the inventory of radioactive material in studies, and an increasing interest on surfaces and interfaces.

## References

- [1] N. Bernhoeft, N. Sato, B. Roessli, N. Aso, A. Hiess, G.H. Lander, Y. Endoh, T. Komatsubara, Phys. Rev. Letters 81 (1998) 4244
- [2] N. Metoki, Y. Haga, Y. Koike, Y. Onuki, Phys. Rev. Letters 80 (1998) 5417
- [3] N. Bernhoeft, B. Roessli, N. Sato, N. Aso, A. Hiess, G.H. Lander, Y. Endoh, T. Komatsubara, invited paper, Conference on "Strongly Correlated Electron Systems", Paris, July 1998, Physica B 259-261 (1999) 614-620
- [4] For a review see, G.H. Lander, E.S. Fisher, S.D. Bader, Adv. in Physics 43 (1994) 1
- [5] J.C. Marmeggi, R. Currat, A. Bouvet, G.H. Lander, Physica B 263-264 (1999) 624-626
- [6] Y. Yamada, Phys. Rev. B 47 (1993) 5614
- [7] L. Fast, O. Eriksson, B. Johansson, J. M. Wills, G. Straub, H. Roeder, L. Nordström, Phys. Rev. Letters 81 (1998) 2978
- [8] N. Bernhoeft, Acta Cryst. A 55 (1999) 274
- [9] N. Bernhoeft, A. Hiess, S. Langridge, A. Stunault, D. Wermeille, C. Vettier, G.H. Lander, M. Huth, M. Jourdan, H. Adrian, Phys. Rev. Letters 81 (1998) 341

## 1.6 Theory

### 1.6.1 Theory of antiferromagnetism for uranium dioxide

Uranium dioxide is an insulating antiferromagnet below 31 K with a saturated magnetic moment of  $1.8 \mu_B$ /atom. There is abundant evidence from measurements that the 5f states are localized in this compound and that they lie in a gap of about 4 eV between the filled valence bands and the empty conduction bands. We have already computed the electronic structure of  $\text{UO}_2$  and its cohesive properties, finding good agreement with measurements [1]. Our knowledge of the electronic structure suggests the following model for the antiferromagnetism: (a) the localized uranium 5f magnetic moment polarizes the uranium 6d states at the uranium site via local exchange interactions; (b) hybridization between the 6d states and the oxygen 2p states leads to coupling between the 6d spin densities on different uranium atoms, hence to an indirect coupling between the corresponding 5f moments. This model is a formulation of the theory of superexchange [2] suitable for multiple scattering band theory.

Application of the Landau theory of phase transitions [3] leads to the following expression for the Neel temperature  $kT_N = \chi_{df} J_{f-d}^2 [(g-1)/g]^2 (\mu_{\text{eff}}^2/3)$  where the effective moment,  $\mu_{\text{eff}}$ , is known from measurements to be  $3.2 \mu_B$  and the g-factor for the localized 5f states is calculated to be 0.821

for a  $5f^2$  configuration. We evaluate the exchange interaction,  $J_{f-d}$ , from self-consistent density functional theory [4] to be 204 meV. The remaining quantity,  $\chi_{df}$ , is the partial susceptibility of the 6d magnetic moment to the exchange field of the 5f moment. We evaluate by making self-consistent calculations for the antiferromagnetic ground state for several values of the 5f moment and using the resulting 6d moment in  $\chi_{df} = \mu_d / \mu_f \approx 0.4$ . The calculated value for  $T_N$  is then 29.6 K. The success of this model for  $\text{UO}_2$  leads us to expect a wide range of application to superexchange in other antiferromagnets.

## References

- [1] P. J. Kelly, M.S.S. Brooks, J. Chem. Soc., Faraday Trans. 83 (1987) 1189
- [2] P.W. Anderson, Phys. Rev. 79 (1950) 350
- [3] L. D. Landau, Soviet Physics JETP 3 (1957) 920
- [4] P. Hohenberg, W. Kohn, Phys. Rev. 136B (1964) 864; W. Kohn, L.J. Sham, Phys. Rev. 140A (1965) 1133

### 1.6.2 Optical properties of $\text{URu}_2\text{Si}_2$

$\text{URu}_2\text{Si}_2$  is a heavy fermion compound in which superconductivity and magnetic order coexist. The latter is characterized by a vanishingly small magnetic moment of  $0.03 \mu_B$  and a Neel temperature of 17.5 K. Moreover there are anomalies in the measured linear and non-linear susceptibility, specific heat and thermal expansion. Conventional electronic structure calculations have failed to reproduce the ordered moment whereas more phenomenological theory has been based upon quadrupolar ordering.

The optical properties have been measured in the paramagnetic phase [1] which presents the opportunity to test whether theory reproduces the electronic structure over a broad energy range. The optical constants and optical conductivity were calculated [2] ab initio using self-consistent density functional theory [3] and the linear muffin tin orbital band structure method [4]. The calculated optical conductivity is compared with measurements in Fig. 1.20. Our conclusion is that the measurements are reproduced well enough for us to conclude that the gross features of the calculated electronic structure are sound.

Contact (1.5): Gerard Lander • tel.: +49 7247 951 382 • fax: +49 7247 951 599 • [lander@itu.fzk.de](mailto:lander@itu.fzk.de)

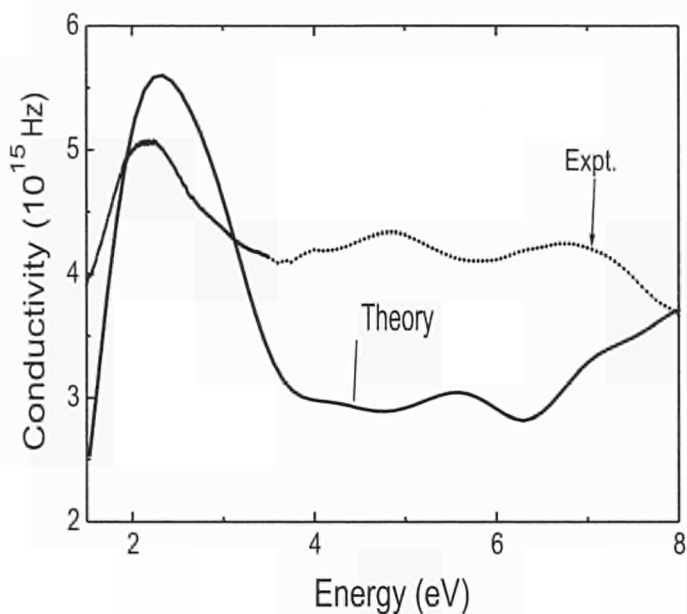


Fig. 1.20 The calculated and measured optical conductivities of  $URu_2Si_2$ .

## References

- [1] J. Schoenes, U. Barkow, M. Broschwitz, J. Lammers, K. Litfin, R. Schulz, D. Kaczorowski, B. Becker, A. Menovski, N. Patil, 28èmes Journées des Actinides, May 14-16, 1998, Uppsala, Sweden
- [2] P. Monachesi, A. Continenza, M.S.S. Brooks, M. Grioni, 28èmes Journées des Actinides, May 14-16, 1998, Uppsala, Sweden
- [3] P. Hohenberg, W. Kohn, Phys. Rev. 136B (1964) 864; W. Kohn, L.J. Sham, Phys. Rev. 140A (1965) 1133
- [4] O.K. Anderson, Phys. Rev. 12 (1975) 3060

## 1.7 Thermodynamic Properties

### 1.7.1 Experiment on high-pressure melting of uranium dioxide: a comparative study

Experimental data on the melting behaviour of  $UO_2$  under pressure are so far completely missing. Recent experimental studies have revealed new aspects of the melting process, which occurs within a complex scenario of first and second order phase transitions [1]. In this context, the dependence of the melting point on pressure defines an important invariant curve, which is a function of the chemical and physical properties of both liquid and solid.

Contact (1.6): Michael S.S. Brooks • tel.: +49 7247 951 476 • fax: +49 7247 951 599 • brooks@itu.fzk.de (1.6)

**Tungsten** was first measured as a reference material. Its melting point at ambient pressure is  $3680 \pm 10$  K [2]. The pressure dependence of  $T_m$  is plotted in Fig. 1.21. The measured slope is 9 K/kbar, whereby the observed increase in the melting temperature between 1 and 2000 bar is approximately 20 K, i.e. five times the measurement precision. Three authors already investigated high-pressure melting of tungsten [3,4,5]; our results are in line with their results.

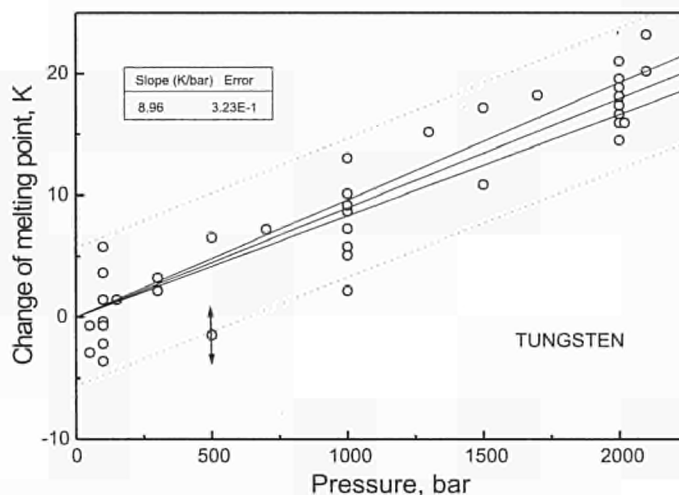


Fig. 1.21 Melting point of tungsten as a function of pressure.

For **uranium dioxide** the variation of the melting point vs. pressure,  $p$ , is shown in Fig. 1.22. The average slope of the line is 41 K/kbar, approximately four times larger than that of tungsten. In order to ascertain that this variation was not due to stoichiometry changes, the samples were submitted to measurement cycling over the full explored pressure range: no hysteresis was detected.

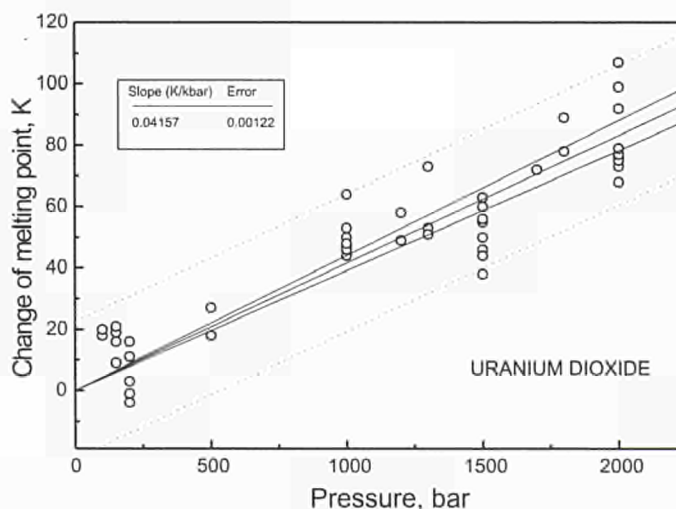


Fig. 1.22 Change of the melting point of  $UO_2$  as a function of pressure.

The obtained data were compared with the values predicted by the Clausius-Clapeyron equation, which asserts that, under equilibrium conditions of liquid and solid, the slope of  $T_m$  vs.  $p$  is equal to the ratio of the volume change across melting to the entropy of fusion.

In the case of tungsten our results reasonably satisfy this thermodynamic equation. The results of  $UO_2$  are more problematic. The measured melting slope is almost four times larger than that predicted by thermodynamics, where the melting expansion and melting entropy are well established. We must therefore conclude that liquid  $UO_2$  was not in thermodynamic equilibrium with the solid and, hence Clapeyron's equation was not valid in the form described above. *It remains, however, unclear, which process could affect the entropy of the liquid (or of the solid) to such an extent as to produce the large pressure dependence of the melting point observed.*

#### References

- [1] C. Ronchi, G.J. Hyland, J. Alloys and Comp. 213 (1994) 159.
- [2] J. P. Hiernaut, F. Sakuma, C. Ronchi, High Temp.-High Press. 21 (1989) 139.
- [3] L. F. Vereshchagin and N. Fateeva, High Temp.-High Press. 9 (1977) 619.
- [4] R.S. Hixson and M.A. Winckler, Int. J. Thermophys. 11 (1990) 709.
- [5] A. Berthault, L. Arles, and J. Matricon, Int. J. Thermophys. 7 (1986) 167.

### 1.7.2 Experiment demonstrates the consistency of the phonon and small-polaron model for thermal conductivity of $UO_2$ up to 2700 K

The new high temperature measurements of the thermal properties of  $UO_2$  reported in the previous report (TUAR97, p. 17 and 61-62) have been connected to measurements at lower temperatures, and to those related to the threshold of the lambda transition (2670 K).

Our measurements of the heat capacity (Fig. 1.23) up to ~2600-2700 K are in good agreement with present recommendations [1,2], but diverge at higher temperatures, necessitating a revision of the current views on the physical heat absorption mechanisms. Actually, at temperatures above 2700 K the effects of the lambda-transition should be negligible (its peak is only 20-30 K wide); therefore the further increase of  $C_p$  must be connected to the creation of a different type of defect, very likely small polarons or Schottky

defects. The value of  $C_p$  we measured at 2850 K is only 10% higher than that we previously measured just below the melting point, using a more sophisticated laser heating technique, requiring, however, a more complicated analysis [3]. Therefore, the high value of  $C_p$  in the vicinity of the solidus confirms the existence of a pronounced fall of the heat capacity across melting [3].

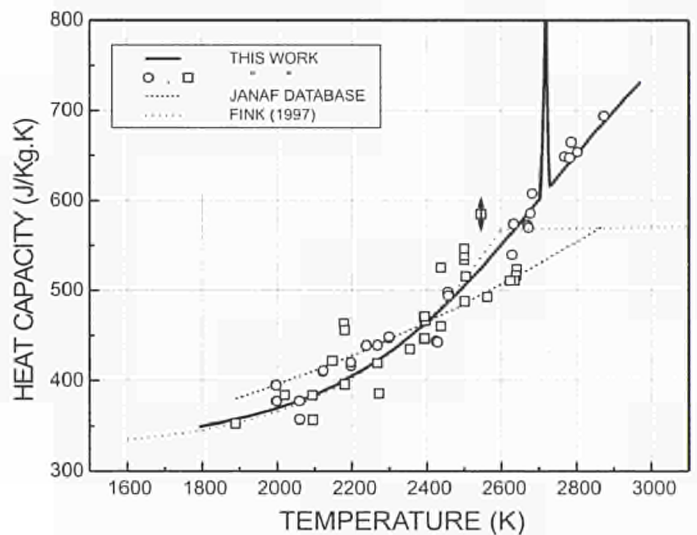


Fig. 1.23 Heat capacity of  $UO_2$  at high temperatures.

In the graph of the inverse of the thermal diffusivity,  $\alpha$ , (Fig. 1.24) as a function of temperature it can be seen that for  $T < 2600$  K the high temperature measurements are reasonably well aligned with the extrapolation of the straight line defined by the low-temperature points. Above the lambda-transition, however, the measured  $1/\alpha$  values fall below this line.

One can see that at high temperature the resistivity values are more scattered, displaying a negative deviation with respect to the straight line defined by the low temperature measurements - although at the highest temperatures this deviation reduces somewhat. For comparison, the data of Bates [4] and Weilbacher [5] are given.

We have analysed our measurements in terms of phonon scattering,  $\lambda_L$ , and small polaron formation  $\lambda_{AP}$  in order to separate the respective (lattice and electronic) contributions to the thermal conductivity.

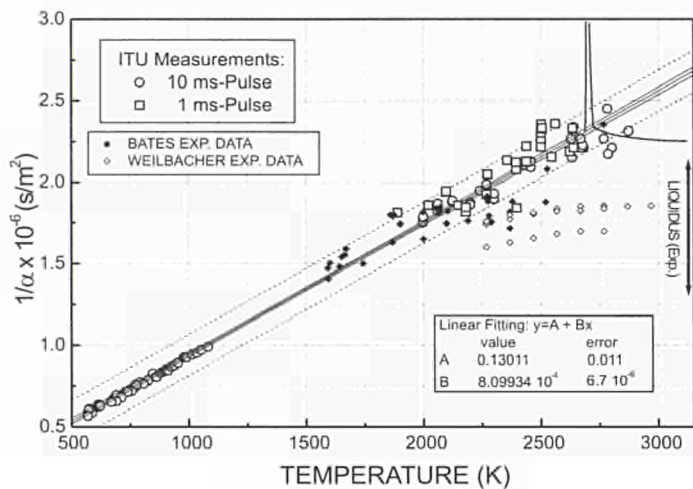


Fig. 1.24 Inverse of thermal diffusivity of  $UO_2$ .

We have interpolated our conductivity measurements with a fifth-order polynomial to give  $\lambda$  as a function of  $T$ ; (Fig. 1.25); this entails obviously an uncertainty band in the extrapolated range from 2900 K to the melting point. Two extremes can be reasonably calculated, between which the real value of  $\lambda$  should fall. The upper one is obtained (i) by assuming a linear extrapolation of  $C_p$ , which gives approximately 800 J/Kg K at 3120 K, and (ii) by a constant extrapolated value of the diffusivity ( $0.45 \text{ cm}^2/\text{s}$ ): the resulting thermal conductivity is in this case 3.5 W/m.K. The lower limit is realised by a linear extrapolation of  $1/\alpha$ , and a constant  $C_p$  (700 J/Kg K) at temperatures above those reached in our experiments: the corresponding conductivity is 2.4 W/m.K.

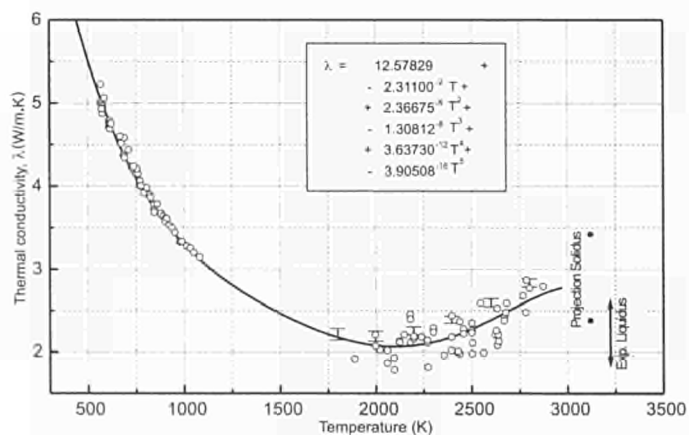


Fig. 1.25 Thermal conductivity of  $UO_2$ : new assessment after recent ITU measurements.

In conclusion, the new measurements of  $\alpha$  reveal a dependence on temperature closer to that predicted by a simple 3-phonon scattering model, whilst  $C_p$  continues to increase with temperature above the lambda transition at 2670K.

The resulting values of  $\lambda$  confirm the existence of a minimum around 2000K, however the upswing at higher temperature is less pronounced than previously assumed.

In particular, following our measurements the conductivity at the solidus point can be extrapolated with a certain confidence obtaining  $\lambda(T_m) \sim 3 \text{ W/m.K}$ . Since the measured drop of the product of heat capacity times density across melting is approximately 40%, this value of the conductivity of the solidus is no longer inexplicably too high compared to that of the liquid ( $2.5 \pm 1 \text{ W/m.K}$ ). It is gratifying that this independently measured value [6] falls in the centre of the band defined by the two extrapolations of the new "experimental" values of  $\lambda$ .

#### References:

- [1] Joint Army-Navy-Air Force (JANAF) Database, Third Edition (1985), United States Department of Commerce
- [2] J.K. Fink, M.C. Petri, Report ANL/RE-97/2, Argonne National Lab., IL USA (1997)
- [3] C. Ronchi, J.P. Hiernaut, R. Selfslag, G.J. Hyland, Nucl. Sci. Eng. 113 (1993) 1-19
- [4] J.L. Bates, Report BNWL-1431, (1970), Battelle Pacific Northwest Lab., Richland, WA (USA)
- [5] J.C. Weilbacher, Report CEA-R-4572 (1974), Commissariat à l'Energie Atomique (France)
- [6] H.A. Tasman, TUAR-88, p. 80-84, Report EUR 12385 EN, European Commission, Joint Research Centre, Karlsruhe, Germany (1988)

### 1.7.3 Ionisation and dissociation potentials of uranium and plutonium oxides

The ionisation and dissociation energies of the different uranium and plutonium oxides have been measured by mass spectrometry of molecular beams produced by Knudsen effusion at high temperature. The values obtained are consistent with the existing thermodynamic data of these oxides. Based on the experimental molecular parameters, a general formula for the ionisation and dissociation/ionisation cross sections through electron inelastic scattering was obtained for collision energies up to 70 eV. This formula can be used to

a) UO <sub>x</sub>								
Daughter Mother	*	U <sup>+</sup>	U	UO <sup>+</sup>	UO	UO <sub>2</sub> <sup>+</sup>	UO <sub>2</sub>	UO <sub>3</sub> <sup>+</sup>
UO <sub>3</sub>	7.8 ±0.1	27.6±0.3	21.7±0.2	19.4±0.2	13.8±0.1	11.3±0.1	5.9±0.1	10.8±0.1
UO <sub>2</sub>	7.2±0.1	21.7±0.3	15.6±0.1	13.4±0.1	7.9±0.1	5.4±0.1	-	
UO	6.5±0.1	14.0±0.2	7.9±0.1	5.6±0.1	-			
U	5.5±0.1	6.1±0.1	-					
b) PuO <sub>x</sub>								
Daughter Mother	*	Pu <sup>+</sup>	Pu	PuO <sup>+</sup>	PuO	PuO <sub>2</sub> <sup>+</sup>		
PuO <sub>2</sub>	7.4±0.1	19.2±0.2	13.0±0.1	12.8±0.2	6.2±0.1	10.1±0.1		
PuO	6.6±0.1	16.2±0.2	6.9±0.1	6.6±0.1	-			
Pu	5.6±0.1	6.1±0.1	-					

\*mean square diameter of the outer orbital (Å)

Tab. 1.5 Measured formation energies (eV) of ions, and neutral and positive single- charged fragments.

calculate the composition of equilibrium vapour mixtures over UO<sub>2</sub> and PuO<sub>2</sub> from mass spectrometric measurements.

The difficulty of the reported experiment are caused by the non-congruent sublimation of uranium and plutonium oxides. Thus a marked increase in the sublimation rate at hyperstoichiometric compositions of UO<sub>2+x</sub> and uranium-rich mixed oxides is a salient aspect of the high-temperature behaviour of this compound, which in nuclear reactor applications may entail considerable technological problems. Experimental data remain scanty and imprecise at high temperatures, where classical thermodynamic measurements are difficult. Endeavours to analyse by mass spectrometry (MS) the equilibrium vapour in Knudsen-effusion experiments were only in part successful: in all cases, only the pressure of MO<sub>2</sub> (g), the major vapour species at O/M ≈ 2.00, could be measured with an adequate precision, whilst the quantitative analysis of the other species led to less precise results. Here oxide vapours of uranium and plutonium were investigated with the aim of providing the necessary experi-

mental data for obtaining the "true" concentrations of the gaseous species MO<sub>x</sub> from ordinary mass spectrometric analysis of an effusing molecular beam.

#### a) Uranium oxide

Mass-spectrometric measurements of molecular beams produced by Knudsen-cell effusion at temperatures above 2200 K were analysed to obtain a self-consistent set of parameters to be fed into the cross section expressions. The results are collected in Tab. 1.5. The values are averages over different measurements; the errors range from 1% for the primary ionisation, to 5% for more complex ionisation processes.

The measured first ionisation potentials of U and UO<sub>2</sub> are, within 2% in agreement with the values published by Rauh and Ackermann [1] and Gurvich [2]. That of UO<sub>3</sub> (10.8 eV) is between 11.1 eV, given by Pattoret [3], and 10.6 eV by Ackermann. The threshold energies for dissociation, calculated from the appearance potentials of the respective ions as

fragments are in good agreement with the thermodynamic values of the total dissociation energies of the reactions  $UO_m \rightarrow U+mO$  reported in the thermodynamic Tables. This agreement is particularly significant, as it corroborates thermodynamic data of uranium oxides, which, so far, have been assigned, in the TPIS Tables, the low-precision class "6-F". This especially regards  $UO_3$ , whose formation energy is rather uncertain, and the dissociation of  $UO$ , for which there exists only one measurement by De Maria [4] (7.7 eV).

Finally, an attenuation factor,  $K$ , was found for the first ionisation rate of  $UO_3$ ; this was evaluated from effusion experiments of largely hyperstoichiometric  $UO_{2+x}$ , obtaining as average:  $K=0.37$ .

This means that, at any energy  $E < 70$  eV, only 37% of the collisions with  $UO_3$  molecules lead to a positive ion formation, whilst the rest results into a dissociation into neutral fragments.

### b) Plutonium oxide

The results for plutonium oxide are collected in *Tab 1.5b*. The only published data are those obtained at ANL in the sixties [5, 6]: our ionisation energy of  $PuO_2$  and  $PuO$  are higher: respectively 10.1 eV (instead of 9.4 eV) and 6.6 eV (instead of 6.2 eV).

From the appearance potential of  $PuO^+$  from  $PuO_2$  (12.8 eV), and of  $Pu^+$  from  $PuO$  (13.0 eV) we deduced from our data a dissociation energy for  $PuO_2 \rightarrow PuO+O$  of 6.2 eV, and for  $PuO \rightarrow Pu+O$  of 6.9 eV, which are close to the recommended formation enthalpies. These data are corroborated by the measured appearance potential of the  $Pu^+$  fragments from  $PuO_2$  dissociation (19.2 eV), which is in line with the latter.

Our results show that, contrary to the case of uranium, the monoxide of plutonium has higher ionisation energy than the metal atom. Rauh and Ackermann [1] observed that monoxides are generally easier ionised than the respective metal, in this context, however, calcium and hafnium represent clear exceptions. Plutonium seems also to exhibit this exception. This effect can be attributed to the strong f-p hybridisation in the oxygen-plutonium bonding [7] leading to the observed high stability of  $PuO_2$ , whose saturated bonding entails a very large ionisation energy (10 eV. compared to 5.4 eV of  $UO_2$ ).

### References

- [1] E.G. Rauh, R.J. Ackermann, *J. Chem. Phys.* 60 (1974) 1396
- [2] L.V. Gurvic, "Termodinamicheskie svoystva individual'nykh veshchestv" (Thermodynamic properties of individual substances) Tome IV, p.181 et sgg., Nauka, Moscow, 1982
- [3] A. Pattoret, J. Drowart, S. Smoes, in "Thermodynamics of Nuclear Materials", p.613 et sgg., IAEA, Vienna (1968)
- [4] G. De Maria, R. P. Burns, J. Drowart, and M. M. Inghram, *J. Chem. Phys.* 32 (1960) 1373
- [5] P. E. Blackburn, A. D. Tevebough, J. D. Bingle, Report ANL-7575, (1968), Argonne National Lab., IL (USA)
- [6] P. E. Blackburn, J. E. Battles, Report ANL-7445, (1968), Argonne National Lab., IL (USA)
- [7] Gubanov, in a series of articles ( see e.g. V.A. Gubanov, A. Rosèn and D. E. Ellis, *J. Phys. Chem. Solids*, 40 (1979) 17) showed that in the actinide oxides f-p hybridisation strength increases with atomic number and attains maxima in Np, Pu and Cm

### 1.7.4 Equation of State of $UO_2$ up to the critical point

The INTAS Project 93-066 on the equation of state of nuclear fuel up to very high temperatures is entering into the concluding phase.

The equation of state of nuclear fuel is generally used for predicting the consequences of severe reactor accidents, in which the fuel is transformed into a hot fluid with an equilibrium vapour at high-pressure. By definition, the equation of state accounts for all the thermodynamic properties of the material at any temperature, so that its theoretical formulation involves a self-consistent analysis of all the possible physical states of the material. In fact, among them, the liquid state is that which presents the greatest difficulties for a theoretical description. Therefore, the principal aim of the Project was to create a theoretical model for *liquid and gaseous*  $UO_2$ , capable of correctly reproducing the available experimental data, and sufficiently well founded to be used for extrapolating thermodynamic properties up to temperatures of the order of 10000 K.

The Project activity consists of both experimental and theoretical work, the former being mainly performed in the IV-TAN Laboratory in Moscow and, in part, in the Institute for Technical Physics in Tashkent. Results concerning the thermal radiative and melting properties of liquid  $UO_2$ , as well as the mechanisms of energy absorption at very high temperatures have been obtained, and in part published in the open

literature. To date, endeavours are still in progress to perform experimental measurements of the total equilibrium partial pressure above 5000 K. The heating experiments, carried out in a high-pressure autoclave by means of laser heating, have faced serious difficulties due to creation of high density plasma in the vapour. Various expedients are still being tested in order to avoid this disturbance that has deleterious effects on both energy deposition and temperature measurements.

The kernel of the project consists of the development of a liquid model, based on a complex "quasi-chemical" approach, involving virtual clusters interacting through *pseudo-potentials*. An exhaustive review work on molecular and thermodynamic data of uranium oxide and analogous materials was carried out in view of selecting the properties, which were to be assumed as distinct "calibration points" of the model. This is intrinsically constructed in order to account for non-congruency of phases in equilibrium, entailing a description of non-stoichiometric states of the fluid. Therefore, the validation of the model presently involves a comparative analysis over an extended field of parameters, which still requires considerable work.

Finally, thermodynamic criticality in such a complex system must be referred to a much more articulate definition than for simple species. This behaviour entails important implica-

tions on the features of the thermodynamic functions at very high temperatures – e.g. the density coexistence curve may assume a shape, by which application of the rectilinear diameter rule would be essentially erroneous.

The model was discussed with specialists of different countries and presented at various Conferences. A monograph is being prepared on the subject.

### 1.7.5 Multi-wavelength pyrometry: recent advances

In the frame of the "Competitive Activities and Technology Transfer Programme" of the European Commission a Project has been launched (DGXIII-ITT CSA98 133) for the development of advanced spectral pyrometry methods for temperature measurements under extreme conditions.

A new set-up has been constructed, where the image of the measured surface is projected onto the entry of an optical fibre, through which the light is conveyed onto a micro-grating, diffracting onto an array detector (Fig. 1.26). Grating and detector (with an integrated pre-amplifier and 16-bit A/D converter) are assembled in a standalone small box. Therefore, the pyrometer merely consists of a suitable objective and a small, loose detecting unit of a few centimetre size.

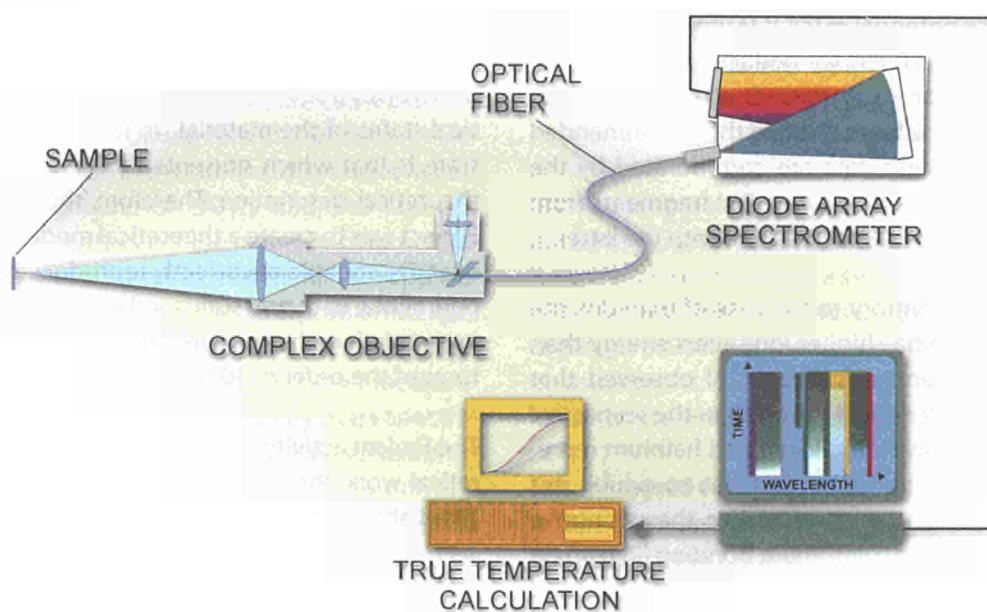


Fig. 1.26 Scheme of the 500-wavelength array pyrometer.

Promising results have been obtained in test experiments carried out with provisional components. A spectral range from 400 to 900 nm was investigated using a Si-array detector with 600 channels. The difficulties related to the dynamic range to be covered in the chosen spectral range (the quality of the temperature measurement increases with its broadness) have been in part resolved, so that temperature measurements could be carried out in a sufficiently large temperature interval. Also the calibration procedure proved to be feasible and easily applicable.

An interesting result of the signal elaboration is the prediction of the detailed spectral emissivity curve. Under standard conditions this output can be compared with real data, and hence be used to estimate the accuracy of the method. As for the precision, the large number of available channels to disposal furnishes an input, which statistically reduces the residual standard deviations (<0.1%) to at least one order of magnitude below the systematic errors.

The inset in Fig. 1.27 shows the measured spectral brightness at 2162 K of one of our tungsten band-lamps, normally used for calibration purposes. The tungsten-band emissivity is certified for one reference wavelength (630 nm), whilst for the other wavelengths it was measured in different laboratories with the maximum achievable accuracy at this temperature. Fig. 1.27 shows the real spectral emissivity of the tungsten band and that obtained from the analysis. The discrepancy is less than 2%, entailing an error in temperature of the order of approximately 4 K.

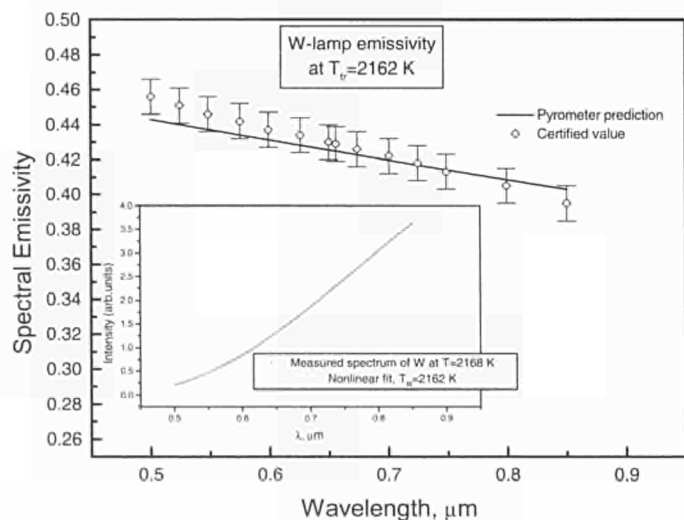


Fig. 1.27 Spectral emissivity measured by the 500-channel pyrometer.

Contact (1.7): Claudio Ronchi • tel.: +49 7247 951 402 • fax: +49 7247 951 591 • ronchi@itu.fzk.de

The development work will continue during 1999, with the aim of constructing a prototype pyrometer for technology transfer applications.

## 1.8 Alpha Immunotherapy

### Introduction

There is a growing interest in using  $^{213}\text{Bi}$  for targeted tumour therapy using specific monoclonal antibodies (mAb) or peptides. ITU has been further approached by clinics for the supply of  $^{225}\text{Ac}$  generators (Tab. 1.6).

As soon as the hospitals will conclude the preclinical studies and start with clinical treatments requiring larger  $^{213}\text{Bi}$  generators, we have to have set up the production by the  $^{226}\text{Ra} (p, 2n) ^{225}\text{Ac}$  process. As described below the feasibility of the production route is established.

### 1.8.1 Ongoing pre-clinical and clinical studies

ITU supplied  $^{213}\text{Bi}$  generators for the ongoing trials. The following summarizes the progress. A more detailed description is available in a special publication which can be received upon request.

For the phase I study at the Memorial Sloan Kettering Cancer Center, New York, several 30 mCi  $^{213}\text{Bi}$  generators were supplied for the treatment of relapsed or refractory myeloid leukemia of now 17 patients.  $^{213}\text{Bi}$  was conjugated to the humanized antibody HuM195 by the bifunctional chelate (CHX-A-DTPA). Ten of 12 evaluable patients had reductions in peripheral blood leukaemia cells, and 12 of the 17 patients had decreases in the percentage of bone marrow blasts. No complete remissions have been observed to date. This is the first study to show that targeted alpha-particle therapy is feasible in humans.

At the Abteilung Nuklearmedizin der Georg-August-Universität Göttingen the toxicity and anti-tumor efficacy with the  $\alpha$ -emitter  $^{213}\text{Bi}$  was assessed as compared to the  $\beta$ -emitter  $^{90}\text{Y}$ , linked to a monovalent Fab' fragment in a human colon cancer xenograft model in nude mice. In the metastatic model, all untreated controls died from rapidly progressing hepatic metastases at 6-8 weeks after tumor inoculation, whereas a histologically confirmed cure was observed in 95% of those

Partner	Cancer type	mAb or peptide
Memorial Sloan Kettering Cancer Center, New York (USA)	acute myelogenous leukaemia (AML)	HuM195
	prostate cancer	J591
INSERM, Nantes (F)	multiple myeloma	B-B4
University of Heidelberg (D)	non-Hodgkin's lymphoma (NHL)	CD-19, 20, 22
Clinic Hasselt, Univ. of Gent (B)	non-Hodgkin's lymphoma (NHL)	CD-19, 20, 22
University of Göttingen (D)	colon cancer	CO17-IA
Kantonsspital Basel (CH)	low grade glioma	peptide: somatostatin
Universitätskliniken München (D)	stomach cancer	7E6 / 6H8

Tab. 1.6 Overview of the present ongoing trials.

animals treated with 700  $\mu\text{Ci}$   $^{213}\text{Bi}$ -Fab' two weeks after model induction, which is in contrast to an only 20% cure rate in mice treated with 250  $\mu\text{Ci}$   $^{90}\text{Y}$ -Fab' [1].

Investigations on the binding characteristics of the  $^{213}\text{Bi}$  labelled monoclonal antibody for the mutant E-Cadherin molecule started with the Nuklearmedizinische Klinik und Poliklinik der Technischen Universität München. In xenotransplanted tumors in nude mice the binding of the mutant specific antibody was higher by a factor of 3 - 4 compared with tumors expressing wild type antigen after  $^{125}\text{I}$  labelling as well as  $^{213}\text{Bi}$  labelling. After intratumoral injection of  $^{213}\text{Bi}$  labelled mutant specific MAb the activity was retained near the injection site 1-2h after administration as demonstrated on frozen sections by a microimager system.

Alpha-Immunotherapy with-peptides for low grade glioma are envisaged at the Kantonsspital Basel, Radiological Center. An improvement compared to the use of DOTA<sup>0</sup>-D-Phe<sup>1</sup>-Tyr<sup>3</sup>-octreotide (DOTATOC) labelled with  $^{90}\text{Y}$  is expected from the  $\alpha$ -emitter  $^{213}\text{Bi}$ . First experiments aimed at the labelling of DOTATOC with  $^{213}\text{Bi}$ .

For the definition phase of the innovation program IN30848 in collaboration with the university hospitals of Heidelberg and Gent and the German Cancer Research Center specific and unspecific cytotoxicity of  $^{213}\text{Bi}$  labelled CD19, CD20 and CD22 antibodies towards B-cell lines Daudi and K422 was studied at dose levels between 0.75 and 1.8  $\mu\text{Ci}/200\mu\text{l}$  [2].

In the two projects CSA 96202/96P04 and CSA 96114/96P03 carried out together with INSERM/SUBATECH in Nantes the feasibility study of B-B4 monoclonal antibody coupled to  $^{213}\text{Bi}$  with CITC-DTPA chelate showed high dose-dependent cell mortality of myeloma cells. In the context of this feasibility study of ex-vivo bone-marrow purging we are concerned with the non-specific irradiation of normal cells. The longer half-life of the  $^{225}\text{Ac}$  (parent nuclide of  $^{213}\text{Bi}$ ) would allow

cancer to be treated with a longer delay between production and administering and a longer irradiation of the tumor. To connect the antibody to the radioisotope the coupling of  $^{225}\text{Ac}$  with existing ligands and newly synthesized compounds using Albumin (HSA) was tested.

### 1.8.2 Direct production of $^{225}\text{Ac}$ through irradiation of $^{225}\text{Ac}$ [3, 4]

The CSA96103/96P02 project was carried out in collaboration with the cyclotron division of the German Research Centre Forschungszentrum Karlsruhe (FZK). In the course of the project the optimal  $^{226}\text{Ra}$  target design was determined as a silver envelope with a thickness of the front and back side of each 250  $\mu\text{m}$ . The results of 8 irradiations and their subsequent analysis at ITU indicate that an one Ci  $^{225}\text{Ac}$  production is feasible.

#### References

- [1] T.M. Behr, R.M. Sharkey, M.E. Juweid., R.D. Blumenthal, R.M. Dunn, G.L. Griffiths, L. Gary, H.-J. Wolf, G. Friedrich, W.S. Becker, D.M. Goldenberg, Cancer Research 55(17) (1995) 3825-3834
- [2] Alpha-Radioimmunotherapy with  $^{213}\text{Bi}$ -labelled CD19, CD20 and CD22 antibodies for B-cell Lymphoma, A. Wilmes, M.T. Voso, C. Apostolidis, R. Molinet, G. Moldenhauer, H. Wesch, G. van Kaick, L. Koch, R. Haas, W. Janssens, ASH (American Society for Hematology) Conference, 5.-8. Dezember 1998
- [3] L. Koch, J. Fuger and J. Van Geel, "Verfahren zur Erzeugung von  $^{225}\text{Ac}$  (durch Bestrahlung von  $^{226}\text{Ra}$  mit Protonen)", Patent No 88636, granted on January 3rd 1997 in Luxembourg and filed as European Patent application in AT, BE, CH, DE, DK, ES, FR, GB, GR, IE, IT, LI, LU, MC, NL, PT, SE
- [4] C. Apostolidis, W. Janssens, L. Koch, J. Mc Ginley, R. Molinet, M. Ougier, J. Van Geel, J. Möllenbeck, H. Schweickert, "Method for producing  $^{225}\text{Ac}$  by irradiation of  $^{226}\text{Ra}$  with protons", Patent filed under Provisional No 98109983.1 on June 2nd 1998 for AT, BE, CH, CY, DE, DK, ES, FI, FR, GB, GR, IE, IT, LI, LU, MC, NL, PT, SE

## 2. Safety of Nuclear Fuel

### 2.1 Structural Investigations and Basic Studies on High Burn-up Fuel

#### 2.1.1 Pre-oxidation studies in the 304 stainless steel - zircaloy system

The interaction and the behaviour of reactor's structural materials under accident conditions or conditions in which accidents could be initiated can be decisive and require further examination. The materials involved are silver absorber material (Ag-15 In- 5 Cd), stainless steel (304 L) for absorber rod cladding and zircaloy-4 fuel rod cladding. During this year the effect of surface layers on the interactions were examined.

For the tests steel was used, which had undergone various pre-oxidations in air at 900°C for 1 to 10 minutes, along with a pre-oxidised zircaloy. In addition control tests with non-oxidised samples were made. The samples were gradually heated (10 °C/min.) in an Argon gas stream and held one on top of the other in firm contact by a spring-loaded Al<sub>2</sub>O<sub>3</sub> rod in an Al<sub>2</sub>O<sub>3</sub> crucible. The elongation of the sample was noted as the temperature was increased until the extensometer indicated a length reduction (i.e. a softening of the material), the furnace was then turned off. The samples were then examined metallographically.

The results show that although there was no great increase in the oxide thickness (3-8 µm in most cases) there was a gradually increasing temperature at which interaction occurs with the increase in steel pre-oxidation time. A further increase was observed with zircaloy pre-oxidation; which appears to be more effective in delaying the interaction than the steel pre-oxidation.

From the above it is deduced that the oxide layer temporarily prevents the interaction between the two metals. With rising temperature interdiffusion between oxide layer and substrate occurs and causes a dispersal of the oxide and enables direct contact between the two metals. The time required for this is a function of the diffusivity of the metals in the oxides (i.e., the stoichiometry of the oxide) and of oxygen in the metals. It is seen in *Tab. 2.1* that the interaction temperature is raised from 1070°C in the metallic state to 1220°C in the doubly pre-oxidised state. Thus surface oxide layers can reduce the interaction occurring between two metallic surfaces and delay the onset of severe interaction in a reactor accident.

Test No.	Test Components	Interaction Temp. °C
1	Zry + 304ss	1070
2	Zry + preoxidised 304ss (900/air/1min)	1070
3	Zry + preoxidised 304ss (900/air/3min)	1120
4	Zry + preoxidised 304ss (900/air/10min)	1170
5	preoxidised Zry (900/air/3min) + preoxidised 304ss (900/air/3min)	1220
6	Zry + preoxidised 304ss (900/argon/5min)	1440 (destroyed)

Table 2.1: Interaction temperature results for various pre-oxidation states.

Fig. 2.1 shows that zircaloy flows and that the pre-oxidized steel remains relatively strong at 1200°C.

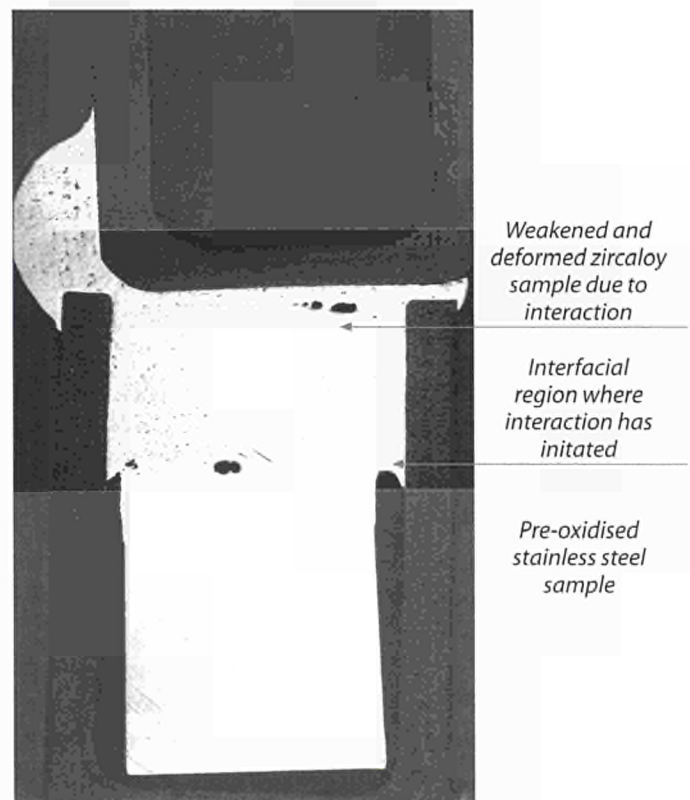


Fig. 2.1 Interaction after heating of zircaloy and pre-oxidised (10min/air/900°C) stainless steel samples in firm contact up to 1200°C under argon atmosphere at 10°C/min.

### 2.1.2 The behaviour of fission gas in the rim region of high burn-up UO<sub>2</sub> fuel

In the reporting period x-ray fluorescence (XRF) and electron probe micro-analysis (EPMA) results for retained Xe from Battelle's high burn-up programme, which ended in 1990 [1, 2] were evaluated. The data reviewed were from commercial low enriched (1.4% <sup>235</sup>U) BWR fuel with burn-ups of 44.8-54.9 GWd/tU and high enriched (7.1-8.3% <sup>235</sup>U) PWR fuel with burn-ups from 62.5-83.1 GWd/tU. The principal aim of this work was to discover whether at high local burn-up fission gas had escaped from the high burn-up structure to the rod free volume.

It was found that the high burn-up structure penetrated much deeper than initially reported (see Tab. 2.2).

Fuel Section	Burn-up GWd/tU	Depth of penetration, μm	
		Ref [1]	This work
BK365-46	83.1	140	2900 a
BSH-06-49	72.2	198	660
3-138-50	70.4	221	960
BK365-86	67.1	160	1410
BLH-64-43	62.5	73	100 b
H8/36-4-220	54.9	159	150
H8/36-4-48.2	44.8	159	150

- The high burn-up structure extended from the pellet rim to the surface of the central hole.
- Ceramography shows patches of pin hole porosity at the pellet rim which could be associated with the formation of the high burn-up structure.

Tab. 2.2 Depth of penetration of the high burn-up structure as found in this work and as reported by Cunningham et al.

Indeed, in the PWR fuel with a burn-up 83.1 GWd/tU it extended over the whole cross-section of the annular pellet, although it was less prominent at intermediate radial positions. The local threshold burn-up for the formation of the high burn-up structure in the BWR fuel with a grain size of 6.6 μm and in the PWR fuel with a grain size of 16 μm was in the range 60-75 GWd/tU. This burn-up range is the same as that found for commercial PWR fuel with 3.0-3.5% enrichment [4]. The high burn-up structure was not detected by

EPMA, however, in the PWR fuel with a grain size of 78 μm obtained by the addition of 0.46 w/o Nb<sub>2</sub>O<sub>5</sub>, although the burn-up at the pellet rim had exceeded 80 GWd/tU. This finding constitutes important evidence that the transformation of the fuel microstructure can be shifted to higher burn-up.

It was concluded that fission gas had been released from the high burn-up structure in three PWR fuels with burn-ups of 70.4, 72.2 and 83.1 GWd/tU. At the locations where XRF indicated gas release in the rim region of the fuels with burn-ups of 70.4 and 83.1 GWd/tU the local burn-up was greater than 75 GWd/tU. The percentage of release involved was small. For example, in the case of the PWR rod with the highest average burn-up, slightly less than 4% of the fission gas inventory had been released to the free volume, although the formation of the high burn-up structure was responsible for approximately 43% release from the fuel grains in the section at peak power and about 11% release from the fuel grains in the section at 80% peak power. In the case of the fuel with a burn-up of 72.2 GWd/tU, apparently all the gas released from the UO<sub>2</sub> grains in the region where the high burn-up structure had formed, which amounted to 6.5% of the fuel cross-section inventory, had escaped from the fuel. In this fuel, however, gas release may have been enhanced by a fabrication anomaly; namely, the presence of islands of high (~90%) enrichment.

#### References

- [1] M.E. Cunningham, M.D. Freshley, and D.D. Lanning, J. Nucl. Mater. 200 (1993) 24
- [2] J.O. Barner M.E. Cunningham, M.D. Freshley, and D.D. Lanning, Nucl. Technol. 102 (1993) 210
- [4] M.E. Cunningham, M.D. Freshley and D.D. Lanning, J. Nucl. Mater. 188 (1992) 210
- [3] K. Lassmann, C.T. Walker, J. van de Laar and F. Lindström, J. Nucl. Mater. 226 (1995) 1

### 2.1.3 The RIM effect irradiation

The work for the international High Burnup Rim Project, HBRP, managed by the Central Research Institute of Electric Power Industry, CRIEPI, and sponsored by 23 different organisations was continued. The aim of the project is to investigate the threshold values (burnup, temperature, pressure and type of fuel) for the formation of the rim structure [1,2]. Five fuel rods were cut and all 168 fuel disks and 68 end disks were recovered and photographed. Optical microscopy was

performed for specimens of 2 rods, scanning electron microscopy, transmission electron microscopy, electron microprobe analysis, burnup analysis, XRD analysis, oxygen potential measurements, gas release measurements in a hot cell furnace and separately in a shielded Knudsen cell apparatus, and thermal diffusivity measurements in a shielded laser flash apparatus were all performed on selected disks. The work will be continued and concluded in 2000.

#### References

- [1] M. Kinoshita, S. Kitajima, T. Kameyama, T. Matsumura, E. Kolstad, Hj. Matzke, ANS Int. Topical Meeting on LWR Fuel Performance: "Going Beyond Current Burnup Limits", Portland, March 2-6, 1997, Proceedings ANS (1997) p.530.
- [2] S. Kitajima, Hj. Matzke, M. Kinoshita, "High Burnup Rim Project" presented at Enlarged Halden Project Meeting, Lillehammer, March 1998, Proceedings Paper F-3.11 (1998).

#### 2.1.4 Supporting nuclear data for advanced MOX fuel

The study is carried out in the frame of a European Community Shared-Cost Action (contract no. FI4I CT 950002). The aim is the determination of nuclear data, i.e. integral cross-sections and fission yields, of various actinides and fission products and hence, the verification of neutron physics calculations.

The targets of actinides ( $^{232}\text{Th}$ .... $^{244}\text{Cm}$  in amounts of about 1 mg) which were irradiated in the KNK II fast reactor, are being chemically analysed, through a range of mass and energy spectroscopy techniques. The resulting composition information will provide the means for verification of nuclear data through appropriate neutronic calculations.

The chemical analysis of the fresh targets (KNK II b) and of the irradiated targets (KNK II a)  $^{233}\text{U}$ ,  $^{238}\text{U}$ ,  $^{238}\text{Pu}$ ,  $^{240}\text{Pu}$ ,  $^{241}\text{Pu}$ ,  $^{242}\text{Pu}$ ,  $^{242}\text{Cm}$ ,  $^{243}\text{Cm}$ ,  $^{245}\text{Cm}$  was completed. The chemical evaluation of the results is in progress.

Neutronic analysis of the results is demonstrated for the  $^{233}\text{U}$  target. A burnup of about 20 a/o was obtained, as determined through the chemical analysis results and on the basis of the  $^{148}\text{Nd}$  concentration. It should be noted that the burnup in this case does not necessarily reflect the fission energy released by the fuel in the reactor core. The irradiated "point" target does not contribute to this energy and it resembles a neutron activation irradiation experiment. KORIGEN [1] in-

ventory calculations (C), simulating the irradiation of the target for a target burnup of 20 a/o, were compared to chemical analysis (E): - C/E for the  $^{148}\text{Nd}/^{233}\text{U}$  ratio is 0.98. A fluence of  $7.5\text{E}22 \text{ n/cm}^2$  is calculated by KORIGEN in comparison to  $8\text{E}22 \text{ n/cm}^2$  declared by the operator.

#### Reference

- [1] U. Fischer and H.W. Wiese, "Verbesserte konsistente Berechnung des Nuclearen Inventars abgebrannter DWR-Brennstoffe auf der Basis von Zell-Abbrand-Verfahren mit KORIGEN", Kernforschungszentrum Karlsruhe, KfK-3014 (1983)

#### 2.1.5 Post-irradiation examination (PIE) of the Phebus FPT1 bundle

The Phebus pf project is an international reactor safety project designed to look at the behaviour of fission products during reactor accidents. It is lead by IPSN Cadarache (France) with support from the European Commission and EdF (France) and has participants from a further six national institutes: NRC (USA), COG (Canada), NUPEC and JAERI (Japan); KAERI (Korea) and PSI and HSK (Switzerland).

ITU is currently undertaking the examination of the degraded FPT1 bundle. In the first "baseline" bundle degradation test in Dec. '93, FPT0 used trace-irradiated fuel and showed a considerable degradation with formation of a molten pool. The 2nd test FPT1 carried out in July '96 using irradiated fuel (~23 GWd/tU) and 2 instrumented non-irradiated rods showed from the  $\gamma$ -tomography to have degraded in the same manner as FPT0 forming a molten pool at one-quarter height.

In 1998 the upper half of the bundle was cut and microphotography on the polished surfaces was carried out. The periscope observations of the upper part of the bundle showed severe oxidation of the outer rods but in the inner ring not only was the cladding "flowered" or missing but the fuel showed considerable porosity and large metallic inclusions.  $\gamma$ -spectroscopy showed  $^{137}\text{Cs}$  as the main isotope in the corium pool section but also  $^{106}\text{Ru}$  in a local hot spot (probably a metallic Ru-rich precipitate). The pool is broad and covers most of the cross section with a porous equi-axed structure at the centre and an outer columnar-grained crust. In the corium, fuel rods are still visible undergoing dissolution.

The section taken for optical microscopy included a zone where there were adjacent irradiated and non-irradiated rods

Contact (2.1.3): Hansjoachim Matzke • tel.: +49 7247 951 273 • fax: +49 7247 951 591 • matzke@itu.fzk.de

Contact (2.1.4): Jean-Paul Glatz • tel.: +49 7247 951 321 • fax: +49 7247 951 561 • glatz@itu.fzk.de

and hence a direct comparison between the melt attack on irradiated fuel and non-irradiated fuel was possible. The optical microscopy shows at low magnification a clear difference between the irradiated and non-irradiated rods. The non-irradiated rods have broken up along major radial fractures and are attacked uniformly along these surfaces (see Fig. 2.2).

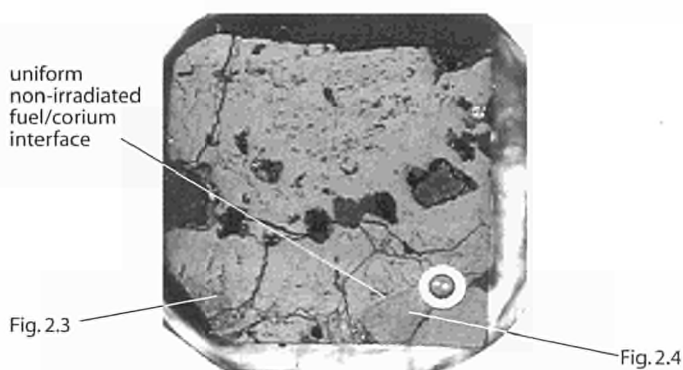


Fig. 2.2 Section of disc Nr. 1 (208 to 228 mm) showing melt in the upper half and in the lower corners remnants of irradiated fuel (left) and non-irradiated fuel (right) with central thermocouple. (Magnification 15x)

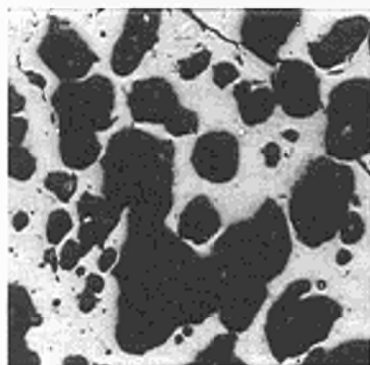


Fig. 2.3 Closer view of the irradiated fuel remnant showing gross porosity presumed due to the fission gas release. (Magnification 200x)

By contrast the irradiated fuel has broken up irregularly and is developing considerable porosity reaching several tenths of millimetres in size under the attack (Fig. 2.3). This leads to swelling of the fuel that is presumed to be due to the pressurised fission gas release as the fuel is attacked and softens. Bundle  $\gamma$ -tomography revealed fuel swelling of the order of 30% in dimension accompanied by a corresponding drop in the density from about  $10 \text{ g.cm}^{-3}$  initially to about  $8 \text{ g.cm}^{-3}$  for badly attacked (and swollen) fuel.

In the case of the non-irradiated fuel there is only limited porosity increase and it retains its structure even 3 mm away from the melt in this sample (see Fig. 2.4).

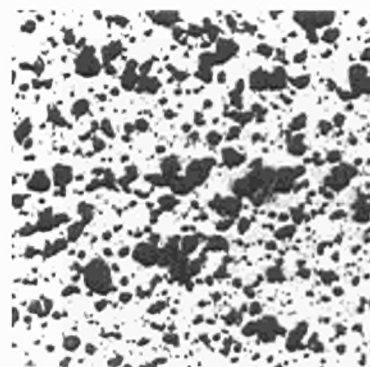


Fig. 2.4 Closer view of the segment of non-irradiated fuel showing relatively little porosity in the fuel. (Magnification 200x)

It is also apparent that this outgassing of the fission product volatiles in irradiated fuel leads to a much greater melt/fuel interface and hence a more rapid fuel dissolution by the melt. Microprobe analysis is currently being performed on this sample.

This will be used to determine the overall melt composition and perform line scans across the melt/fuel interfaces for irradiated and non-irradiated fuels to see whether differences in dissolution kinetics exist. The metallographic examination of the six selected zones is due to be completed by end of February '99.

### 2.1.6 Post-irradiation examination of pressurised and boiling water reactor fuel rods

In the framework of the contract with Siemens AG-Bereich Energieerzeugung (KWU), non-destructive and destructive examinations of power reactor fuel rods were carried out. The work performed and described in the last seven annual reports [1] has continued and a list of types and number of examinations carried out on different fuel rods in 1998 is given in Tab. 2.3.

Three fuel rods from a PWR and one fuel rod from a BWR were transferred to the hot cells in ITU. In the case of the PWR rods, the goal of the examinations was to provide experimental data on the corrosion behaviour of different cladding mate-

rials at high average burn-up (up to about 100 GWd/tM). The focal point of the studies was dimensional stability of the fuel as well as the corrosion behaviour of the cladding (improved Zr-alloys). In the case of the BWR rod, the phenomenon called "shadow corrosion", was to be studied, including detailed oxide layer thickness determination and metallography at the spacer positions. In addition, structural components from two PWR's were received for destructive examinations, including metallography and hydrogen uptake determination. The aim of these examinations was to obtain information on the dimensional stability and oxidation behaviour.

Finally, 22 capsules containing fuel rod remnants were shipped back to the reactor pool of the appropriate utility.

TYPE OF EXAMINATION	BWR	PWR	TOTAL
Visual examination	1	10	11
Defects (cladding)	1	-	1
Oxide layer thickness	1	4	5
Gamma scanning	2	2	4
Fission gas analysis	-	2	2
Free volume determination	-	2	2
Metallography	15	28	43
Ceramography	9	-	9
Burn-up determination	-	1	1
Density	4	1	5
H <sub>2</sub> -determination	3	26	29
Burst test	6	6	12
EMPA-cladding	1	-	1

Tab. 2.3 Number and type of examinations carried out on different fuel rods.

#### Reference

- [1] EUR 14493 (TUAR-91), p. 199, EUR 15154 (TUAR-92), p. 199, EUR 15741 (TUAR-93), p. 227, EUR 16152 (TUAR-94), p. 205, EUR 16368 (TUAR-95), p. 199, EUR 17296 (TUAR-96), p. 127, EUR 17746 (TUAR-97), p. 74

### 2.1.7 Innovative non-destructive techniques (NDT) for spent fuel

One of the most important NDT methods used for post irradiation examination (PIE) of spent fuel rods is the determination of the axial-distribution of  $\gamma$ -emitters. For the measurement the fuel rod is fixed horizontally on a metrology bench. Then the fuel rod is displaced axially at a constant speed during the examination in front of the collimator of a high purity germanium  $\gamma$ -detector. The resolution of the measurement depends upon of the collimator aperture, which varies from 0.6 to 2 mm. In the integral measurement, the pulses sent by the germanium detector are analysed by a ratemeter provided with a proportional analogue output. The axial position of a particular measurement can be determined from tick marks generated by the translation system. Both signals are recorded continuously on paper and simultaneously in digital form on floppy discs.

For the evaluation of the digital files, the new computer Code GAMBLE was developed.

The program has the following features:

- Internal length calibration using the tick data or alternative external calibration by the user.
- Peak search criteria can be changed by the user to achieve more flexibility.
- Automatic or manual determination of beginning and end of the fuel stack.
- Calculation of fuel stack length.
- Automatic peak search and evaluation gives complete description of peak properties: FWHM (full width at half depth), FWTD (full width at tenth depth) which are related to the maximal axial gap width. The peak area is proportional to the gap volume.
- Calculation of individual pellet length and mean pellet length.
- Detection of pellet defects like cracks with a special check algorithm.
- Calculation of the effective gap width, which is the gap volume between two pellet calculated from the peak area given as the thickness of a disc with the pellet's diameter.

- Axial distribution of effective gap widths, peak areas, FWHM, FWTD and further peak-related properties.
- Determination of the total number of pellets.

The algorithms used are based on differentiation of the axial  $\gamma$ -distribution and the analysis of the derivative. To also handle "noisy" data sets two different smoothing algorithms, 5 point smoothing and locally weighted regression scatter plot smoothing (LOWESS) [1], are used.

A usual  $\gamma$ -scan taken with a step width of less than 0.1 mm on a fuel pin of 4.5 m length yields 45000 data points. Such a pin contains approximately 300 pellets. The complete evaluation of such a data set with the code GAMBLE takes about half an hour, whereby the obtained axial profile information is just determined by the chosen step width.

#### Reference

[1] W.S. Cleveland, Amer. Statistician 35 (1981) 54

## 2.2 Studies of High Temperature Properties of Nuclear Fuels

### 2.2.1 High-temperature thermophysical properties of MOX fuel

Heat capacity, thermal diffusivity, and thermal conductivity of MOX fuel were measured at temperatures from 1800 to 2600 K in argon atmosphere. The results are presented in Fig. 2.5-2.7. The oxide, in the form of a solid solution, was stoichiometric with a sintered density of 95% th.d.. The results show that both heat capacity and thermal diffusivity – and, consequently, the thermal conductivity – decrease with the increase of plutonium content. At temperatures above 2400 K, the material undergoes a marked restructuring – observed by metallography of the samples – leading to a larger scatter of the measurements, whereby, however, an average increase of diffusivity of approximately 10% is observed (Fig. 2.5).

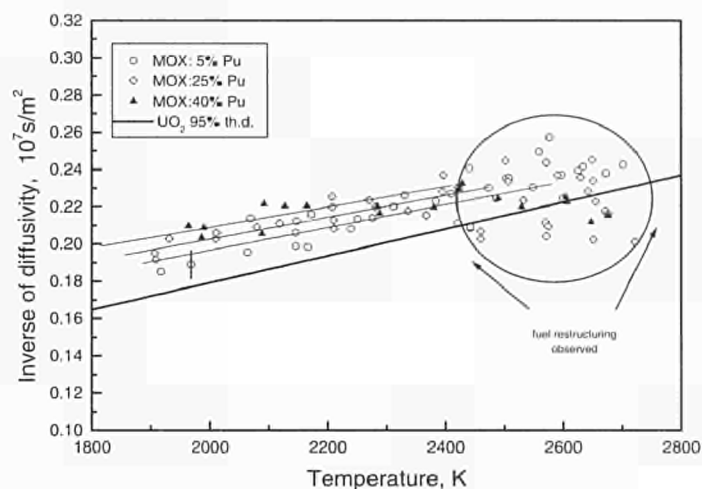


Fig. 2.5 Inverse of thermal diffusivity of MOX as a function of temperature as a function of temperature.

The effect on the heat capacity ( $C_p$ ) due to addition of 5%, 25% and 40% Pu in  $UO_2$  (Fig. 2.6a-c) is a slight increase of  $C_p$  below 2200 K and a decrease of  $C_p$  above 2200 K. In MOX (5% Pu) the  $C_p$  appears to be slightly higher than in  $UO_2$  (Fig. 2.6a).

Particularly interesting is the dependence of the MOX thermal conductivity,  $\lambda$ , as a function of temperature at different plutonium contents (Fig. 2.7).

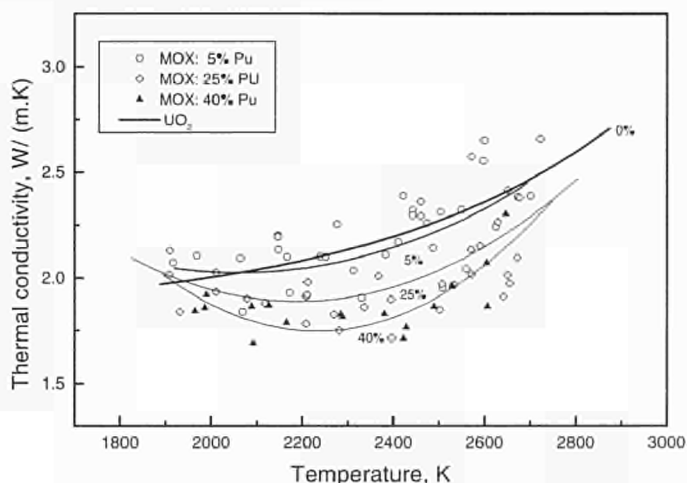


Fig. 2.7 Thermal conductivity of MOX as a function of temperature.

A flat minimum in  $\lambda$  at approximately 2000 K, as in the case of uranium dioxide, is also observed in the mixed oxide. However, whilst in  $UO_2$  the conductivity slowly increases from this temperature to the melting point, in MOX the curve of  $\lambda$  vs. T is flatter, and only above 2400 K does it markedly

increase, with  $\lambda$  attaining values near to those of  $UO_2$ . Due to experimental limitations the measurements could not be carried out at absolute temperatures above 90% of the melting point. It is however very likely that above 2400 K the thermal conductivity of MOX is effectively equal to that of uranium oxide. Since the upswing of the conductivity at high temperatures is due to electronic defect contributions to the heat capacity (mainly small polarons), this property of the mixed oxide may cast new light on the formation and activation of lattice defects. A study is in progress in this direction.

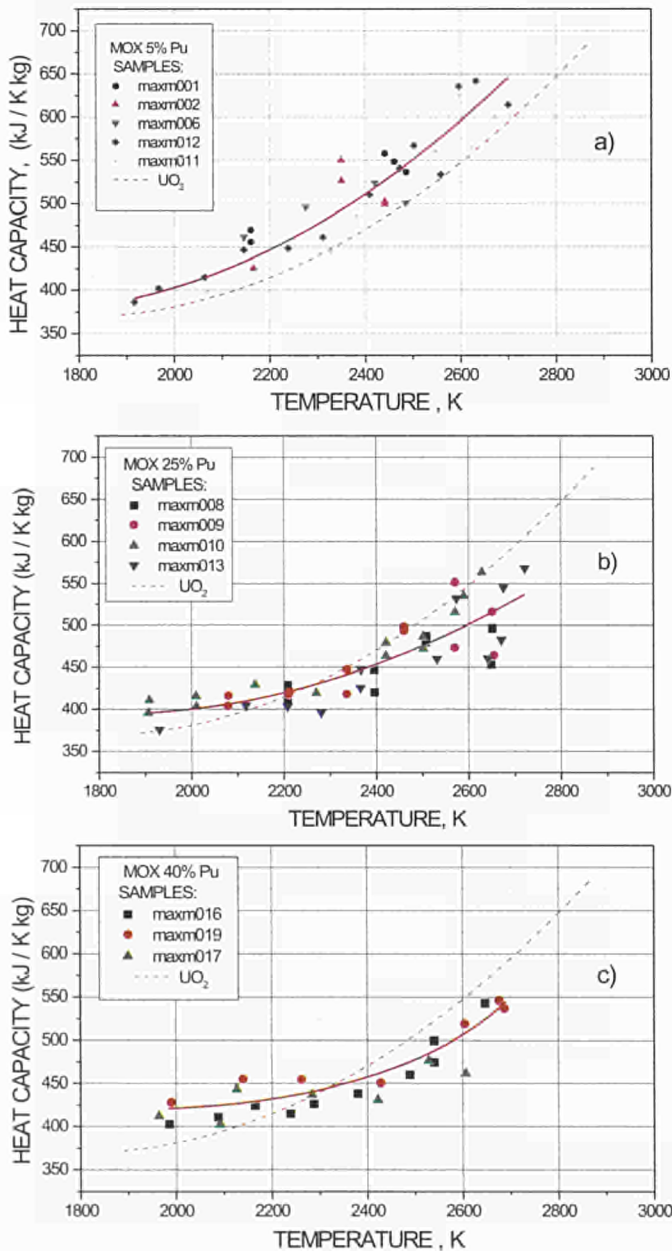


Fig. 2.6 Heat capacity of MOX a)  $(U_{0.95}Pu_{0.05})O_2$  b)  $(U_{0.75}Pu_{0.25})O_2$  c)  $(U_{0.60}Pu_{0.40})O_2$ .

Contact (2.2.1): Claudio Ronchi • tel.: +49 7247 951 402 • fax: +49 7247 951 591 • ronchi@itu.fzk.de

Contact (2.2.2): Jean-Pol Hiernaut • tel.: +49 7247 951 385 • fax: +49 7247 951 591 • hiernaut@itu.fzk.de

## 2.2.2 Revaporisation of Phebus pf FPT1 samples

This shared cost-action, co-financed by the EC, is in its second year and has ITU, AEA Technology plc and VTT Finland as partners. The aim is to examine the possibility of fresh fission product revaporisation in the primary circuit due to the decay heat during a reactor accident. This phenomenon is to be examined using the Phebus FPT1 samples from the vertical line deposit above the bundle.

There had been delays in the previous year as the special aerosol furnace designed by VTT required considerable redesign to reduce the size and permit adequate shielding before installation in a glove box and modifications to allow use with active samples. After final alterations were agreed at an ITU/VTT meeting in March, VTT delivered the rig at ITU in July '98. Installation in the glove-box and shielding is in progress.

The FPT 1 samples were cut in May '98 and one half of the samples from the vertical line along with back-up vertical line and steam generator samples were transported to AEA Technology plc, Winfrith in August '98 for characterization of deposits by electron microscopy.

Knudsen cell testing of the vertical line samples has been performed at ITU in Dec '98 and the results will be analysed in the coming year. This will give an indication of the volatilisation temperatures of the fission products under near-equilibrium conditions. Adjacent samples have been mounted for metallography and will be examined by optical microscopy and later by scanning electron microscopy.

## 2.2.3 Analysis of filter samples of the Phebus FPT1 experiment

ITU, under a contract from IPSN, Cadarache, undertook the analysis of filter samples of the Phebus FPT1 experiment which was the first of the series to use irradiated fuel (burn-up 23 GWd/tU). The results of the analysis (along with the results of other laboratories: AEA Technologies plc, Winfrith; CEN, Grenoble; CEN, Marcoule; Siemens Erlangen) will help to explain the behaviour and provide information about the mass balance of the fission products released during accident conditions.

The selected samples were filters located in the simulated

primary circuit *before* the steam generator (at 700°C) and *at* the steam generator inlet (at 150°C). Three filters were exposed at the power plateau before the final power rise (oxidation phase), while 2 filters were taken at the moment of maximum degradation as the reactor was shut down. The filters were examined by  $\gamma$ -spectroscopy and were seen to have the fission products Cs-134, Cs-137, Sb-125 and Eu-154, as well as the irradiation product Ag-110m. These were concentrated in the centre in the upstream filters (see Fig. 2.8) but were more uniformly distributed in the back-up or downstream filters.

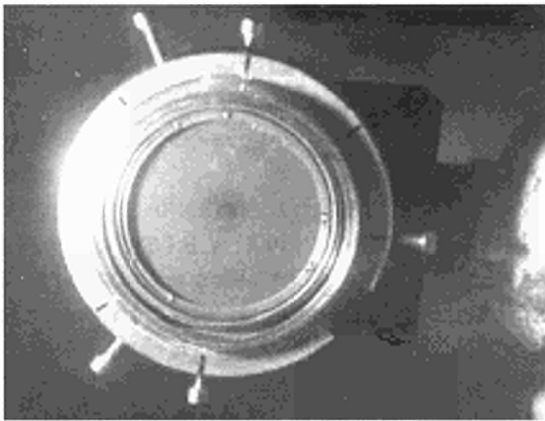


Fig. 2.8 Filter 701 from the FPT1 test exposed to the aerosol-laden atmosphere at 700°C during bundle degradation, showing the concentration of deposits in the central zone.

ICP-MS analysis shows that further fission products were present such as Mo, Ru and Tc as well as U and Zr (from cladding) and Ag+In+Re from the absorber and thermocouples. The optical microscopy showed that the upstream filters were fully blocked in the centre with a heterogeneous deposit. The SEM-EDX analysis shows part to be powdery and composed of final aerosol agglomerates and indicates some U both uniformly deposited as well as U, Zr droplets that have been carried over from the melting bundle. Cd was found particularly on the low temperature filters, along with some In. There was maximum deposition of Re at the highest temperatures, while absorber materials such as Ag, In, Cd were volatilising earlier, prior to the final degradation.

A final report summarizing the results of all participating laboratories is due to be issued by IPSN, Cadarache in 1999.

#### 2.2.4 Corium interaction thermochemistry

The Corium Interaction Thermochemistry project is an 8 partner shared cost action project examining the properties and behaviour of reactor core melt (corium) that may be formed during a severe accident. It is co-ordinated by IPSN Cadarache (France) and forms part of a series of in-vessel reactor accident projects along with the Core Behaviour and Oxidation Phenomena in Severe Accidents projects. ITU's contribution to this project is the examination of the irradiated  $\text{UO}_2$  dissolution by zircaloy. Other institutes have done thermodynamic modelling of the U-Zr-O system and investigation of non-irradiated  $\text{UO}_2$  dissolution by zircaloy and modelling of the kinetics of  $\text{UO}_2$ -Zr dissolution.

ITU carried out two sets of experiments using a direct electrical heating (DEH) oven with graphite crucibles and Ar atmosphere. The second set was a scoping test, which used various non-irradiated  $\text{UO}_2$  fuel segments with the aim of seeing what segment size was suitable for the oven.

In the first set segments of  $\text{UO}_2$  2, 3, 5 and 10 mm high with cladding were tested at 2000°C. Upto 5 mm high segments appeared to be almost completely dissolved while the 10 mm high segment appeared to have been too large for the crucible and may not have reached the full temperature.

The second set of experiments were performed at a fixed temperature of 2000°C but for different durations (25s up to 229s) using 3 mm irradiated  $\text{UO}_2$  fuel segment with cladding and 3 mm non-irradiated  $\text{UO}_2$  fuel segments with cladding. The irradiated fuel was BR3 fuel with a high burn-up of 53 GWd/tU and low linear power. The repetition of the experiments with non-irradiated and irradiated  $\text{UO}_2$  fuel enabled a direct comparison to be made under identical experimental conditions.

The importance of maintaining similar experimental conditions has been stressed by the  $\text{UO}_2$ -Zr modellers. They have noted that the  $\text{UO}_2$  crucible's wall thickness effects its dissolution rate by liquid zircaloy because the supply of fresh  $\text{UO}_2$  is rapidly exhausted.

The samples were cross-sectionally mounted and then examined by optical microscopy, with selected samples undergoing microprobe analysis to determine the melt compositions as well as confirming the fuel composition. Melt interaction with the crucible was also checked, as there had been sug-

gestions that the graphite crucibles would react with the molten zircaloy to form carbides. In one non-irradiated sample blocky precipitates in the melt typical of carbide were seen. However microanalysis of the irradiated samples showed no evidence of carbon in the melt. Phase analysis of the samples was also carried out.

The overall dissolution by zircaloy appears to be noticeably faster with irradiated fuel than with non-irradiated fuel: there was a more rapid break-up of the irradiated fuel into pieces. Moreover, more porosity was seen in the irradiated fuel samples as fission product volatiles are released. (This also corresponds to the swelling that was seen in the Phebus FPT1 bundle examination). The melt phase progression (amount of  $\text{UO}_2$ -containing phase in the melt versus the metallic Zr-rich phase in the melt) was also estimated from phase analysis to follow the total  $\text{UO}_2$  fuel dissolved. When these results are compared with those of other workers using non-irradiated  $\text{UO}_2$ , they indicate that at  $2000^\circ\text{C}$  irradiated fuel dissolves at rates found at  $2150^\circ\text{C}$  for non-irradiated  $\text{UO}_2$  fuel. There are also indications from a preliminary test that  $\text{UO}_2$  dissolution can start from the zircaloy melting point in the range  $1760$  to  $1800^\circ\text{C}$ .

Further tests at  $2000^\circ\text{C}$ , using TaC crucibles, are foreseen to confirm these findings.

## 2.3 The Fuel Performance Code TRANSURANUS

### 2.3.1 The TRANSURANUS research network

TRANSURANUS is a computer program, for the thermal and mechanical analysis of fuel rods in nuclear reactors, which has been developed at the European Institute for Transuranium Elements [1]. It is fully described in the literature and has been outlined in previous Annual Reports. The code is in use in several European organisations, both research and private industry and has been further developed.

The close collaboration with several groups has been intensified. The development of the TRANSURANUS-WWER version has reached a mature level. This development was carried out within the frame of the PHARE 92-94 programme in co-operation with a) the Institute for Nuclear Research and Nuclear Energy in Bulgaria and b) the Nuclear Research Institute Rez plc. in the Czech Republic (see below). The TRANSURANUS-WWER version has been verified successfully employing

**Contact (2.2.2.-2.2.4): David Bottomley • tel.: +49 7247 951 364 • fax: +49 7247 951 591 • bottomley@itu.fzk.de**

the Kola and Sofit irradiation data from the International Fuel Performance Experiments Data Base (IFPE) developed by IAEA-OECD/NEA. Within the IAEA regional technical co-operation program RER/4/019 the latest version of the TRANSURANUS code, V1M2J98, the pre- and post processors has been released to 7 Eastern European countries.

One training course was given:

- Within the IAEA RER/4/019 Seminar "Implementation of the WWER version of the TRANSURANUS code and its application to safety criteria", held at Sofia, Bulgaria, between December 7-11, 1998, a TRANSURANUS Training Course was offered. More than 30 participants from 15 countries discussed WWER related problems, the application of the TRANSURANUS-WWER version and its application to safety criteria. The course was supported by the IAEA under the regional technical co-operation program RER 4/019 ("Licensing fuel and modelling codes for WWER reactors").

### 2.3.2 Specific TRANSURANUS model developments and results

The structural investigations and basic studies on high burn-up fuel outlined in the previous section were augmented by further development and verification of the high burn-up models described in references [2,3]. The burn-up equations of the TRANSURANUS code were extended to include the burnable absorbers Gadolinia ( $\text{Gd}_2\text{O}_3$ ) and Zirconium diboride ( $\text{ZrB}_2$ ). Extensive verification work has been done [4].

The treatment of fission products in the TRANSURANUS code has been completely revised. The code structure has been extended in such a way that in principle an arbitrary number of fission products can be considered. This modification will allow more detailed studies on fission gas behaviour.

An improved model for the fission yields has been developed that allows the study of Kr/Xe ratios under a wide range of conditions, especially at high burn-up. This model will be used in 1999 for the analysis of the most important question in fuel performance behaviour:

Where does the increased fission gas release come from that is observed at extended burn-up in all reactor irradiations?

1. from the inner hot regions by thermal gas release processes or
2. by an a-thermal process from the outer cold regions that show the High Burn-up Structure.

The relevance is obvious. If the increased fission gas release at high burn-up originates from an a-thermal processes associated with the formation of the High Burn-up Structure, then this effect could limit the life time of fuel rods due to the build-up of the inner pin pressure.

### 2.3.3 Phare project "Fuel Rod Modelling and Performance (FERONIA)", Bulgaria

This project was a co-operation between the Bulgarian Academy of Sciences, Institute of Nuclear Research and Nuclear Energy and the ITU. It finished in June 1998. The main activities in 1998 focused on the following areas:

1. Development of the TRANSURANUS-WWER version.
2. Verification of the TRANSURANUS-WWER version employing data cases (SOFIT and Kola) from the International Fuel Performance Experiments Data Base (IFPE) developed by IAEA-OECD/NEA. During the evaluation several problems came up that need further clarification with the Russian colleagues.

Details are given in the Final Report and 9 Quarterly Reports which are available on request.

### 2.3.4 Phare project "Fuel Rod Modelling and Performance (FERONIA)", Czech Republic

This project was a co-operation between the Nuclear Research Institute Rez plc. in the Czech Republic and the ITU. It finished in June 1998. The goal of this project was to provide to the Czech Republic a modern fuel rod performance code to be use in licensing of the nuclear power plants Dukovany (WWER 440) and Temelin (WWER 1000 with Westinghouse fuel assemblies). The main activities in 1998 focused on the following areas:

1. Application of the TRANSURANUS code to the licensing of the nuclear power plant Dukovany (VVER 440)

2. Application of the TRANSURANUS code to the licensing of the nuclear power plant Temelin (WWER 1000 with Westinghouse fuel assemblies).

The TRANSURANUS code has been applied successfully in the licensing of the two different nuclear power plants. Details are given in a report which is available on request.

#### References

- [1] K. Lassmann, Journal of Nuclear Materials 188 (1992) 295-302
- [2] K. Lassmann, C.T. Walker, J. van de Laar, F. Lindström, Journal of Nuclear Materials 226 (1995) 1-8
- [3] K. Lassmann, C.T. Walker, J. van de Laar, Journal of Nuclear Materials 255 (1998) 222-233
- [4] K. Lassmann, J. van de Laar, TRANSURANUS Handbook, Document Number: Version 2, Modification 2, Year 1998 (V1M2J98), November 1998, internal ITU document

## 2.4 Development of Advanced Fuel Fabrication Techniques

### 2.4.1 Target fabrication by the infiltration of porous beads

Fabrication of targets for transmutation and incineration of actinides and fission products will require increased radiation protection, in the form of lead and water shielding, than currently necessary for the manufacture of conventional UO<sub>2</sub> and MOX fuels. In addition, the development of new advanced fabrication processes, compatible with the high activity of these materials, must be pursued. Sol-gel droplet to liquid conversion [1,2] and infiltration of radioactive materials (INRAM) [3] are two fabrication processes being developed to meet these requirements.

The INRAM process has been used successfully for the fabrication of targets for the EFTTRA-T4 irradiation experiment in HFR Petten [4]. In this case porous (50% porosity) spinel (MgAl<sub>2</sub>O<sub>4</sub>) pellets were infiltrated with an Am nitrate solution and after thermal conversion the final product pellets contained 11 w/o Am in oxide form. The quantity of Am in spinel can be increased to 40 w/o in a further variation of the INRAM process, in which porous (80% porosity) spinel beads are infiltrated by the Am solution (see Fig. 2.9).

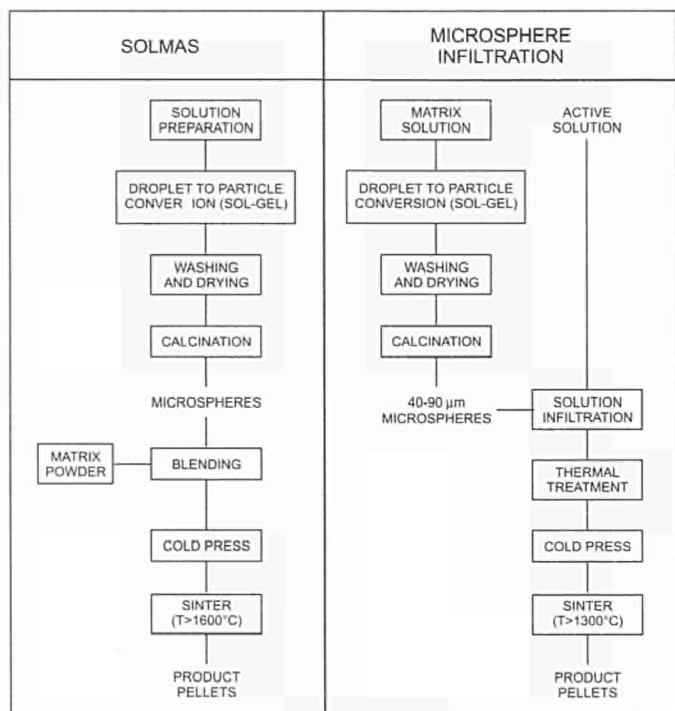


Fig. 2.9 Flow sheets for the SOLMAS and INRAM processes.

Porous spinel beads have been produced by the sol-gel process [5]. Pellets were pressed and the dependence of their density and height, at a constant fill height of the press, has been investigated as a function of the metal concentration in the original sol-gel feed solution. The results (shown in Fig. 2.10) indicate that the pellet density increases with metal concentration, but the height decreases. The measurements show that at a total metal concentration of about 0.4 M a compromise condition is found, where the pellets meet envisaged specifications for a PWR reactor, namely a height of 8 mm and a density greater than 90% of the theoretical value.

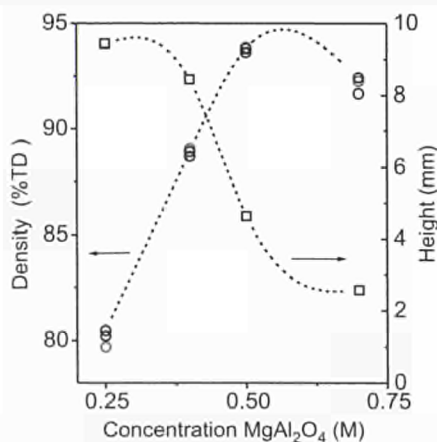


Fig. 2.10 Dependence of spinel pellet height and density on initial concentration of metal in the sol-gel feed solution.

Infiltration of the porous spinel beads is achieved by adding a solution of the actinide nitrate just until the point of incipient wetness is reached. The material is then thermally treated at 100°C to evaporate water and residual nitric acid and at 800°C to convert the nitrate to oxide. Flowable dust free beads containing the actinide oxide are retrieved. Following compaction of the infiltrated beads, the resulting pellets are sintered at 1650°C to obtain the final product.

Spinel pellets containing 10 w/o Pu and 20 w/o Am have been fabricated using this technique. Ceramographic analysis (see Fig. 2.11) reveals that the actinide particles are about 2-3 μm in diameter and are distributed uniformly, on a macroscopic scale at least, throughout the sample. The micrograph indicates that the individual particles are located near the surface regions of the original beads.

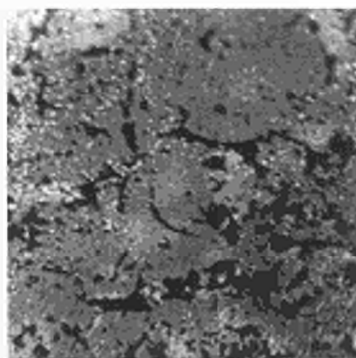


Fig. 2.11 Micrograph of Am containing particles (in white) in a spinel-20 w/o Am target prepared by the INRAM process based on the infiltration of porous spinel beads.

X-ray diffraction has been used to identify the actinide within the spinel matrix during the fabrication process. Following infiltration of spinel by a Pu nitrate solution and subsequent calcination at 800°C, XRD identifies  $\text{PuO}_2$  along with the peaks due to spinel. Sintering of the sample at 1650°C induces a reaction between plutonium and spinel to form a new species with a perovskite structure, which is identified as  $\text{PuAlO}_3$ . Additional investigations have shown that a similar reaction occurs between Ce, Nd and Am oxides and spinel, and in all cases a compound with a perovskite structure is formed. In the case of Ce and Nd these compounds have been identified as  $\text{CeAlO}_3$  and  $\text{NdAlO}_3$ . This would indicate that  $\text{AmAlO}_3$  is also formed by the reaction of Am oxide with spinel. Further experiments are underway to confirm the identification of this reaction product, and to investigate the thermal and physical properties of actinide and lanthanide aluminate species vis à vis their irradiation suitability.

#### 2.4.2 Fabrication of macrosphere targets by combined sol gel powder blending (SOLMAS)

The results obtained from the EFTTRA-T4 irradiation experiment on Am transmutation [6] show a large swelling of the spinel ( $\text{MgAl}_2\text{O}_4$ ) matrix, in which the Am matrix was supported. This swelling could be due to He production or matrix damage caused by  $\alpha$  particles and fission products. If the latter is the major cause, its effect could be minimised by increasing the size of the Am containing particles (2-3  $\mu\text{m}$  in EFTTRA T4) to 50-100  $\mu\text{m}$ , so that the volume of the matrix damaged by the fission products is reduced [7]. In addition, the reaction between Am and spinel could be hindered by incorporation of Am in the matrix as an  $(\text{Am,Zr})\text{O}_2$  solid solution, rather than as  $\text{AmO}_{2-x}$ . This concept will be tested in the EFTTRA-T5 irradiation programme.

A SOLMAS fabrication procedure (see Fig. 2.10) is being developed for the fabrication of targets containing  $(\text{Am,Zr})\text{O}_2$  macrospheres, with diameters between 50 and 150  $\mu\text{m}$ , dispersed in an inert matrix (e.g. spinel, MgO or Y stabilised  $\text{ZrO}_2$ ). During the development work,  $(\text{Am,Zr})\text{O}_2$  is simulated by  $(\text{Ce,Zr})\text{O}_2$ .

Macrospheres of  $(\text{Ce}_{0.5}\text{Zr}_{0.5})\text{O}_2$  were made by the Sol-Gel method, and have been compacted into pellets and sintered at 1650°C under reducing ( $\text{Ar}/\text{H}_2$ ) and oxidising atmospheres (air), to give the  $(\text{Ce}_{0.5}\text{Zr}_{0.5})\text{O}_{2-x}$  final products. XRD measurements indicate that under the former conditions a f.c.c phase is formed with a minority secondary phase (possibly pyrochlore [8]), while under the latter conditions, a tetragonal phase is formed. Measurements of the O/M ratio are currently being pursued.

Target fabrication tests for the EFTTRA-T5 irradiation experiment have concentrated on the blending of  $(\text{Ce}_{0.5}\text{Zr}_{0.5})\text{O}_2$  macrospheres with  $\text{MgAl}_2\text{O}_4$  powder, pellet pressing, and sintering under reducing and oxidising atmospheres. Pellet densities in the 91-93% TD range have been obtained. A macrograph of a macromass pellet produced in this way is shown in Fig. 2.12. The distribution of the macrospheres is rather inhomogeneous, which is attributed to the different densities of the macrospheres and spinel powders. XRD and EPMA measurements find no evidence for a reaction between  $(\text{Ce}_{0.5}\text{Zr}_{0.5})\text{O}_2$  and spinel, when the pellets are sintered under air, but an additional species, apparently  $\text{MgAl}_{11}\text{CeO}_{19}$ , is detected when the pellets are sintered under  $\text{Ar}/\text{H}_2$ .



Fig. 2.12 Macrograph of a macromass pellet containing  $(\text{Ce}_{0.5}\text{Zr}_{0.5})\text{O}_2$  dispersed in a spinel matrix.

Further fabrication tests are in progress to improve the homogeneity of the distribution of the macrospheres within the matrix pellet. These include blending of

- (i)  $(\text{Ce}_{0.5}\text{Zr}_{0.5})\text{O}_2$  macrospheres with the matrix powder sieved at 50, 100 and 200  $\mu\text{m}$ ,
- (ii)  $(\text{Ce}_{0.5}\text{Zr}_{0.5})\text{O}_2$  macrospheres with macrospheres of the matrix powders also produced by the Sol-Gel method.

#### References

- [1] P. Gerontopolous, G. Cogliati, K. Richter, in ENC'79 Nuclear Power – Option for the World, Trans. ANS 31 (1979) 175
- [2] A. Fernández, K. Richter, J.C. Closset, S. Fourcaudot, C. Fuchs, J. F. Babelot, R. Voet, J. Somers, Proceedings of the 9th CIMTEC Conference, Florence, 1998, in press
- [3] K. Richter, A. Fernández, J. Somers, J. Nucl. Mater. 249 (1997) 121
- [4] J.F. Babelot, J.C. Closset, A. Fernández, C. Fuchs, J.F. Gueugnon, J. McGinley, K. Richter, J. Somers, ITU Technical Note K0297190 (1997)
- [5] A. Fernández, K. Richter, J. Somers, Proceedings of the 9th CIMTEC Conference, Florence, 1998, in press
- [6] R.J.M. Konings, R. Conrad, D. Haas, G. Mühling, J. Rouault, G. Vanbenepe, Proceedings of the Fifth International Exchange Meeting on Actinide and Fission Product Partitioning and Transmutation, Mol, 25-27th Nov. 1998, in press
- [7] N. Chauvin, R.J.M. Konings, H.J. Matzke, J. Nucl. Mater., in press.
- [8] P.E. Raison, R.G. Haire, T. Sato, T. Ogawa, Proceedings of the MRS Fall Meeting, Symposium QQ: Scientific Basis for Nuclear Waste Management, Nov. 30 - Dec. 4, 1998

### 3. Mitigation of Long Lived Actinides and Fission Products

#### 3.1 Fabrication of Fuels and Targets for Transmutation Experiments

##### 3.1.1 TRABANT2

Within the framework of the CAPRA programme, three fuel pins for the irradiation experiment TRABANT2 have been fabricated. The fuel for two of these pins have a Pu content (Pu/(U+Pu)) of 40% and were manufactured by mechanical mixing and blending of UO<sub>2</sub> and PuO<sub>2</sub> powders. Two different O/M ratios were obtained by sintering the pellets in Ar or Ar/H<sub>2</sub> atmospheres. The fuel for the third pin has a Pu content of 45% and was fabricated using the sol-gel process [1,2]. The main fuel characteristics are summarized in Tab. 3.1.

Fuel	Fabrication Process	Pu Content Pu/(U+Pu)	Pellet Density (%TD)	Grain Size (µm)	O/M
(U,Pu)O <sub>2</sub>	MIMAS	0.40	94.2	10-25	1.971
(U,Pu)O <sub>2</sub>	MIMAS	0.40	93.4	10-25	1.995
(U,Pu)O <sub>2</sub>	SOL-GEL	0.45	86.3	10-20	1.990

Tab.3.1 TRABANT2 fuels.

The pellets were loaded into three stainless steel tubes (15/15 Ti) of the design shown in Fig. 3.1, and were welded using the TIG method. The fuel column length is 340 mm in all cases. The fuel pins will be transported to HFR Petten in the first quarter of 1999, where irradiation will be made in the TRIOX facility. A burn-up of 10 a/o should be achieved in 300 EFPD. Calculations using the GERMINAL code at CEA indicate that the linear power should not exceed 450-490 W.cm<sup>-1</sup>.

#### References

- [1] P.Gerontopolous, G.Cogliati, K.Richter, in ENC'79 Nuclear Power – Option for the World, Trans. ANS 31 (1979) 175
- [2] A. Fernández, K. Richter, J.C. Closset, S. Fourcaudot, C. Fuchs, J. F. Babelot, R. Voet, J. Somers, Proceedings of the 9th CIMTEC Conference, Florence, 1998, in press

##### 3.1.2 PIMPOM

During this period, the design of a new experiment called PIMPOM (Plutonium Inert Matrix in the POMpei device) has been finalized with our partners CEA, FZK and PSI. The main objective of this experiment is to test the chemical compatibility of the fuels and targets (listed in Tab.3.2) with the fission products, and their restructuring, including phase changes,

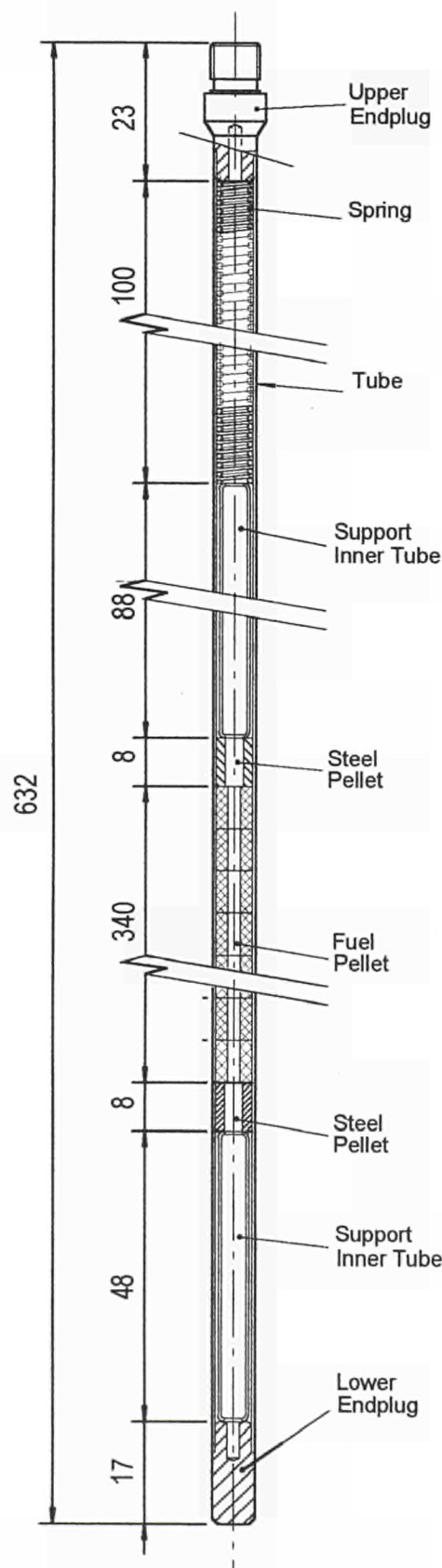


Fig.3.1 Capsule design for the TRABANT2 irradiation experiment.

Contact (3.1.1.-3.1.2.): Joseph Somers • tel.: +49 7247 951 359 • fax: +49 7247 951 566 • somers@itu.fzk.de

and material swelling. In the irradiation device, up to 12 thin disks of these materials can be loaded (diameter 9 mm, height 1.5 mm). The burnup to be achieved in HRF Petten amounts to 20 a/o per year of irradiation. Between one and two years of irradiation are planned.

MATERIAL	FABRICANT	PROPERTIES	PURPOSE
PuN	ITU	Good thermal conductivity, dense fuel	Study of thermal stability in presence of fission products
PuN + W	ITU	Confine helium gases (in case of Am) in a metallic matrix Good compatibility of W with cladding and with fissile support	Same as PuN + study of behaviour of metallic matrix
PuO <sub>2</sub> + W	CEA	Same as PuN + W. However, reaction of PuO <sub>2</sub> with Na	Study of behaviour of metallic matrix.
(Pu,Zr)N	PSI	Same as PuN, with the chemical stabilization by Zr in the PuN	Comparison with PuN
PuN + Al or TiN	ITU	Better thermal stability than PuN expected	Comparison with PuN
(U,Pu)O <sub>2</sub>	ITU	Reference Material	Comparison purpose
(Th,Pu)O <sub>2</sub>	ITU	Easiness of fabrication and licensing Lower material properties	Fuel swelling

Tab.3.2 *Materials for the PIMPOM irradiation experiment.*

All these materials will be irradiated with substitutive Pu instead of Am, if the Am compounds cannot be fabricated within the time schedule. They simulate different types of Am- or Cm-based targets for fast reactors or for sub-critical devices.

### 3.1.3 Development of advanced fuel fabrication techniques: Metallic fuels

Among the various possibilities presently being investigated for minor actinides transmutation and burning, one considers the utilisation of metallic (matrix) fuels based on U-Pu-Zr or Th-U alloys. One advantage of this concept is the possibility of performing repeated irradiation cycles, where the fuel fabrication and reprocessing steps could be easily linked, if a pyrochemical or pyrometallurgical method is used for fuel reprocessing. The largest experience gained up to now with this technology was in the Experimental Breeder Reactor (EBR I-II) of the Argonne National Laboratory in USA. The metallic fuels used were fabricated by injection casting after melt refining.

For the purposes of transmutation, where the fuel contains additions of minor actinides, a heterogeneous distribution of these elements can appear if the direct casting method is used. To avoid this, an alternative fabrication route is being

studied, in which direct casting is substituted by melt-atomisation and hot-compaction of the pre-alloyed powders. The powder size is selected such that critical conditions for autoignition (pyrophoricity) are excluded. For a failure free in-reactor behaviour, fuel properties such as creep, gas swelling and compatibility with the cladding have to be optimised. Since these properties largely depend on the alloy composition and microstructure, a study of the influence of these parameters in the irradiation behaviour is foreseen at a later stage in the programme. The experimental techniques for powder production and compaction are being optimised with a simulated fuel alloy U-Ce-Zr. After optimisation, the techniques will be applied to the real system, U-Pu-Zr-MA.

### 3.1.4 Minor actinide laboratory

The main purpose of the Minor Actinide Laboratory is to fabricate fuel pellets and fuel pins containing large amounts of minor actinides. Up to 50 g Am can be loaded in each batch of fuel. The complete fabrication chain includes 10 glove-boxes located in two laboratory rooms, F105 and F106. The operators are protected by lead reinforced water wall shieldings. Work is carried out using manipulators, or in remote manner, in the pellet handling boxes. The reference fabrication processes are the sol-gel and INRAM (Infiltration of Radioactive Materials) processes [1,2].

At present, all major equipment has been ordered and is partially delivered. The year 1999 will be devoted to the installation of the equipment in the glove-boxes, and to the construction of the laboratory in room F106.

The Minor Actinide Laboratory will be used to fabricate Am containing fuel pins for irradiation in PHENIX, and in Material Testing Reactors such as HFR in Petten. Pellets will also be prepared for their characterization and specific testing e.g. leaching experiments or solubility tests. Finally, this laboratory will also be used to develop conditioning processes (ceramization) of highly radioactive laboratory wastes.

### References

- [1] P. Gerontopolous, G. Cogliati, K. Richter, in ENC'79 Nuclear Power – Option for the World, Trans. ANS 31 (1979) 175
- [2] K. Richter, A. Fernández, J. Somers, J. Nucl. Mater. 249 (1997) 121

### 3.1.5 Evaluation of minor actinide target fabrication processes

Within the framework of a Shared Cost Action of the 4th FWP, ITU participated in a project on the evaluation of possible P&T strategies, in particular, minor actinides target fabrication. The work was performed in collaboration with BELGONU-CLEAIRE (Belgium) and ENEA (Italy).

A tentative comparison of the three processes which are analyzed in the frame of the present study contract, for the fabrication of advanced MOX fuels and of targets containing minor actinides (particularly Am), is presented in *Tab. 3.3*. The comparison is based on selection criteria in order to evaluate the feasibility of each process.

PROCESS	MIMAS	SOL-GEL	INRAM
Dust formation	C	B	A
Radioactivity handling	C	B	A
Fuel homogeneity	B	B	C
Radwaste production	B	C	A
FEASIBILITY	A	B	B
Improvement potential	C	B	A

A = Satisfactory, B = Additional development required, C = Weak point / still to be demonstrated

*Tab. 3.3 Tentative assessment of the feasibility of fabrication processes for advanced MOX fuel or targets with minor actinides.*

The MIMAS process can be considered as a reference, as several hundreds of tons of standard MOX fuel have been and are being fabricated using this method. For the fabrication of fuels and targets containing minor actinides, however, processes that produce minimal quantities of dust and waste are recommended.

In the case of americium target rods, the radioprotection constraints due to the handling of highly radioactive materials are cumbersome, but they can be managed. As these constraints are mostly conditioned by the radiation sources (proportional to the Am content of the pellets), and by the density of the pellet matrix, the fabrication technique has only a very limited influence on the order of magnitude of the dose rate due to a target rod and the additional protec-

tion is similar for each technique. However, the fabrication technique has an important effect on the secondary radiations due to dust, waste, and possible contamination. One advantage of the INRAM process is due to the reduced number of steps involving highly radioactive materials and to the liquid nature of the infiltrant, so that the hazard of radioactive dusts can be minimized, as well as the risk of contamination within the glove-boxes.

In particular, ITU has demonstrated on a laboratory scale, the feasibility of the infiltration (INRAM) technique consisting of the infiltration of the active solution (Am nitrate) into a non-active matrix (a porous pellet in this case) by capillary forces. Tests are still required to permanently avoid the heterogeneity sometimes observed in the americium distribution, which did probably occur by diffusion during thermal treatment.

The final recommendation of these studies is to pursue R/D effort in the development and testing of the new or improved techniques for the fabrication of advanced MOX fuels and of targets including minor actinides.

## 3.2 Basic Work on Inert Matrices

### 3.2.1 Simulation of fission and $\alpha$ -damage in inert matrices for the transmutation of minor actinides

#### Spinel, $MgAl_2O_4$

New samples of spinel  $MgAl_2O_4$  were irradiated with 70 MeV I-ions (fission product of fission energy) at the Tandem of the TU München, with Bi-ions of 2.38 GeV and 120 MeV energy, respectively, at GSI Darmstadt, with 2 MeV and 260 keV He-ions at INFP, FZK Karlsruhe and with 30 MeV C<sub>60</sub>-buckminsterfullerenes at the Tandem of IPN Orsay. These new experiments extend the work performed on spinel (see TUAR-97, p.85) to study its behaviour against the impact of energetic ions simulating fission damage [1] or against the impact of He-ions simulating the alpha-particle from decaying actinides (mainly <sup>242</sup>Cm).

#### He-behaviour in spinel

*Tab. 3.4* summarizes the irradiation conditions of the He-irradiated spinel specimens. In the EFFTRA-T4 experiment (see TUAR 97, p. 89) for the transmutation of <sup>241</sup>Am in the HFR re-

Contact (3.1.4.-3.1.5.): **Didier Haas** • tel.: +49 7247 951 367 • fax: +49 7247 951 566 • dhaas@itu.fzk.de

actor, the swelling of a  $MgAl_2O_4$  matrix containing initially 11%  $AmO_{2-x}$  was measured to be 18 v/o. As reported before (TUAR 97, p. 86), spinel samples irradiated with 72 MeV I-ions at different fluences and temperatures showed a similarly pronounced swelling [2]. As spinel was shown to be stable against neutrons, the scientific reasons being known, one has to consider the two other damage sources that will be present during reactor irradiations, i.e. the fission products and the alpha decay yielding an alpha particle and a recoil atom. In the host matrix,  $^{241}Am$  forms  $^{242}Am$  ( $T_{1/2} = 16$  h) by neutron capture which decays into  $^{242}Cm$  ( $T_{1/2} = 162.8$  d) decaying itself into  $^{238}Pu$  ( $T_{1/2} = 87.7$  y) [e.g. 3]. As a consequence of this decay chain, large quantities of He are incorporated into the matrix hosting the americium to be transmuted. The ratio of He to fission gases is  $\sim 10$  at the end of the irradiation. If this helium is retained in the matrix, it may induce swelling (e.g. bubbles formation can occur). To study the He-behaviour, the temperature dependence of He-release from implanted spinel single crystals (see Tab. 3.4) was measured using the Knudsen-cell- technique, using mass spectrometry to measure the He-concentration.

Energy (MeV)	Range ( $\mu m$ )	Straggling ( $\mu m$ )	Dose (ion/cm <sup>2</sup> )	Remarks
2	4.29	0.32	$5 \cdot 10^{16}$	2 spots – average dose
0.260	0.79	0.08	$10^{16}$	All surface implanted

Tab. 3.4 Irradiation parameters and TRIM96-code calculations of range and straggling of He-ions in  $MgAl_2O_4$ .

The samples were placed in a tungsten Knudsen cell and heated in steps of  $\sim 50$  K up to 2100 K. At 2000 K, the release of He is practically completed and the spinel is not yet molten. Fig. 3.2 shows the 2 MeV He-irradiated sample before and after the heating treatment. Part a) of this figure is showing two irradiated spots without visible swelling. Part b) is a profile recorded with a Dektak 8000 profilometer after heating the specimen up to 2100 K, showing that the whole irradiated volume was lost, i.e. the measured depth of the two holes corresponding to the two beam spots was identical to the range calculated with the TRIM96 code. This could indicate that overpressurized He bubbles formed at the end of the range of the  $\alpha$ -particles which upon heating caused the damaged overlying lid to spall off. In this case, release would be due to mechanical disintegration rather than long-range diffusion.

Curves of fractional release of He vs. temperature are shown in Fig. 3.3. The release of He starts for both implanted specimens at around 1100 K. The release curve for the specimen implanted with 2 MeV He-ions is shifted to higher temperatures. Essentially no release is seen below 1000 K and the release of He is complete for both specimens at 2100 K. At high temperatures ( $> 1600$  K) enhanced Mg-evaporation (not shown on the curve) was seen.

New experiments will be performed on other He-implanted specimens (other heating schedules and other He-concentrations) to determine the release mechanisms, i.e. to deter-

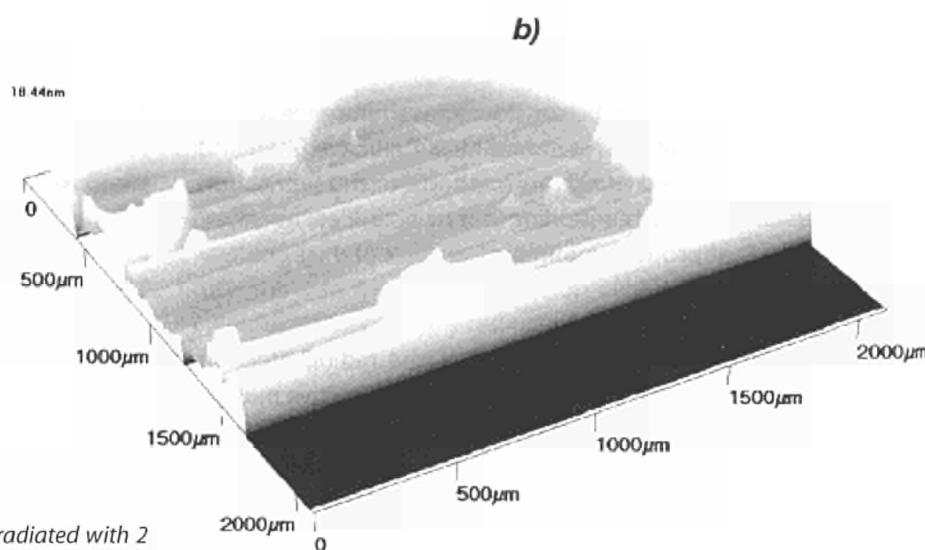
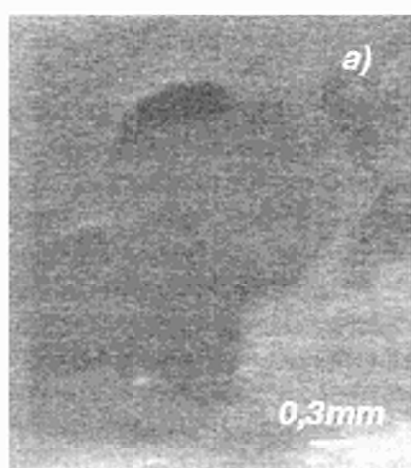


Fig. 3.2 a) SEM micrograph of an  $MgAl_2O_4$  crystal irradiated with 2 MeV He-ions at an average dose of  $5 \cdot 10^{16}$  ions/cm<sup>2</sup>. b) Profile recorded after thermal treatment of the same specimen.

mine if and how much He diffuses through the matrix or if the release is due to the degradation of the matrix connected with the observed spalling of the damaged layer.

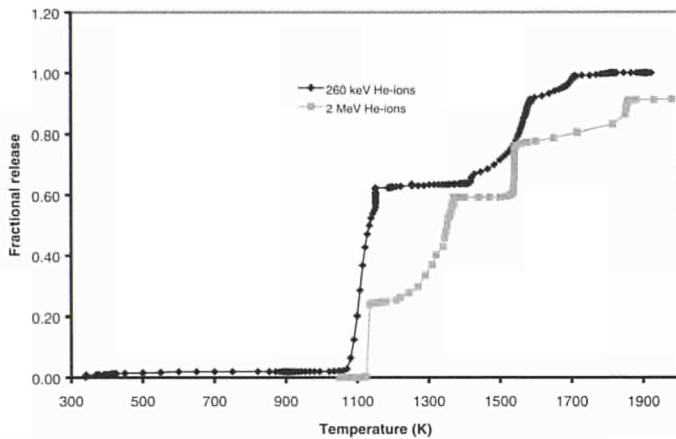


Fig. 3.3 He-release from spinel irradiated samples vs. temperature.

### TEM studies on spinel irradiated with heavy ions

Tracks were observed in plan view by transmission electron microscopy in the spinel implanted with high-energy Bi-ions (2.38 GeV and 120 MeV) and with 30 MeV Buckminster fullerenes (see Fig. 3.4a-3.4c) showing that spinel is sensitive to electronic energy loss, and giving an explanation of the observed large swelling. For the fullerenes, the shape of the tracks indicates that the initial fullerenes were frequently split into 2 and sometimes into 3 fragments. The mean track diameter is about 20 nm corresponding to the juxtaposition of two tracks of 10 nm diameter due to the two fragments. The samples irradiated with Bi-ions also show clearly visible tracks of  $3.5 \pm 0.5$  nm diameter for both the 2.38 GeV ions and for the 120 MeV ions (see Figs. 3.4b and 3.4c). In parallel work, performed in co-operation with S.J. Zinkle (Oak Ridge Nat. Lab., USA) and V.A. Skuratov (Flerov Lab., Dubna, Russia), similar track diameters were found in sintered spinel (2.0 and 2.6 nm for 430 MeV Kr and 614 MeV Xe-irradiations, respectively) [4]. The nature of the track is not yet clear. The question is still open whether the track core is amorphous or whether overlapping of tracks is necessary to induce the amorphization which is found at high fluences [4,5]. The mechanisms for track formation will be carefully further investigated by both high resolution TEM and by theoretical treatments of the existing data.

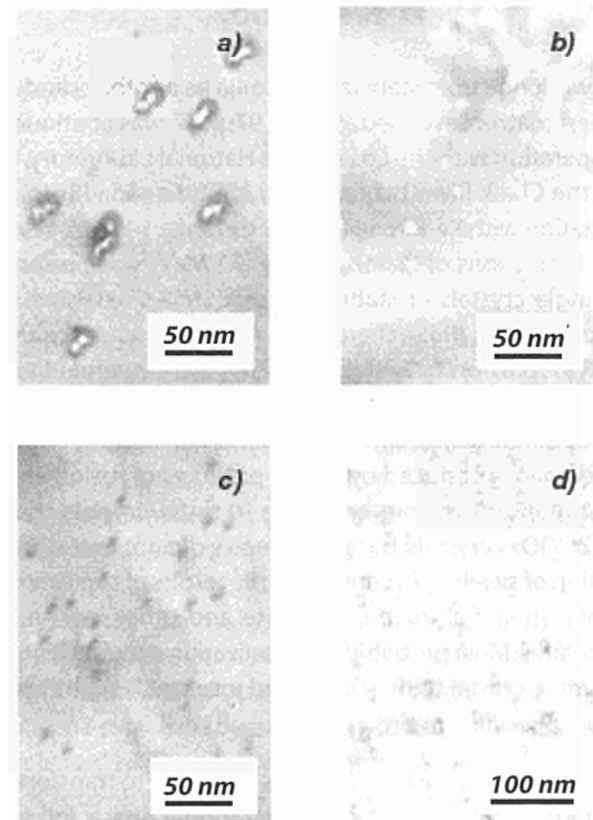


Fig. 3.4 TEM viewgraphs of  $MgAl_2O_4$  irradiated with a) 30 MeV C60 Buckminster fullerenes b) 2.38 GeV Bi-ions c) 120 MeV Bi-ions and d)  $CeO_2$  irradiated with 70 MeV I-ions.

### Ceria, $CeO_{2-x}$

$CeO_{2-x}$  is a further candidate inert matrix. It is isostructural to  $UO_2$  and is also studied at present for Pu-incineration. Sintered disks of  $CeO_2$  were irradiated with fission products of fission energy. Fig. 3.4d shows that tracks also form in  $CeO_2$  due to the impact of 70 MeV I-ions, and thus that  $CeO_2$  is more sensitive to high electronic energy losses than  $UO_2$ . The tracks formed are about 3 nm in diameter. This type of investigation applying low irradiation fluences constitutes a rapid and easy way to determine if microstructural modifications can be expected from heavy ions (fission products) irradiation. The thermal spike model of Toulemonde et al. [6] has been shown to quantitatively describe measured track diameters in different insulators following irradiations with swift heavy ions (e.g. in  $UO_2$ , [7]). We will apply this and other models to the present results on  $CeO_2$  and spinel in continued research.

## Zirconia, ZrO<sub>2</sub>

The work on cubic-stabilized zirconia as another candidate as inert matrix described in TUAR 97, p. 87, was continued, in co-operation with the Los Alamos National Laboratory, USA, and the Chalk River Laboratories, AECL, Canada [8]. Ion implantation with Xe-ions in the energy range 340-400 keV and with iodine ions of fission energy (72 MeV) was performed on single crystals of stabilized cubic ZrO<sub>2</sub>. The Rutherford backscattering (RBS)/channeling experiments described in TUAR 97, p. 87 on Y<sub>2</sub>O<sub>3</sub>-stabilized ZrO<sub>2</sub> were extended to stabilized ZrO<sub>2</sub> additionally doped with Ce (simulation of Pu or Am) or different rare earths (simulation of neutron poisons). The damage produced by fission products of fission energy was significantly more extensive in these crystals than in the (Zr,Y)O<sub>2-x</sub> crystals, but profilometry did not reveal any indication of swelling, in contrast to the results of similar experiments on spinel, zircon, monazite and other inert matrix candidates. Most probably, polygonization occurred causing the single crystal to be subdivided into small, slightly misaligned crystalline grains.

Unstabilized, monoclinic ZrO<sub>2</sub> was observed to transform into a higher symmetry, cubic or tetragonal phase, following irradiation with 380 keV Xe<sup>++</sup>-ions to fluences in excess of 5x10<sup>14</sup> ions/cm<sup>2</sup> at 120 K. Simultaneously, the ZrO<sub>2</sub> densified by ~ 5%. No amorphization of the pure ZrO<sub>2</sub> was observed to a Xe-dose equivalent to a peak displacement damage level of ~ 680 dpa.

In conclusion, pure ZrO<sub>2</sub> was shown to be very radiation resistant, similar to ThO<sub>2</sub> and UO<sub>2</sub>. Stabilization of the cubic structure with Y<sub>2</sub>O<sub>3</sub>, in particular when accompanied by doping with rare earths, caused the zirconia to accumulate damage much faster, probably related to the large concentration of oxygen vacancies introduced by the three valent ions causing the zirconia lattice to be less stable.

### References

- [1] Hj. Matzke, Proceedings Frederic Joliot Summer School in Reactor Physics, "Innovative Nuclear Fuels and Applications", part II, edited by CEA Cadarache, 1998
- [2] T. Wiss and Hj. Matzke, Proceedings of 19th International Conference on Nuclear Tracks in Solids, Besançon, France, 31/08/98-04/09/98, to be published in "Radiation Measurements"
- [3] N. Chauvin, R.J.M. Konings and Hj. Matzke, J. Nucl. Mater. special issue "Inert Matrix Fuels", Ed. C. Degueldre (1999)
- [4] S.J. Zinkle, Hj. Matzke and V.A. Skuratov, MRS 1998 Fall Meeting, Nov. 30-Dec. 4, 1998, Boston.

- [5] S.J. Zinkle and V.A. Skuratov, Nucl. Instrum. Meth. B 141 (1998) 737-746
- [6] M. Toulemonde, E. Paumier and C. Dufour, Radiat. Eff. Def. Solids 126 (1993) 205
- [7] T. Wiss, Hj. Matzke, C. Trautmann, M. Toulemonde and S. Klaumünzer, Nucl. Instrum. Methods Phys. Res. B 122 (1997) 583
- [8] K.E. Sickafus, Hj. Matzke, T. Hartmann, K. Yasuda, J.A. Valdez, P. Chodak III, M. Nastasi and R. Verrall, presented at Inert Matrix Workshop, PSI, Switzerland, October 1998, and special issue J. Nucl. Mater., in press

## 3.3 Partitioning and Transmutation Experiments

### 3.3.1 New partitioning techniques using centrifugal contactors

The improvements and the extension of the centrifugal extractor battery from 12 to 16 stages, reported in the previous annual report (TUAR-97, p.92) has permitted more complete tests of different process schemes. During the present reporting period significant progress was made at ITU, especially concerning the integral counter current extraction tests to improve and verify the DIAMEX process scheme. A number of preparative experiments were carried out, followed by the hot verification using High Level Liquid Waste (HLLW); namely:

- PUREX reprocessing of commercial LWR fuel using centrifugal extractors installed in a hot cell in order to produce genuine HLLW feed for the DIAMEX process.
- Inactive experiments (cold test), using 8 centrifugal extractors with simulated HLLW solution (only Ln) as feed in order to determine the performance of the extractor battery and optimise the process scheme.
- Batch extraction tests using HLLW.
- Continuous counter current extractions of An/Ln from HLLW using 16 centrifugal extractor to verify an optimised process scheme.

For the DIAMEX process the flow-sheet was optimised on the basis of data obtained from the cold test with a simulated lanthanide solution (3.44 M in nitric acid and 0.1 M in oxalic acid). Oxalic acid was added to prevent the extraction of Zr and Mo. Using results from this test and from a hot batch

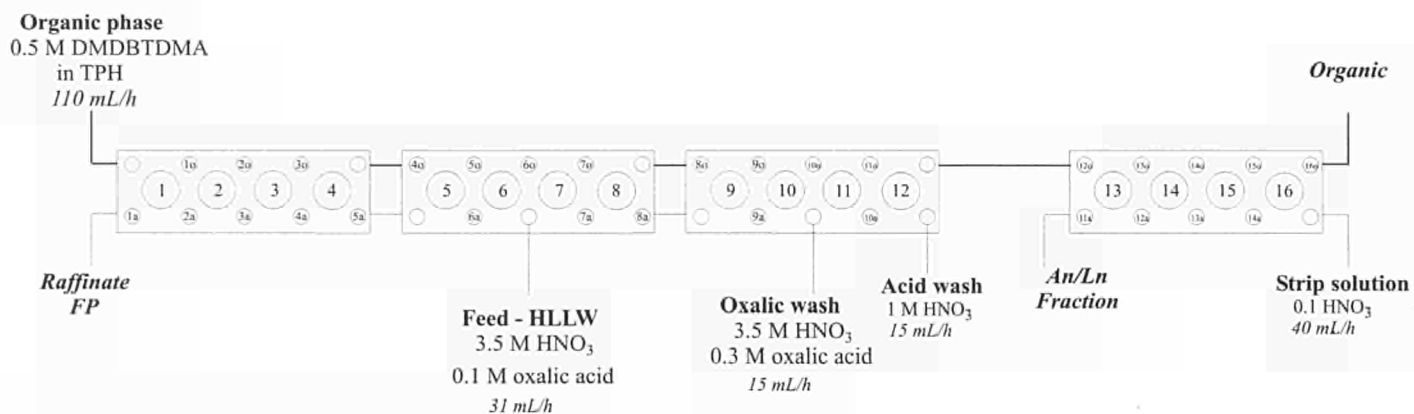


Fig. 3.5 The flow sheet used in the DIAMEX test.

test, an optimised process scheme was developed using the PAREX code [1] see Fig. 3.5.

The aqueous concentration profiles show that all minor actinides (MA), Am, Cm and also Np, are efficiently extracted, similar to the lanthanides. The back-extraction of the actinides and lanthanides (stage 13-16) is even more efficient, except for Np, where kinetic effects might have a significant influence on the extraction process.

The profiles in the oxalic scrubbing section (stage 7-10) show that co-extracted Zr and Mo is almost completely back-extracted to the aqueous phase. For co-extracted Tc and Pd, and to some extent Ru, oxalic scrubbing is not efficient. In the back-extraction section, the Pd and Ru profiles indicate a slow back-extraction, and the efficiency could probably be increased using more stages. In this section the Tc profile indicates also an accumulation in the organic phase. Additional process development is needed to solve the problem related to these difficult fission products.

Ln/An isotopes	DF
La-139	650
Ce-140	815
Pr-141	835
Nd-146	609
Sm-152	426
Eu-153	438
Gd-156	189
Np-237	1020
Am-243	1000
Cm-144	1167

FP isotopes	DF
Zr-91	3.7
Mo-98	3.8
Tc-99	462.0
Ru-101	4.9
Pd-105	610.0

Tab. 3.5 Decontamination factors (DF) achieved in the DIAMEX process (Feed/Raffinate).

The decontamination factors of the feed for the major isotopes analysed are shown in Tab. 3.5.

The MA elements show higher DF values compared with the lanthanides. In the lanthanide series DF values vary with the element number and are at maximum for Ce and Pr. This result can be explained by a different stability of the extracted complexes. From the analyses of aqueous and organic effluents, a recovery of more than 99.9% of Am and Cm in the process was calculated, *i.e.*, the losses of these elements in the process are very low. With the present experiments it could be demonstrated, that by means of the DIAMEX process an efficient separation of MA from genuine HLLW (obtained from PUREX type reprocessing of commercial LWR fuel) is possible. The process represents an excellent compromise between reasonably good extraction and even better back-extraction properties for MA. The An/Ln fraction produced from the DIAMEX process, permitted new extractive molecules for the separation of actinides from lanthanides to be tested (see chapter 3.3.2).

#### Reference

- [1] B. Dinh, B. Mauborgne, P. Baron, "Dynamic Simulation of Extraction Operations: Application in Nuclear Fuel Reprocessing" ESCAPE 2, Toulouse-France (1992)

### 3.3.2 Separation of An(III) from Ln(III)

In the previous report the lanthanide separation from minor actinides (MA), could be demonstrated on a genuine TRPO partitioning effluent. A separation factor > 400 was achieved in a 3 stage extraction by commercially available dithiophosphonic acid (see TUAR-97, p. 92). Unfortunately the separa-

tion is efficient only at pH > 2, thus a denitration of the feed, with a considerable risk of precipitation, is necessary. This drawback can be avoided and the separation factors can be increased with chlorophenyl substituted dithiophosphinic acid.

It has been shown from inactive and spiked tests performed in the Forschungszentrum Jülich that a successful separation of trace amounts of An(III) from Ln(III) is possible from 0.5 M HNO<sub>3</sub> using the system 0.5 M bis(chlorophenyl)dithiophosphinic acid + 0.25 M TOPO in tertbutylbenzene. At ITU, the method was tested under real conditions using the genuine An/Ln effluent of the DIAMEX process (see chapter 3.3.1). The high radiation dose delivered, especially from alpha decay, might cause significant damage to the solvent and thereby affect the extraction efficiency. Batch extraction tests have been carried out at 0.5 and 1 M HNO<sub>3</sub>. The distribution factors are shown in Tab. 3.6.

Isotope	D – Value <sup>1</sup>	
	0.5 M An/Ln sol.	1.0 M An/Ln sol.
<sup>99</sup> Tc	> 21000	> 4000
<sup>101</sup> Ru	1.0	0.3
<sup>105</sup> Pd	> 2200	> 1400
<sup>139</sup> La	1.1	0.1
<sup>140</sup> Ce	1.7	0.2
<sup>141</sup> Pr	1.7	0.2
<sup>146</sup> Nd	1.1	0.2
<sup>152</sup> Sm	1.4	0.3
<sup>153</sup> Eu	1.4	0.4
<sup>237</sup> Np	600	13
<sup>243</sup> Am	25.2	2.5
<sup>244</sup> Cm	7.8	0.8
SF <sub>2</sub> <sup>2</sup>	18.3	5.6

<sup>1</sup>) Distribution value, [Metal]<sub>organic</sub>/[Metal]<sub>aqueous</sub>

<sup>2</sup>) Separation factor, D<sub>Am</sub>/D<sub>Eu</sub>

Tab.3.6 Distribution factors obtained from the batch tests.

From the D-values obtained it is clear that Tc, Pd and Np are co-extracted with the MA. Furthermore, the results show that, as expected, the extraction is strongly dependent on the acid concentration. However, both the distribution factors for the MA and the separation factors from Ln are even at 1.0 M HNO<sub>3</sub> large enough to obtain in several stages a MA fraction with sufficiently low lanthanide content.

### 3.3.3 Am transmutation (EFTRA-T4 and EFTRA-T4bis)

In 1995 the T4 experiment was initiated by the EFTRA partners to study the feasibility of americium transmutation in a so-called once-through mode. In this scenario the fissioning extent should be very high (> 90%). The T4 experiment was performed as a shared cost action project in the cluster "P&T strategy studies and transmutation experiments" of the Fourth Framework Programme of the EC.

For the T4 experiment, pellets of magnesium aluminate spinel (MgAl<sub>2</sub>O<sub>4</sub>) containing about 10-12 w/o <sup>241</sup>Am were fabricated by the infiltration method (INRAM) at ITU [1]. This method yields a relatively fine distribution of the americium in the pellet. However, it was observed that this distribution is not uniform and that the americium, intended to be present as an oxide, formed a compound during sintering, which is probably AmAlO<sub>3</sub>. Two irradiation capsules were prepared, T4 and T4bis.

The irradiation of the T4 target in the HFR at Petten has been performed from August 1996 to January 1998 (358.4 full power days), during which a burnup of 32% FIMA (value obtained from post-test burnup calculation) has been achieved. During the irradiation a neutron radiograph was made. After the irradiation the fuel was examined non-destructively in the hot-cell laboratories in Petten. The following results are now available [2]:

- Neutron radiography of the sample holder at mid-of-life shows no visible damage of the fuel pin and an increase of the length of the pellet stack.
- Gamma-spectrometry and gamma-tomography of the fuel pin show that the distribution of the fission products is correlated to the initial americium concentration of the pellets, and an increase in length of the pellet stack and in the diameter of the pellets.
- Profilometry of the fuel pin showed an increase of the diameter of the cladding from the original 6.55 mm to a maximum of 6.75 mm after irradiation.

From the results it is clear that considerable swelling of the fuel occurred: about 18% in volume. This swelling can be caused by two different processes: (i) the damage of the spinel matrix by fission fragments, which can be extensive in this type of fuel due to the relatively small size of the americium containing particles (< 3 μm), and (ii) the formation of gas bubbles containing helium produced by the alpha de-

cay of  $^{242}\text{Cm}$ , one of the isotopes in the transmutation chain of  $^{241}\text{Am}$ . Destructive examinations to be performed at ITU will investigate the relevance in these phenomena.

The results of the T4 test, combined with results of theoretical studies and other experiments, are being used to modify the design of the targets. It is proposed to use a so-called "hybrid" fuel, a dispersion of spherical inclusions (between 50 and 300  $\mu\text{m}$ ) - containing americium, in a dense inert matrix. For the host phase the cubic solid solution  $(\text{Zr},\text{Am})\text{O}_2$ , possibly stabilised by yttrium, and for the inert matrix  $\text{MgO}$  (fast reactors) and  $\text{MgAl}_2\text{O}_4$  (thermal reactors) are the most likely candidates. These materials will be tested in a new experiment (EFTTRA-T5) to be loaded in HFR. The targets will be fabricated at the ITU, and the necessary fabrication development work is already underway, as described in section 2.4.2 of this report.

The T4bis pin is still in HFR and its irradiation will be pursued until 1999.

#### References

- [1] K. Richter, A. Fernández, J. Somers, J. Nucl. Mater. 249 (1997) 121
- [2] R.J.M. Konings, R. Conrad, D. Haas, G. Mühlhling, J. Rouault, G. Vambenepe, Transmutation of Am and Tc: recent results of EFTTRA, OECD/NEA Fifth International Information Exchange Meeting on Actinide and Fission Product Partitioning and Transmutation, Mol, 25-27 Nov. 1998

### 3.3.4 Technetium transmutation (EFTTRA T2)

Technetium is a non-natural element that is present in significant amounts in spent fuel from nuclear reactors. Upon reprocessing of the spent fuel, technetium remains in the high level waste (HLW), which is then vitrified, temporarily stored and eventually disposed of by geological burial. Studies on the long-term radiological effects of this HLW show that  $^{99}\text{Tc}$  is among others a highly radiotoxic and one of the risk dominating isotopes. Therefore transmutation of such isotopes to short-lived or stable ones will significantly reduce the radiotoxicity and further potential risks of such a waste.

The study of the transmutation of the technetium was started in 1992 when irradiation tests of targets of  $^{99}\text{Tc}$  metal were planned for the High Flux Reactor (HFR) at Petten as well as the PHENIX fast reactor at Cadarache. The fabrication of the

targets for these tests was studied at ITU, where a technique was developed for the fabrication of cylinders/pellets by casting of liquid technetium metal in a water-cooled copper mould. The targets that were fabricated for the irradiation tests each contained two of such cylinders (4.8 mm diameter, 25 mm length).

The results of the T1 test showed good behaviour of the technetium metal at a transmutation extent of about 6%. To study the behaviour at a higher transmutation, one of the targets (2 cylinders) of the T1 test was re-encapsulated and irradiated again in the HFR. The T2 test has been completed successfully in 1997 and the results of the post-irradiation examinations have become available recently.

The cumulative irradiation time for the T2 experiments was 24 reactor cycles (579.3 full power days) during which the total neutron fluency was about  $5.8 \times 10^{26} \text{m}^{-2}$ . The post-irradiation examination (PIE) revealed an excellent in-pile behaviour of the metallic technetium rods. Metallographic examinations showed no changes in the microstructure compared to the unirradiated material. Electron probe microanalysis (EPMA) of the radial distribution of ruthenium, the product of the transmutation process, showed an increase from about 15-16% in the centre to 30-40% near the rim of the pellets, giving a pellet-average Ru concentration of about 18%. Mass spectrometric analysis of the pellet-average Ru concentration showed that the extent of transmutation is about 16%.

The results of the T2 test indicate that there are no technical limitations to the use of metallic technetium as a target for transmutation.

### 3.3.5 Transmutation studies of $^{99}\text{Tc}$ with high Ru content (Pompei experiment)

As shown in section 3.3.4,  $^{99}\text{Tc}$  can be irradiated without difficulties to achieve up to the level of 16% transmutation to  $^{99}\text{Ru}$  [1]. In order to test the materials performance at even higher rates of transmutation, ITU fabricated two relevant Ru alloys with a higher Ru content:  $\text{Tc}_{0.5}\text{Ru}_{0.5}$  and  $\text{Tc}_{0.2}\text{Ru}_{0.8}$ . These alloys together with pure Tc sample have been irradiated for 240 days reaching a (calculated) transmutation of 7.0 a/o in the HFR reactor in Petten (Netherlands) within the frame of the POMPEI programme. In the following, the analysis of the material before irradiation is reported. The irradiated speci-

Contact (3.3.3-3.3.4): Rudy Konings • tel.: +49 7247 951 391 • fax: +49 7247 951 566 • konings@itu.fzk.de

mens are recovered but proved to be very difficult to be etched for metallography. The complete analysis of the irradiated specimens will therefore be reported in the next report.

The Ru containing samples were polished, chemically etched using a Murakami modified solution, developed in our laboratories and analyzed by optical microscopy (Fig. 3.6a and 3.6b). The pure Tc sample was observed under polarized light. (Fig. 3.6c)

In addition the Ru containing samples revealed microstructure differences as compared to the pure technetium, and exhibit columnar grains with a combination of growth orientations along the  $\{0\ 0\ 0\ 1\}$  and the  $\{1\ 0\ \bar{0}\}$  crystallographic directions.

The  $Tc_{0.5}Ru_{0.5}$  sample presents a microstructural feature located in the initial grains. Two explanations might apply in order to understand the appearance of such a structural feature. The first is that etching has brought out some dendritic nature of the growth process by which the individual grains were formed. Similar phenomena have been reported to appear in Mo-V alloys [2]. The second is that some kind of surface effect was produced during etching. The pure Tc material on the other hand, showed columnar grains with an homogeneous growth habit preferentially oriented along the  $\{0\ 0\ 0\ 1\}$  crystallographic direction, Fig. 1c, starting at the periphery of the cylinder towards the center.

EPMA of the Ru containing specimens, confirmed their theoretical concentration showing very slight differences in the Ru content between the center and the periphery of the sample.

#### References

- [1] R.J.M. Konings, A.D. Stalios, C.T. Walker, N. Cocuau, J. Nucl. Mater. 254 (1998) 122
- [2] W. Rostoker, J. R. Dvorak, "Interpretation of Metallographic Structures" 3rd edit. Academic Press Inc. (1990) p.102

#### 3.3.6 Postirradiation examination of high plutonium content fuels (Trabant 1)

Trabant 1 is a high plutonium content ( $U_{0.55}Pu_{0.45}O_{2-x}$ ) pin that was irradiated to a high burn-up (9.5 a/o in 12 cycles over one year) as part of the CAPRA project in HFR Petten. The pin was located in a molybdenum shroud and was

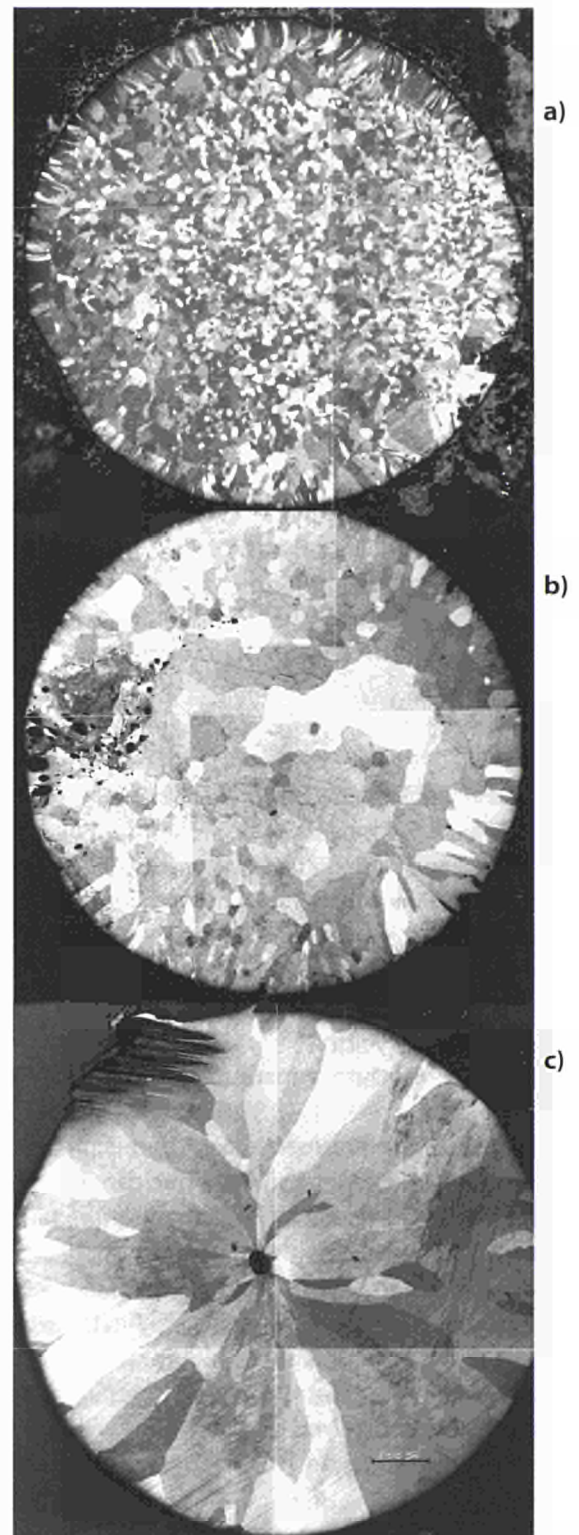


Fig. 3.6 Structural details of the as fabricated material; (a) top,  $Tc_{0.5}Ru_{0.5}$ ; (b) middle,  $Tc_{0.2}Ru_{0.8}$  and (c) bottom, Tc pure. Note the structural differences such as e.g. grain size, orientation and planar defects. (Magnification: 50X.)

sodium cooled. After it became defective it was in operation for at least further 5 cycles during which fuel displacements occurred. The Non-Destructive Testing (NDT) metallographic examination were requested by CEN Cadarache to determine:

- the cause of the failure
- the extent and mechanism of the translocations.

The radiography shows a 6 cm long ruptured zone at the top end of the fuel stack. In this area the pin has two major defects where molten fuel had escaped from the cladding. Light shadows through the whole defect zone indicate a longitudinally cracked cladding. The pin has also ballooned in this zone. A sample cut from this zone confirms a longitudinal crack but shows also a partially molten cladding with candling and in the fuel, metallic particles were detected (Fig. 3.7).

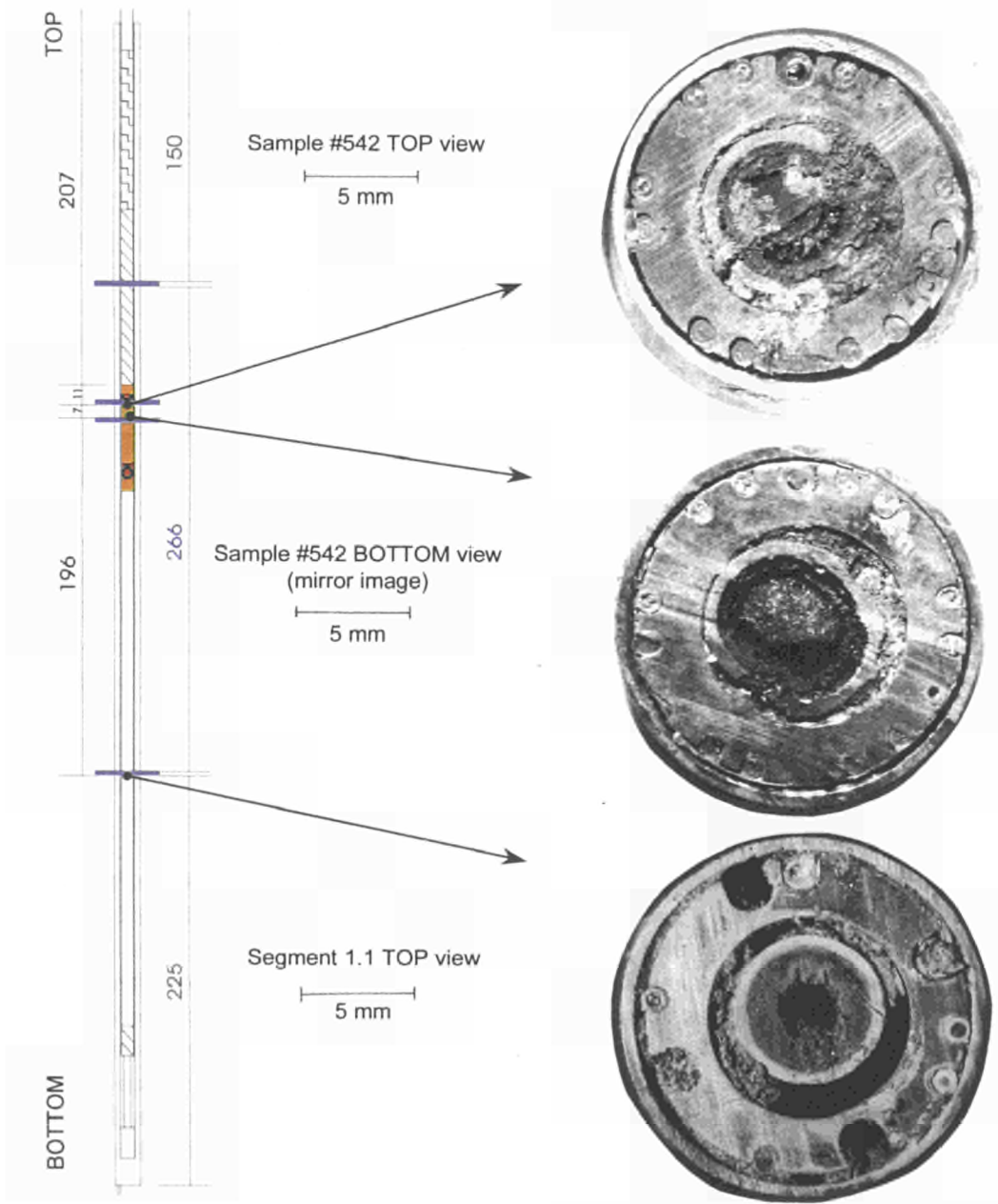


Fig. 3.7 Trabant 1 Pin 1: Locations of cuts and macrographs of surfaces (as cut).

This behaviour is evidently the result of severe overheating. The fuel pellets central channel at the fuel top is filled with dense fuel from condensation and/or relocation processes. In contrast, a second cut made in the lower half of the fuel stack showed the central channel in this region to be open. To prove the hypothesis of fuel condensation, a further cut should be made at the cooler bottom end of the fuel stack to check the central channel. If fuel condensation has occurred, it should also be filled with material.

The results obtained from micro  $\gamma$ -scanning at the fuel top are in good agreement with those given by ECN. They show a significant release of volatile fission products, which are condensed to a large extent between the steel cladding of the pin and the molybdenum shroud. This could happen in the case of interrupted sodium cooling. Ceramographic studies show a severe intrusion of sodium in the fuel and the formation of a highly porous material that is assumed to be a sodium uranate or plutonate. Only the dense condensate in the central channel, which has metallic inclusions (cladding material?), has withstood the sodium attack.

At present, it is assumed that the primary cause of failure was an interruption of, or reduction in cooling at the fuel top, which lead to a break in the cladding and subsequent sodium ingress. An alternative explanation could be stress corrosion cracking. Indications of stress corrosion cracking in the cladding have been found in a metallographic specimen originating from near the longitudinal cladding defect.

More investigations are planned to clarify the course of events that lead to the development of the major (though probably not primary) failure at the top of the fuel stack.

### 3.3.7 New approaches in partitioning and transmutation

The transmutation of radiotoxic waste resulting from nuclear energy generation has been proposed as a medium term option for waste management. This involves the development of a subcritical fast reactor driven by a spallation source. Because of the accumulated experience one would regard as the best choice as fuel: oxides or metals. In the following therefore the potential of oxide and metal fuel will be discussed in view of the newly proposed reactor concept and its fuel reprocessing.

Looking back in the history of nuclear power reactor develop-

ment there was a parallel use of oxide and metal fuels which determined the reactor design according to the compatibility with moderator and/or coolant. Since for fast reactors the need for moderation does not exist, Na is used as the coolant for both fuel types. Considering the experienced difficulties with sodium future designs conceive alternate coolants. Pb-Bi is being used in propulsion reactors of small size. An upscale for nuclear power plants is being investigated. However, Pb would exclude the use of metallic fuel since it forms low melting alloys with actinides (see Fig. 3.8). Pb similar to Na forms also ternary oxides with oxide fuels with the same disadvantages. The problems to use lead cooling in large size power plants are not yet solved, so that He cooling is considered as an alternative. Helium would be of course compatible with metal fuels.

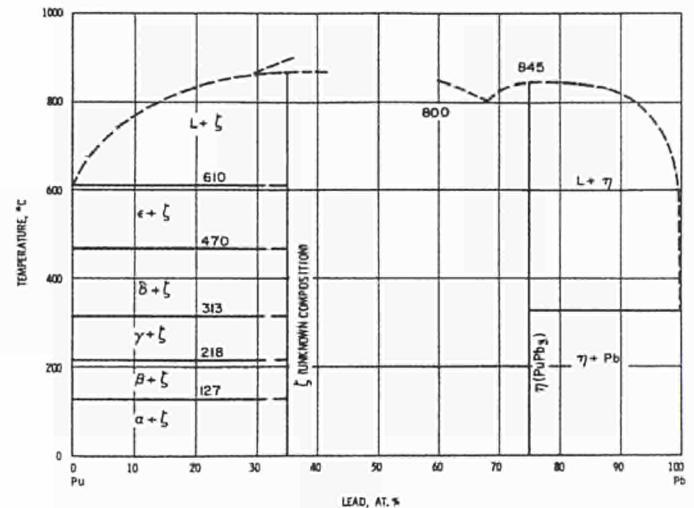


Fig. 3.8 Phase diagram of Pb-Pu [1].

Any transmutation concept requires a rework of the fuel to partition the remaining long term toxic from the less toxic nuclear waste. Here the question arises whether to use the well established aqueous or the pyrochemical reprocessing. The latter was developed so far only for special applications. There are incentives to use the dry route because the partitioning installations would be more compact, the radiolytic effects observed in aqueous solutions could be eliminated and the fuel could be reprocessed with short delay thus reducing the out of pile inventory. The pyrochemical reprocessing has been exercised for oxide at the RIAR installations at Dimitrovgrad. However, the there developed DOVITA process [2] so far is not capable of separating the minor actinides.

The foreseen fractionated precipitation to separate lanthanide from actinides might be too complicated for industrial application. But also the electrochemical separation of the metallic actinides from alkaline chloride melts - as being developed by CRIEPI [3] - has so far not achieved a sufficient separation of americium from lanthanide. Here the reductive extraction of the actinides into liquid Cd or Bi seems a promising route. Therefore, the metallic separation pyroprocessing seems to be the more promising technique and consequently would favour the use of metallic fuels in advanced reactors. A pilot installation is being set up at ITU under a joint research agreement with CRIEPI.

In this new pyrometallurgical project (within the Joint Research Agreement with the Central Research Institute of Electric Power Industry - CRIEPI) the feasibility and optimization of the actinide recycling technology of spent metallic nuclear fuel will be demonstrated. Another item of the contract is the recovery of minor actinides from high level liquid waste (HLLW) originating from aqueous PUREX reprocessing.

The processes applied are electrolytic and liquid-liquid extraction based on the use of molten salt and liquid metal (Cd or Bi) and comprise the following experiments:

- electrorefining of metallic fuels consisting of the anodic dissolution of the fuels, the U recovery on a solid cathode followed by the recovery of Pu and the remaining U into a liquid Cd cathode in molten LiCl-KCl salt / liquid Cd system at about 500°C
- chlorinating of fission products oxides obtained by calcination of HLW in a LiCl-KCl mixture at about 700°C in a Cl<sub>2</sub>/CO gas mixture. The volatile elements will be trapped in a molten salt bath heated at the temperature of about 500°C
- reductive extraction for the separation of transuranium elements (TRU) from RE in a molten salt / liquid metal system
- recovery of TRU by the distillation of Cd.

All these experiments have to be performed in an argon atmosphere with an oxygen and water content less than 10 ppm respectively. The conceptual design of an installation composed of a new stainless-steel box (caisson) and an argon purification is given in *Fig. 3.9*.

## References

- [1] Plutonium Handbook – A Guide to the Technology. O. J. Wick, Gordon and Breach, Science Publishers, New York, London, Paris, p. 211 (1967)
- [2] A.V. Bychkov; O.V. Skiba; A.A. Mayershin, V.A. Kisly, S.K. Vavilov, M.V. Kormilitzyn, L.S. Demidova, L.G. Babikov, R.A. Kuznetsov, GLOBAL '97. Proceedings International Conference on Future Nuclear Systems, Yokohama, Japan, Oct. 5-10, 1997. Vol. 1, p. 657-662
- [3] T. Inoue, H. Tanaka, GLOBAL '97. Proceedings International Conference on Future Nuclear Systems, Yokohama, Japan, Oct. 5-10, 1997. Vol. 1, p. 646-652

### 3.3.8 Minor actinide containing Zr-alloy based fuel (CRIEPI III)

The irradiation of the U, Pu, ZrMA (RE) alloy in the PHENIX reactor is further delayed. So far all the acceptance tests are completed. The foreseen short irradiation of 3 pins during the last months of 1998 did not take place due to the earlier shut-down of the reactor. After the maintenance period in 1999 the reactor is planned to restart in 2000 and would then begin with the foreseen irradiation experiment.

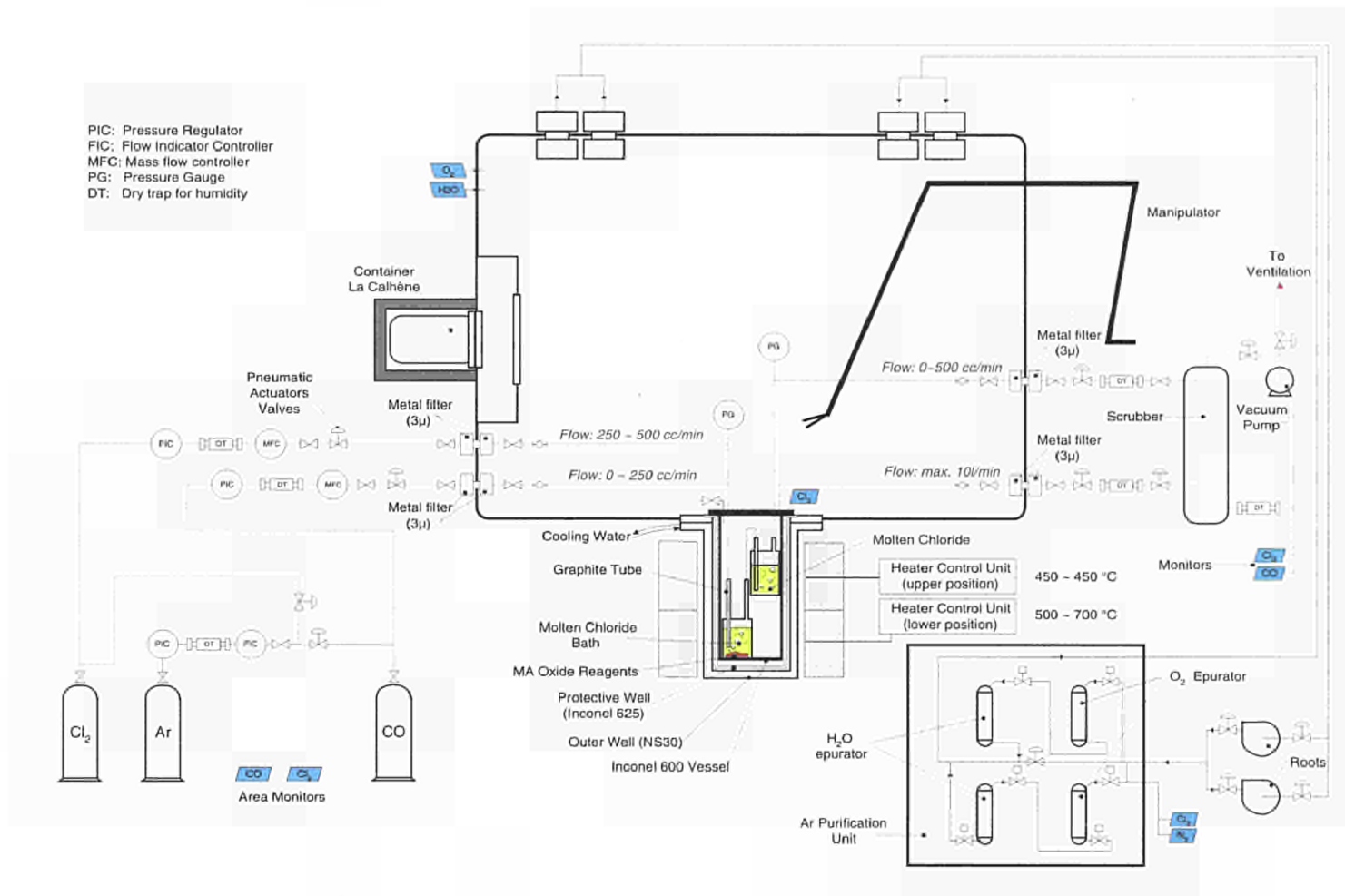


Fig.3.9 Caisson for pyrochemistry.

## 4. Spent Fuel Characterization in View of Long Term Storage

### 4.1 Characterization and Leaching Experiments

#### 4.1.1 Local phase examination of an oxidized spent fuel by micro-X-ray diffraction

High burn-ups affect significantly the microstructure and the thermophysical properties of LWR-fuels, especially at the pellet edge. The determination of potential crystal-structure changes in small pellet regions, occurring either due to irradiation, or during waste disposal, is therefore an important part of the fuel characterization. For this purpose, a micro X-ray diffraction technique for local analysis of fuel pellets was developed, whose first results on a pre-oxidated fuel, simulating an accidental exposure to air in a repository, are reported here.

A powder diffractometer installed in a lead shielded glove was used to study the phases formed at the surface of a slightly oxidized irradiated fuel. The sample, a longitudinal cut of a spent fuel pellet with burn-up 67 GWd/tM, was scanned by the line focus micro X-ray beam (dimensions at the opening of the collimator: 20  $\mu\text{m}$  x 2.8 mm) and the diffraction spectrum was obtained at several surface positions. Only the  $\text{UO}_2$  and  $\text{U}_4\text{O}_9$  fluorite structures were detected, which is in agreement with most of the reported observations on oxidized spent fuels [1-4]. The periphery (rim) region was examined in detail and the characteristic (111), (200) and (220) Bragg-peaks are presented in Fig. 4.1. It can be seen from the relative peak heights (most clearly from the (111) planes) that there is a radial variation of the oxidation degree. The bulk fuel is partially oxidized and the spectra from this area (not shown in Fig. 4.1) are similar to those obtained at  $r/r_o=0.892$ , while the outer rim area is completely oxidized and  $\text{U}_4\text{O}_9$  is the only phase existing.

The complete oxidation at the rim is due to the special structure characteristics of the material in this area: The higher burn up at the pellet rim compared with the bulk material, the increased surface area associated with the higher porosity [5] and radiation damage of the lattice, accelerate  $\text{O}_2$  diffusion and the conversion of  $\text{UO}_2$  to  $\text{U}_4\text{O}_9$ , which is then stabilized by the present fission products [4].

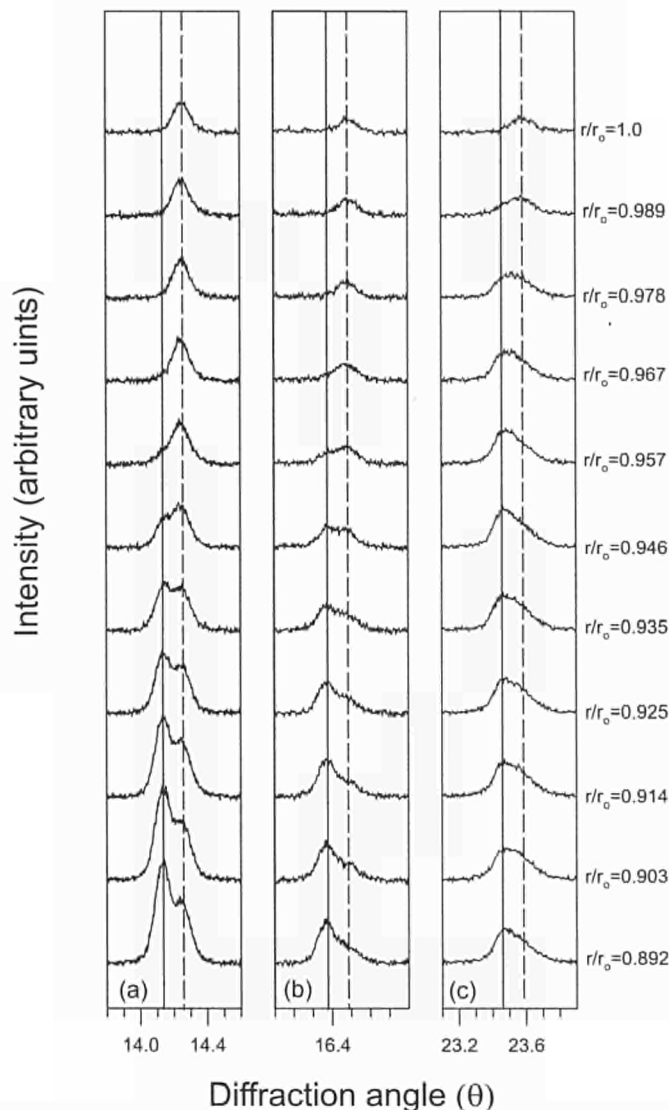


Fig. 4.1 X-ray diffraction peaks at several sample locations in the range between  $r/r_o=0.892$  and pellet edge (a): (111) plane, (b): (200) plane and (c): (220) plane; Solid line:  $\text{UO}_2$  peak positions, dashed line:  $\text{U}_4\text{O}_9$  peak positions.

#### References

- [1] L.E.Thomas, R.E. Einziger and R.E.Woodley, J. Nucl. Mater. 166 (1989) 243-251
- [2] L.E.Thomas, O.D. Slagle and R.E. Einziger, J. Nucl. Mater. 184 (1991) 117-126
- [3] R.E. Einziger, L.E. Thomas, H.C. Buchanan and R.B. Stout, J. Nucl. Mater. 190 (1992) 53-60
- [4] R.E. Thomas, R.E. Einziger and H.C. Buchanan, J. Nucl. Mater. 201 (1993) 310-319
- [5] J. Spino, K. Vennix and M. Coquerelle, J. Nucl. Mater. 231 (1996) 179-190

#### 4.1.2 Spent fuel characterization for interim dry storage- STEP 2 (CRIEPI X)

The project is being carried out under a contract with the Central Research Institute of the Electric Power Industry (CRIEPI) Japan. The purpose of this project, namely to characterize high burnup UO<sub>2</sub> and MOX spent fuel, is twofold: to assess their interim dry storage behaviour, and to obtain experimental data for the verification of computer codes used to evaluate their radiation source term. Destructive and non-destructive techniques are being used to characterize different fuel. The project began in 1998 and will be concluded in 2002.

Initial work performed included chemical analyses of the actinide and fission product content and axial neutron emission distribution determinations.

#### 4.1.3 $\alpha$ -radiolysis and $\alpha$ -radiation damage effects on UO<sub>2</sub> dissolution

##### Introduction

By the time the spent fuel containers in a geological repository may fail, i.e. after a few hundred years,  $\alpha$ -decay will constitute almost entirely the radiation field in and around spent nuclear fuel. Although the repository is characterized by reducing conditions, the presence of radiolysis products like H<sub>2</sub>O<sub>2</sub>, O<sub>2</sub> and OH radicals may cause oxidizing conditions near the fuel surface, which would enhance the dissolution of uranium. The activity of the spent fuel available today is dominated by  $\beta, \gamma$ -decays; hence, it is not representative of aged fuel in the repository. In order to simulate high levels of  $\alpha$ -decays at the surface of the fuel, pellets of UO<sub>2</sub> containing ~0.1 and ~10 w/o <sup>238</sup>Pu were fabricated and tested [1], comparing their leaching behaviour and properties to those of undoped UO<sub>2</sub>. In parallel to the leaching tests, characterization and radiation damage studies were performed on the  $\alpha$ -doped UO<sub>2</sub>, in order to investigate the build up of  $\alpha$ -decay damage (He-ion and ~100 keV daughter recoil ion) in the structure.

##### Experimental

The powders were prepared using a sol-gel method. This method was adopted to ensure a uniform distribution of the  $\alpha$ -activity in the final product. *Tab 4.1* shows the composition,

specific activity, and specific surface activity of a pellet for each of the materials used in this work. The specific surface activity was estimated as the activity of a volume at the pellet surface, with a thickness equal to half the range of  $\alpha$ -particles in UO<sub>2</sub>, i.e. ~7  $\mu$ m [2]. For these preliminary experiments, relatively high values of  $\alpha$ -activity were chosen, especially in the case of the UO<sub>2</sub>-10, in order to highlight the effects of radiolysis and  $\alpha$ -damage. Samples with lower  $\alpha$ -activities will be fabricated to simulate quantitatively the  $\alpha$ -activities of spent fuel in a repository.

Material	weight fraction of additive (%)	$\alpha$ -activity of mixture (Bq·g <sup>-1</sup> )	$\alpha$ -activity on pellet surface (Bq·cm <sup>-2</sup> )
UO <sub>2</sub> -10	10	3.76·10 <sup>10</sup>	2.71·10 <sup>8</sup>
UO <sub>2</sub> -01	0.1	3.76·10 <sup>8</sup>	2.71·10 <sup>6</sup>

Tab 4.1 Summary of the  $\alpha$ -activity for the materials used in this work.

Static batch leaching tests (i.e. new sample, leachant, and vessel for each contact time) were performed at room temperature in 20 ml of demineralized water under N<sub>2</sub> atmosphere (<10 ppm O<sub>2</sub>). The samples consisted of discs of ~6 mm diameter and ~1 mm thickness. The leachant was purged with pure N<sub>2</sub> for several hours prior to the tests. The leaching duration was 1 h, 10 h, 100 h, and 1000 h. Some of the longest duration tests are still continuing. After each test the leachate and the acid rinse solution of the leaching vessel were analyzed using ICP-MS.

##### Results

*Fig. 4.2* shows the concentrations of U and Pu in the leachates of the batch tests.

All the data points on *Figs 4.2* and *4.3* have error bars of  $\pm 5\%$ , smaller than the symbol size. The concentration of U released from the UO<sub>2</sub>-10 increased with leaching time up to 100 h, and was higher than the values for the UO<sub>2</sub>-01; after 1000 h, however, the value for UO<sub>2</sub>-01 became higher. The value for UO<sub>2</sub>-01 after 100 h is most probably an outlier. Pu was clearly detected only in the leachate of the UO<sub>2</sub>-10, starting at 100 h of leaching, and in significant amounts. The ratio Pu/U in solution was higher than 0.1; after the longest leaching time the concentration of Pu was actually slightly higher than that for U. The concentration values of U in the leachate for undoped UO<sub>2</sub> were significantly lower than those for the doped materials. Relatively large amounts of U were found in the rinse solutions, often in quantities higher than the cor-

responding values in the leachate. This indicates that significant adsorption on the walls of the leaching vessel occurred.

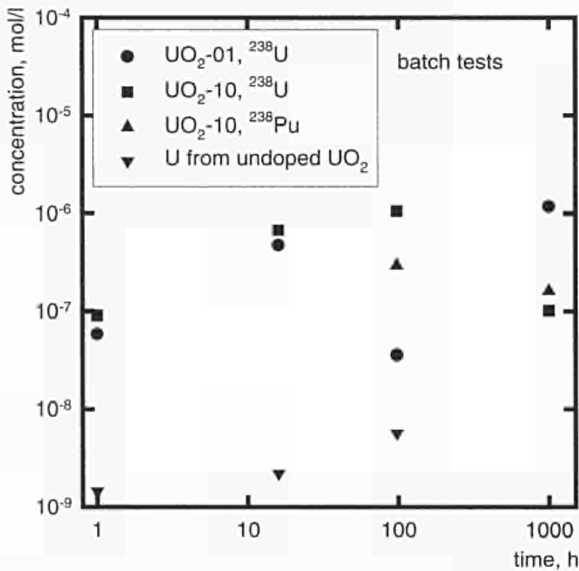


Fig. 4.2 Concentration of <sup>238</sup>U and <sup>238</sup>Pu measured in the leachates for UO<sub>2</sub>-01, UO<sub>2</sub>-10 and UO<sub>2</sub> undoped.

Fig. 4.3 shows the ICP-MS results in terms of Total Fraction of Inventory Released (TFIR), i.e. the sum of the fractions found in the leachate and in the acid rinse solutions.

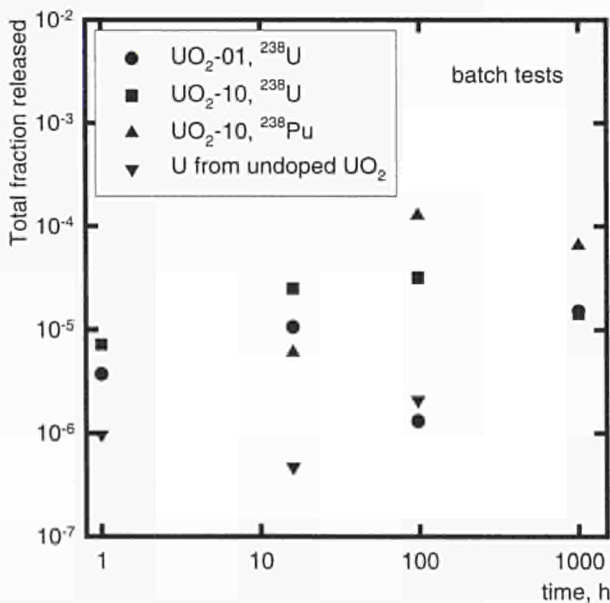


Fig. 4.3 Total fraction of inventory released for <sup>238</sup>U and <sup>238</sup>Pu from UO<sub>2</sub>-01, UO<sub>2</sub>-10 and UO<sub>2</sub> undoped.

As for the leachates, Pu was detected only in the rinse of UO<sub>2</sub>-10. The amounts of Pu in the rinse solutions were smaller than the corresponding ones in the leachate, with the exception of the value found in the rinse after 10 h. The U rinse contribution was proportionally higher for UO<sub>2</sub>-10 than for UO<sub>2</sub>-01. The fraction of Pu released from the UO<sub>2</sub>-10 for leaching times  $\geq 100$  h is significantly high, almost one order of magnitude higher than the fraction for U. It is not clear what causes this high release. The data points in Fig. 4.4 also show a strong rinse contribution to the TFIR for the undoped UO<sub>2</sub>. It must be noted that there is always a certain degree of uncertainty as to the source of the material found in the acid rinse solutions: although the vessels were visually inspected prior to rinsing, the presence of small fines from the samples could not be entirely ruled out.

The overall measurable effect of the  $\alpha$ -decays in the material is the increase of the lattice parameter. Fig. 4.4 shows the results of the XRD measurements on the UO<sub>2</sub>-10.

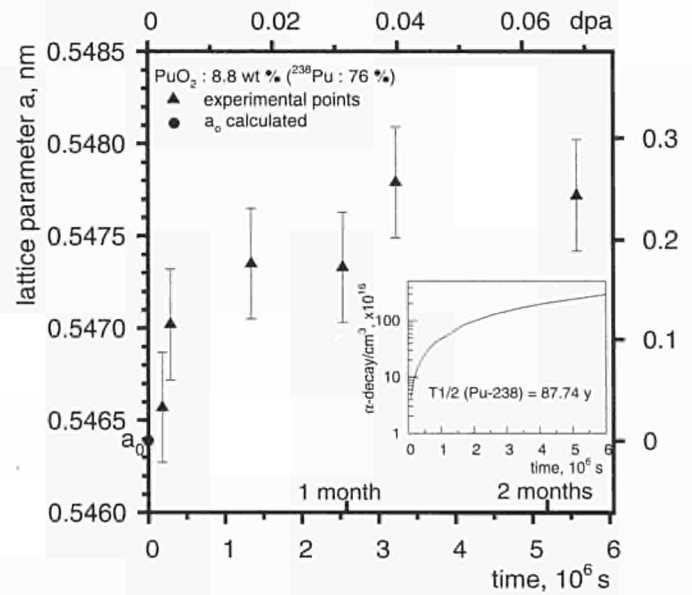


Fig. 4.4 Lattice parameter,  $a$ , as a function of time and displacements per atom (dpa axis) for the UO<sub>2</sub>-10 material. The  $\alpha$ -decay evolution with time for <sup>238</sup>Pu is also shown in the small insert.

The absolute values and the fractional variation of the lattice parameter (respectively, on the left and right vertical axes) are plotted as a function of time. The measurements were started with essentially no initial damage. The top axis on the figure reports the displacements per atom (dpa) values corresponding to the time evolution of the decay of the <sup>238</sup>Pu contained in the UO<sub>2</sub>-10. The evolution with time of

the  $\alpha$ -decay for  $^{238}\text{Pu}$  is also shown in the small insert. The initial lattice parameter value,  $a_0$ , was calculated assuming that each fluorite type phase (i.e.  $\text{UO}_2$  and  $\text{PuO}_2$ ) contributes proportionally to its concentration. The experimental results show an increase of the lattice parameter with time (corresponding to increasing damage). After approximately 2 months, the lattice parameter value had increased by  $\sim 0.25\%$ , similarly to reported values [3-5] for  $\text{UO}_2$  and  $\text{PuO}_2$  at the same dpa level (approximately 0.07). The  $\text{UO}_2\text{-01}$  did not show, during the same time interval, appreciable variations of the lattice parameter. This was expected because of the one hundred-fold lower decay rate. A behaviour similar to that observed with the XRD was found by performing periodically repeated Vickers hardness measurements. While the  $\text{UO}_2\text{-01}$  did not show significant variations of the hardness, the values measured for  $\text{UO}_2\text{-10}$  increased, and after approximately 2 months appeared to have reached a maximum value, corresponding to an increase of hardness of  $\sim 20\%$ .

### Conclusions

Under the experimental conditions of the present leaching tests a clear difference between doped and undoped  $\text{UO}_2$  was observed, which indicates a clear effect due to  $\alpha$ -radiolysis, also for the lower  $^{238}\text{Pu}$ -content material. With the partial exception of the amounts released from  $\text{UO}_2\text{-01}$  after 100 h of leaching, the concentrations of U in solution for the  $\alpha$ -doped samples were  $\sim 2$  to 3 orders of magnitude higher than those for "inactive"  $\text{UO}_2$ . Relatively high fractions of Pu were released. In terms of radiation damage and solid characterization studies, the behaviour of  $\text{UO}_2\text{-10}$ , subject to more intense  $\alpha$ -damage, was different from that of  $\text{UO}_2\text{-01}$  and undoped  $\text{UO}_2$ .

### References

- [1] V.V. Rondinella, Hj. Matzke, J. Cobos, and T. Wiss, Mat. Res. Soc. Symp. Proc., in press
- [2] Hj. Matzke, J. Nucl. Mater., in press
- [3] W.J. Weber, J. Nucl. Mater. 98 (1981) 206
- [4] Hj. Matzke, Radiat. Eff. 64 (1982) 3
- [5] M. Noe and J. Fuger, Inorg. Nucl. Chem. Letters 10 (1974) 7

## 4.2 Corrosion Measurements with Electrochemical Techniques

Measurements of the leach rates of spent fuel in groundwater is vital for the evaluation and design of a repository for

final fuel storage. Electrochemical techniques provide a sensitive although difficult method to measure such low corrosion rates as exist in underground final storage conditions.

There are strong indications of a pitting corrosion on  $\text{UO}_2$  in carbonate-containing solution. The extent of this mechanism can be obtained from electrochemical noise measurements.

Furthermore, first electrochemical experiments carried out with unirradiated Pu-containing fuels ( $\text{PuO}_2$ ,  $(\text{U,Pu})\text{O}_2$  and irradiated MOX) show a different behaviour compared to unirradiated and irradiated  $\text{UO}_2$  fuel, e.g. very low corrosion potentials of  $\text{PuO}_2$ . Therefore there are also indications of a galvanic coupling between the different uranium- and plutonium-rich phases.

In order to prove these phenomena in the hot cells a special electrochemical cell has been developed (Fig. 4.2). It is designed for remote handling and kept as flexible as possible. Two working electrodes (electrodes that contain the material under investigation) can be introduced into the cell. Both can be easily centred in the electrolyte chamber (volume  $\sim 5$  ml) and then adjusted to a fixed distance ranging from 1 to 20 mm. Different types of reference electrodes can be fitted in the cell and at the end of an experiment the electrolyte can be easily released through a drain and collected for analysis.

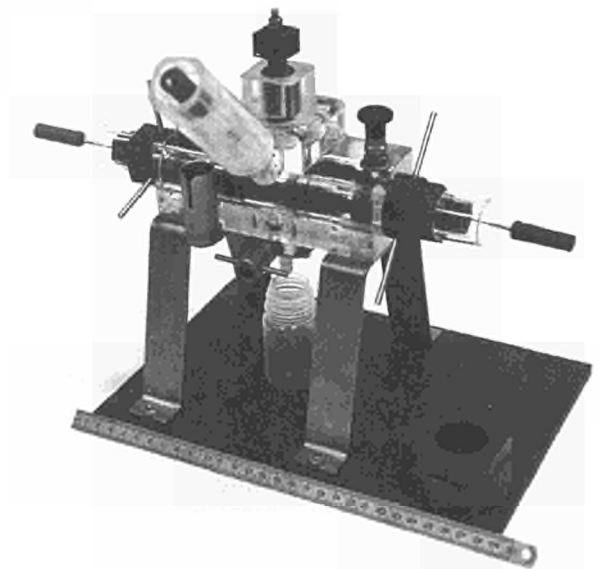


Fig. 4.5 Newly developed cell for electrochemical experiments on spent fuel in hot cells.

Contact (4.1.3): Vincenzo V. Rondinella • tel.: +49 7247 951 279 • fax: +49 7247 951 591 • wiss@itu.fzk.de

The cell is ideally suited for contact corrosion experiments in which different materials are electrically short-circuited in a controlled manner to measure the current flowing between these materials. By performing such measurements a direct comparison of the different electrochemical behaviour of the materials under investigation is possible.

### 4.3 Source Term of Spent Fuel

Final results on the dissolution behaviour of spent nuclear fuels were obtained in the last year of this shared-cost action programme (INE, Karlsruhe; CIEMAT/ENRESA, Madrid; UPC, Barcelona; FU, Berlin; SCK-CEN, Mol; CEN, Marcoule and ITU, Karlsruhe).

The study of defective  $\text{UO}_2$  and MOX fuel rodlets simulates the case of groundwater intrusion into the fuel pin in case of cladding failure. It shows that the dissolution process can be described by a two-step dissolution model with a fast initial dissolution of an oxidised layer on the pellet surface followed by a slower oxidative matrix dissolution.

The fraction of inventory in the aqueous phase (FIAP) values shows that during the fast initial dissolution the uranium release is almost the same for  $\text{UO}_2$  and MOX fuels. However the release of plutonium and fission products is higher compared to uranium for both fuels. Higher release rates in MOX fuels compared to  $\text{UO}_2$  fuels may be due to the special two-phase structure of MOX fuel, leading to an increased fission product inventory at the peripheral agglomerate grain boundaries, i.e. the surface in contact with the leachant. This explanation is supported by the especially high FIAP values found for caesium and iodine; these radionuclides are known to migrate to the outer zone of the pellet upon irradiation.

The long-term dissolution rates are similar for uranium, plutonium and strontium in MOX fuels appear to be independent of the fuel's burn-up. In the case of  $\text{UO}_2$  fuels these dis-

solution rates seem to increase slightly with burn-up, with plutonium having always the lowest values.

Electrochemical studies of  $\text{UO}_2$  and spent fuels were carried out at constant potential, and combined with additional impedance measurements, gave relevant information about electrical conductivity, corrosion rate and the inner resistance of the specimen. Knowledge of the latter is important to obtain the correct value of the corrosion-determining potential at the surface - electrolyte interface.

Corrosion rates estimated from the open circuit potentials using the Tafel relation are in the range of 0.1 – 10  $\text{mg/m}^2\text{d}$  for unirradiated  $\text{UO}_2$ ; irradiated fuel exhibited lower corrosion rates. Experiments carried out using MOX fuel show a different behaviour with a much lower open circuit potential. This may be related to the plutonium-rich agglomerates in the fuel.

Liquid mercury porosimetry measurements were used to calculate the effective pore surface of two non-irradiated samples, namely  $\text{UO}_2$  and SIMFUEL. The results gave similar values compared to data obtained with the Brunauer, Emmet and Teller (BET) surface gas adsorption technique.

In the case of spent fuel samples the effective surface measurements by Hg pycnometry in the hot cells proved to be extremely difficult, due to the complexity of the equipment and the delicate manipulations necessary for the specimen preparation. The operation of an automated gas absorption pycnometer is much easier and more appropriate. A new apparatus is presently being tested before installation in the hot cells.

#### References

- [1] D.W. Shoesmith, S. Sunder, AECL Report 10488, Pinawa, Canada (1991)
- [2] S. Sunder, D.W. Shoesmith, M. Kolar, D.M. Leneveu, Mat. Res. Soc. Symp. Proc. 506 (1998) 273



## 5. Safeguards Research and Development

### Introduction

Following developments in Irak, the international nuclear safeguards regime was recently strengthened in order to cope better with the proliferation of nuclear material. So far, the "classical" nuclear material safeguards concentrated on the detection of the diversion of nuclear material from the declared facilities. For this purpose ITU has developed a number of measurement techniques to analyse nuclear materials in samples taken during inspection. The on-site laboratories (see chapter 6) being set up at the reprocessing plants in La Hague and Sellafield consist of equipment designed or adapted by ITU.

To cope with clandestine operation of facilities or clandestine production of nuclear materials, environmental monitoring techniques (as defined in the 93 + 2 programme of the IAEA) and the HPTA (High Performance Trace Analysis) of Euratom were developed. These techniques which are based either on the analysis of particles taken at or nearby the plants or from bulk samples originating from the environment.

The following contributions describe additional development work carried out in support of forensic analysis (5.1 and 5.4), environmental monitoring (5.2), and interim and final storage of spent fuel (5.3).

### 5.1 High Sensitivity Isotope Mass Spectrometry

The new thermal ionization mass spectrometer (TIMS) that had been installed at ITU, was thoroughly tested and first samples were measured using the high sensitivity ion counting mode. The instrument shall allow precise isotope ratio measurements on samples of only a few picograms. During the testing it was noted that the micro channeltron detectors required further improvement to optimize instrument performance.

Measurements were carried out in total evaporation mode on uranium oxide samples in order to determine the  $^{18}\text{O}/^{16}\text{O}$  ratio. Other measurements on minute amounts of uranium (obtained by decay of plutonium) were successfully performed and revealed the age of the plutonium. Separation of (sub-)nanogram quantities of actinides requires a special separation process. For this purpose we developed a rapid column extraction chromatography procedure for the separation of uranium, neptunium and plutonium. This separation chemistry elegantly complements the high sensitivity TIMS instrument.

Contact (5.1.): Klaus Mayer • tel.: +49 7247 951 545 • fax: +49 7247 951 595 • mayer@itu.fzk.de

Contact (5.2.): Maria Betti • tel.: +49 7247 951 363 • fax: +49 7247 951 595 • betti@itu.fzk.de

ration of uranium, neptunium and plutonium. This separation chemistry elegantly complements the high sensitivity TIMS instrument.

### 5.2 Environmental Monitoring / High Performance Trace Analysis

#### 5.2.1 Methods for the analysis of uranium particles and bulk analysis

Different techniques for the collection of particles from swipe samples have been studied. An apparatus for the production of  $\text{UO}_2$  particles with known isotope composition and size has been built. Particles of  $\text{UO}_2$  with a size distribution of around  $1 \mu\text{m} \pm 0.3 \mu\text{m}$  have been produced and characterized by SEM and SIMS. These particles will be used to produce control swipe samples and verify the efficiency of the methods for the recovery of particles from real swipe samples. Procedures for leaching and complete dissolution of swipes as well as for other environmental samples have been established.

In order to increase the capacity of particle analysis of samples by SIMS a concept for a new sample changer has been developed. The prototype realized allows 8 samples to be loaded simultaneously in the sample chamber of the machine. The changing of the samples as well as the complete operation of the sample changer will be controlled by computer.

#### 5.2.2 Screening methods for hot spot detection

Systems based on  $\alpha, \beta, \gamma$  autoradiography as well as methods based on  $\alpha$ -track and fission tracks have been investigated for the application to environmental and swipe samples. From the first investigations it was possible to detect hot spots in contaminated soil from Chernobyl. The hot spots have been characterized by SEM and SIMS.

#### 5.2.3 Instrumental analytical techniques

New sources have been prepared for the calibration of the high-resolution low-background gamma spectrometry to exploit this technique for the analysis of environmental samples.

New methods based on liquid scintillation counting were investigated for the measurement of Am, Pu and Cm in envi-

ronmental samples. Specific chromatographic phases are under investigation for the separation of actinides at trace levels and the direct coupling to an ICP-MS detector.

### 5.3 Non-Destructive Assay of Spent Nuclear Fuel

The aim of this work was to evaluate the performance capabilities of a CdZnTe detector for gamma spectroscopy of spent fuel. A planar CdZnTe detector (9 mm<sup>2</sup> sensitive area and 2 mm thickness, bias 400 V), cooled by a thermoelectric circuit at a temperature of -30°C, coupled to an electronic module comprising a power supply, amplification and pulse shaping, was used for this study.

Gamma spectroscopy was performed on power reactor spent nuclear fuel rods stored inside a β-γ hot cell at the Institute. The spectroscopy was performed under the following experimental set-up: the detector is situated outside the cell (wall thickness 1 m) facing the fuel under investigation through a collimator, made of lead and tungsten, incorporated into the cell wall (1 m thickness); rectangular apertures 10 mm in height and between 0.6 mm to 1.2 mm wide were available.

A typical gamma spectrum is shown in Fig. 5.1. The small detector size and the use of cooling and charge loss correction resulted in improved energy resolution (6 keV at 662 keV), peak-to-compton and peak-to-valley ratios. The fission products <sup>134</sup>Cs and <sup>137</sup>Cs and <sup>106</sup>Ru are visible in the γ-spectrum. The 605 keV and 662 keV lines of <sup>134</sup>Cs and <sup>137</sup>Cs are well resolved. The 796 keV and 802 keV lines of <sup>134</sup>Cs are not resolved, which is also the case for the 512 keV of <sup>106</sup>Ru and the 511 keV annihilation radiation. The energy lines of 605 keV and 662 keV are thus the only ones suitable for interpretation purposes of spent fuel, i.e. burnup and cooling time verification.

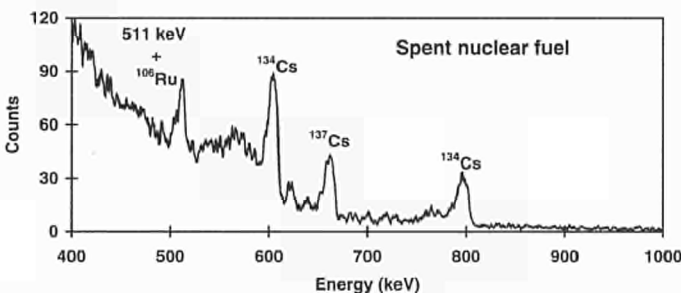


Fig. 5.1 Gamma-spectrum of spent nuclear fuel with a small CdZnTe detector.

### 5.4 Relational Database for Identification of Nuclear Material of Unknown Origin

In the framework of ITU's activities for analytical identification of nuclear material of unknown origin, the relational database system dedicated to support and guidance of such analyses was updated and extended. In June 1998, a bilateral workshop on analytical methods in nuclear forensics was held with participation of experts from VNIINM Moscow and ITU Karlsruhe. It allowed the exchange of information and experience in applying the expertise of both laboratories in nuclear analytics for the identification of nuclear material of unknown origin. In addition, recommendations for prioritization of the analytical parameters included in the common database were given, in particular in the field of impurity and microstructure analysis. In the database, a relational system of tables provides the backbone for systematic queries and a step-by-step narrowing of origin and intended use of the nuclear material. Details are available in ref. [1].

For nuclear material used in power reactors, this year's activities in structure development focused on impurity parameters which, from the statistical viewpoint, are available in 4 categories:

- specification limits provided and assured by the material manufacturers (IMPURITY\_LIMIT)
- typical ranges with 95% confidence level, taken from 2σ of an assumed Gaussian distribution (IMPURITY\_MEAN)
- real minimum and maximum values encountered for a specific fuel type and origin (IMPURITY\_REAL)
- example cases with known origin (IMPURITY\_EX)

During an additional stay of two guest scientists from the Bochvar All-Russia Research Institute for Inorganic Materials (VNIINM) in Moscow, the database has been further extended. It now covers also basic parameters characteristic for nuclear fuel used in research reactors as well as analytical methods and equipment used in both VNIINM and ITU.

A retrieval system with a graphical interface has been developed using the ORACLE Developer 2000™ package. The system provides user-friendly access to the database and consists of the three modules:

- NucSearch - for retrieving characteristic parameters,
- NucEquip - for queries on available analytical equipment,

- NucVisual - for additional visualization purposes e.g. to display abundance distributions.

An example display showing the entrance screen of the module NucSearch is given in Fig. 5.2.

The dedicated ORACLE™ Database Management System has been upgraded to the most recent version available on the market. The migration to the WindowsNT operating system is under way. A symmetric installation of both the relational database and the retrieval software package has been per-

formed at VNIINM Moscow. The database installations at VNIINM and ITU are mutually updated on a regular basis.

#### Reference

- [1] Schubert A., Janssen G., Koch L., Peerani P., Bibilashvili Yu.K., Chorokhov N.A., Dolgov Yu.N.: A Software Package for Nuclear Analysis Guidance by a Relational Database, Proceedings of the ANS International Conference on the Physics of Nuclear Science and Technology, Long Island, New York, October 5-8, 1998, p.1385-1392

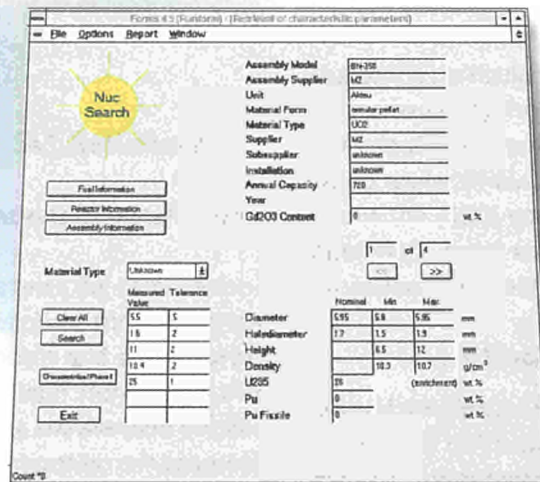


Fig. 5.2 Typical entrance screen for the software module "NucSearch"



# 6. Scientific and Technical Support to DG XVII

## Introduction

The provision of scientific and technical support in the area of nuclear material analysis to DG XVII-E is one of the core activities of the Institute and was continued during the reporting period. The efforts covered development work, analytical measurements, training and consultancy in the following areas:

- Development and further improvement of analytical methodologies to meet present and future safeguards challenges.
- Design, installation and commissioning of on-site laboratories at the site of the large reprocessing plants at Sellafield (UK) and La Hague (F) and the performance of verification measurements on-site.
- In-field measurements, using mobile equipment, for verification measurements at low enriched uranium fuel production facilities.
- Analytical measurements of samples of nuclear material transported to the Institute.

## 6.1 On-Site Laboratory (OSL), Sellafield

### 6.1.1 Commissioning and modifications of installations

After completion of the infrastructure tests, the commissioning activities were started. During this phase the functionality and safety of operation of gloveboxes and analytical instrumentation was subject to tests with non-radioactive material. These activities included data transfer and the implementation of the computerized laboratory management system. The results of the inactive commissioning demonstrated compliance with previously established safety documentation. At the end of the year the first uranium solution was received in the OSL and active tests of the NDA equipment could be started.

Minor modifications of equipment and software were carried out as consequence of the results of inactive commissioning activities. Two major modifications shall be mentioned explicitly:

- Titration had initially been foreseen as an analytical technique for element assay for 20% of the product samples for quality control purposes. Due to the considerable amount of waste and the related costs generated by this

technique, it was decided to change the analytical procedure of the OSL. Another primary method of measurement namely Isotope Dilution Mass Spectrometry (IDMS), will replace titration. As a consequence, the entire titration equipment including the robot was removed. The box will stay in the OSL and will be used for storage of spikes and for dilution within the IDMS analysis procedure.

- Bagless transfer ports (BTPs) had been foreseen for simple and rapid material transfers between the different glove boxes. The development of the BTPs by BNFL Engineering Ltd. (BEL), however, did not work as expected. The ports finally designed and released proved to be not suitable for a powder handling environment. Consequently, BTPs were removed from boxes involving powder samples so-called "dry boxes". The ports remaining on the "wet boxes" have been modified to the latest BNFL design. After execution of these modifications the glove-box integrity was thoroughly retested.

Due to the particular nature of the project (an analytical laboratory owned by the European Safeguards Directorate (ESD), operated by ITU staff using ITU equipment, within a building being under BNFL responsibility, B229) BNFL is concerned about the OSL's compliance with safety regulations. OSL operations need to be in accordance with relevant B229 procedures and instructions.

### 6.1.2 Finalisation of data management

Several modules of ITU software for data management (see TUAR-97, p. 107) were finalised together with their operating manuals, independently validated and implemented in the pre-OSL prior to use on-site.

Modules for sample management, data compilation and data treatment were fully implemented in the OSL. All these modules had undergone long and thorough testing under routine operation conditions in the pre-OSL. Other modules are aimed to support accountancy and criticality control in the OSL and had been developed especially for on-site application. Validation is scheduled for the active commissioning phase.

### 6.1.3 Management of the safety of the OSL

After handover and start of inactive commissioning, ITU became fully responsible for the management of safety of the

on-site laboratory. In compliance with site specific safety regulations, ITU staff were therefore nominated for different functions such as Duly Authorised Person/Radioprotection Supervisor (DAP/RPS), Material Custodian etc. The DAP/RPS has entire responsibility on-site for the different safety aspects. It has to assure that the laboratory is at any given time managed according to the fully developed Safety Case (fd-SC) and its interpretation into local rules and operating instructions. The responsibility for the accountancy of fissile material and criticality control within the OSL is assured by designated personnel, the Material Custodian, who followed a specific training and is assisted by software tools specifically developed at ITU.

Discussions on the running costs of the OSL led to a closer examination of the amount of waste generated in the laboratory. The largest proportion of liquid waste is generated by potentiometric titration, a technique which had been foreseen to serve as quality control for the predominantly applied radiometric techniques. This triggered a review of the analytical concept of the OSL /1/ resulting in a drastical reduction of the costs for waste.

Maintenance of the OSL is split into three parts and will be undertaken by either BNFL (B229 Engineering Services) covered by an appropriate maintenance contract, by ITU or by subcontractors for specialist work. ITU will restrict their maintenance to the analytical equipment and the instrumentation of the gloveboxes. In some specific cases subcontractors may be involved (mass spectrometers, X-ray generator etc.).

#### **6.1.4 Training of inspector analysts followed by assessments**

Training of OSL analysts was continued, with emphasis on the aspects related to B229 working practice, rules and procedures the OSL has to comply with. Additionally, also training on analytical techniques and familiarisation with ITU software were intensively pursued, in this context the pre-OSL proved to be an invaluable tool.

Training topics were in particular:

- to run the pre-OSL at ITU to gain practical experience on analytical techniques,
- lectures and practical training sessions at Karlsruhe on ITU software modules,
- site specific courses provided by the Sellafield Training Department,

- DAP trainees were involved with on-the-job training on-site,
- Self training followed by an assessment on training modules identified together with B229.

As OSL-teams are rotating on a weekly basis, several DAP/RPS candidates were approved by B229 management following an assessment on an individual basis. DAP trainees were involved with on-the-job training along with a DAP in charge whilst on-site prior to nomination by ITU management.

Training and further qualification of staff will continue to be an important issue.

## **6.2 Laboratoire Sur Site (LSS), La Hague**

The LSS project is being executed according to schedule. The efforts for implementation of the LSS are twofold:

- ITU continued development, testing, construction or adaptation of analytical equipment, as illustrated in more detail below.
- The installation of the laboratory infrastructure is carried out under supervision of the engineering company "Société Générale pour les techniques Nouvelles" (SGN). In particular the installation of the glove-box chains (dedicated to the handling of PuO<sub>2</sub>, uranyl nitrate and for sample preparation prior to mass spectrometry) started on site in September. ITU participated actively in the installation. Inactive testing is scheduled for summer 1999.

Three gloveboxes were delivered to ITU for modification and installation of instruments and components that were specifically developed in the Institute. Installation of a laboratory robot (with its auxiliary equipment for chemical separation, alpha spectrometry and filament preparation) was completed in the IDA box (Isotope Dilution Analysis). The analytical set-up and adaptation of the product boxes (PuO<sub>2</sub> and uranyl nitrate) was achieved according to the time schedule. After modification, the boxes were shipped to the La Hague site.

Scientific equipment was installed in the hot cell suite, including three hybrid K-Edges, a gamma spectrometry device and two PAAR densitometers. The early installation of these items

allow the completion of the shielding. The mass spectrometer was received at La Hague. Its installation however, will be completed in June 99.

The pré-LSS IDA box has been constructed after having developed and successfully tested the separation chemistry [2] which enables the handling of samples containing only 500 ng plutonium. This allows to comply with the specific rules which are in force at La Hague. The pré-LSS box will be used at the ITU to test and optimize the robotized chemical separation procedure. It will also serve for training purposes and for demonstration.

Issues like site specific training for inspector analysts, medical and dosimetry follow up of the ITU staff working on site have been discussed. A first group of three analysts inspectors was sent in a pilot training session, the contents of which is based on COGEMA's requirements. This session was given by INSTN (Institut National des Sciences et Techniques Nucléaire), La Hague and lead to the obtention of three distinct diploma for each participant, related to general nuclear knowledge, site specific rules and glovebox operation.

The general planning for the project (Tab. 6.1) remains valid and the hand-over of the LSS is foreseen by the end of October 1999 [1].

	1999				2000			
	1	2	3	4	1	2	3	4
Suppliers tests	■	■						
Specifics tests		■						
Integration of EURATOM equipment		■						
Inactive testing	■	■	■	■				
Active commissioning				■	■			

Tab. 6.1 General planning of the LSS project.

## References

- [1] U. Blohm-Hieber, P. Chare, W. Kloeckner, H. Ottmar, P. Daures, M. Ougier, L. Koch, K. Mayer, X. Rincel, R. Vinoche, A. Barrier, D. Willocquet and M. Brucy, Proc. 19th Annual ESARDA Symposium, Montpellier, France, 13-15 May, 1997, EUR 17665 (1997) p.211
- [2] C. Apostolidis, R. Molinet, P. Richir, M. Ougier, K. Mayer; Development and Validation of a simple, rapid and robust method for the chemical separation of uranium and plutonium; Radiochimica Acta 83 (1998) 21-25

## 6.3 Developments for the LSS and OSL

The new generation of Hybrid K-Edge Densitometers (HKED's) developed for the LSS differs from the previous instrument layout in two important items:

- The parallel K-edge densitometry (KEDG) and X-ray fluorescence (XRF) measurements are now performed directly on a single sample as presented by the plant operator;
- The new HKED incorporates a sample changer for automated measurements on up to 6 samples. For this feature a patent application has been filed.

Both modifications were intended to enhance significantly the sample throughput on the one side, and to further simplify the operational procedures on the other side. The changes were stimulated by the foreseeable workload in the LSS, where the HKED's will have to take over a large fraction of the on-site analytical work.

One of the new HKED systems has also replaced the previous Euratom HKED at La Hague, which has been in use for on-site verification measurements since 1989. The new installation, completed in the month of September at an active hot-cell in the high active laboratory of UP2, offered a good opportunity for acquiring operational experiences and performance data.

In both on-site laboratories the technique of energy-dispersive X-ray fluorescence analysis (XRF), partly in combination with K-edge densitometry (KEDG), will now take over the role of a second method for the element assay in PuO<sub>2</sub> and MOX product samples. As an example, Fig. 6.1 outlines the adopted analytical scheme for PuO<sub>2</sub> materials. This analysis will be performed on a weight basis using an internal uranium standard, which simplifies and speeds up the analytical procedure by avoiding the time-consuming density measurement. A series of comparison analyses between XRF, titration and IDMS were carried out to evaluate the performance of the XRF technique.

The analysis of precise passive neutron coincidence measurements, previously performed at ITU with the OSL neutron/gamma counter on a variety of small plutonium samples, suggested the need for better defined <sup>240</sup>Pu effective responses for <sup>238</sup>Pu and <sup>242</sup>Pu. More accurate weighting factors for both isotopes in the expression for the <sup>240</sup>Pu effective mass are of importance particularly for the assay of high-burnup pluto-

ni-238, where the two minor isotopes account for up to 40% of the spontaneous fission neutrons. This has prompted ITU to undertake, in co-operation with the Euratom Safeguards Directorate and AEA Harwell, an experimental determination of the  $^{238}\text{Pu}$  and  $^{242}\text{Pu}$  coincidence rate per unit mass relative to that of  $^{240}\text{Pu}$ . For this purpose three  $^{238}\text{PuO}_2$  samples, two  $^{240}\text{PuO}_2$  and two  $^{242}\text{PuO}_2$  samples, all in the approximate mass range 25 - 500 mg, were prepared in standard type X.2 capsules at Harwell (UK). Prior to their shipment to ITU the samples have been counted, for later comparison, in the N95 Harwell high efficiency neutron counter. The counting of the samples in two OSL neutron-gamma counters at ITU started in December and will be completed early in 1999.

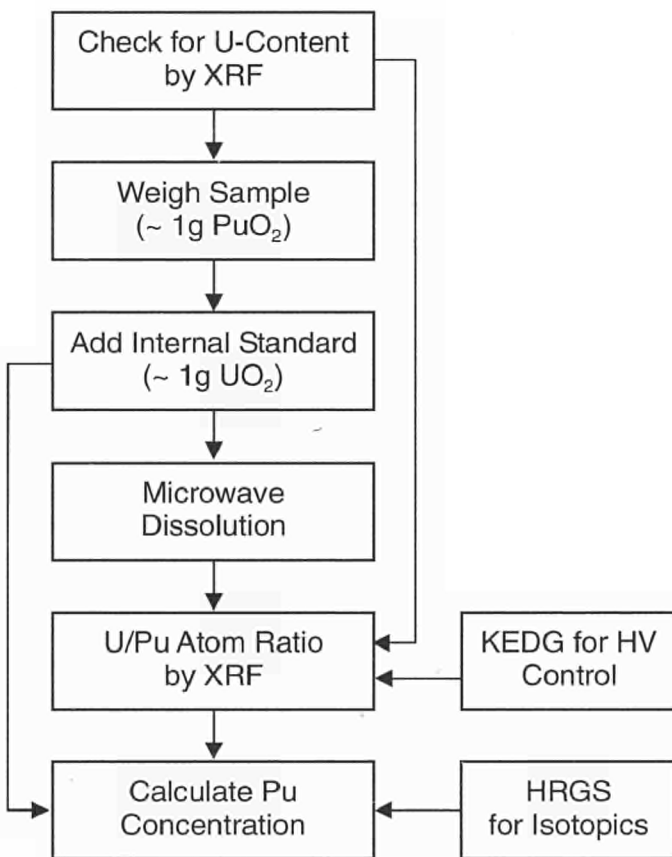


Fig. 6.1 Scheme of the XRF analysis for  $\text{PuO}_2$  samples.

To aid the evaluation of the final  $^{240}\text{Pu}$ -effective responses for  $^{238}\text{Pu}$  and  $^{242}\text{Pu}$ , Monte Carlo calculation capabilities using the MCNPTM code for the modelled OSL counter have been set up at ITU. The MCNP calculations will be used to determine the leakage self multiplication factors for each sample.

Developments for IDMS were continued, particularly in view of the boundary conditions applicable at La Hague. A prototype glove box was designed and constructed for implementation of the new separation procedure that had been developed [1]. A number of auxiliary equipment was developed for improving the efficiency of the robotized sample treatment which comprises U/Pu/fission product separation, alpha spectrometry of the U and Pu fraction respectively and filament preparation for mass spectrometric measurement. Programming of the robot and the alpha spectrometry was completed as well as the interfacing with the TAMS (Transuranium Institute Analysis Management System). The glove box layout is schematically shown in Fig. 6.2.

The box was leak-tested and is being finalized for introducing active material. A view of the interior of the box during construction is given in Fig. 6.3.

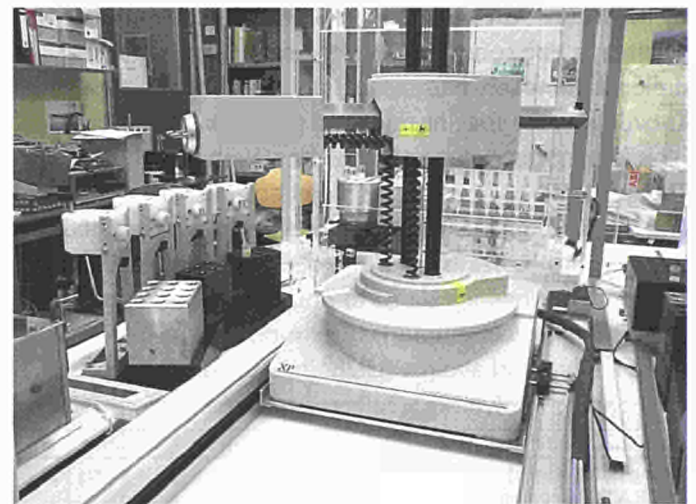
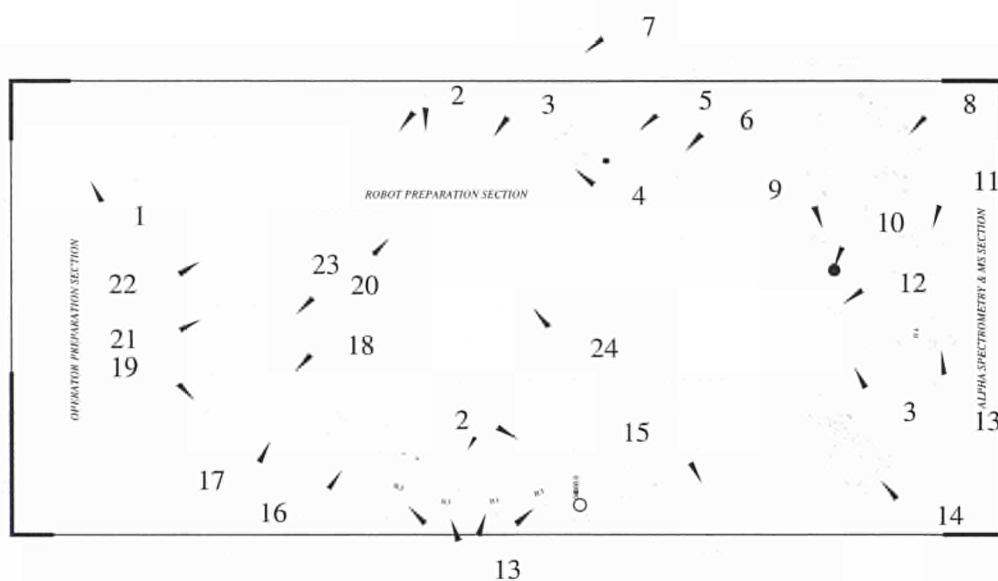


Fig. 6.3 View of the pre-LSS IDA box.

A specific software package (TAMS) has been developed at ITU in order to assist in the analysis management. It is composed of interactive modules that are tailored to the particularities of a nuclear analytical laboratory. The expert system for sample initialization, the sample preparation and data compilation and evaluation module were amended to enable the utilization of the Large Size dried spike (LSD) [TUAR-97, p. 111], and the spiking of plutonium samples with uranium followed by X-ray fluorescence measurement. Traditional multi-channel analyzers for alpha spectrometry were replaced by compact modules for PC operation. The software for spectra evaluation was adapted and interfaced with the ro-



- |                      |                             |                           |
|----------------------|-----------------------------|---------------------------|
| 1 preparation rack   | 9 alpha target waste        | 17 hotplate               |
| 2 tube racks         | 10 alpha disk stock         | 18 cooler                 |
| 3 U-Pu fraction rack | 11 10 $\mu$ L pipette tips  | 19 mixer                  |
| 4 capper             | 12 "clean discs"            | 20 chromatography system  |
| 5 tube caps          | 13 robot hands              | 21 reagent dispenser      |
| 6 solid waste        | 14 MS turret                | 22 liquid waste           |
| 7 barcode reader     | 15 balance                  | 23 robot railroad         |
| 8 alpha chamber      | 16 1 mL & 5 mL pipette tips | 24 robot (2 working pos.) |

Fig. 6.2 Layout of the new robotized glove box for preparation of U/Pu samples.

bot operation and isotope dilution modules. The Accountancy Management System (AMAS) was completed and tested. It shares the information contained in TAMS and allows one to follow the flow of samples of nuclear material throughout the laboratory. Using bar code labels on the sample vials and bar code readers in most of the glove boxes allows a simple and near real time inventory update. This is essential for accountancy and criticality control.

#### Reference

- [1] P. Richir, B. Brandalise, K. Mayer, Proc. Int. Workshop on Appl. of Extr. Chromatography in Radionuclide Measurements, Geel, Belgium, 9 - 11 Nov. 1998

### 6.4 In-Field Verification Activities

Inspector analysts from ITU travelled on a regular basis to La Hague, France, to carry out measurements with the EURATOM Hybrid K-Edge (HKED) instrument. These measure-

ments and the associated instrument maintenance work are carried out on a permanent basis throughout the year, hence ITU staff travel on a weekly basis.

In 1998, more than 750 samples were measured at La Hague. Taking into account the control samples, repeat measurements, passive spectra and reference spectra taken, a total number of more than 1200 measurements were carried out as shown in Tab. 6.2

Year	Number of input samples	Number of measurements (total)	Effective working days	Measurements per day (average)
1989	15	33	11	3.00
1990	107	234	66	3.55
1991	175	317	98	3.24
1992	199	335	85	3.94
1993	305	435	104	4.18
1994	407	597	109	5.48
1995	573	917	144	6.37
1996	618	1067	156	6.84
1997	663	1068	171	6.25
1998	785	1246	172	7.24

Tab. 6.2 Evolution of the number of samples measured by the Hybrid K-Edge at La Hague.

Contact (6.3): Klaus Mayer • tel.: +49 7247 951 545 • fax: +49 7247 951 595 • mayer@itu.fzk.de

Contact (6.4): Pascal Daures • tel.: +49 7247 951 211 • fax: +49 7247 951 595 • daures@itu.fzk.de

The Hybrid K-Edge instrument was replaced in summer (during the La Hague plant maintenance period) by a new set-up equipped with a sample changer developed at ITU allowing high precision sample positioning. The software was modified accordingly, in close co-operation with Canberra. It enables the automated sequential measurement of five samples plus one standard, hence making optimum use of the instrument by minimizing operator intervention and allowing overnight operation. The new HKED set-up streamlines the procedure even further by enabling measurements directly on the COGEMA sample vials, a transfer of the spent fuel solutions into special measurement cells is no longer necessary. This development also leads to a reduction of the volume of waste by about 30% while at the same time increasing the efficiency.

A set of U/Pu standard solutions was prepared at ITU and shipped to La Hague in order to perform an initial calibration of the new HKED. This became necessary due to the temporary unavailability of certified reference solutions, and to enable taking up operation of the instrument and to continue verification measurements for the reprocessing plants. These materials were gravimetrically prepared from primary reference materials and verification analysis was performed by potentiometric titration and by IDMS.

At Sellafield, the maintenance of the HKED instrument at the THORP plant, was carried out by ITU staff. EURATOM inspectors were trained in instrument operation.

The mobile COMPUCEA instrument was operated by specialised ITU staff to directly support inspection campaigns at low enriched uranium (LEU) fuel production facilities all over Europe. The instrument is specifically designed for uranium enrichment and concentration measurements. Almost 130 samples were measured during such campaigns, in plants in France, Belgium, United Kingdom, Sweden and Spain.

### 6.5 European Commission's Safeguards Analytical Measurements

Samples of nuclear material are taken by EURATOM inspectors and analyzed for safeguards verification purposes. ITU is the major laboratory carrying out measurements in the framework of the European Commission's Safeguards

Analytical Measurements (ECSAM). In 1998 more than 150 samples were analyzed and the results were reported to the Euratom Safeguards Directorate (ESD). The analytical techniques applied range from potentiometric titration, thermal ionization mass spectrometry to high level neutron coincidence counting, gamma spectrometry and X-ray techniques.

A trend to lower sample numbers but more demanding analytical requirements and more sophisticated measurement procedures was observed. This is aimed at improving the overall uncertainty and at quantification of the uncertainty components comprising the sampling step at the facility.

Participation in the external quality control programme EQRAIN (organized by CETAMA, France) was started. Four uranium and two plutonium solutions were analyzed "blindly". The results showed that the analytical techniques routinely applied for uranium and plutonium assay are well under control and deliver results well within the International Target Values [1]. At the same time the successful participation in the external quality control programme confirms the proper operation of the internal quality control scheme.

#### Reference

- [1] S. Deron et al., 1993 International Target Values for Uncertainty Components in Measurements of Amount of Nuclear Material for Safeguards Purposes, ESARDA Bulletin No. 23, March 1994

### 6.6 High Performance Trace Analysis

During 1998 swipe samples collected both in enrichment plants and hot cell facilities by the Euratom Safeguards Directorate (ESD) have been analyzed. Uranium and plutonium isotope compositions in particles have been measured by Secondary Ion Mass Spectrometry (SIMS). Low background  $\gamma$ -spectrometry along with IC-ICP-MS have been extensively applied for the measurements of fission products.

As in 1997 [TUAR-97, p. 112] a training course on High Performance Trace Analysis and Environmental Sampling (HPTA/ES) has been organized in June 1998 for ESD, the IAEA and the Argentine-Brazil Inspectorate. An additional exercise for collectors of swipes in hot cell facilities was performed.

## 7. Scientific and Technical Support to DG I (Safeguards)

### 7.1 Support to IAEA

ITU continued to support IAEA in the area of robotized analysis. The IAEA intends to set up an on-site laboratory at the reprocessing plant of Rokkasho-Mura (Japan). In this context the robotization of a number of laboratory components is being studied. Based on the unique expertise gathered over many years at ITU, consultancy and assistance is provided to the IAEA safeguards analytical laboratory.

Since ITU entered the network of analytical laboratories of IAEA for project 1993 + 2, environmental monitoring (TUAR 97, p. 113), the Agency has regularly sent swipe samples for isotopic analysis by Secondary Ion Mass Spectrometry (SIMS) for particles containing uranium. New materials and tools for the collection of swipe samples inside hot cells have been tested under request of IAEA.

Consultancy for the purchase of a SIMS at the clean laboratory in Seibersdorf as well as on the development and implementation of analytical techniques has been provided.

During 1998 Np and Am along with Cm and Pu have been determined by IC-ICP-MS in spent fuel solutions from samples sent by IAEA. The results and the analytical methods used have been reported to the Agency.

### 7.2 Assistance to Central and East European Countries

Co-operations with three East European countries (Czech Republic, Hungary, Bulgaria) to combat nuclear trafficking are running under the acronym FONSAFE (FOrensic Nuclear analysis for SAFeguards) under the EC's PHARE programme (see *Tab. 7.1*). Their main aim is to upgrade local nuclear analysis capabilities to perform a maximum fraction of fissile material characterisation in the country of seizure, if possible directly on-site. ITU is contributing to this task by consultancy as well as for test runs. In addition, ITU will receive input for its nuclear material data bank and offers assistance in complementary analyses which can be performed upon request in the Institute's specialized laboratories and with participation of experts from the partner country involved. Contacts have been established with both the State authorities responsible for nuclear safeguards as well as the analytical laboratories charged with the first phases of analyses in potential cases of vagabonding nuclear material.

Contact (7.1): Klaus Mayer • tel.: +49 7247 951 545 • fax: +49 7247 951 595 • mayer@itu.fzk.de

Contact (7.2): Arndt Schubert • tel.: +49 7247 951 289 • fax: +49 7247 951 595 • schubert@itu.fzk.de

COUNTRY	NUCLEAR SAFEGUARDS AUTHORITY	ANALYTICAL LABORATORY
Czech Republic	State Office for Nuclear Safety (SONS)	Nuclear Research Institute Rez near Prague, Central Analytical Laboratory (NRI-CAL)
Hungary	Hungarian Atomic Energy Authority (HAEA)	Institute of Isotopes and Surface Chemistry, Budapest (IoI)
Bulgaria	Committee for Use of Atomic Energy for Peaceful Purposes (CPUAEP)	Institute for Nuclear Research and Nuclear Energy, Sofia (INRNE)

Tab. 7.1 Overview of FONSAFE partners in the East European Countries.

Official visits were paid to those countries and details of the work programmes adopted. In the case of the Czech Republic the procurement procedure for purchase of an inductively-coupled plasma mass spectrometer (ICP-MS) was completed. By end of 1998 a trilateral agreement on transfer of data between SONS, NRI-CAL and ITU was ready for signature.

For Hungary and Bulgaria a market survey on portable non-destructive equipment was performed. The devices selected will allow to characterise the U and Pu isotopic composition of nuclear material by low-energy gamma-spectrometry at the location of seizure.

### 7.3 Design and Set-up of Analytical Laboratories at the Bochvar Institute, Moscow

In the framework of the Commission's TACIS programme (Technical Assistance to the Commonwealth of Independent States), a project on the installation of laboratory facilities for nuclear metrology, safeguards analysis and analysis of nuclear material of unknown origin at the Bochvar Institute (VNIINM) in Moscow was set up. In discussions with the Russian partner institute, the technical details of the laboratories were defined.

Eleven VNIINM staff were trained at ITU in scientific/technical areas and on modern instrumentation relevant to the operation of the laboratories, i.e. in metallography, electron microscopy, titration and mass spectrometry. During the individual four weeks training periods, also technical specifications for large measurement instrumentation were finalized. Instrument purchases were initiated through the TACIS procurement procedure. Further training sessions are foreseen for 1999 in the area of radiometric measurements. In a bilateral workshop on analytical methods for nuclear forensics, the complementarity of the data base project and the forensic laboratory were emphasized.

During a visit to VNIINM the status of the rooms that shall house the new instrumentation were inspected. A conceptual study on the implementation of the laboratories was developed by VNIINM and serves a basis of information for the next steps.

## Annex I

## Books and Periodicals - Conferences - Reports &amp; Special Publications

## Books and Periodicals

(22 of these publications had been submitted or presented at conferences in 1997 and appeared in print in 1998).

*Abbas K., Morel J., Etcheverry M., Nicolaou G.*

Use of Miniature CdZnTe X/Gamma Detector in Nuclear Safeguards: Characterisation of Spent Nuclear Fuel and Uranium Enrichment Determination.

Nuclear Instruments and Methods in Physics Research A 405 (1998) 153-158.

*Apostolidis C., Molinet R., Richir P., Ougier M., Mayer K.*

Development and Validation of a Simple, Rapid and Robust Method for the Chemical Separation of Uranium and Plutonium.

Radiochimica Acta 83 (1998) 21-25.

*Apostolidis C.; Carvalho A., Domingos A., Kanellakopoulos B., Maier R., Marques N., Pires de Matos A., Rebizant J.*

Chloro-lanthanide, and plutonium complexes containing the hydrotris(3,5-dimethylpyrazol-1-yl)borate ligand: the crystal and molecular structures of

[PrCl( $\mu$ -Cl)Tp<sup>Me2</sup>(3,5-Me<sub>2</sub>pzh)]<sub>2</sub> and YbCl<sub>2</sub>Tp<sup>Me2</sup>(THF).  
Polyhedron 18 (1998) 263-272

*Arico E.M., Kanellakopoulos B., Apostolidis C., Zinner L.B.*

Synthesis and Magnetic Properties of (C<sub>5</sub>H<sub>5</sub>)<sub>3</sub>Ce.HMPA.

Journal of Alloys and Compounds 275-277 (1998) 798-800.

*Babelot J.F., Conrad R., Konings R.J.M., Mühling G., Salvatores M., Vambenepe G.*

The EFTTRA Experiment on Irradiation of Am Targets.

Journal of Alloys and Compounds 271-273 (1998) 606-609.

*Bakker K., Hein H., Konings R.J.M., van der Laan R.R., Matzke Hj., van Vlaanderen P.*

Thermophysical Property Measurements and Ion-Implantation Studies on CePO<sub>4</sub>.

Journal of Nuclear Materials 252 (1998) 228-234.

*Bernhoeft N., Hiess A., Roessli B., Sato N., Aso N.A., Endoh, Y., Lander G.H., Komatsubara, T.*

UPd<sub>2</sub>Al<sub>3</sub>: An Analysis of the Inelastic Neutron Scattering Spectra. "Itinerant Electron Magnetism: Fluctuation Effects", p. 43-60. Proceedings of the Conference of the NATO Advanced Study Institute held in Moscow (Russia) Sept. 1-5, 1997, Kluwer Academic Publishers, 1998, (eds.) D. Wagner et al.

*Bernhoeft N., Hiess A., Langridge S., Stunault A., Wermeille D., Vettier C., Lander G.H., Huth M., Jourdan M., Adrian H.*

Probe Coherence Volume and the Interpretation of Scattering Experiments.

Physical Review Letters 81 No. 16 (1998) 3419-3422.

*Bernhoeft N., Sato N., Roessli B., Aso N., Hiess A., Lander G.H., Endoh Y., Komatsubara T.*

Enhancement of Magnetic Fluctuations on Passing below T<sub>c</sub> in the Heavy Fermion Superconductor UPd<sub>2</sub>Al<sub>3</sub>.

Physical Review Letters 81 No. 19 (1998) 4244-4247.

*Blank H.*

Fractional Packing Densities and Fast Diffusion in Uranium and Other Light Actinides.

Journal of Alloys and Compounds 268 (1998) 180-187.

*Borwieck H., Walter O., Dinjus E., Rebizant J.*

Organometallic Chemistry in Supercritical Water:

Metallorganic Products of the CpCo-Catalyzed.

Cyclotrimerization of Acetylenes.

Journal of Organometallic Chemistry 570 (1998) 121-127.

*Bottomley P.D.W., Montigny F., Stalios A.D., Walker C.T.*

EPMA of Melted UO<sub>2</sub> Fuel Rods from the Phebus-FP Reactor Accident Experiment.

Mikrochimica Acta (Suppl.) 15 (1998) 191-200

*Braithwaite D., Demuer A., Goncharenko I.N., Ichas V., Mignot J.M., Rebizant J., Spirlet J.C., Vogt O., Zwirner S.*

Pressure Effects on Magnetism in the Uranium and Neptunium Monopnictides.

Journal of Alloys and Compounds 271-273 (1998) 426-432.

*Brooks M.S.S., Eriksson O., Wills J.M., Johansson B.*

Reply to a Comment "Density Functional Theory of Crystal Field Quasiparticle Excitations and the ab initio Calculation of Spin Hamiltonian Parameters".

Physical Review Letters 80 (1998) 4108.

*Burghartz M., Matzke Hj., Léger C., Vambenepe G., Rome M.*

Inert Matrices for the Transmutation of Actinides: Fabrication, Thermal Properties and Radiation Stability of Ceramic Materials.

Journal of Alloys and Compounds 271-273 (1998) 544-548.

*Cobos J., Papaioannou D., Spino J., Coquerelle M.*

Phase Characterisation of Simulated High Burn-up UO<sub>2</sub> Fuel.

Journal of Alloys and Compounds 271-273 (1998) 610-615.

Cottenier S., Demuynck S., Kaczorowski D., Spirlet J.C., Meersschaut J., Rots M.

The Magnetic Structure of  $UIn_3$ :PaC on a Polycrystal.  
Journal of Physics Condensed Matter 10 (1998) 8381-8387.

Cross J.O., Newville M., Rehr J.J., Sorensen L.B., Bouldin C.E., Watson G., Gouder T., Lander G.H., Bell M.I.

Inclusion of Local Structure Effects in Theoretical X-ray Resonant Scattering Amplitudes using ab initio X-ray-absorption Spectra Calculations.  
Physical Review Condensed Matter 58 No. 17 (1998) 11215-11225.

Dervenagas P., Paolasini L., Hiess A., Lander G.H., Panschulla A., Canfield P.

Competing Exchange Interactions in Ferromagnetic  $CeFe_2$ .  
Physica B, Condensed Matter 241-243 (1998) 649-650.

Estrela P., Pereira L.C.J., de Visser A., de Boer F.R., Almeida M., Godinho M., Rebizant J., Spirlet J.C.

Structural, Magnetic and Transport Properties of Single-Crystalline  $U_2Pt_2In$ .  
Journal of Physics Condensed Matter 10 (1998) 9465-9475.

Fernández A., Richter K., Somers J.

Fabrication of Transmutation and Incineration Targets by Infiltration of Porous Pellets by Radioactive Solutions.  
Journal of Alloys and Compounds 271-273 (1998) 616-619.

Gouder T.

Thin Layers in Actinide Research.  
Journal of Alloys and Compounds 271-273 (1998) 841-845.

Heathman S., Haire R.G.

High-Pressure X-ray Diffraction Studies of Cm-Bk Alloys: Contribution to the Actinide Pressure-Phase Diagram.  
Journal of Alloys and Compounds 271-273 (1998) 342-346.

Kaczorowski D., Kruk R., Sánchez J.P., Malaman B., Wastin F.

Magnetic and Electronic Properties of Ternary Uranium Antimonides  $UTSb_2$  (T = 3d, 4d-, 5d-electron Transition Metal).  
Physical Review B Condensed Matter 58 No. 14 (1998) 9227-9237.

Kinoshita M., Kameyama T., Kitajima S., Matzke H.

Temperature and Fission Rate Effects on the Rim Structure Formation in a  $UO_2$  Fuel with a Burnup of 7.9% FIMA.  
Journal of Nuclear Materials 252 (1998) 71-78.

Konings R.J.M., Stalios A.D., Walker C.T., Cocuau N.

Transmutation of Technetium: Results of the EFTTRA-T1 Experiment.  
Journal of Nuclear Materials 254 (1998) 122-128.

Kopmann W., Litterst F.J., Klauß H.H., Hillberg M., Wagener, W., Kalvius, G.M., Schreier, E., Burghart, F.J. Rebizant, J., Lander, G.H.

Magnetic Order in  $NpO_2$  and  $UO_2$  Studied by Muon Spin Rotation.  
Journal of Alloys and Compounds 271-273 (1998) 463-466.

Lassmann K., Walker C.T., van de Laar J.

Extension of the TRANSURANUS Burnup Model to Heavy Water Reactor Conditions.  
Journal of Nuclear Materials 255 (1998) 222-233.

Lindbaum A., Hafner J., Gratz E., Heathman S.

Structural Stability of  $YM_2$  Compounds (M = Al, Ni, Cu) studied ab initio Total-Energy Calculations and High-Pressure X-ray Diffraction.  
Journal of Physics Condensed Matter 10 No. 13 (1998) 2933-2946.

Matzke H., Beauvy M., Wiss T.

Simulation of Fission Damage in Materials Candidate for the Transmutation of Minor Actinides.  
Annual Report Grand Accélérateur National d'Ions Lourds (1998) 159-160.

Massiot P., Leprince B., Lizon C., Rateau G., Richter K., Fritsch P.

Chemical Composition of Inhalable MOX Powders Prepared According to a SOLGEL Process: an Energy Dispersive X-ray Analysis of Individual Particles.  
Journal of Alloys and Compounds 271-273 (1998) 38-41

Merli L., Rorif F., Fuger J.

The Enthalpies of Solution of Lanthanide Metals in Hydrochloric Acid at Various Concentrations. Relevance to Nuclear Waste Long Term Storage.  
Radiochimica Acta 82 (1998) 3-9.

Musella M., Ronchi C., Brykin M., Sheindlin M.

The Molten State of Graphite - An Experimental Study.  
Journal of Applied Physics 84 No.5 (1998) 2530-2537.

Nowicki L., Turos A., Garrido F., Choffel C., Thomé L., Jagielski J., Matzke H.

Lattice Location of Oxygen Atoms in  $UO_2$  Single Crystals Leached in Water.  
Nuclear Instruments and Methods B 136-138 (1998) 447-452.

Oppeneer P.M., Perlov A.Ya., Antonov V.N., Yaresko A.N., Kraft T., Brooks M.S.S.

Optical and Magneto-optical Spectroscopy of Uranium and Plutonium Compounds: Recent Theoretical Progress.

Journal of Alloys and Compounds 271-273 (1998) 831-836.

Paixao J.A., Waerenborgh J.C., Rogalski M.S., Conçalves A.P., Almeida M., Gukasov A., Bonnet M., Spirlet J.C., Sousa J.B.

Magnetization Density in  $UFe_{10}Si_2$ .

Journal of Physics Condensed Matter 10 No.18 (1998) 4071-4080.

Paolasini L., Dervenagas P., Vulliet, P., Sánchez J.P., Lander G.H., Hiess A., Panchula A., Canfield P.

Magnetic Response Function of the Itinerant Ferromagnetic  $CeFe_2$

Physical Review B Condensed Matter 58 No.18 (1998) 12117-12124.

Paolasini L., Caciuffo R., Roessli B., Lander G.H.

Unusual Fe-Fe Interactions in the Itinerant Magnet  $UFe_2$ .

Physica B, Condens Matter 241-243 (1998) 681-683.

Raptis K., Mayer K., Hendricks F., Debievre P.

Preparation and Certification of New Thorium Isotopic Reference Materials.

Fresenius Journal of Analytical Chemistry 361 No.5 (1998) 400-403.

Rebizant J., Wastin F., Rijkeboer C., Bednarczyk E., Lefévre P.

Preparation and Electrical Resistivity of  $(Pu_{1-x}U_x)Sb$  and  $(Pu_{1-x}Y_x)Sb$  Single Crystals.

Journal of Alloys and Compounds 271-273 (1998) 490-494.

Sato, N., Aso, N., Roessli, B., Lander, G.H., Komatsubara, T., Endoh, Y., Sakai, O.

Observation of Two Low-Energy Responses in  $UPd_2Al_3$  - Interaction of Magnetism and Superconductivity?

Journal of Alloys and Compounds 271-273 (1998) 433-436.

Schenkel R., van Geel J.

ITU Karlsruhe goes East: toward a common safety & safeguards culture.

Nuclear Europe Worldscan 1-2 (1998) 68.

Serrano J.A., Glatz J.P., Toscano E.H., Papaioannou D., Barrero J., Coquerelle M.

Influence of Low Temperature Air Oxidation on Dissolution Behaviour of  $UO_2$  and MOX Spent Fuel.

Journal of Alloys and Compounds 271-273 (1998) 573-576.

Serrano J.A., Rondinella V.V., Glatz J.P., Toscano E.H., Quinones J., Diaz-Arocas P.P.

Comparison of the Leaching Behaviour of Irradiated Fuel, SIMFUEL, and Non-Irradiated  $UO_2$  under Oxidic Conditions.

Radiochimica Acta 82 (1998) 33-37.

Sheindlin M., Halton D., Musella M., Ronchi C.

Advances in the Use of Laser-flash Techniques for Thermal Diffusivity Measurement.

Review of Scientific Instruments 69 No. 3 (1998) 1426-1436.

Sikafus K.E., Matzke H.J., Yasuda K., Chodak P., Verrall R.A., Lucuta P.G., Andrews H.R., Turos A., Fromknecht R., Baker N.P.

Radiation Damage Effects in Cubic-Stabilized Zirconia Irradiated with 72 MeV  $I^+$  Ions.

Nuclear Instruments & Methods in Physics Research B 141 No. 1 (1998) 358-365.

Spino J., Baron D., Coquerelle M., Stalios A.D.

High Burn-up Rim Structure: Evidences that Xenon-Depletion, Pore Formation and Grain Subdivision start at Different Local Burn-ups.

Journal of Nuclear Materials 256 No.2,3 (1998) 189-196.

Tamborini G., Betti, M., Forcina V., Hiernaut T., Giovannone B., Koch L.

Application of Secondary Ion Mass Spectrometry to the Identification of Single Particles of Uranium and their Isotopic Measurement.

Spectrochimica Acta Part B 53 (1998) 1289-1302.

Vogt O., Mattenberger K., Löhle J., Rebizant J.

High Temperature Susceptibilities of Actinide Monopnictides and Monochalcogenides.

Journal of Alloys and Compounds 271-273 (1998) 508-512.

Wasserman S.R., Soderholm L., Rebizant J., Lander G.H.

Surface Contamination of Single-Crystal  $PuSb$ .

Journal of Alloys and Compounds 271-273 (1998) 882-886.

Wastin F., Bednarczyk E., Rebizant J.

Transport Properties of  $(U_{1-x}Np_x)Pd_2Al_3$  and  $(U_{1-x}Pu_x)Pd_2Al_3$  Intermetallic Solid Solutions.

Journal of Alloys and Compounds 271-273 (1998) 437-443.

Wastin F., Rebizant J., Stalios A.D., Walker C.T.

On the Characterization of  $(U,Np)_xT_yX_z$  Intermetallic Solid Solutions.

Journal of Alloys and Compounds 271-273 (1998) 513-516.

Weber W.J., Ewing R.C., Catlow C.R.A., Díaz de la Rubia T., Hobbs L.W., Kinoshita C., Matzke, H.J., Motta A.T., Nastasi M.A., Salje E.H.K. et al.

Radiation Effects in Crystalline Ceramics for the Immobilization of High-level Nuclear Waste and Plutonium.

Journal of Materials Research 13 No.6 (1998) 1434-1484.

Wermeille C., Vettier C., Bernhoeft N., Stunault A., Langridge S., de Bergevin F., Yakhov F., Lidström E. Flouquet J., Lejay P.

Resonant Magnetic X-ray Scattering in  $UPd_2Si_2$  at the Uranium L-2, L-3 Edges.

Physical Review B Condensed Matter 58 No. 14 (1998) 9185-9193

## Conferences

Conference papers published in 1998 in journals or special conference proceedings volumes may appear also under paragraph 1 (Books and Periodicals).

### **1998 Winter Conference on Plasma Spectrometry January 5-12, 1998 Scottsdale, AZ (USA)**

*Barrero Moreno J.M., Betti M.*

Determination of the Isotopic Composition of Cesium in Radioactive Samples by Ion Chromatography Inductively Coupled Plasma Mass Spectrometry.

*Barrero Moreno J.M., Betti M., Menchichetti L., Fuoco R.*

Ion Chromatography Inductively Coupled Plasma Mass Spectrometry for the Determination of Ru, Mo, and Tc Fission Products in Samples of Nuclear Concern.

*Betti M., Actis-Dato L.O., Rasmussen G., Toscano E.H., Giannarelli S., Ruhmann H.*

Depth Profiling of Impurities in Zirconium Oxide Layers by DC Glow Discharge Mass Spectrometry.

*Betti M., Gouder T., Actis-Dato L.O., Rasmussen G., Tocci U., Fuoco R.*

Characterization of Thin Film Samples by Glow Discharge Mass Spectrometry and X-ray Induced Photoelectron Spectroscopy.

### **Journées Annuelles Groupe Français de la Céramique "Céramiques Nucléaires" February 3-4, 1998 Cadarache (France)**

*Matzke, Hj.*

Radiation Damage in Inert Matrices for Transmutation.

### **5th Fissile Materials Workshop Lawrence Livermore National Laboratory February 3-4, 1998 Livermore, CA (USA)**

*Koch L.*

International Co-operation in Nuclear Forensics.  
Proceedings of the Conference.

### **International Seminar on "Thermal Performance of high Burn-up LWR Fuel" March 3-6, 1998 Cadarache (France)**

*Lassmann K., Walker C.T., van de Laar J.*

Thermal Analysis of Ultra-high-burn-up Irradiations Employing the TRANSURANUS Code.

Proceedings of the Seminar, OECD/NEA (1998) 359-367.

*Lassmann K.*

Numerical Algorithms for Intragranular Fission Gas Release.

### **Fachgespräch "Neue Nukleartechnologien im Spannungsfeld von Naturwissenschaft und Ethik" March 11-14, 1998 Darmstadt (Germany)**

*Magill J., Peerani P., Schenkel R., van Geel J.*

Accelerator Driven System -An Ecological and Sustainable Nuclear Option for Future Energy Generation?

Proliferation and Waste Toxicity Considerations.

Proceedings of the Conference.

### **Enlarged Halden Programme Meeting "High Burn-up Fuel Performance, Safety & Reliability and Degradation of In-core Materials and Water Chemistry" March 15-20, 1998 Lillehammer (Norway)**

*Kitajima S., Matzke H., Kinoshita M.*

High Burnup Rim Project.

Proceedings Halden Project Report (1998) F-3.11.

*Lassmann K., Walker C.T., van de Laar J.*

The TRANSURANUS Burnup Model for Light and Heavy Water Reactor Conditions.

### **Frühjahrstagung der Deutschen Physikalischen Gesellschaft March 23-27, 1998 Regensburg (Germany)**

*Schenkel R., Koch L., van Geel J.*

Neue Entwicklungen im Bereich der Verifizierung von Kernmaterial  
Proceedings "Nuklearwaffen- Neue Rüstungstechnologien", 1998,  
p. 81-88, Neuneck, G., Altmann, J. Scheffran, J. (eds.) DPG/FONAS.

### **13th Radiochemical Conference April 19-24, 1998 Prague (Czech Republic)**

*Koch L., Apostolidis C., Janssens W., Molinet R., van Geel J.*

Production of AC-225 and Application of the Bi-213 Daughter in Cancer Therapy.

**Workshop on Innovative Options in the Field of  
Nuclear Energy**

**April 27-May 1, 1998 Les Houches (France)**

*Magill J., Peerani P., van Geel J.*

(Non-) Proliferation Aspects of Accelerator Driven Systems.  
Proceedings of the Conference.

**12th International Conference on Packaging and  
Transportation of Radioactive Materials**

**May 10-15, 1998 Paris (France)**

*Matsumura T., Sasahara A., Takei M., Takekawa T., Kagehira K., Nicolaou G., Betti M.*

Analysis of Burnup Credit on Spent Fuel Transport/Storage Casks -  
Estimation of Reactivity Bias.  
Proceedings of the Conference.

**ESARDA Seminar on "Modern Verification Systems: Similarities,  
Synergies and Challenges"**

**May 12-14, 1998 Helsinki (Finland)**

*Mayer K.*

Destructive Analytical Measurement Techniques in Nuclear Mate-  
rial Safeguards Accountancy and Control.  
Proceedings ESARDA Bulletin.

**EMAS Regional Workshop on Modern Developments and  
Application in Microbeam Analysis**

**May 13-16, 1998 Barcelona (Spain)**

*Walker C.T.*

Electron probe Microanalysis of Actinide Elements.  
Proceedings of the Conference.

**28. Journées des Actinides**  
**May 14-16, 1998 Uppsala (Sweden)**

*Ahuja R., Auluck S., Eriksson O., Brooks M.S.S., Johansson B.*  
Fermi Surface of Uranium Carbide.

*Bernhoeft N., Sato N., Roessli B., Aso N., Hiess A., Lander G.H., Endoh Y.,  
Komatsubara T.*

Superconductivity and Magnetism in UPd<sub>2</sub>Al<sub>3</sub> - New Results.

*Brooks M.S.S.*

Calculated X-ray Magnetic Circular Dichroism for Actinide Com-  
pounds.

*Colineau E., Wastin F., Higgins E.J.*

Magnetism of U<sub>4</sub>(Ru<sub>1-x</sub>OS<sub>x</sub>)<sub>7</sub>Ge<sub>6</sub> Solid Solutions (Poster).

*Colineau E., Wastin F., Rebizant J.*

Mössbauer Investigations on Np<sub>2</sub>Ir<sub>2</sub>In.

*Demuyneck S., Cottenier S., Spirlet J.C., Rots M.*

The Magnetic Structure of UPb<sub>3</sub> Studied by Perturbed Angular Cor-  
relations Spectroscopy.

*Griveau J.C., Braithwaite D., Thomasson J., Geibel C., Assmuss W.,  
Flouquet J.*

Heavy Fermion Superconductors UPd<sub>2</sub>Al<sub>3</sub> and CeCu<sub>2</sub>Si<sub>2</sub> under High  
Pressure (Poster).

*Ichas, V., Rebizant, J., Spirlet, J.C.*

Pressure Effects on the Resistivity of PuTe.

*Javorsky P., Wastin F., Havela L., Griveau J.C., Bednarczyk E., Rebizant J.*

Magnetic Properties of NpNiSn and NpIrSn (Poster).

*Lidström E., Hiess A., Longfield M., Mannix D., Lander G.H., Wastin F.,  
Rebizant J.*

Element Specific Magnetism in U<sub>1-x</sub>Np<sub>x</sub>Ru<sub>2</sub>Si<sub>2</sub> Compounds.

*Méresse Y., Heathman S., Le Bihan T., Darracq S., Rebizant J., Spirlet J.C.,  
Benedict U.*

X-ray Diffraction Studies of Neptunium Compounds under High  
Pressure (Poster).

*Monachesi P., Continenza A., Brooks M.S.S., Griioni M.*

Electronic Properties of URu<sub>2</sub>Si and URhSi.

*Oppeneer P.M., Brooks M.S.S., Kraft T.*

Electronic Structure Investigation of the Plutonium Monochalco-  
genides.

*Wachter P., Rebizant J.*

The Electronic Structure of NpTe and AmTe.

**CIMTEC 98, World Congress on Ceramics**  
**June 14-19, 1998 Firenze (Italy)**

*Fernández A., Richter K., Closset J.C., Fourcaudot S., Fuchs C., Babelot  
J.F., Voet R., Somers J.*

Fabrication of Targets for the Transmutation and Incineration of Ac-  
tinides.

*Fernández A., Richter K., Somers J*

Preparation of Spinel (MgAl<sub>2</sub>O<sub>4</sub>) Spheres by a Hybrid Sol-Gel Technique.

*Lucuta P.G., Matzke H.J., Andrews H.R., Verrall R.A.*

Simulated Fission Radiation Effects in UO<sub>2</sub> and SIMFUEL.  
Proceedings of the Conference.

*Matzke H.J.*

Ceramics in Fission Energy - Current Developments and Problems.  
Proceedings of the Conference.

**5th Subsecond Thermophysics Conference  
June 16-19, 1998 Aix-en-Provence (France)**

*Musella M., Ronchi C., Sheindlin M.*

Dependence of Melting Temperature on Pressure up to 2500 Bar in Tungsten, Uranium Dioxide and Graphite.  
Proceedings International Journal of Thermophysics.

*Salikhov T.P., Kan V.V., Ronchi C.*

Radiative Properties of Uranium Dioxide near its Melting Point.  
Proceedings International Journal of Thermophysics.

**Gordon Research Conference on Research at High Pressure  
June 21-26, 1998 Mériden, NH (USA)**

*Méresse Y., Heathman S., Le Bihan T., Darracq S., Rebizant J., Spirlet J.C., Benedict U.*

X-ray Diffraction Studies of Neptunium and Uranium based-compounds under High Pressure.

**Nuclear Disarmament, Safe Disposal of Nuclear Materials or  
New Weapons Development  
July 2-4, 1998 Como (Italy)**

*Koch L.*

How can we Detect Clandestine Nuclear Activities?  
Proceedings of the Conference.

**International Conference on Strongly Correlated  
Electron Systems (SCES)  
July 15-18, 1998 Paris (France)**

*Bernhoeft N., Sato N., Roessli B., Aso N., Hiess A., Lander G.H., Endoh Y., Komatsubara T.*

Magnetic Fluctuations Above and Below T<sub>c</sub> in the Heavy Fermion Superconductor UPd<sub>2</sub>Al<sub>3</sub>.  
Proceedings Physica B.

*Hiess A., Bernhoeft N., Langridge S., Vettier C., Huth M., Jourdan M., Adrian H., Lander G.H.*

Magnetic Properties of UPd<sub>2</sub>Al<sub>3</sub> Thin Film Investigated by Resonant X-ray Scattering.

Proceedings Physica B.

*Hiess A., Coad S., Buschinger B., Trovarelli O., Boucherle J.X., Givord F., Hansen T., Lelievre-Berna E. Suard E., Geibel C., Steglich F.*

Magnetism in R<sub>2</sub>T<sub>3</sub>X<sub>9</sub> (R = Ce, Yb, U; T = Rh, Ir; X = Al, Ga) Intermetallic Compounds.

Proceedings Physica B.

*Paolasini L., Dervenagas P., Lander G.H., Hiess A., Panchula A., Canfield P.*

Antiferromagnetic Fluctuations Observed in the Itinerant Ferromagnetic CeFe<sub>2</sub>.

**INMM Annual Meeting  
July 26-30, 1998 Naples, FL (USA)**

*Mayer K., Ottmar H., Richir P., Brandalise B., Koch L.*

Development and Analytical Measurements for Safeguards.  
Proceedings INMM Journal.

**International Conference on Phonons  
July 27, 1998 Lancaster (United Kingdom)**

*Marmeggi, J.C., Curat, R., Bouvet, A., Lander, G.H.*

Phonon Softening in Alpha-Uranium Associated with the CDW Transition.

Proceedings Physica B.

**12th International Conference on Vacuum  
Ultraviolet Radiation Physics  
August 3-7, 1998 San Francisco (USA)**

*Gouder T.*

Photoemission Study of the 5f Localization in Thin Films of Pu.  
(Poster), Proceedings of the Conference.

**Sixth Summer School on Neutron Scattering Complementarity  
between Neutron and Synchrotron X-ray Scattering  
August 8 -14, 1998 Zuoz (Switzerland)**

*Lander G.H.*

Seminar on "Magnetism".

World Scientific Publishing, Ed. A. Furrer (1998) 163-165.

**FJSS '98 - 1998 Frédéric Joliot Summer School in Reactor Physics**  
**August 17-26, 1998 Cadarache (France)**

*Matzke HJ.*

Innovative Nuclear Fuels and Applications. Part I: Limits of Today's Fuels and Concepts for Innovative Fuels.

Proceedings CEA.

*Matzke HJ.*

Innovative Nuclear Fuels and Applications. Part II: Materials Properties, Irradiation Performance and Gaps in our Knowledge.

Proceedings CEA.

**15th International Congress on X-ray Optics and Microanalysis**  
**August 24-27, 1998 Antwerp (Belgium)**

*Walker, C.T.*

Electron Probe Microanalysis of Irradiated Nuclear Fuel.

Proceedings Journal Microanalysis & Trace Elements.

**Joint Meeting of European Physical Society & French Physical Society on Condensed Matter**  
**August 24-29, 1998 Grenoble (France)**

*Martin-Martin A., Pereira L.J., Lander G.H., Rebizant J.*

Singly Crystal Neutron Diffraction on  $U_2T_2In$  ( $T=Pt, Ni$ ) Compounds.

*Paolasini L., Caciuff R., Lander G.H., Hennion B., Roessli B., Myers K., Canfield P.*

Anomalous Spin-Lattice Dynamics in the Itinerant  $UFe_2$ .

**International Conference on Weak Interacting Plasma**  
**August 25-28, 1998 Boston (USA)**

*Gryaznov V.K., Iosilevski I.L., Yakub E.S., Fortov V.E., Hyland G.J., Ronchi C.*

Ionic Model for Liquid Uranium Dioxide.

Proceedings of the Conference.

**Asian Conference on Thermophysical Properties**  
**August 30-September 2, 1998 Seoul (Republic of Korea)**

*Salikhov T.P., Kan V.V., Ronchi C.*

Thermal Radiation Properties of Uranium Dioxide at High Temperatures.

Proceedings of the Conference.

**19th International Conference on Nuclear Tracks in Solids**  
**August 31-September 4, 1998 Besançon (France)**

*Wiss T., Matzke HJ.*

Heavy Ion Induced Damage in  $MgAl_2O_4$ , an Inert Matrix Candidate for the Transmutation of Minor Actinides.

Proceedings Journal "Radiation Measurements".

**7th European Magnetic Materials and Applications Conference**  
**September 9-12, 1998 Zaragoza (Spain)**

*Pereira L.C.J., Almeida M., Estrela P., Godinho M., Rebizant J., Spirlet J.C., Pinto R.P., Amado M.M., Braga M.E., Sousa J.B.*

Magnetic and Transport Properties of  $U_2Pt_2In$  Single Crystals.

Proceedings J. of Magnetism and Magnetic Materials.

**5th Euroconference "Bulk Magnetic and Superconducting Novel Materials"**  
**September 18-22, 1998 Patras (Greece)**

*Hiess A., Bernhoeft N., Langridge S., Vettier C., Roessli B., Huth M., Jordan M., Adrian H., Sato N., Aso N., Endho Y., Komatsubara T., Lander G.H.*

Magnetic Properties of  $UPd_2Al_3$  Single Crystals and Thin Films Investigated by X-ray and Neutron Scattering Experiments.

**Fermi-Liquid Instabilities in Correlated Metals (FERLIN)**  
**September 23-25, 1998 Bad-Herrenalb (Deutschland)**

*Ichas V., Rebizant J., Spirlet J.C.*

Pressure Effects on the Resistivity of PuTe.

**Environmental Radiochemical Analysis, Radiochemical Methods Group**  
**September 23-25, 1998 Blackpool (United Kingdom)**

*Tamborini G., Betti M., Koch L., Carbol P.*

Secondary Ion Mass Spectrometry for the Detection of Radionuclides in Particles from Environmental Materials.

**International Conference on the Physics of Nuclear Science and Technology**  
**October 4-8, 1998 Islandia, New York (USA)**

*Schubert A., Janssen G., Bibilashvili Yu.K., Chorokhov N.A., Dolgov Yu.N., Koch L., Peerani P.*

A Software Package for Nuclear Analysis Guidance by a Relational Database.

**24th Annual Meeting of the Spanish Nuclear Society  
October 14-16, 1998 Valladolid (Spain)**

*Cobos J., Rondinella V.V., Wiss T., Matzke Hj.*

Effect Alpha-Radiolysis on the Dissolution of UO<sub>2</sub> Doped with Alpha Emitters under Anoxic Conditions.

Proceedings of the Conference.

*Fernández A., Somers J., Richter K., Haas D., Fourcaudot S., Fuchs C., Voet R.*

Fabrication of Fuels and Targets for the Transmutation and Incineration of Actinides.

Proceedings of the Conference.

**Inert Matrix Fuel Workshop  
October 19-20, 1998 Villigen (Switzerland)**

*Chauvin N., Konings R.J.M., Matzke Hj.*

Optimization of Inert Matrix Fuel Concepts for Americium Transmutation.

Journal of Nuclear Materials.

*Matzke Hj., Rondinella V.V., Wiss T.*

Materials Research on Inert Matrices: a Screening Study.  
Proceedings Journal of Nuclear Materials.

**OECD/NEA Workshop on Advanced Reactors with  
Innovative Fuels  
October 21-23, 1998 Villigen (Switzerland)**

*Matzke Hj.*

Radiation Stability of Inert Matrix Fuels.

Proceedings of the Conference.

**GLOBAL '98 - International Conference on Preparing  
the Ground for Renewal of Nuclear Power  
October 22-23, 1998 Paris (France)**

*van Geel J., Schenkel R., Magill J.*

Innovative Fuel Cycles.

Proceedings of the Conference.

**Congress "Legislation on Radioprotection in  
the European Union"  
October 27-28, 1998 Bologna (Italy)**

*Betti M.*

Detection of Release of Radioactivity into the Environment by modern Analytical Instrumental Techniques.

Proceedings of the Conference.

**Tripartite Seminar on Radiochemical Plants  
November 2-6, 1998 Obninsk (Russia)**

*Mayer K., Ottmar H., Cromboom O., Daures P., Schneider H.G., Brandalise B., Koch L.*

Analytical Measurements for Safeguarding Large Reprocessing Plants.

Proceedings of the Conference.

**International Workshop on the Application of Extraction  
Chromatography in Radionuclide Measurement  
November 9-10, 1998 Geel (Belgium)**

*Richir P., Brandalise B., Apostolidis C., Molinet R., Mayer K.*

Development of a Robotized Separation Method for U-Pu Samples Using UTEVA Resin.

Proceedings EUR-Report.

**43rd Conference on Magnetism & Magnetic Materials  
November 9-12, 1998 Miami, FL (USA)**

*Amoretti G., Caciuffo R., Santini P., Lander G.H., Kulda J., de V. du Plessis P.*

Polarized Neutron Scattering Study of the Magnetic Response across TN in a Single Crystal of UO<sub>2</sub>.

Proceedings Journal of Applied Physics.

*Caciuffo R., Griveau J.C., Kolberg D., Wastin F., Rinaldi D., Canfield P., Panchula A.*

Static and Dynamic Magnetic Response of CeFe<sub>2</sub>.

Proceedings Journal of Applied Physics.

**International Workshop on "Quality Requirements  
in NDA Measurements"  
November 17-19, 1998 Ispra (Italy)**

*Cromboom O.*

Implementation and use of the DIN EN ISO 9001 Quality Management System at ITU.

Proceedings ESARDA.

**OECD Fifth International Information Exchange Meeting on Actinide and Fission Product Partitioning and Transmutation**  
**November 25-27, 1998 Mol (Belgium)**

*Haas D., Somers J., La Fuente A., Renard A.*  
Feasibility of the Fabrication of Americium Targets.  
Proceedings NEA.

**1998 Autumn Meeting of the Materials Research Society**  
**November 30-December 4, 1998 Boston (USA)**

*Rondinella V.V., Matzke H.J., Cobos J., Wiss T.*  
Alpha-Radiolysis and Alpha-Radiation Damage Effects on UO<sub>2</sub> Dissolution under Spent Fuel Storage Conditions.  
Proceedings Materials Research Society Symposium.

*Zinkle S.J., Matzke H.J., Skuratov V.A.*  
Microstructure of Swift Heavy Ion irradiated MgAl<sub>2</sub>O<sub>4</sub> Spinel.  
Proceedings Materials Research Society Symposium.

**Workshop "Implementation of the WWER Version of the TRANSURANUS Code and its Application to Safety Criteria"**  
**December 7-11, 1998 Sofia (Bulgaria)**

*Lassmann K., van de Laar J.*  
Release of the TRANSURANUS Version V1M2J98: General and Practical Aspects.

*Lassmann K., van de Laar J.*  
The TRANSURANUS WWER Version.

*Lassmann K., van de Laar J.*  
Fission Gas Release Models of the TRANSURANUS Version V1M2J98.

*Lassmann K., van de Laar J.*  
Burnup Models of the TRANSURANUS Code Version V1M2J98.

*Lassmann K., van de Laar J.*  
The TRANSURANUS Gd Version.

*Lassmann K., van de Laar J.*  
The Transient TRANSURANUS Version.

**Conference on Condensed Matter**  
**December 13-17, 1998 Manchester (United Kingdom)**

*Bernhoeft N., Roessli B., Sato N., Hiess A., Lander G.H.*  
Evidence for Quasiparticle Renormalisation by the Low Frequency Exchange Field in UPd<sub>2</sub>Al<sub>3</sub>.

## Reports & Special Publications

*Huber, U. (Ed.)*  
ITU - Institute for Transuranium Elements Karlsruhe.  
Special Publications: S.P./I.98.37 (1998).

*Schenkel R., Richter J., Magill J., Pel D.*  
Annual Report 97 - Institute for Transuranium Elements.  
EUR 17746 EN (1998).

*Janssens, W. (compiler)*  
α-Immuno '97 Symposium organized by the European Commission, Institute for Transuranium Elements, October 27-28, 1997 (Karlsruhe (Germany))  
EUR 18089 EN (1998), ISBN 92-828-4617-2

*Adroguer B., Barrachin M., Coquerelle M., Bottomley D., Hofmann P., Steinbrück M., Chevalier P.Y., Cheynet B., Fischer M., Hellmann S. et al.*  
Corium Interactions and Thermochemistry (CIT Project).  
FISA-97 EU Research on Severe Accidents, November 17-19, 1997 Luxembourg.  
EUR 18258 EN (1998) 103-112 Eds. G. Van Goethem et al.

*Bowsher B.R., Bottomley D., Jokiniemi J.K.*  
Revaporization of Tests on Samples from Phebus Fission Products.  
FISA-97 EU Research on Severe Accidents, November 17-19, 1997 Luxembourg.  
EUR 18258 EN (1998) 213-222 Eds. G. Van Goethem et al.



# Annex II

## Collaborations with External Organizations

### Argentina

**Brazilian-Argentine Agency for Accounting and Control of Nuclear Materials (ABACC), Rio de Janeiro:** Safeguards (E. Palacio, C. Feu Alvim, O. Mafra Guidicini).  
CNEA Buenos Aires: Diffusion in solids (F. Dyment).

### Armenia

**Armenian Nuclear Regulatory Authority, Yerevan:** TRANSURANUS fuel pin code development (A. Martirosian).

### Austria

**International Atomic Energy Agency (IAEA), Vienna:** Evaluation and automation of techniques for safeguards analysis (K. Lessmon); *Division of Safeguards Directorate:* Environmental analysis (E. Kuhn, J. Cooley); *Seibersdorf Analytical Laboratory (SAL):* Cooperative Support Programme (S. Deron); *Division of Nuclear Fuel Cycle and Waste Management:* TRANSURANUS fuel pin code development (M. Samiei)  
**Technical University of Vienna:** Resistivity of alloys and high-pressure effects (E. Gratz).

### Belgium

**Belgonucléaire:** Ariane project: properties of irradiated cladding (M. Lippens); Post irradiation examinations (S. Pilate, M. van den Borck, M. Lippens, J. Basselier); Measurements of thermal conductivity of high burn-up MOX fuel (GERONIMO) (M. Lippens).  
**University Hospital Gent, Clinic for Radiotherapy and Nuclear Medicine:** -immunotherapy (F. Offner).  
**University of Leuven:** Xe-implantation (H. Pattyn).  
**University of Liège:** Single crystal growth, X-ray diffraction, and analysis (J.F. Desreux, L. Martinot, M.R. Spirlet).  
**University of Namur, Laboratoire Interdisciplinaire de Spectroscopie Electronique:** Surface spectroscopy and electrochemistry (R. Caudano, J. Riga).  
**Virga Jesse Clinik, Hasselt:** -immunotherapy (D. Vanstraelen).

### Brasil

**Brazilian-Argentine Agency for Accounting and Control of Nuclear Materials (ABACC), Rio de Janeiro:** Safeguards (E. Palacio, C. Feu Alvim, O. Mafra Guidicini).

### Bulgaria

**Bulgarian Academy of Sciences, Institute of Nuclear Energy:** Illicit trafficking, FONSAFE (A. Strezov).  
**Committee on the Use of Atomic Energy for Peaceful Purposes, Sofia:** TRANSURANUS fuel pin code development (P. Ardenska); Illicit trafficking; FONSAFE (N. Todorov).  
**Institute of Nuclear Research and Nuclear Energy, Bulgarian Academy of Science, Sofia:** Fuel rod modelling and performance, FERONIA (D. Elenkov).

### Canada

**AECL Chalk River:** Gas release, SIMFUEL production and property studies (I. Hastings, P. Lucuta, R. Verrall); Behaviour of Rb and Cs in SIMFUEL (W. Hocking).  
**University of Kingston:** Inert matrices (P.G. Lucata).

### Czech Republic

**Nuclear Research Institute Rez plc, Rez:** TRANSURANUS fuel pin code development (F. Pazdera).  
*Central Analytical Laboratory:* Illicit trafficking, FONSAFE (F. Sus).  
**State Office for Nuclear Safety, Prague:** TRANSURANUS fuel pin code development (P. Krs); Illicit trafficking, FONSAFE (L. Bartak).  
**University of Prague:** Magnetic and electrical measurements (V. Sechovsky, L. Havela, P. Jaworsky); Gas release measurements (V. Balek).

### Denmark

**Risø National Laboratory:** Neutron scattering (B. Lebech).

### Finland

**STUK: Finnish Centre for Radiation and Nuclear Safety:** Illicit trafficking, FONSAFE (E.: Kainulainen).  
**VTT Energy Aerosol Technology:** shared cost actions "Revaporisation of Phebus PF samples" (J. Iokiniemi, A. Auvinen); Spent fuel source term (K. Oilila).

### France

**Commissariat à l'Énergie Atomique (CEA)**  
CEA, Cadarache: Transmutation of actinides - irradiation experiments: DNR (J.L. Faugère, N. Chauvin, S. Pillon, J.-C. Garnier, D. Warin, A. Languille, J. Rouault, M. Salvatores); PHEBUS PF programme, ThO<sub>2</sub> tube production (R. Zeyen); Bundle post irradiation examinations and sample post-test analysis (M. Schwartz, R. Zeyen); Melting point of PHEBUS pf corium (M. Schwartz); Examination of FP deposits of PHEBUS PF by mass spectrometry (M. Schwartz); Inert matrices (M. Beauvy and N. Chauvin); shared cost action "Corium Interaction Thermochemistry" (B. Adroguer, M. Barrachin).  
CEA, Marcoule: Partitioning of actinides, DIAMEX process (C. Madic); Characterization of transuranium cyano-complexes (D. Meyer, C. den Auwer); behaviour of He in waste glasses (D. Ghaleb).  
CEN, Grenoble: Neutron diffraction, magnetic studies; transport properties and Mössbauer studies (P. Bulet, N. Bernhoeft, J.P. Sánchez, D. Braithwaite and F. Bourdarot).  
CEA Palaiseau: Radiation Damage (A. Dunlop).  
CEN, Saclay: Neutron diffraction (J.M. Mignot, B. Hennion); Post-irradiation examinations (J.I. Blanc, F. Couvreur).  
**CERCA, Romans:** MTR fuel development (J.P. Durand, B. Lelievre).

**CNRS, Lab. de Cristallographie, Grenoble:** Crystallography of phase transitions (J.C. Marmeggi); Orsay: Basic studies on spent  $UO_2$  fuel (J.C. Dran); ARAMIS accelerator, radiation damage, ion implantation (L. Thomé).

**COGEMA, La Hague:** Laboratoire sur Site (G. Decobert).  
*Branche Retraitement et Combustible:* Development of MOX fuels (J. Nigon, Mme M. Trotabas), Thermophysical measurements on ECRIX material " $MgO-AmO_2$ " (T. Albiol, Y. Croixmarie).

#### Électricité de France (EDF)

Septen, Villeurbanne: Transmutation of actinides (G. Vambenepe); Div. Recherche, Paris: RIM effect (M. Baron); Chemical and mechanical interactions fuel/cladding (thermal reactor) and determination of mechanical properties of irradiated  $UO_2$  (M. Baron).

**ESRF, Grenoble:** Synchrotron studies on actinides (C. Vettier, G. Grübel, P. Carra).

**FRAMATOME, Nuclear Fuel Division, Lyon:** Post-irradiation examinations (P. Blanpain, E. Van Schel, O. Gentil).

**Grand accélérateur National d'ions Lourds, GANIL, Caen:** Radiation damage in inert matrices (M. Toulemonde).

**ILL, Grenoble:** Polarized neutron diffraction and neutron inelastic scattering (P.J. Brown, A. Hiess).

**Institut National de la Santé et de la Recherche Médicale (INSERM), Nantes:**  $\alpha$ -immunotherapy by Bi-213 (J.F. Chatal).

**OECD Nuclear Energy Agency, AEN-NEA, Paris:** Database on fuel performance (E. Sartori).

**Subatech, Ecole des Mines, Nantes:** production of Ac-225 (H. Gutbrod).

#### Germany

**Bundesministerium für Umwelt, Naturschutz, und Reaktorsicherheit:** Vagabonding nuclear material (J. B. Fechner); Treatment of nuclear fuels (H. Dumpich).

**Bundesministerium für Bildung und Forschung:** Environmental sampling (H. Remagen).

**Deutsches Krebsforschungszentrum, Biophysik und Medizinische Strahlenphysik, Heidelberg:**  $\alpha$ -immunotherapy (G. van Kaick).

**Forschungszentrum Jülich, Institut für Festkörperforschung:** spin dynamics in  $UO_2$  (U. Köbler).

#### Forschungszentrum Karlsruhe (FZK)

*Hauptabteilung Zyklotron (HZY):* production of Ac-225 (H. Schweikert).

*Institut für Nukleare Entsorgung (INE):* shared cost action: Spent fuel source term (T. Fanghaenel).

*Institut für Nukleare Festkörperphysik (INFP):* Radiation damage studies, RBS analyses, channeling, ion implantation (R. Fromknecht, G. Linker).

*Institut für Technische Chemie (ITC):* Susceptibility and crystal preparation (B. Kanellakopoulos).

*Projekt Nukleare Sicherheitsforschung (PSF):* Irradiation experiment CAPRA-TRABANT (G. Heusener).

*Technologie Transfer:* KEIM initiative (J. Wüst).

**Hahn-Meitner-Institut (HMI), Berlin:** High-energy ion implantation (S. Klumünzer).

**Max-Planck Research Group "Theory of Complex and Correlated Systems", Dresden:** Theory of the Kerr-effect (P.M. Oppeneer).

**Siemens/KWU, Erlangen:** Post-irradiation fuel rod examination (R. Manzel).

#### Technischer Überwachungsverein Bayern e.V., München:

TRANSURANUS fuel pin code development (G. Sauer).

#### Technischer Überwachungsverein Hannover/Sachsen-Anhalt e.V.:

TRANSURANUS fuel pin code development (H. Märtens, D. Bour).

#### Technischer Überwachungsverein Norddeutschland e.V.,

Hamburg: TRANSURANUS fuel pin code development (J.F. Schriek).

#### Technischer Überwachungsverein Südwest e.V., Mannheim:

TRANSURANUS fuel pin code development (I. Brestrich).

**Technische Universität München:** Mössbauer and SR studies (M. Kalvius, W. Potzel, L. Asch).

*Nuklearmedizinische Klinik und Poliklinik der TU München:*

$\alpha$ -immunotherapy (R. Senekowitsch-Schmidtke).

**Universität Augsburg:** Resistivity of transuranium samples at low temperature high pressure (G. Stewart).

**Universität Göttingen, Zentrum Radiologie:**  $\alpha$ -immunotherapy (T.M. Behr, W. Becker).

**Universität Heidelberg, Medizinische Klinik und Poliklinik V, Heidelberg:**  $\alpha$ -immunotherapy (R. Haas).

**Universität Mainz, Institut für Kernchemie:** Analytical techniques for particle characterization (J.V. Kratz).

**Universität München-Garching:** High-energy ion implantation (W. Assmann).

#### Hungary

**Hungarian Academy of Sciences, Institute of Isotopes, Budapest:** Forensic nuclear analysis for safeguards (J. Safar).

**KFKI Atomic Energy Research Institute, Budapest:** TRANSURANUS fuel pin code development (S. Elo).

**Hungarian Atomic Energy Commission, Budapest:** TRANSURANUS fuel pin code development (M. Gado), Illicit trafficking, FONSAFE (I. Czoch).

#### Israel

**Technion, Haifa:** Waste glass studies (Y. Eyal).

### Italy

**Centro Ceramico Bologna:** Leaching studies, Indentation techniques (L. Esposito).

**Centro Legnaro/Padova:** RBS, Ion implantation, H-analysis on leached waste matrices (G. Della Mea, V. Rigato).

**ENEA:** Partitioning and Transmutation, Accelerator Driven Systems (G. Gherardi).

**University of Ancona:** Neutron and bulk magnetization studies (R. Caciuffo).

**University of Aquila, Physics Department:** Theory of optical properties (P. Monachesi).

**University of Bologna, Ravenna, Environmental Science:** Measurements of environmental radioactivity (Prof. Bruzzi).

**University of Padova:** Analysis of glass surfaces (P. Mazzoldi).

**University of Pisa, Chemistry Department:** Instrumental analytical techniques for traces analysis (R. Fuoco).

**University of Parma, Physics Department:** Theory of oxides (G. Amoretti).

### Japan

**Central Research Institute of Electricity Producing Industries (CRIEPI), Tokyo:** Preparation and characterization of minor actinide alloys (T. Inoue); Pyro-reprocessing studies (T. Inoue, T. Koyama); Spent fuel characterization for interim dry storage (T. Matsumura); Rim effect studies (M. Kinoshita); Measurements of thermal conductivity of irradiated fuel up to high burnup (M. Kinoshita).

**JAERI, Tokai Mura:** Radiation damage in oxide fuels (K. Fukuda).

**Nuclear Material Control Center, Tokai:** Safeguards (T. Tsujino).

**Tohoku University, Inst. for Materials Research, Sendai, Japan:** Reduction of Np metal, solid states physics (Y. Shiokawa).

**Tokohu University, Sendai, Japan:** Studies of heavy fermion uranium compounds (N. Sato, T. Komatsubara, Y. Endoh).

### The Netherlands

**Interfaculty Reactor Institute, Delft:** Gas release (A. van Veen).

**Mallinckrodt, Medical bv, Petten:**  $\alpha$ -immunotherapy (G. Ensing).

**NRG, Petten:** Transmutation of fission products (H.U. Staal, M. Grupelaar).

### Norway

**OECD Halden Reactor Project:** High Burnup Rim Effect irradiation (E. Kolstad).

### Poland

**Institute of Atomic Energy, Otwock/Swierk:** TRANSURANUS fuel pin code development (M. Szuta).

**Institute for Low Temperature and Structure Research, Warsaw:** Bulk properties and neutron scattering (R. Troc, W. Suski, D. Kaczorowski).

### Portugal

**Instituto Tecnológico e Nuclear (ITN), Sacavem:** Physical chemistry of actinides (A. Pires de Matos, M. Almeida).

**University of Aveiro, Department of Physics:** Kerr effect theory (T. Gasche).

**University of Coimbra:** Neutron and X-ray studies (J.A. Paixão).

### Romania

**Institute for Nuclear Research, Nuclear Fuel Performance Analysis, Pitetsi:** TRANSURANUS fuel pin code development (G. Horhoianu).

### Russia

**Academy of Sciences, IVTAN, Moscow:** Equation of uranium dioxide (I. Iosiliewski); Studies on high-melting materials (V. Fortov).

**All Russia Research Institute of Inorganic Materials (A.A. Bochvar Institute), Moscow:** Setting up of three laboratories for safeguards, metrology, nuclear forensics (A. Petrov).

**ENIL, Moscow:** Thermophysical properties of high temperatures (E. Volkov).

**Flerov Laboratory, Dubna:** Radiation damage in ceramics (V.A. Skuratov).

**GOSATOMNADZOR, Moscow:** Nuclear Safeguards (A. Dimitriev).

**High Temperature Institute, Moscow:** Thermodynamic database (V. Yungman, L. Gorokhov).

**Institute of Chemical Physics, Chernogolowka:** Critical Point of  $UO_2$  (V. Gryaznov).

**MINATOM, Moscow:** Nuclear Safeguards (N. Redin).

**Nuclear Power Plant, Leningrad:** PIE, non destructive examinations (V.C. Shevchenko) Nuclear.

### Slovak Republic

**Nuclear Power Plant Research Institute, Trnava:** TRANSURANUS fuel pin code development (M. Cvan).

### South Africa

**University of Witwatersrand, Johannesburg:** Transport measurements (P. du Plessis).

### Spain

**Ministerio de Industria y Energia, CIEMAT, Instituto de Technologica Nuclear, Madrid:** TRANSURANUS fuel pin code development (J. López Jiménez).

**ENRESA:** Waste management, leaching tests (J.A. Esteban-Hernández).

### Sweden

**SKB:** Spent fuel disposal (K. Spahiu).

**University of Uppsala:** Solid state theory of actinides (B. Johansson, O. Eriksson).

### Switzerland

**ETH, Zürich:** Single crystal growth, magnetic, optical and transport properties, preparation of U and Th compounds (O. Vogt, P. Wachter, K. Mattenberger).

**Kantonsspital Basel, Institut für Nuklearmedizin,**  $\alpha$ -immunotherapy (H.R. Mäcke).

**Paul-Scherrer-Institut, Villigen** TRANSURANUS fuel pin code development (C. Hellwig); Post-irradiation structural investigations by electron microscopy, PHEBUS PF FPT1 bundle post irradiation examination (D. Gavillet); Inert matrix studies (M. Burghartz, G. Ledergerber).

**University of Lausanne:** Theory of oxides (P. Santini).

### Ukraine

**Ministry for environmental protection and nuclear safety of Ukraine:** Illicit trafficking, FONSAFE (A. Smyshliaiev).

**State Scientific and Technical Centre on Nuclear and Radiation Safety, Kyiv:** TRANSURANUS fuel pin code development (M. Yermenko).

**University of Odessa:** Liquid state models (E. Yakub).

### United Kingdom

**AEA Technology, Winfrith:** shared cost action "Revaporisation effects of PHEBUS samples" (B. Bowsher).

**Birkbeck College:** neutron and magnetization studies (K. McEwen).

**BNFL, Sellafield:** On-site laboratory (R. Strong, J. Reed); PIE examination of MOX spent fuel (S. Fisher); Melting point of irradiated MOX (S. Fisher).

**BFNL Eng. Department, Risley:** Laboratory infrastructure (R. Johnson).

**NNC, Risley:** Engineering design support (B. Rowney).

**NCC, Workington:** QA consultancy (W.G. Smith).

**University of Bristol, Interface Analysis Centre:** Surface corrosion (G. Allen).

**University of Glasgow, Dept. of Physics and Astronomy / Rutherford Appleton Laboratory, Chilton:** Laser induced fission (K.W.D. Ledingham).

**University of Liverpool:** X-ray and neutron scattering (W.G. Stirling).

**University of Warwick:** Compton scattering (M.J. Cooper); Equation of state of irradiated fuel (G. Hyland); Radiative properties at high temperatures (G. Hyland).

### United States of America

**Argonne National Laboratory, IL:** Neutron scattering and X-ray absorption spectroscopy (L. Soderholm).

**Battelle Pacific Northwest Laboratories, Richland, WA:** Irradiation damage studies (W. Weber).

**Brookhaven National Laboratory, NY:** High-resolution and magnetic X-ray scattering (D. Gibbs).

**Colorado State University, Fort Collins, CO:** Studies of oxides (S. Kern).

**Lawrence Berkeley National Laboratory, CA:** Synchrotron studies of actinide surfaces and thin films (D. Shuh).

**Lawrence Livermore National Laboratory, CA:** Forensic nuclear analysis (S. Niemeier).

**Los Alamos National Laboratory, NM:** Materials preparation and photoemission (B. Cort, A.J. Arko, R. Robinson, A. Lawson); Radiation damage in ceramics (K. Sickafus).

**Memorial Sloan Kettering Cancer Center, New York, NY:**  $\alpha$ -immunotherapy by Bi-213 (D.A. Scheinberg).

**National Institute of Health, Bethesda, MD:**  $\alpha$ -immunotherapy by Bi-213 (M.W. Brechbiel).

**Oak Ridge National Laboratory, TN:** Material preparation, high pressure X-ray and optical studies (R.G. Haire, J.R. Peterson); Radiation damage in ceramics (S.J. Zinkle).

**University of Maryland, Baltimore, MD:** Studies of surfaces (G. Watson).

**University of Michigan, Ann Arbor, MI:** High resolution TEM, radiation damage (R. Ewing, L.M. Wang).

**University of West-Virginia, Morgantown, WV:** Actinide theory (B.R. Cooper).

### Uzbekistan

**Physical Technical Institute, Tashkent:** Radiative properties of UO<sub>2</sub> at high temperatures (T. Salikhov).

# Annex III

## List of Contributors to the Various Chapters

### PART A

#### Review Article

L. Koch, I.L.F. Ray, M. Betti, A. Schubert.

#### Highlights

V. Ichas (H1), T. Gouder (H2), C. Ronchi (H3), Hj. Matzke, V.V. Rondinella, T. Wiss (H4), Hj. Matzke, V.V. Rondinella, J. Cobos, T. Wiss, J. Somers (H5), J.-P. Glatz (H6), J. Magill (H7), J.-F. Babelot (H8).

### PART B

#### 1. Basic Actinide Research

G.H. LANDER, N. Bernhoeft, A. Bombardi, M.S.S. Brooks, S. Coad, E. Colineau, T. Gouder, J.C. Griveau, S. Heathman, V. Ichas, D. Kolberg, K. Litfin, D. Mannix, A. Martín-Martín, J. Rebizant, F. Wastin  
Hj. MATZKE, M. Cheindlin, J.-P. Hiernaut, C. Ronchi  
L. KOCH, C. Apostolidis, W. Janssens.

#### 2. Safety of Nuclear Fuels

J.-P. GLATZ, D. Bottomley, D. Papaioannou, J. Spino, A. Stalios, E. Toscano, C. Walker, D.H. Wegen  
Hj. MATZKE, M. Cheindlin, K. Laßmann, M. Musella, C. Ronchi, V.V. Rondinella, T. Wiss  
D. HAAS, J. Somers, F. Charollais, N. Boucharat, A. Fernández  
L. KOCH, G. Nicolaou.

#### 3. Mitigation of Long Lived Actinides and Fission Products

Hj. MATZKE, J.-P. Hiernaut, T. Sonoda, T. Wiss,  
J.-P. GLATZ, O. Courson, R. Malmbeck, B. Sätmark, A. Stalios, C. Walker,  
D.H. Wegen  
L. KOCH, M. Ougier  
D. HAAS, J. Somers, N. Boucharat, A. Fernández.

#### 4. Spent Fuel Characterization in View of Long Term Storage

J.-P. GLATZ, J. Giménez, D. Papaioannou, J. Spino, A. Stalios,  
D. H. Wegen  
Hj. MATZKE, J. Cobos, V. Rondinella, T. Wiss,  
L. KOCH, G. Nicolaou.

#### 5. Safeguards Research and Development

L. KOCH, M. Betti, P. Carbol, O. Cromboom, G. Janssen, K. Mayer,  
G. Nicolaou, L. Pajo, A. Schubert, D. Solatie, M. Wallenius, G. Tamborini.

#### 6. Scientific and Technical Support to DG XVII

L. KOCH, M. Betti, P. Daures, K. Mayer, H. Ottmar, H.-G. Schneider

#### 7. Scientific and Technical Support to DG I

L. KOCH, M. Betti, K. Mayer, A. Schubert.



## Glossary of Acronyms and Abbreviations

**ABACC:** Agência Brasileiro-Argentina de Contabilização e Controlo dos Materiais Nucleares.

Argentinian-Brazilian Agency for Accounting and Control of Nuclear Material.

**ACTINEAU:** Incinération des ACTINides dans les réacteurs à EAU.

**AEA:** Atomic Energy Authority (United Kingdom).

**AECL:** Atomic Energy of Canada Ltd.

**ADS:** Accelerator Driven hybrid reactor Systems.

**AMAS:** Accountancy Management Systems.

**a/o:** (at.%) atomic percent.

**ARTINA:** Analysis of Radioisotope Traces for the Identification of Nuclear Activities.

**BET:** Brunauer, Emmet and Teller surface gas asorption technique.

**BNFL:** British Nuclear Fuel plc, Springfields (United Kingdom).

**BWR:** Boiling Water Reactor.

**CAPRA:** Consommation Accrue de Plutonium dans les (réacteurs) RAPides.

**CEA:** Commissariat à l'Énergie Atomique (France).

**CEN:** Centre d'Études Nucléaires.

**CdZnTe:** Cadmium-Zinc-Telluride (detector).

**CDW:** Charge Density Wave.

**CETAMA:** Commission d'établissement des méthodes d'analyses (France).

**CIEMAT:** Centro de Investigaciones Energéticas, Medioambientales y Tecnológicas, Madrid (Spain).

**COG:** CANDU Owners' Group, Toronto, ON (Canada).

**COGEMA:** COmpagnie GÉnérale des MATériaux nucléaires, Vélizy (France).

**COMPUCEA:** COMBined Product-Uranium Concentration and Enrichment Assay.

**CORDIS:** Community Research and Development Information Service, Luxembourg.

**CRIEPI:** Central Research Institute of the Electric Power Industry, Tokyo (Japan).

**DEH:** Direct Electrical Heating.

**DESY:** Deutsches Elektronen-Synchrotron, Hamburg (Germany).

**DG IA:** Directorate General "External Relations: Europe and the New Independent States, Common Foreign and Security Policy, External Service" of the European Commission.

**DG XIII:** Directorate-General XIII "Information Society, Telecommunications, Markets, Technologies – Innovation and Exploitation Research" of the European Commission.

**DG XVII:** Directorate-General "Energy" of the European Commission.

**DIAMEX:** DIAMide EXtraction process.

**DIN:** Deutsche Industrienorm; Deutsches Institut für Normung.

**DOVITA:** Dry reprocessing, Oxide fuels, Vibropac, Integral, Transmutation of Actinides.

**DQS:** Deutsche Gesellschaft zur Zertifizierung von Qualitätssicherungssystemen.

Deutsche Gesellschaft zur Zertifizierung von Managementsystemen mbH.

**EBR:** Experimental Breeder Reactor, Argonne National Laboratory (USA).

**ECN:** Energie Centrum Nederland, Petten (Netherlands).

**ECSAM:** European Commission's Safeguards Analytical Measurements.

**EDAX:** Energy-Dispersive Analysis with X-rays.

**EDF:** Électricité de France.

**EDX:** Energy-Dispersive X-ray analysis.

**EFQM:** European Foundation for Quality Management.

**EFTRA:** Experimental Feasibility for Targets and TRANsmutation.

**EFPD:** Effective Full Power Days.

**EMPA:** Electron Micro-Probe Analysis (also EPMA).

**ENRESA:** Empresa Nacional de Residuos Radioactivos SA (Spain).

**EOS:** Equation Of State.

**EPMA:** Electron Probe Micro-Analysis (also EMPA).

**ESARDA:** European SAFeguard Research and Development Association.

**ESD:** European Safeguards Directorate, Luxembourg.

**ESRF:** European Synchrotron Radiation Facility, Grenoble (France).

**ETH:** Eidgenössische Technische Hochschule, Zürich (Switzerland).

**EURATOM:** EUROpean ATOMIC energy community.

**EXAFS:** Extended X-ray Absorption Fine Structure.

**FARO:** fuel melting and release oven, JRC Ispra (Italy).

**FBR:** Fast Breeder Reactor.

**FCCI:** Fuel Clad Chemical Interaction.

**FCMI:** Fuel Clad Mechanical Interaction.

**FERONIA:** fuel rod modelling and performance project.

**FIAP:** Fraction of Inventory in the Aqueous Phase.

**FONSAFE:** Forensic Nuclear analysis for SAFEGuards.

**FP:** Fission Products.

**FWP:** FrameWork Programme.

**FZK:** ForschungsZentrum Karlsruhe (Germany).

**FWHD:** Full Width at Half Depth.

**FWHM:** Full Width at Half Maximum.

**FWTD:** Full Width at Tenth Depth.

**GDMS:** Glow Discharge Mass Spectrometry (Spectrometer).

**GSP:** Gel Supported Precipitation.

**GWd/tM:** Gigawatt-day per (metric) ton metal.

**GWd/tU:** Gigawatt-day per (metric) ton Uranium (metal).

**HBRP:** High Burnup RIM Project.  
**HEU:** Highly Enriched Uranium.  
**HFR:** High Flux Reactor, Petten (Netherlands).  
**HKED:** Hybrid K-Edge Densitometer.  
**HLW:** High Level Waste.  
**HLLW:** High Level Liquid Waste.  
**HPTA:** High Performance Trace Analysis.  
**HWHM:** Half-Width at Half Maximum.

**IAEA:** International Atomic Energy Agency, Vienna (Austria).  
**ICP-MS:** Inductively Coupled Plasma Mass Spectrometry.  
**IDA:** Isotope Dilution Analysis.  
**IDMS:** Isotope Dilution Mass Spectrometry.  
**ILL:** Institut Max von Laue - Paul Langevin, Grenoble (France).  
**IMF:** Institut für Materialforschung, FZK (Germany).  
**INE:** Institut für Nukleare Entsorgungstechnik, FZK (Germany).  
**INR:** Institut für Neutronenphysik und Reaktortechnik, FZK (Germany).  
**INRAM:** INFiltration of RAdioactive Materials.  
**INRNE:** Institute for Nuclear Research and Nuclear Energy, Bulgarian Academy of Science.  
**INSERM:** Institut National de la Santé et de la recherche médicale.  
**INSTN:** Institut National des Sciences et Techniques Nucléaires, La Hague (France).  
**INTAS:** INTernational ASSociation for the promotion of Cooperation with Scientists from the Independent States of the former Soviet Union.  
**IPSN:** Institut de Protection et de Sûreté Nucléaire, Cadarache (France).  
**ISO:** International Organisation for Standardisation.  
**ISTC:** International Science and Technology Center, Moscow (Russia).  
**ITU:** Institute for Transuranium Elements, Karlsruhe (Germany).  
**ITN:** Instituto Tecnológico e Nuclear, Savacem (Portugal).  
**IVTAN:** Institute for High Temperature Physics, Moscow (Russia).

**JAERI:** Japan Atomic Energy Research Institute (Japan).  
**JEF:** Joint Evaluated File, decay library, NEA-OECD, Paris.  
**JRC:** Joint Research Centre, European Commission.

**KAERI:** Korea Atomic Energy Research Institute, (Republic of Korea).  
**KEDG:** K-EDGe densitometer.  
**KEIM:** Karlsruher Existenzgründer Impuls (Germany).  
**KNK II:** Kompakte Natriumgekühlte Kernreaktoranlage (Germany).  
**KWU:** KraftWerk-Union, Germany.

**LEU:** Low Enriched Uranium.  
**LSD:** Large Size Dried spikes.  
**LSS:** Laboratoire Sur Site, La Hague (France).  
**LWR:** Light Water Reactor.

**MA:** Minor Actinides (Np, Am, Cm).  
**MOX:** Mixed OXide fuel.  
**MWd/tM:** Megawatt day per (metric) ton of (heavy) Metal.  
**MWd/tU:** Megawatt day per (metric) ton of Uranium.

**NDA:** Non-Destructive Assay (Analysis).  
**NDT:** Non-Destructive Testing.  
**NEA:** Nuclear Energy Agency, OECD, Paris (France).  
**NNC:** National Nuclear Corporation, Ltd. Risley (U.K.).  
**NRC:** Nuclear Regulatory Commission, Washington DC (USA).  
**NRI-CAL:** Nuclear Regulatory Institute Rez near Prague, Central Analytical Laboratory.  
**NSLS:** National Synchrotron Light Source, Brookhaven, NY (USA).  
**NUPEC:** Nuclear Power Engineering Corporation (Japan).

**OECD:** Organization for Economic Cooperation and Development, Paris (France).  
**ORACLE:** Relational database program.  
**ORNL:** Oak Ridge National Laboratory, Oak Ridge, TN (USA).  
**OSL:** On-Site Laboratory.

**PCI:** Pellet Clad Interaction.  
**PHARE:** Pologne-Hongrie: Aide à la Reconstruction Économique.  
**PHEBUS:** French test reactor, Cadarache (France).  
**PHEBUS-FP:** Programme to study fission product release and their distribution in the primary circuit.  
**PHENIX:** French prototype fast reactor.  
**PIE:** Post-Irradiation Examination.  
**PIMPOM:** Plutonium Inert Matrix in the POMpei device.  
**PSI:** Paul Scherrer Institut, Würenlingen, (Switzerland).  
**PUREX:** Plutonium and Uranium Recovery by EXtraction.  
**PWR:** Pressurized Water Reactor.

**QM:** Quality Management.

**RBS:** Rutherford Backscattering Spectroscopy.  
**RIAR:** Research Institute of Atomic Reactors, Dimitrovgrad (Russia).

**SAL:** Seibersdorf Analytical Laboratory, Vienna (Austria).  
**SCK-CEN:** Studiecentrum voor Kernenergie - Centre d'Etude de l'Energie Nucleaire, Mol (Belgium).  
**SEM:** Scanning Electron Microscopy.  
**SGN:** Société Générale pour les Techniques Nouvelles, (France).  
**SIMFUEL:** SIMulated high burnup FUEL (with major non-volatile fission products).  
**SIMS:** Secondary Ion Mass Spectrometry.  
**SOLMAS:** Sol-gel master blend.

**SONS:** State Office for Nuclear Safety, Czech Republic.  
**SQUID:** Superconducting QUantum Interference Device.  
**SUBATECH:** Laboratoire de physique SUBAtomique et de TECHnologies associés, Nantes (France).  
**TACIS:** Technical Assistance to the Commonwealth of Independent States.  
**TAMS:** Transuranium institute Analysis Management System.  
**TEM:** Transmission Electron Microscopy.  
**THORP:** Thermal Oxide Reprocessing Plant, Sellafield (U.K.).  
**TIG:** Tungsten Inert Gas welding.  
**TIMS:** Thermal Ionization Mass Spectrometry.  
**TOPO:** TriOctyl Phosphine Oxide.  
**TRABANT:** TRAnsmutation and Burning of Actinides in TRIOX.  
**TRANSURANUS:** Fuel behaviour code (ITU), Karlsruhe (Germany).  
**TRIOX:** HFR irradiation capsule, Petten (The Netherlands).  
**TRPO:** TRiAlkyl Phosphine Oxide.  
**TRU:** TRansUranium.  
**TUAR:** Annual Report of the Institute for Transuranium Elements (ITU), Karlsruhe (Germany).

**UPC:** Universitat Politecnica de Catalunya, Barcelona (Spain).  
**VNIINM:** All-Russia Research Institute of Inorganic Materials, Moscow (Russia).  
**v/o:** (vol %) volume percent.  
**VVER:** (also WWER) Voda-Vodyanoi Energetichesky Reaktor. Pressurized Water Reactor (PWR) built by Russia.  
**w/o:** (wt %) weight percent.  
**WWER:** (also VVER) Pressurized Water Reactor (PWR) built by Russia.  
**XPS:** X-ray induced Photoelectron emission Spectroscopy.  
**XRD:** X-Ray Diffraction.  
**XRF:** X-Ray Fluorescence analysis.



# Annex V

## Previous Progress Reports of the Institute for Transuranium Elements

TUSR	Period	COM Nr	EUR-Nr	TUAR	Period	COM Nr	EUR-Nr
1	Jan - Jun 1966	1580	-	86	Jan - Dec 1986	4302	12233 EN
2	Jul - Dec 1966	1522	-	87	Jan - Dec 1987		11783 EN
3	Jan - Jun 1967	1745	-	88	Jan - Dec 1988		12385 EN
4	Jul - Dec 1967	2007	-	89	Jan - Dec 1989		12849 EN
5	Jan - Jun 1968	2172	-	90	Jan - Dec 1990		13815 EN
6	Jul - Dec 1968	2300	-	91	Jan - Dec 1991		14493 EN
7	Jan - Jun 1969	2434	-	92	Jan - Dec 1992		15154 EN
8	Jul - Dec 1969	2576	-	93	Jan - Dec 1993		15741 EN
9	Jan - Jun 1970	2664	-	94	Jan - Dec 1994		16152 EN
10	Jul - Dec 1970	2750	-	95	Jan - Dec 1995		16368 EN
11	Jan - Jun 1971	2833	-	96	Jan - Dec 1996		17269 EN
12	Jul - Dec 1971	2874	-	97	Jan - Dec 1997		17746 EN
13	Jan - Jun 1972	2939	-	98	Jan - Dec 1998		18715 EN
14	Jul - Dec 1972	3014	-				
15	Jan - Jun 1973	3050	-				
16	Jul - Dec 1973	3115	-				
17	Jan - Jun 1974	3161	-				
18	Jul - Dec 1974	3204	-				
19	Jan - Jun 1975	3241	-				
20	Jul - Dec 1975	3289	-				
21	Jan - Jun 1976	3358	-				
22	Jul - Dec 1976	3384	-				
23	Jan - Jun 1977	3438	6475 EN				
24	Jul - Dec 1977	3484	7209 EN				
25	Jan - Jun 1978	3526	7459 EN				
26	Jul - Dec 1978	3582	7227 EN				
27	Jan - Jun 1979	3657	7483 EN				
28	Jul - Dec 1979	3714	7509 EN				
29	Jan - Jun 1980	3822	7857 EN				
30	Jul - Dec 1980	3846	8230 EN				
31	Jan - Jun 1981	3898	8447 EN				
32	Jul - Dec 1981	3927	8777 EN				
33	Jan - Jun 1982	3990	9581 EN				
34	Jul - Dec 1982	4048	10251 EN				
35	Jan - Jun 1983	4094	10266 EN				
36	Jul - Dec 1983	4117	10454 EN				
37	Jan - Jun 1984	4150	10470 EN				
38	Jul - Dec 1984	4165	11013 EN				
39	Jan - Jun 1985	4201	11835 EN				
40	Jul - Dec 1985	4263	11836 EN				

Previous Programme Progress Reports were confidential for a period of two years. Between 1977 and 1987 they had been made freely accessible after that period as EUR-Reports (on microfiches) and since 1988 they have been issued as regular EUR-Reports.



European Commission

**EUR 18715 EN - Institute for Transuranium Elements - Annual report 1998**

*Editors: R. Schenkel, J. Richter, J. Magill, D. Pel*

Luxembourg: Office for Official Publications of the European Communities

1999 - 138 pp. - 21.0 x 29.7 cm

Scientific and Technical Research series

ISBN 92-828-6580-0

**Abstract**

The 1998 annual report of the Institute for Transuranium Elements (ITU) of the JRC is divided in two parts, a more general part (A) reflecting management and infrastructure and a scientific-technical part (B) in which progress over the last year is detailed.

Included in part (A) is a review article nuclear forensics – the investigation of smuggled nuclear materials which describes in detail the Institute activities in this important field. In addition there is a series of highlights, i.e. short articles describing work of particular interest or where important results have been obtained. In the present report, there are highlight articles on:

- Strong Pressure Dependence of the Transport Properties of PuTe.
- Thin Films of Actinides and their Study by Photoemission.
- High-Precision Melting Point Measurement of MOX Nuclear Fuel.
- Interaction of an Oxidic Corium Melt with Water: the Puzzle of H<sub>2</sub>-Production.
- Effect of Alpha-Radiolysis on Leaching of UO<sub>2</sub> in Water.
- Partitioning of Minor Actinides from Genuine High Level Waste by Means of the DIAMEX process.
- NUCLIDES 2000: An Electronic Chart of the Nuclides on Compact Disc.
- ISO 9001 Certificate for ITU.

Part B of the report contains a detailed description of the progress made in the fields of basic actinide research, alpha-immunotherapy, safety of nuclear fuels, partitioning and transmutation of long lived actinides and fission products, spent fuel characterization in view of long term storage and safeguards research. Finally a list of publications is given together with collaborations with external organizations.









The mission of the JRC is to provide customer-driven scientific and technical support for the conception, development, implementation and monitoring of EU policies. As a service of the European Commission, the JRC functions as a reference centre of science and technology for the Union. Close to the policy-making process, it serves the common interest of the Member States, while being independent of special interests, whether private or national.



OFFICE FOR OFFICIAL PUBLICATIONS  
OF THE EUROPEAN COMMUNITIES

L-2985 Luxembourg

ISBN 92-828-6580-0



9 789282 865804 >